12-4-2006

Synthesis of Boronic Acid Based Sensors for Glucose and Sialic Acid and Synthesis of Novel and Selective PDE4 Enzyme Inhibitors

Gurpreet Kaur

SYNTHESIS OF BORONIC ACID BASED SENSORS FOR GLUCOSE AND SIALIC ACID

AND

SYNTHESIS OF NOVEL AND SELECTIVE PDE4 ENZYME INHIBITORS

by

GURPREET KAUR

Under the Direction of Binghe Wang

ABSTRACT

The boronic acid functional group is known to bind compounds with the diol group tightly and reversibly in aqueous environment and has been used as a recognition moiety for the design of carbohydrate sensors. The first chapter of the dissertation studies the synthesis and substitution effect on the affinity and selectivity of a known boronic acid-based glucose sensor. In such a sensor design effort, the availability of a signaling event, whether it is fluorescence or UV, is crucial. The second chapter studies the detailed mechanism on how a well-known fluorescent boronic acid compound changes fluorescent properties upon binding. A new mechanism has been established which corrected a decade old mistake. In the third chapter, a series of boronic acid-based sensors were designed and synthesized for sialic acid, which is part of tetrasaccharide found on many cell surface carbohydrates. Such sialic acid sensors could be very useful for the development of new type of anti-influenza therapy. The fourth is on the design and synthesis novel and selective inhibitors for phosphodiesterase 4 (PDE4), which are potential anti-asthma agents.

INDEX WORDS: Boronic acid, PDE4, enzyme inhibitors, sialic acid sensors, glucose sensors, fluorescence

SYNTHESIS OF BORONIC ACID BASED SENSORS FOR GLUCOSE AND SIALIC ACID

AND

SYNTHESIS OF NOVEL AND SELECTIVE PDE4 ENZYME INHIBITORS

by

GURPREET KAUR

A Dissertation Submitted in Partial Fulfillment of the Requirements for the Degree of

Doctor of Philosophy

in the College of Arts and Sciences

Georgia State University

2006

SYNTHESIS OF BORONIC ACID BASED SENSORS FOR GLUCOSE AND SIALIC ACID

AND

SYNTHESIS OF NOVEL AND SELECTIVE PDE4 ENZYME INHIBITORS

by

GURPREET KAUR

Major Professor:	Binghe Wang
Committee:	David Boykin
	Shahab Shamsi
Chair of Department	A.L. Baumstark

Electronic Version Approved:

Office of Graduate Studies

College of Arts and Sciences

Georgia State University

December 2006

DEDICATION

To my late father (Manjit Singh), mother (Jaspal Kaur), and brother (Harmeet Singh). Your love, kindness, and motivation have made this possible. I also dedicate my work to Navjot, new addition to my life. Your love and encouragement made it possible.

ACKNOWLEDGMENTS

I would like to thank my family.

I would like to thank my research advisor Dr. Binghe Wang for his guidance and encouragement during my graduate work.

I would like to thank the Wang group, and especially Hao Fang and Shilong Zheng for all the helpful discussions and ideas.

I would also like to acknowledge Molecular Disease Fellowship and National Institutes of Health for their financial support.

TABLE OF CONTENTS

LIST OF TABLES

LIST OF FIGURES

LIST OF SCHEMES

Chapter 1. Substituent effect on anthracene-based bisboronic acid glucose sensors

Abstract: Anthracene-based boronic acid has been studied as potential sensors for glucose detection. Aimed at understanding the substituent effect, various functional groups were introduced, such as the cyano, nitro, and fluoro group on the boronic acid moiety of the glucose sensor. Fluorescent binding studies indicated that the cyano-substituted sensor has the highest affinity (K_{eq} 2540 M^{-1}) for glucose, but the lowest selectivity (3-fold over fructose); the fluoro-substituted compound shows the lowest affinity (630 M^{-1}) and a modest selectivity (15-fold over fructose); and the unsubstituted one shows the highest selectivity over fructose (43-fold) and a modest affinity (1472 M^{-1}).

1.1. Introduction

Carbohydrates are considered critical to various biological processes.[1-5] The most prominent among them is glucose which is a critical energy supplier to cells, and its elevated concentration is the primary symptom of diabetes.[6] Sensors for the biologically important carbohydrates have the potential to be used as diagnostics, new imaging agents, as well as therapeutics.[7-9] Generally, selective sensors consists of three components: a) proper functional groups that afford strong intermolecular interactions (boronic acid), b) a 'reporter' event/moiety (stars) that allows the binding event to be recognized, and c) the appropriate three-dimensional scaffold that allow for necessary complementarily in terms of size, shape, and functional group orientation (bridge) as shown in Figure 1.1. There is especially strong interest in developing boronic acid-based sensors[10-16] because of the ability of the boronic acid group to form reversible and tight complexes with diol-containing compounds.[10, 13, 14, 17-25] Boronic acids have been used to develop fluorescent sensors,[11, 13, 14, 21, 22, 26-28] color sensors,[8, 11-13, 15, 16, 26, 29-36] sensors for cell recognition based on surface carbohydrate biomarkers,[22] carbohydrate transporters,[37-42] and chromatographic stationary materials.[43-48]

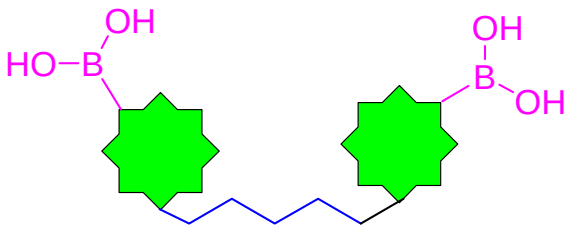

Figure 1.1. Three components of a "selective" sensor

1.1.1. Interaction between boronic acid and carbohydrate containing diols

Boronic acids covalently react with 1,2 or 1,3 diols to form reversible five- or six-membered cyclic esters in aqueous media. The *cis* diols of saccharides normally form stronger cyclic esters than the *trans* or acyclic diols. Boronic acids are Lewis acids and can react with water to form the neutral trigonal form (**1**) to the anionic tetrahedral form (**2**) (Scheme 1). The same is true for the diol – boronic complex or the boronic ester (**3**).

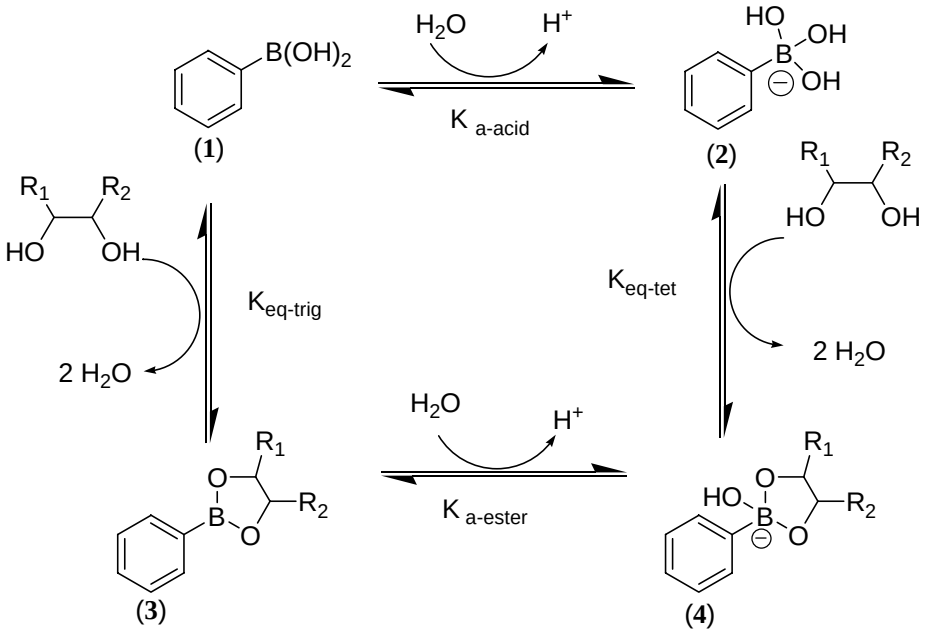

Scheme 1.1. Binding process between phenylboronic acid and a diol

1.1.2. Design of fluorescent boronic acid sensor

As mentioned above, a selective sensor requires proper functional groups that afford strong intermolecular interactions and a 'reporter' event/moiety that allows the binding

event to be recognized. The boronic acid moiety fulfills the requirement of strong intermolecular interaction needed for the sensor design. It is known that the monoboronic acids have certain intrinsic preference for various carbohydrates, the design of selective sensors for a particular sugar often relies on the introduction of additional functional group interactions, such as a second boronic acid unit, with a proper scaffold to afford selectivity.[22] Such an approach has been successfully used in various examples.[10, 11, 15, 32, 49] Modulation of the affinity of a monoboronic acid for diols can be achieved through the introduction of various substituents on an arylboronic acid. Generally speaking, arylboronic acids with lower p*K*a values tend to have higher affinities for diols, although one also needs to consider the pH of the solution and other factors.[19] For example, 2-fluoro-5-nitrophenylboronic acid has a p*K*a of about 6.0, which is 2.8 p*K*a units lower than that of phenylboronic acid. Consequently, the binding constant between glucose and 2-fluoro-5-nitrophenylboronic acid at physiological pH is about 10-fold higher than that of phenylboronic acid.[19] A fluorophore fulfills the signaling event for the binding process of sensor. A fluorophore that can change fluorescence upon binding to a saccharide is an ideal for fluorescent sensor design. One way to design a fluorescent sensor is through the modulation of an excited state photoelectron transfer (PET) process that is responsible for the quenching of fluorescence.

The first fluorescence PET sensors for saccharides, the anthrylboronic acids (**5** and **6**), showed significant fluorescence intensity changes upon binding with saccharide.[13] The fluorescence intensity change was due to the change in the hybridization state of the ester, which has lower p*K*a than the boronic acid (p*K*a about 8.8). Specifically, the

boronic acid should exist mostly in the neutral trigonal state at the physiological pH and at such a state PET to the open shell of the boron can happen in the excited state leading to fluorescence quenching. However, upon ester formation, the boron functionality would exist in the anionic tetrahedral because of a decreased p*K*a and such a hybridization change abolishes the excited PET and therefore removes fluorescence quenching mechanism.

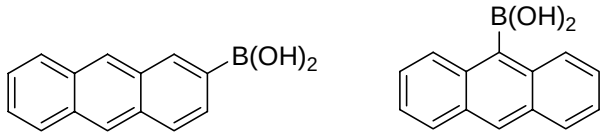

5 **6**

Figure 1.2. First fluorescence PET sensor developed

A second PET system was developed by Shinkai, where the amino group was positioned in a 1,5- relationship with the boronic acid. Such an arrangement promoted dative B-N bond formation.[50] It was proposed for the anthracene system that the anthracene fluorescence can be quenched by the lone pair electrons of the amino group through excited state photoelectron transfer (PET). It was further proposed that the B-N bond strengthens upon sugar binding, which "ties up" the lone pair electrons, abolishes the PET, and results in a fluorescence intensity increase. Although the mechanism proposed has proven to be incorrect (this will be discussed in detail in Chapter 2), indeed, upon sugar binding, **7** (Scheme 1.2) shows much higher fluorescent intensity. The positioning of an amino group also lowers the p*K*a of the boronic acid, and increases its

binding affinity for diols. Therefore, **7** showed much higher binding affinity to glucose and fructose compared with phenyl boronic acid. Shinkai et al also developed a similar anthracene system with bisboronic acid unit (**9**).[10] Compound **9** was selective for glucose over fructose.

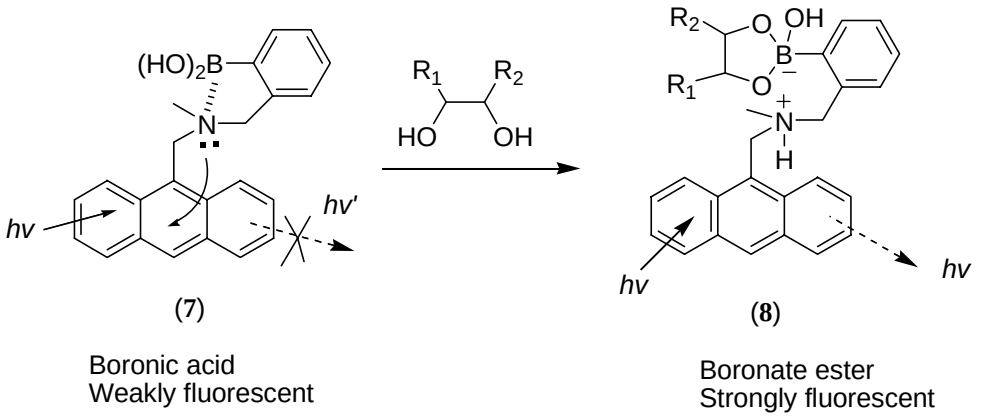

Scheme 1.2. Mechanism of an anthracene-based photoinduced electron transfer system

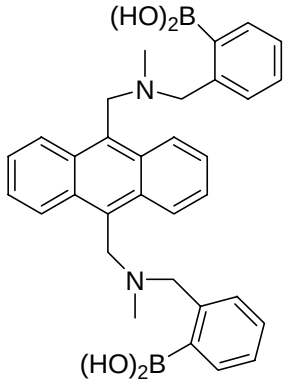

9

Figure 1.3. First bisboronic acid sensor developed by Shinkai

Our group has designed a highly selective anthracene-based boronic acid sensor for glucose (**10a**, Figure 1.4).[22] The sensor design used the Shinkai fluorescent reporter[10] which showed an increase in fluorescence intensity upon binding with a diol due to protonation of the amine nitrogen upon binding, the details of which will be discussed in Chapter 2.[51] Compound **10a** showed about 43-fold selectivity for glucose over fructose and 49-fold selectivity over galactose.

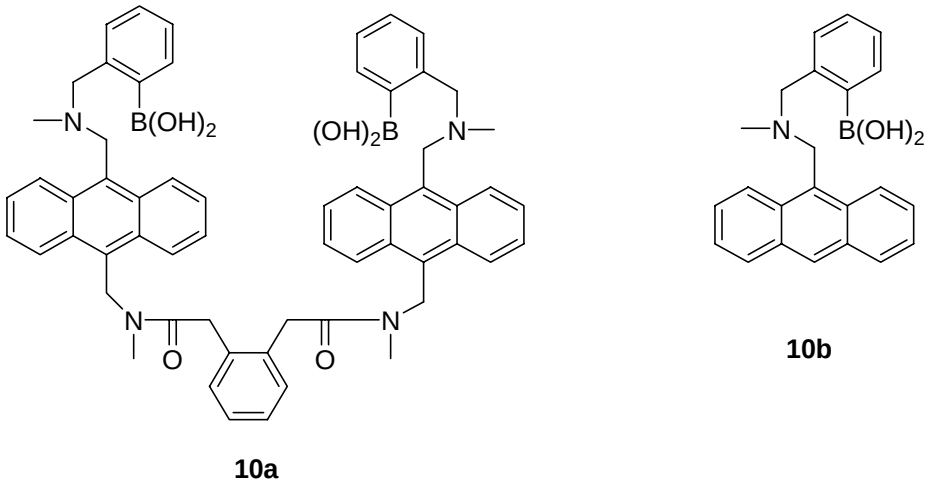

Figure 1.4. Dianthraceneboronic acid (**10a**) and anthracenemonoboronic acid (**10b**)

1.2. Project Objective

In this study, we are interested in studying the effect of electron withdrawing groups on the binding affinity between the bisboronic acid and various saccharides. We designed and synthesized analogs of **10a** and **10b** with different electron-withdrawing

substitutents on the arylboronic acid portion of the bisboronic acid sensor aimed at achieving a better understanding of the substituents effect. Specifically, there are two questions we wish to answer: (1) will the affinity-enhancing effect of electron withdrawing groups such as fluoro, nitro, and cyano substituents be translated into enhanced affinity of the bisboronic acid sensors for saccharide and (2) how will such electron-withdrawing groups affect the selectivity of the parent boronic acid sensors **10a** and **10b**. With that in mind three analogs of **10a**[22] and **10b**[10] with the cyano, nitro, and fluoro functional groups para position to the boronic acid were synthesized. Their binding constants with various sugars were determined.

1.3. Synthesis

Well established routes were used to synthesis the building blocks and final bisboronic acids compounds.[22, 36, 52] Figure 1.5 shows the target anthracene based bisboronic and monoboronic acids compounds that were synthesized.

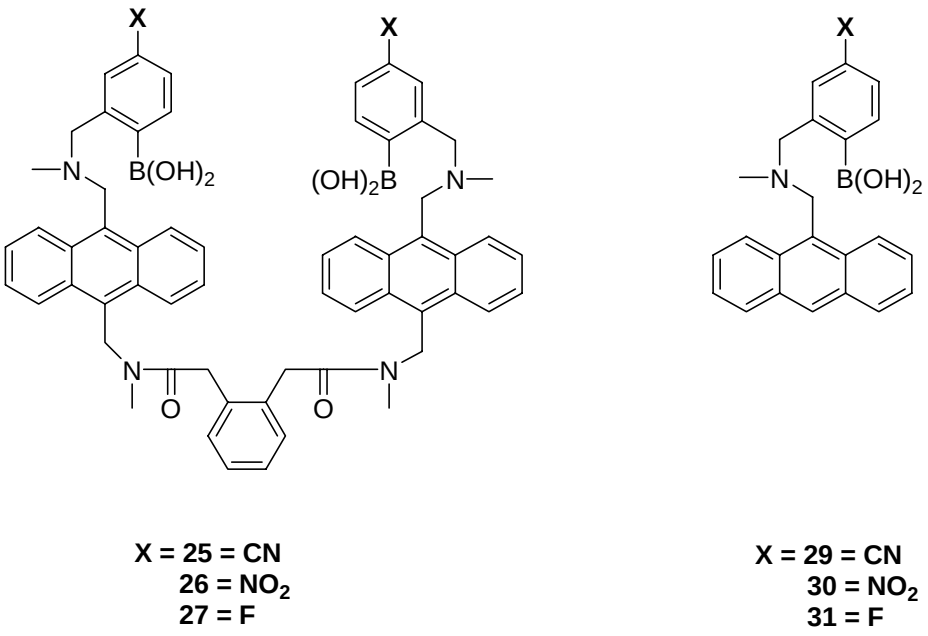

Figure 1.5. Synthesized target bisboronic and monoboronic acids compounds

1.3.1. Synthesis route to the common building block, bisanthracene amide

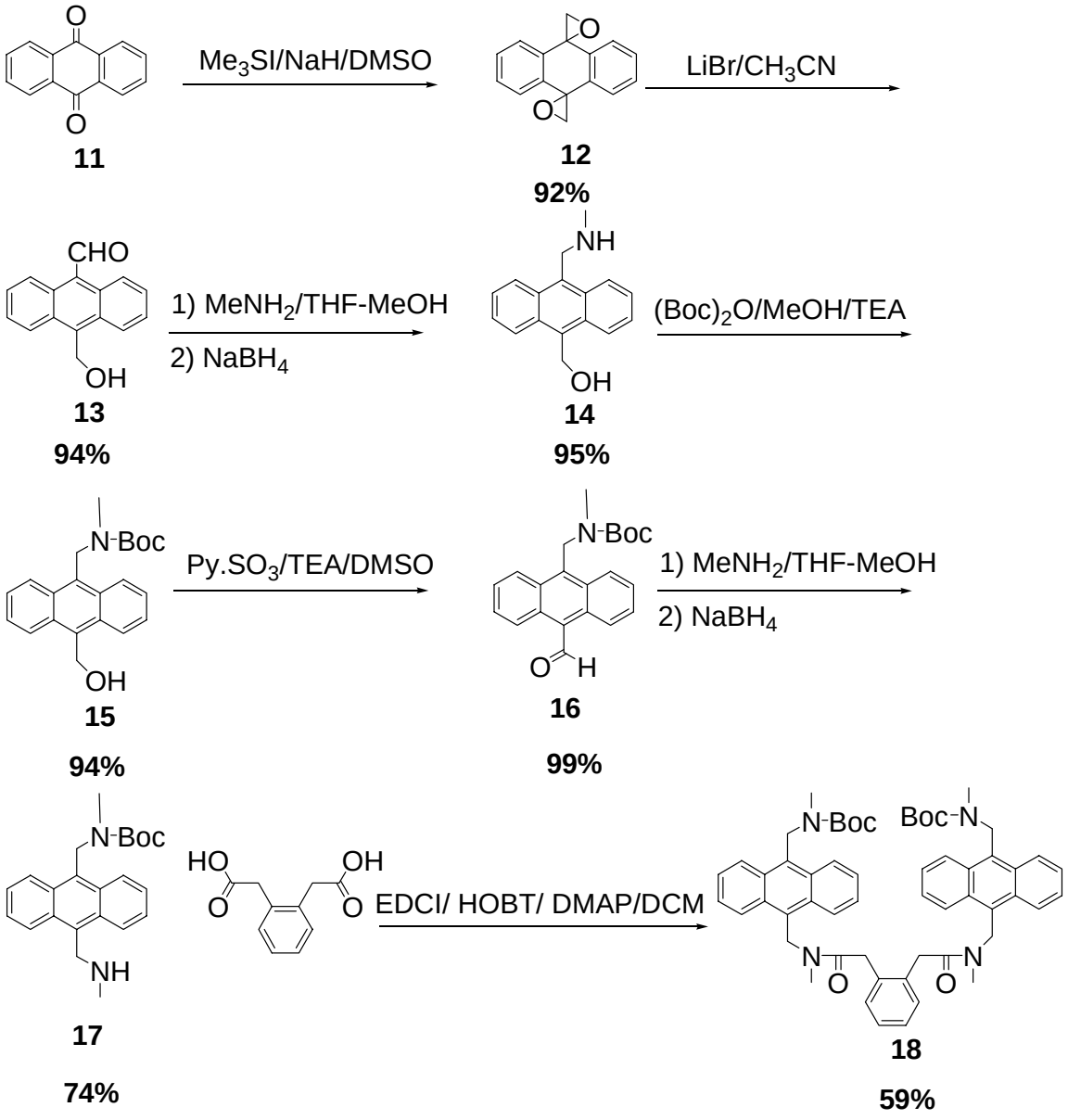

Scheme 1.3. Synthesis of intermediate Boc-protected diamides **18**

The synthesis of intermediate **18** took seven steps starting from the commercially available anthraquinone (**11**). **11** was first reacted with the trimethyl sulfonium *ylide* in dimethyl sulfoxide (DMSO) to give bis(epoxide), which then underwent rearrangement in the presence of lithium bromide in refluxing acetonitrile to give hydroxyaldehyde (**13**) in 94% yield.[52] Reductive amination of hydroxyaldehyde with methyl amine in MeOH/THF and $NaBH_4$ gave secondary amine (**14**) in 95% yield. The amine was protected with di-*tert*-butyldicarbonate in methanol in the presence of triethyl amine (TEA) to give **15** in 94 % yield. The hydroxyamine (**15**) was oxidized with pyridine sulfur trioxide complex in DMSO to give aldehyde (**16)** in quantitative yield. The resulting aldehyde underwent reductive amination to give amine (**17)** in 74% yield. The coupling reaction between amine (**17**) and the acid linker in the presence of 1-(2-diemthyl-amino propyl)-3-ethylcarbodiimide hydrochloride (EDCI) gave the intermediate **18** in 59 % yield.

1.3.2. Synthesis of *para* substituted arylboronic esters

To study the effect of electron withdrawing groups on the binding affinity of the boronic acid for the saccharide, *para* substituted arylboronic acids were needed. For the study, three para substituted arylboronic acids were synthesized with cyano, nitro, and fluoro as electron withdrawing groups. They were then introduced to the intermediate **18** to give the final bisboronic acids. Here only the syntheses of fluoro substituted arylboronic acid I prepared is reported (Scheme 1.4). The other two substituted aryl boronic acids (**19**, **20**) were synthesized by Mr. Haibo Li using similar procedures.

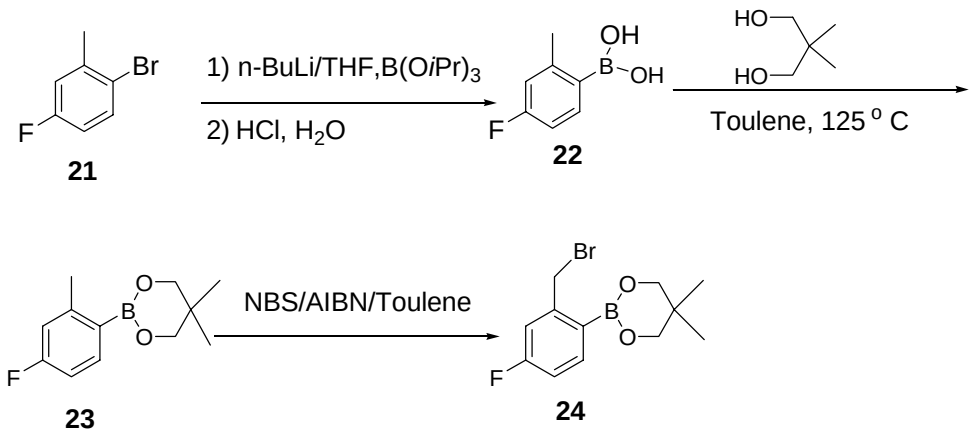

Scheme 1.4. Synthesis of 4-fluoro-2- phenylboronic acid (**24**)

Commercially available bromo-2-methyl-4-fluoro-benzene (**21**) was transmetalated with *n*-butyl lithium and then quenched with trisopropyl borate to give protected boronic acid which was cleaved during acidic work up to give free boronic acid (**22**). Free boronic acid was then protected with neopentyl glycol at 115 °C for the ease of deprotection at the end of the synthesis. Bromination of **23** in presence of NBS and AIBN yielded **24** in 68% yield.

The above method for the synthesis of neopentyl protected boronic acid (**24**) took three steps whereas a recently developed palladium catalyzed borylation method can be done in two steps for the same compound (**24**). Also, the palladium-catalyzed method can be used for the borylation of substrates that contain functional groups such as cyano, nitro, amino, hydroxyl, which may not be compatible with organometallic agents such as *n*-butyllithium. A separate study was conducted to examine the new bis(neopentyl glycolato)diboron borylating agent for the palladium catalyzed reaction with substrates substituted with various functional groups (see section 1.6).

1.3.3. Synthesis of bisboronic acid and monoboronic acid compounds

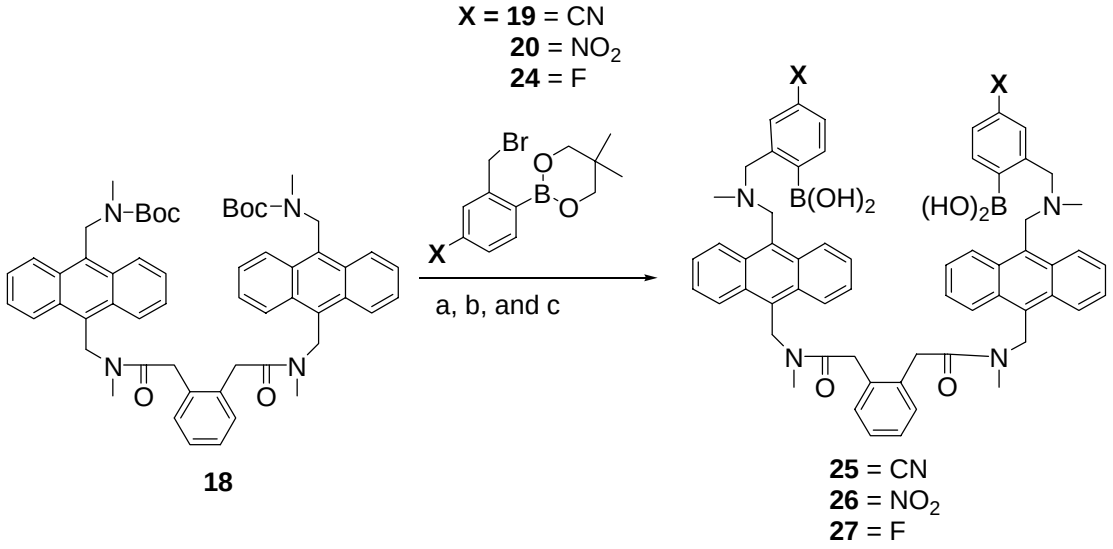

Scheme 1.5. (a) TFA, DCM; (b) **19, 20, 24**, K_2CO_3, KI, CH_3CN; (c) **25** and **26**: DCM, 10%$NaHCO_3$, H_2O; **27**: acetone: H_2O (4:1), 1*N* HCl

Bisboronic acid sensors, compound (**25-27**) were prepared through alkylation of intermediate **18** with substituted arylboronic acids. **18** was deprotected using trifluoroacetic acid (Scheme 1.5) and the free amino group was then reacted with **19**, **20**, and **24**, respectively**,** in the presence of K_2CO_3 in acetonitrile at room temperature to give the corresponding boronate esters of **25-26**. Hydrolysis of the protected boronic acids under basic conditions in the presence of $NaHCO_3$ gave the free boronic acids **25** and **26**; whereas free boronic acid **27** was obtained under acidic condition in the presence of HCl.[22]

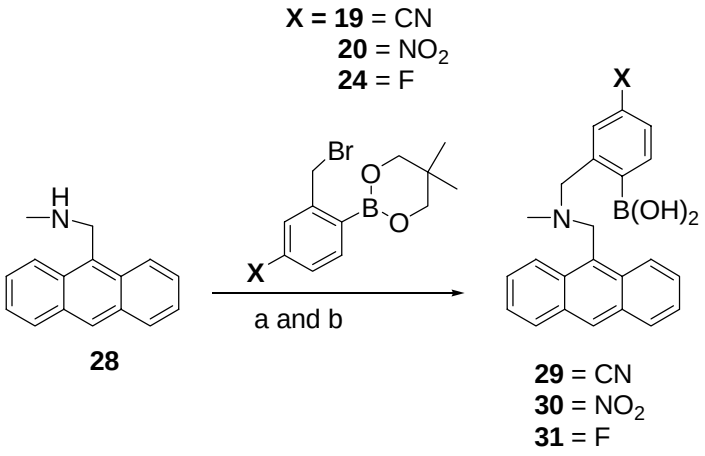

Scheme 1.6. (a) **19**,**20**,**24**, K_2CO_3, KI, CH_3CN; (b) **29** and **30**: DCM, 10%$NaHCO_3$, H_2O; **31**: acetone: H_2O (4:1), 1*N* HCl

For the synthesis of the monoboronic acids, commercially available anthracen-9-ylmethyl-methylamine (**28**) was reacted with **19**, **20**, and **24**, respectively, in the presence of K_2CO_3 in acetonitrile at room temperature to give the corresponding boronate esters (Scheme 1.6). Hydrolysis of the protected boronic acids was done under the same conditions as mentioned above to obtain free boronic acids **29-31**.[22]

1.4. Binding Studies

The bisboronic acid and monoboronic acid compounds mentioned above were expected to show increase in fluorescence upon sugar binding. Furthermore, we were interested in seeing whether substitutions would change the binding affinity of the bisboronic acid sensors for diols parallel to that of the monoboronic acid unit. Therefore, fluorescence experiments were conducted to determine the appropriate binding constants of **25-27** and **29-31** for various sugars. Since the anthracene-based compounds are fairly

lipophilic, a 1:1 mixture of methanol and phosphate buffer (pH 7.4) was used as the solvent with a sensor concentration of about 1×10^{-6} M. The sugars studied include glucose, fructose, and galactose. As expected, upon sugar addition, all three substituted glucose sensor analogs (**25-27**) showed dramatically increased fluorescence intensity. Figure 1.6 shows two typical sets of fluorescent spectral changes upon sugar addition using compound **25-27** as examples. It has been proposed in literature that the increase in fluorescence intensity for such anthracene based boronic acids upon addition of a saccharide was due to increased B-N bond strength upon sugar binding, which in turn resulted in reduced fluorescence quenching by photoinduced electron transfer (PET).[10] Whereas we have established a different mechanism, the hydrolysis mechanism, for the increase in the fluorescence intensity upon addition of a sugar. The hydrolysis mechanism will be discussed in detail in Chapter 2. One would expect these new analogs to have a similar mechanism in inducing the fluorescent changes upon sugar binding, although this was not specifically studied.

With the four analogs of dianthraceneboronic acid in hand, the cyano-substituted compound **25** showed the highest change in fluorescence intensity with a 10-fold increase upon glucose addition. It also showed the highest binding affinity with an apparent binding constant (K_a) of 2540 M^{-1} for glucose (Table 1.1). It is interesting to see that the nitro-substituted compound (**26**) showed the lowest fluorescent intensity changes (a maximum of 2 fold), while having the second highest affinity for glucose (1808 M^{-1}). The fluoro-substituted analog (**27**) showed only 4-fold fluorescent intensity change with a binding constant (630 M^{-1}) that is even smaller than that of the parent compound (**10a**,

1472 M^{-1}). The binding of these bisboronic acids was compared with that of the corresponding monoboronic acid analogs (**29-31**, Table 1.2)**.** It is interesting to note that the cyanophenylboronic acid compound (**25**) also showed much higher affinity than either the nitro (**26**) or fluoro (**27**) substituted ones. Therefore, the results of the bisboronic acids parallel that of the monoboronic acids in this case.

a)

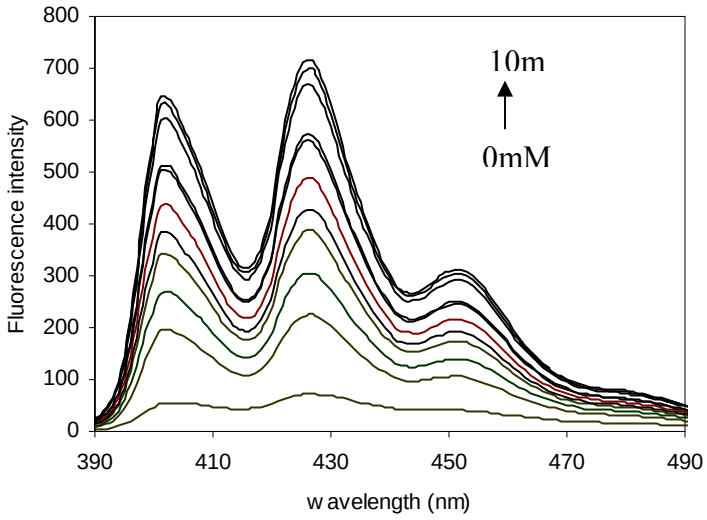

b)

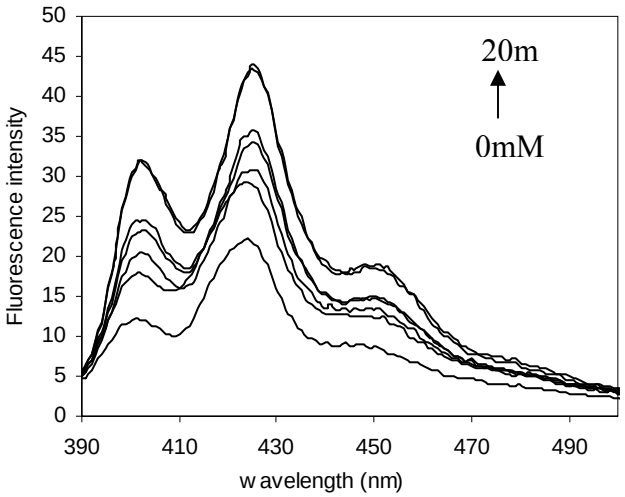

Figure 1.6. a) Fluorescence spectra of **25** (1.0×10^{-6} M) with D-glucose (0 mM-10 mM); b) Fluorescence spectra of **26** (1.0×10^{-6} M) with D-glucose (0 mM-20 mM) at 25 ^{o}C in 50% MeOH/0.1 M aqueous phosphate buffer at pH 7.4: λ_{ex} = 370 nm.

The comparison between the nitro and fluoro-substituted compounds did not yield the same conclusions. In the monoboronic acid series, the nitro and fluoro-substituted boronic acids (**30** and **31**) had similar affinities for both fructose and glucose. On the other hand, in the bisboronic acid series, the nitro-substituted compound (**26**) showed a much higher affinity than the fluoro-substituted one (**27**). It is also worth noting that the fluoro-substituted bisboronic acid has an even lower affinity than that of the unsubstituted control (**10a**). Such results were somewhat unexpected because fluoro-substitution is electron-withdrawing. Furthermore, the size of the fluorine atom is small and one would not expect much perturbation of the conformation of the bisboronic acid compound by the fluorine atom. Consequently, one would expect **27** to have a higher affinity for glucose than does **10a**.

The results of the selectivity studies were also somewhat surprising. Sensor **25**, although having the highest affinity for glucose, showed the lowest selectivity with a 3-fold preference for glucose over fructose in terms of the binding constants. This is in direct contrast to the 43-fold selectivity of **10a** for the same pair of sugars.[22] Compounds **26** and **27** were somewhere in between. In comparison with the monoboronic acids, it seems that the cyano-substituted one has a low selectivity problem too, only in this case it was the selectivity for fructose. Such results could mean that the cyano-substituted boronic acids have a lower propensity to discriminate among different sugars. However, the underlying reason for this is not clear.

Table 1.1. Binding Constant (K_a) for compounds **25-27** and **10a** with different saccharides

Compound	K_a (M^{-1}) glucose	K_a (M^{-1}) fructose	K_a (M^{-1}) galactose	Selectivity $K_{a\ glucose}/K_{a\ fructose}$	Fluorescence intensity changes for glucose
25	2540 ± 90.1	968 ± 126.6	271 ± 37.5	3	10-fold increase
26	1808 ± 130.6	198 ± 32.8	132 ± 60.5	9	2-fold increase
27	630 ± 48.6	42 ± 7.2	46 ± 6.6	15	4-fold increase
10a	1472	34	30	43	7-fold increase

Table 1.2. Binding Constant (K_a) for monoboronic acids **29-31** and **10b** with different saccharides

Compound	Ka (M^{-1}) fructose	Ka (M^{-1}) glucose	Selectivity $K_{a\ fructose}/K_{a\ glucose}$	Fluorescence intensity changes for fructose
29	1350 ± 68.4	101 ± 5.2	13	2.3-fold increase
30	714 ± 51.3	40 ± 4.0	18	2-fold increase
31	650 ± 29.2	26 ± 8.3	25	2.3-fold increase
10b	940	50	18	2- fold increase

Overall, the results indicate that the substituent effect on monoboronic acids can only be partially translated into the same kind effect when used for the preparation of bisboronic acid compounds. Other factors such as conformational changes may also need to be considered in designing analogs aimed at optimizing the affinity and selectivity of the interested sensors.

There is one additional point that is worth discussing, *i.e.,* why the substituent electron-withdrawing ability did not correlate with the apparent binding constants of the monoboronic acids (**10b**, and **29-31**) (Tables 1 and 2). As has been reported previously, the apparent binding constant of a particularly boronic acid can be affected by several factors including (1) the pKa values of the boronic acid and the diol, (2) the optimal pH for a particular complexation reaction, (3) steric factors, (4) the concentration and nature of the buffer, (5) whether trivalent interaction is involved, and (6) other idiosyncratic factors that have not been identified.[19] Among these factors, a shift of the optimal pH

away from 7.4 to a lower pH is most likely the reason for the diminished intrinsic affinity of **29** and **30** for diols at pH 7.4 compared with the un-substituted one (**10b**). Similar examples have been reported before, especially with boronic acids that have a very low pKa value.[19]

1.5. Conclusions

Three new fluorescent anthracene-based bisboronic sensors (**25-27**) and three monoboronic fluorescent sensors (**29-31**) were synthesized. Both cyano- (**25**) and nitro-substituted (**26**) sensors had higher apparent binding constant for glucose (*K* 2540 M^{-1} and 1808 M^{-1} respectively) than the parent sensor (**10a**) (1472 M^{-1}). Whereas fluoro-substituted bisfluoroboronic acid (**27**) had a lower apparent binding constant (*K* 630M^{-1}) but it has the most appropriate affinity and selectivity for glucose sensing under physiological conditions. The selectivity between glucose and fructose did diminish for all the new sensors (**25-27**) compared to **10a**. The monoboronic acid series sensors (**29-31**) also showed similar trend in the affinity for saccharides compared with their bisboronic acid analogs. Again, monofluoroboronic acid sensor (**31**) had the lowest binding constant but showed a greater selectivity (25 fold) than **29** for fructose over glucose. Overall, the introduction of an electron-withdrawing group does not always directly translate into enhanced affinity, and the affinity of the bisboronic sensors only partially tracks that of the monoboronic building blocks. The effect of the electron-withdrawing group in the selectivity of the bisboronic acid sensors is hard to predict.

1.6. Palladium catalyzed synthesis of sterically hindered arylboronic esters

1.6.1. Contributions

The goal of this project was to study the new borylating agent (bis(neopentyl glycolato)diboron) for the palladium catalyzed synthesis of hindered arylboronic acid. In this methodology study 12 ortho substituted boronic esters were synthesized. Dr. Hao Fang synthesized 7 boronic esters and I synthesized 5 boronic esters. Detailed synthesis of boronic esters that I performed will be given with full characterization.

1.6.2. Introduction

Generally, two methods are used to synthesize arylboronic acid or ester compounds. One is the transmetalation between an arylmetal and a boron halide or alkoxide;[53] the other is the recently developed $PdCl_2$(dppf)-catalyzed borylation of aryl halides,[54] triflates[55, 56] and diazonium[57, 58]with a tetra(alkoxy)diboron [54, 55, 57] or dialkoxyborane reagent.[56, 59] The palladium-catalyzed method can be used for the borylation of substrates that contain functional groups such as cyano, nitro, amino, hydroxyl, ester and carbonyl groups, which may not be compatible with organometallic agents such as *n*-butyllithium. Currently, bis(pinacolato)diboron (**32**) is the most widely used agent in palladium mediated borylation reactions due to its commercial availability and good stability in the presence of water and during chromatography.[60]

In the synthesis of boronic esters, many problems were encountered when bis(pinacolato)diboron was used as the borylation agent. For example, complicated reaction mixtures were obtained in the preparation of *ortho*-methoxy-substituted phenylboronic acid, which led to low yields (about 20%).[61] Similar results have also been

reported in the literature,[54]although a few exceptions were reported when aryltriflates were used instead of arylhalides.[55] Baudoin and coworkers utilized pinacolborane $(Me_4C_2O_2)BH$ to synthesize phenylpinacol boronic esters from *ortho*-substitued aryl bromides and found the best catalyst being $Pd(OAc)_2$ in the presence of 2-(dicyclohexyl phosphino)biphenyl which is a sterically hindered phosphine ligand,[59] although the yields were still poor when functional groups such as nitro (20%), acetyl (0%), and Boc protected amino group (40%) were present. Later Miyaura's group reported that $Pd(dba)_2/PCy_3$ could be used to carry out borylation of some *ortho*-substituted chloroarenes (nitro and methoxy) by using bis(pinacolato)diboron (70% yield based on GC after 48 hours of reaction).[62] Most recently, a new *N*-heterocyclic carbene-palladium catalyst was used to borylate *ortho*-methoxy substituted aryldiazonium with good yields using bis(pinacolato)diboron.[58]

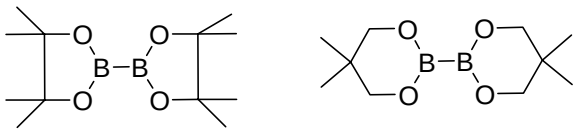

32 **33**

Figure 1.7. Bisborylating agents (a) bis(pinacolato)diboron (b) bis(neopentylglycolato)diboron

So far, research in this area has been focused on examining the effect of different leaving groups or designing or experimenting new palladium catalysts. We envisioned that some of the problems might be overcome by manipulating the steric bulkiness of the borylation agent. In our very first example, we examined the borylation of 2-methoxy-5-

nitrophenylbromide using the new commercially available bis(neopentyl glycolato)diboron **33** in the presence of $PdCl_2$(dppf) and observed much improved yield compared with the reaction using bis(pinacolato)diboron as the borylation agent (72% vs. 20%) under similar conditions (Scheme 1.7.). Such results suggested that the steric bulkiness of the tetra(alkoxy)diboron agent may play an important role in the borylation of other *ortho*-substitutent arylhalide (bromide in this case) and a less hindered bis(neopentyl glycolato)diboron might be used to overcome the side reaction problems associated with the use of sterically bulky bis(pinacolato)diboron.

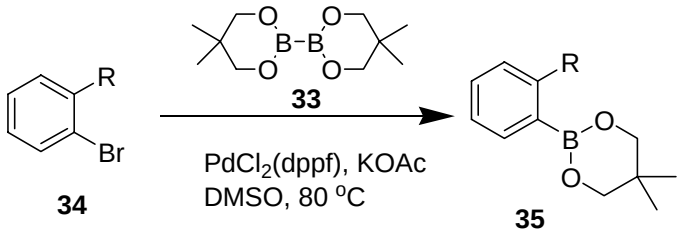

Scheme 1.7. General synthesis route to neopentyl protected boronic ester

1.6.3. Synthesis of ortho-substituted aryl boronic esters

In order to understand the scope of the effect of the steric bulkiness of the borylation agent, we were interested in examining the borylation of a series *ortho*-substituted arylhalides. As a first step, we optimized the reaction conditions with respect to the solvent and base used. As expected and has been observed with reactions using the bis(pinacolato)diboron borylation agent, DMSO was the best solvent and KOAc was the best base. Toluene and dioxane exhibited low reaction rate with more debromo product. The reaction did not work when using triethylamine as base.

The borylation of 12 additional arylhalides were studied using this method (entry 2-13, Table 1.3). In most cases, the reaction was completed within 4 hours. Good (65%) to excellent (90%) yields were obtained in most cases except with 8-quinoline analog (entry 9, 35%), 2-bromophenol (entry 11, 5%), and 2-bromobenzaldehyde (entry 13, 7%). Unexpectedly, borylation of Boc protected 2-bromoaniline (entry 3) gave the deprotected aniline neopentyl glycolato boronate. The mechanism through which the Boc group was cleaved is unclear. Comparing with literature and our own research results, the yields were much better than the reactions using bis(pinacolato)diboron or pinacolborane as the borylating agent. For example, *ortho*-bromonitrobenzene (entry 4) and 2-bromomethylphenylketone (entry 8) gave yields in the range of 0-20% when pinacolborane was used as the borylating agent.[59] Even when the corresponding iodoarene was used for the nitrobenzene analog, the yield was still low (44%).[59] In contrast, the corresponding reactions using bis(neopentyl glycolato)diboron as the borylation agent gave over 68% isolated yields for both nitro (entry 4) and acetyl substituent (entry 8).

Table 1.3. Representative Reactions

Entry	**1**		Product **3**		Time (h)	**3** (%)[a]
1	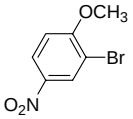	**34a**	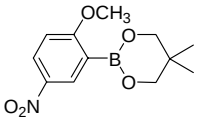	**35a**	2	72
2	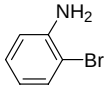	**34b**	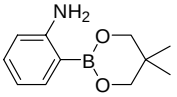	**35b**	2	69
3	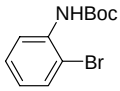	**34c**	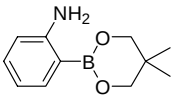	**35b**	4	65
4	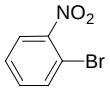	**34d**	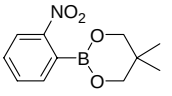	**35d**	3	68
5	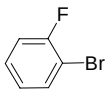	**34e**	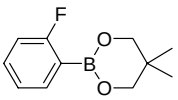	**35e**	4	(90)
6	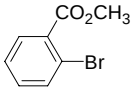	**34f**	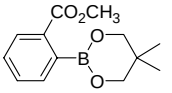	**35f**	4	80
7	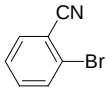	**34g**	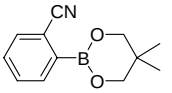	**35g**	6	73
8	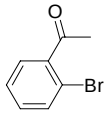	**34h**	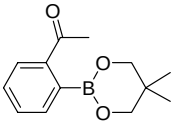	**35h**	3	70
9	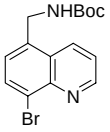	**34i**	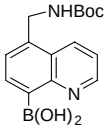	**35i**	12	35
10	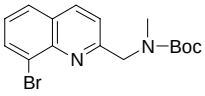	**34j**	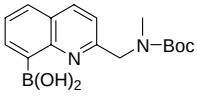	**35j**	12	85
11	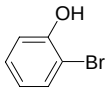	**34k**	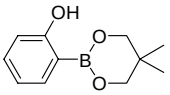	**35k**	12	5
12	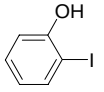	**34l**	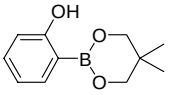	**35k**	8	70
13	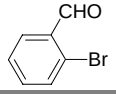	**34 m**	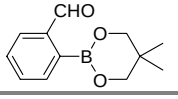	**35 m**	12	7

[a] isolated yield after flash chromatography. Yields in parentheses are GC yields.

On a somewhat different note, where steric hindrance may not necessarily be a factor, the borylation of quinoline bromide also benefited from using bis(neopentyl glycolato)diboron instead of bis(pinacolato)diboron as the borylation agent. For example, in the borylation of 8-bromoquinoline derivatives (Entries 9 and 10), Suzuki coupling product was the major product when bis(pinacolato)diboron was used as a borylation agent in the presence of KOAc.[63] However, when bis(neopentyl glycolato)diboron was used, Suzuki coupling product was not formed in the reaction mixture and the corresponding 8-quinoline boronic acid was easily obtained.

It does need to be noted that entry 13 (with a formyl substituent) gave less than 10% yield of the desired product with the formation of 20% Suzuki coupling product and the recovery of 50% of the starting material. In addition, entry 11 (hydroxyl group) gave only 5% yield of the desired product with over 85% of the starting material recovered, while the corresponding iodide (entry 12) gave a good yield (70%). It is not clear why the hydroxyl group (entry 11) and the formyl group (entry 13) presented special problems. In an effort to improve the yields for entries 11 and 13, we also examined whether different catalysts would be able to facilitate these two reactions. Previous work in the Baudoin[59] and Miyaura groups[62] indicates that a more reactive palladium catalyst may be able to improve yield of entry 11. Several air stable and more active palladium catalysts, such as $[(t\text{-Bu})_2\text{P(OH)}]_2\text{PdCl}_2$ (POPd), $\{[(t\text{-Bu})_2\text{P(OH)}][(t\text{-Bu})_2\text{P(O}^-)]\text{PdCl}\}_2$ (POPd1), and $[(t\text{-Bu})_2\text{P(OH)PdCl}_2]_2$ (POPd2), have been employed for cross-coupling reactions of aryl chloride,[64-66] and also for borylation of 5-bromofluorescein diacetate.[67] Therefore,

the new active palladium catalyst, POPd, was examined in the borylation of 2-bromophenol and 2-bromobenzaldehyde.

Different palladium catalysts and solvents were examined in order to search for a condition that would give a reasonable borylation yield from 2-bromophenol (Table 1.4). The results showed that the POPd facilitates the borylation reaction and works better than $Pd(PPh_3)_4$ and $PdCl_2(dppf)$ in DMSO (entries 1-3). When the temperature was raised to 120 °C, 40% of the desired borylation product was obtained, with the remaining portion being the un-reacted starting material (entry 4). When the solvent was changed to toluene and dioxane, the debromo product (**36**) was the main product (entries 6 and 7). Therefore, it seems that for the borylation of 2-bromophenol using POPd in DMSO at 120 °C gives the best yield. When applying the same conditions to the borylation of 2-bromobenzaldehyde, the starting material completely disappeared with the formation of 35% (isolated yield) of the desired borylation product and the remaining being the Suzuki coupling product

Table 1.4. Different Palladium Catalysts in the Borylation of 2-bromophenol and 2-bromobenzaldehyde

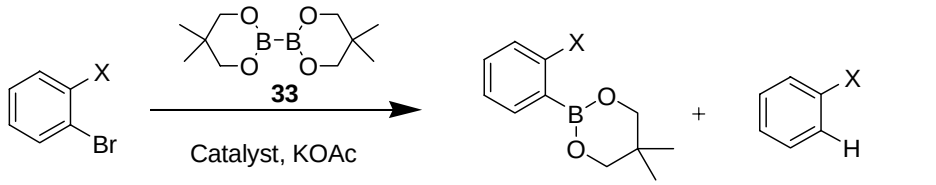

34 k X = -OH
m X = -CHO

35 k X = -OH
m X = -CHO

36 k X = -OH
m X = -CHO

Entry	Catalyst	Solvent	Heating method (temp. °C, time)	Product ratio **34k**:**35k**:**36k**[a]
1	$Pd(PPh_3)_4$ (6%mol)	DMSO	100, 12h	100:0:0

2	$PdCl_2$(dppf) (6% mol)	DMSO	100, 12h	93:7:0
3	POPd (3% mol)	DMSO	80, 12h	78:22:0
4	POPd (3% mol)	DMSO	120, 12h	60:40:0
5	POPd (3% mol)	DMF	80, 12h	74:27:0
6	POPd (3% mol)	Toluene	80, 12h	0:27:73[b]
7	POPd (3% mol)	Dioxane	80, 12h	0:10:80[b]

[a]Determined by GC-MS
[b]Determined by ^{1}H-NMR

1.7. Conclusions

Palladium catalyzed borylation of arylbromide is a very convenient way for the preparation of arylboronic acids. However commonly used borylation reagent, bis(pinacolato)diboron, gives low yields and side reactions for *ortho*-substituted bromoarenes, possibly due to the steric hinderance presented by the *ortho* substitutent. This problem can be overcome by using a less hindered borylation agent, bis(neopentyl glycolato)diboron, in most of cases. With the two cases (*ortho* substituent being a hydroxyl or a formyl group) that give low yields of the borylation product, the problem can be addressed by using a new and more active palladium catalyst, such as POPd.

1.8. Experimental

1.8.1. General Procedures

All air- and water sensitive reactions were performed under dry Nitrogen in oven dried glassware. Commercially available reagents were used without additional purification unless otherwise indicated. Dichloromethane was distilled from CaH_2. THF was distilled from sodium and benzophenone.

Analytical thin layer chromatography (TLC) was performed with Scientific Adsorbents plastic-baked TLC silica gel 60 F hard layer plates. TLC plates were

visualized with UV light (254 nm) or with 5% (w/v) solutions of phosphomolybidic acid in ethanol. Flash chromatography was performed with Scientific Adsorbents silica gel (flash 32-63 nm).

Mass spectrometry (MS) analyses were performed by the Mass Spectrometry Laboratories of Georgia State University. ^{1}H and ^{13}C NMR spectra were recorded at 75 MHz and 100 MHz. Chemical Shifts (δ) are given in ppm relative to TMS for ^{1}H spectra and relative to residual solvent for ^{13}C spectra.

1.8.2. Fluorescence Binding Study Procedure

Fluorescence measurents were used to determine the bidning between boronic acid (BA) and saccharide. Fluorescence polarization is a measure of rotatational relaxation time, so upon binding of a small molecule to a large molecule the fluorescene polarization of small molecule changes which in turn reflects the relaxation time of the large molecule. This effect indicates the binding event. The relationship between fluorescence intensity change and the equilibrium constant can be expressed using equation 1. At sufficiently low concentration where a plot of ΔI_f vs. concentration sugar complex is linear:

$$\Delta I_f = 1 + K_1 [\text{Sugar}] \qquad \text{Equation 1}$$

A plot of $1/\Delta I_f$ vs $1/[\text{Sugar}]$ gives K_1= intercept / slope

A Shimadzu RF-5301PC fluorometer was used for all the fluorescent studies. For a typical fluorescent measurement, a 2 mL of sensor stock solution in methanol (2.0×10^{-6} M) was mixed with 2 mL of saccharide solution in 0.1 M of phosphate buffer (pH 7.4) at various concentrations. The apparent pH was checked with pH meter and

corrected if necessary. The mixture was allowed to mix for 20 min and fluorescence intensity was recorded. Triplicate measurements were taken for each sugar. The correlation coefficients for all determinations in fitting the 1:1 model were over 0.98.

1.8.3. General Procedure for the Synthesis of Arylboronates

A mixture of palladium catalyst (0.03eq), potassium acetate (3eq), bis(neopentyl glycolato)diboron (1.2eq) and arylbromide was added to a flask in a glove box under anhydrous condition. After addition of anhydrous DMSO (8 mL/mmol), the mixture was stirred at 80 ^{0}C several hours checked by TLC. The reaction solution was cooled to room temperature and poured into ice-water. The mixture was extracted with ethyl acetate and the combined organic layers was washed with saturated brine, dried over $MgSO_4$, and concentrated *in vacuo*. The residue was purified by flash column chromatography to give the corresponding arylboronates.

1, 10-Diexpoxide-anthracene (**12**). The preparation followed the literature procedure.[52] A stirred suspension of anthraquione (4.0 g, 1mmol) and sodium hydride (2.2 g, 2.5 mmol) in ahydrous DMSO was added dropwise to a solution of trimethylsulfonium iodide (11.0 g, 2.5 mmol) in anhydrous DMSO at room temperature over a period of 30 min and stirred for another 3h. The mixture was filtered and the filtrate was poured into 350 ml ice water. The mixture was allowed to stand for 2h, and then the precipitate was washed with water and dried under vacuum at 45 ^{o} C overnight giving the diexpoxide in 92 % yield with no further purification. ^{1}HNMR (300 MHz, $CDCl_3$) δ: 3.25 (4H, s), 7.38 (8H, d, J = 1.2 Hz) ppm, was in agreement with the literature data.[52]

10-Hydroxymethyl-anthracene-9-carbaldehyde (**13**). Compound **12** (3.3 g, 1mmol) was added to stirred solution of lithium bromide (19.3 g, 5 mmol) in dry CH_3CN, and the mixture was stirred at 60 ^{o}C in the dark for 16h and then was cooled to -40 ^{o}C in a dry ice-acetonitrile bath. The resulting product were collected by filtration, washed with water, and dried overnight under vacuum to give **13** in 94% yield. ^{1}HNMR (300 MHz, $CDCl_3$) δ: 5.67 (2H, s), 7.64 (4H, m), 8.54 (2H, d, *J* = 8.4 Hz), 8.87-8.89 (2H, q, *J* = 1.5, 6 Hz), 11.47 (1H, s) ppm, was in agreement with the literature data.[52]

10-Methylaminomethyl-anthracen-9-yl)-methnaol (**14**). An aqeous solution of methylamine (40% wt, 25 mL) was added to the solution of compound **13** (0.48 g, 1mmol) in MeOH (10 mL) and THF (5 mL) and stirred at room temperature for 16h. To the stirred mixture was added sodium borohydride (0.39 g, 5 mmol). The solution was stirred for another 30 min. After solvent evaporation, the resulting solid was dissolved in EtOAC (10 mL). The solution was washed with water (2 x 20 mL) and brine (20 mL), dried over MgSO4 and concentrated. The resulting crude product was purified with silica gel column with eluent of MeOH/CH_2Cl_2 to give compound **14** in 95 % yield. ^{1}HNMR (300 MHz, $CDCl_3$) δ: 2.68 (3H, s), 4.69 (2H, s), 5.67 (2H, s), 7.55 (4H, m), 8.40-8.46 (4H, m) ppm, was in agreement with the literature data.[36]

(**10-Hydroxymethyl-anthracene-9-ylmethyl)-methyl-carbamic acid *tert*-butyl ester** (**15**). Compound 9 (0.49 g, 1mol), di-tert-butyl dicarbonate (2.5 g, 2.5 mmol) and triethylamine (5 mL) were mixed in MeOH (30 mL), and the mixture was stirred at room temperature for 30 min. After removal of the solvent, the resulting residue was dissolved in DCM (10 mL). The solution was washed with water (3 x 10 mL), and saturated brine

(15 mL), dried over $MgSO_4$ and concentrated. The resulting compound was dried under vacuum to give **15** in 94 % yield. ^{1}HNMR (300 MHz, $CDCl_3$) δ: 1.57 (13H, s), 2.48 (3H, s) 5.50 (2H, s), 5.70 (2H, s), 7.59-7.52 (4H, m), 8.50-8.42 (4H, m) ppm, was in agreement with the literature data.[36]

(**10-Formyl-anthracene-9-ylmethyl**)**-carbamic acid *tert*-butyl ester** (**16**). Compound **15** (0.64 g, 1 mmol) was dissolved in the mixture of dry DMSO (10 mL) and triethylamine (15 mL). To the solution was added the solution of pyridine sulfur trioxide (1.76g, 6 mmol) dissolved in dry DMSO (5 mL) over period of 30 min, and then was poured into ice water (200 mL). The mixture was extracted with EtOAc (3 x 20 mL), dried over MgSO4 and concentrated. The resulting solid gave **16** in 99 % yield. ^{1}HNMR (300 MHz, $CDCl_3$) δ: 1.56 (9H, s), 2.50 (3H, s), 5.56 (2H, s), 7.64-7.25 (4H, m), 8.53 (2H, d, J = 8.4 Hz), 8.91 (2H, d, J = 9.6 Hz), 11.51 (1H, s) ppm, was in agreement with the literature data.[36]

Methyl-(10-methylaminomethyl-anthracen-9-ylmethyl)-carbamic acid tert-butyl ester (**17**). Compound **16** (0.61 g, 1 mmol) was dissolved in THF (10 mL) and MeOH (20 mL). To this solution was added an aqueous solution of methylamine (40%, wt, 20 mL), and the resulting reaction mixture was then stirred at room temperature under N_2 for 12h. Sodium borohydride (0.33 g, 5 mmol) was added, and the reaction mixture was stirred for 30 min. The mixture was concentrated and dissolved in CH_2Cl_2. The solution was washed with water (2 x 10 mL) and brine (20 mL), dried over $MgSO_4$ and concentrated. The resulting crude product was purified on silica column, eluting with CH_2Cl_2/MeOH (20/1), giving compound **17** in 74% yield. ^{1}HNMR (300 MHz, $CDCl_3$) δ:

1.56 (9H, s), 2.48 (3H, s), 2.70 (3H, s), 4.72 (2H, s), 5.51 (2H, s), 7.25-7.58 (4H, m), 8.38-8.42 (4H, dd, *J* = 2.4, 1.2 Hz) ppm, was in agreement with the literature data.[36]

Boc-protected diamides (**18**). Compound **17** (0.73 g, 1 mmol), was added to a solution of (2-Carboxymethyl-phenyl)-acetic acid (0.19 g, 0.5 mmol), 1-(2-diemthyl-aminopropyl)-3-ethylcarbodiimide hydrochloride (EDC· HCl, 0.77 g, 2 mmol), (HOBT, 0.27g, 1 mmol), (DMAP, 49 mg, 0.2 mmol), TEA (200 μL) in dry CH_2Cl_2 (60 mL), and the mixture was stirred at room temperature at room temperature under N_2 for 12h. The solution was washed with 10% citric acid (10 mL), and water (2 x 20 mL), and was dried over $MgSO_4$ and concentrated under *vacuo.* The residue was purified on silica gel column, eluting with Hexane/EtOAc (1/1) to give **18** in 54% yield. ^{1}HNMR (300 MHz, $CDCl_3$) δ: 1.59 (22H, s), 2.27 (6H, s), 2.36 (6H, s), 3.71 (4H, s), 5.46 (4H, s), 5.66 (4H, s), 7.27 (4H, s), 7.49 (8H, t, *J* = 8.1 Hz), 8.42 (8H, t, *J* = 7.2 Hz) ppm, was in agreement with the literature data.[36]

4-Fluoro-2-methyl-boronic acid (**22**). Commercially available 1-bromo-4-fluoro-2-methyl-benzene **21** (1.02 g, 1mmol) was dissolved in dry THF (15 ml) and treated with *n*-BuLi (2M in pentane, 1.3 mmol) at -78 ^{o}C for 1 hour under N_2. Trisopropyl borate (1.62 ml, 1.3 mmol) was added drop wise into the flask and reaction was mixed for overnight at room temperature. The reaction was treated with 1*N* HCl (20 mL) for 1 hour and extracted with ethyl acetate (3 x 10 mL), and was dried over $MgSO_4$ and concentrated under *vacuo* to give free boronic acid **17** in 75 % yield. ^{1}HNMR (400 MHz, $CDCl_3$) δ: 2.42 (3H, d, *J* = 36.8 Hz), 6.81- 6.92 (2H, m), 7.25-7.45 (1H, t(t), *J* = 7.6 Hz) ppm, was in agreement with the literature data.[68]

2-(4-Fluoro-2-methyl-phenyl)-5-methyl-[1,3,2] dioxaborinane (**23**). Compound **22** (0.64 g, 1 mmol) and neopentyl glycol (0.52 g, 1.2 mmol) were mixed in toluene and refluxed for 18 hours in a Dean-Stark setup. Reaction was cooled to room temperature and solvent was evaporated. Crude product was chromatographed on silica column using hexane-ethyl acetate as eluent to give **23** in 83%. ^{1}HNMR (300 MHz, $CDCl_3$) δ: 1.03 (6H, s), 2.51 (3H, s), 3.76 (4H, s), 6.81(2H, m), 7.88 (1H, t, *J* = 6.9 Hz) ppm, was in agreement with the literature data.[68]

2-(2-Bromomethyl-4-fluoro-phenyl)-5,5-dimethyl-[1,3,2]dioxaborinane (**24**).

Compound **23** (0.66g, 1mmol) was brominated in the presence of NBS (0.58g, 1.1mmol) and catalytic amount of AIBN (10mg) and refluxed in benzene for 18 hours. Crude product was chromatographed on silica column using hexane-ethyl acetate as eluent to give **24** in 68%. ^{1}HNMR (300 MHz, $CDCl_3$) δ: 1.09 (6H, s), 3.84 (4H, s), 4.94 (2H, s), 7.02 (1H, t, *J* = 8.4 Hz), 7.10-7.15 (1H, dd, *J* = 2.4, 7.5 Hz), 7.88 (1H, t, *J* = 6.9 Hz) ppm, was in agreement with the literature data.[68]

(**25**)**.** BOC protected diamide compound **18** (127 mg, 14 mmol) was dissolved in 4ml dry DCM and 2 ml of trifluoroacetic acid (TFA) was added to the flask. Reaction was stirred for 30min at rt and solvent was removed and dried under vacuum. The deprotected product, **19** (156mg, 0.50 mmol), potassium carbonate (175 mg, 1.27 mmol) and KI (6 mg) was dissolved in dried acetonitrile and mixed for 12 hours at rt. Solvent was removed and resulted yellow precipitate was dissolved in (10 ml) DCM and 5ml 10% $NaHCO_3$ and stirred for 1 hour at rt. The organic phase was washed with water (2 × 10ml), and dried over $MgSO_4$ and solvent was removed *in vacuo*. The resulted residue

was re-precipitated from DCM-ether to give **25** in 39%. ^{1}HNMR (400 MHz, CD_3OD) δ: 2.37 (6H, s), 2.63 (6H, s), 3.81 (4H, s), 4.22 (4H, s), 5.06 (4H, s), 5.74 (4H, s), 7.24 (4H, s), 7.57 (9H, t, *J* = 8.8 Hz), 7.83 (4H, d, *J* = 7.2 Hz), 8.31 (4H, d, *J* = 7.6 Hz), 8.45 (4H, d, *J* = 8 Hz) ppm. HRMS (ESI+): calcd for $C_{62}H_{58}B_2N_6O_6$: 1005.4663; found: 1005.4663. We were unable to remove cleaved neopentyl glycol, in order to confirm the structure; the boronic acid was oxidized in the presence of acetic acid/water (1:1) and H_2O_2 to obtain pure NMR. ^{1}HNMR (400 MHz, CD_3Cl_3) δ: 2.41 (6H, s), 2.64 (6H, s), 3.81 (8H, s), 4.71 (4H, s), 5.72 (4H, s), 6.66 (2H, d, *J* = 8.4Hz), 7.23 (6H, s), 7.34-7.32 (3H, dd, *J* = 2, 6.4 Hz), 7.54 (4H, t, *J* = 8.8 Hz), 7.63 (4H, t, *J* = 6.4 Hz) 8.44 (8H, q, *J* = 9.2, 12 Hz) ppm. ^{13}C NMR (100 MHz, $CDCl_3$) δ: 22.58, 29.62, 33.37, 39.35, 41.85, 53.59, 59.52, 102.32, 116.85, 119.12, 122.84, 124.37, 124.76, 125.28, 125.64, 126.26, 126.42, 127.32, 128.55, 129.98, 130.52, 130.89, 131.17, 132.22, 132.42, 132.98, 133.12, 134.42, 161.58, 170.77 ppm. HRMS (ESI+): calcd for $C_{62}H_{56}N_6O_4$: 949.4442; found: 949.4479.

(**26**)**.** The procedure was same as the preparation of **25** from **18.** Yield (20%). ^{1}HNMR (400 MHz, $CD_3OD/CDCl_3$) δ: 2.37 (6H, s), 2.63 (6H, s), 3.80 (4H, s), 4.21 (10H, s), 5.73 (4H, s), 7.23 (4H, s), 7.56 (6H, t, *J* = 8.0 Hz), 7.86 (2H, d, *J* = 8.0 Hz), 8.07 (2H, s), 8.12 (2H, d, *J* = 8 Hz) 8.30 (4H, d, *J* = 8.4 Hz) 8.43 (4H, d, *J* = 8.4 Hz) ppm. HRMS (ESI+): calcd for $C_{60}H_{58}B_2N_6O_{10}$: 1045.4479; found: 1045.4523. We were unable to remove cleaved neopentyl glycol, in order to confirm the structure; the boronic acid was oxidized in the presence of acetic acid/water (1:1) and H_2O_2 to obtain pure NMR. ^{1}HNMR (400 MHz, $CDCl_3$) δ: 2.44 (6H, s), 2.64 (6H, s), 3.80 (4H, s), 3.88 (4H, s), 4.73 (4H, s), 5.72 (4H, s), 6.64 (2H, d, *J* = 6 Hz), 7.26 (3H, s), 7.52 (4H, t, *J* = 8 Hz), 7.62 (4H, t, *J* = 6.8

Hz), 7.87 (2H, s), 7.95-7.93 (4H, dd, *J* = 2.4, 2.4 Hz), 8.41 (4H, t, *J* = 10 Hz) ppm. ^{13}C NMR (100 MHz, $CDCl_3$) δ: 29.71, 33.48, 39.36, 41.66, 42.01, 53.50, 59.39, 116.17, 121.81, 124.36, 124.65, 125.22, 125.32, 126.36, 126.57, 127.44, 128.38, 130.04, 130.82, 131.10, 134.35, 140.05, 163.70, 170.74 ppm. HRMS (ESI+): calcd for $C_{60}H_{56}N_6O_8$: 989.4238; found : 989.4252.

(**27**)**.** The procedure was same as the preparation of **25** from **18,** but the hydrolysis was done in solution of acetone and water (1:4) in total volume of 150 ml and 1N HCl (10 ml). The reaction was stirred vigorously for 1hour at rt. The organic phase was washed with water (2 × 10ml), and dried over $MgSO_4$ and solvent was removed *in vacuo*. The resulted residue was re-precipitated from DCM-ether to give **27** in 20%. ^{1}HNMR (400 MHz, $CD_3OD/CDCl_3$) δ: 2.21 (6H, s), 2.42 (6H, s), 3.72 (4H, s), 4.11 (4H, s), 4.60 (4H, s), 5.68 (4H, s), 7.09 (4H, q, *J* = 8.4, 9.6 Hz), 7.24 (4H, s), 7.48 (8H, s), 7.68 (2H, s), 8.27 (4H, s), 8.42 (4H, d, *J* = 6.4 Hz) ppm. HRMS (ESI+): calcd for $C_{60}H_{58}B_2F_2N_4O_6$- H_2O: 973.4483; found: 973.4464. We were unable to remove cleaved neopentyl glycol, in order to confirm the structure; the boronic acid was oxidized in the presence of acetic acid/water (1:1) and H_2O_2 to obtain pure NMR. ^{1}HNMR (400 MHz, $CDCl_3$) δ: 2.34 (6H, s), 2.61 (6H, s), 3.79 (8H, s), 4.67 (4H, s), 5.29 (4H, s), 6.62 (2H, q, *J* = 4.4, 4.8 Hz), 6.71 (2H, dd, *J* = 2.8 Hz), 6.77 (2H, d, *J* = 2.8 Hz), 7.23 (4H, s), 7.52 (4H, t, *J* = 8.4 Hz), 7.60 (4H, t, *J* = 8.4 Hz), 8.40-8.42 (8H, dd, *J* = 2.4, 2.8 Hz) ppm. ^{13}C NMR (100 MHz, $CDCl_3$) δ: 29.71, 39.31, 41.66, 41.75, 53.59, 59.97, 114.78 (s (d_{C-F}), *J* = 14 Hz), 115.01 (s (d_{C-F}), *J* = 14 Hz), 116.49 (s (d_{C-F}), *J* = 8 Hz), 122.69, 122.75, 124.63, 125.19, 126.29, 127.42, 129.14, 129.58, 130.08, 130.85, 131.07, 134.38, 153.11, 157.15 (s (d_{C-F}), *J* =

220 Hz), 170.72 ppm. HRMS (ESI+) calcd for $C_{60}H_{56}F_2N_4O_4$: 935.4348 ; found: 935.4351.

2-[(Anthracen-9-ylmethyl-methyl-amino)-methyl]-4-cyano-boronic acid (**29**). Anthracen-9-ylmethyl-methyl-amine (120 mg, 0.54 mmol), **19** (183 mg, 0.60 mmol), potassium carbonate (299 mg, 2.17 mmol) and KI (7.2 mg) was dissolved in dried acetonitrile and mixed for 12 hours at rt. Solvent was removed and resulted yellow precipitate was dissolved in (10 ml) DCM and 5ml 10% $NaHCO_3$ and stirred for 1 hour at rt. The organic phase was washed with water (2 × 10ml), and dried over $MgSO_4$ and solvent was removed in vaccum. The resulted residue was re-precipitated from DCM-hexane to give **29** in 12%. ^{1}HNMR (300 MHz, $CDCl_3$) δ: 2.44 (3H, s), 4.23 (2H, s), 5.03 (2H, s), 7.55 (4H, m), 7.67 (1H, d, *J* = 7.8 Hz), 7.89 (1H, d, *J* = 7.5 Hz), 8.10-8.19 (4H, dd, *J* = 8.4 Hz), 8.59 (1H, s) ppm. ^{13}C NMR (100 MHz, $CDCl_3$) δ: 43.15, 51.55, 112.24, 119.33, 124.92, 125.88, 128.08, 128.34, 129.08, 129.32, 130.09, 131.00, 131.39, 131.72, 133.79, 144.71 ppm. HRMS (ESI+): calcd for $C_{24}H_{21}BN_2O_2$: 381.1774; found: 381.1774.

2-[(Anthracen-9-ylmethyl-methyl-amino)-methyl]-4-nitro-boronic acid (**30**). The procedure was same as the preparation of **29**. Yield (29%). ^{1}HNMR (400 MHz, $CDCl_3$) δ: 2.25 (3H, s), 4.54 (2H, s), 5.15 (2H, s), 7.58 (4H, m), 7.97 (1H, d, *J* = 8 Hz), 8.14 (2H, d, *J* = 8 Hz), 8.24-8.28 (4H, dd, *J* = 5.6, 6 Hz), 8.64 (1H, s) ppm. ^{13}C NMR (100 MHz, $CDCl_3$ / CD_3OD) δ: 42.29, 121.80, 124.24, 124.90, 126.08, 126.77, 128.57, 129.17, 131.38, 131.95, 135.88, 141.96, 143.07, 148.50 ppm. HRMS (ESI+): calcd for $C_{23}H_{21}BN_2O_4$: 401.1672; found: 401.1670.

2-[(Anthracen-9-ylmethyl-methyl-amino)-methyl]-4-fluoro-boronic acid (**31**). The procedure was same as the preparation of **29**. Yield (53%). ^{1}HNMR (300 MHz, CD_3OD) δ: 2.24 (3H, s), 3.98 (2H, s), 4.57 (2H, s), 7.06 (2H, m), 7.42-7.44 (4H, dd, *J* = 2.7, 3.3 Hz), 7.79 (1H, s), 7.94-8.00 (4H, dd, *J* = 3, 13.2 Hz), 8.39 (1H, s) ppm. ^{13}C NMR (100 MHz, $CDCl_3$ / CD_3OD) δ: 38.39, 61.24, 112.81 (s (d_{C-F}), *J* = 18 Hz), 115.52 (s (d_{C-F}), *J* = 19 Hz), 122.32, 123.64, 125.38, 127.84, 128.28, 130.01, 130.16, 134.69, 141.96, 162.69 (s (d_{C-F}), *J* = 243 Hz) ppm. HRMS (ESI+): calcd for $C_{23}H_{21}BFNO_2$: 374.1727; found: 374.1717.

2-(2-fluorophenyl)-5,5-dimethyl-1,3,2-dioxaborinane (**35e**).

^{1}HNMR (400 MHz, $CDCl_3$) δ: 1.03 (6H, s), 3.79 (4H, s), 6.99 (1H, t, *J* = 9.2, 9.6 Hz), 7.11 (1H, t, *J* = 7.6 Hz), 7.37 (1H, m), 7.72 (1H, t) ppm. ^{13}C NMR (100 MHz, $CDCl_3$) δ: 21.86, 31.81, 72.45, 115.45 (s (d_{C-F}), *J* = 24Hz), 123.48 (s (d_{C-F}), *J* = 3 Hz), 132.55 (s (d_{C-F}), *J* = 8 Hz), 136.21 (s (d_{C-F}), *J* = 8 Hz), 165.90, 168.38 ppm. GCMS (EI): calcd for $C_{11}H_{14}BFO_2$: 208; found: 208.

Methyl 2-(5,5-dimethyl-1,3,2-dioxaborinan-2-yl)benzoate (**35f**).

^{1}HNMR (300 MHz, $CDCl_3$) δ: 1.13 (6H, s), 3.82 (4H, s), 3.94 (3H, s), 7.40 (1H, s), 7.53 (2H, d, *J* = 2.7 Hz), 7.79 (1H, s), 7.95 (1H, d, *J* = 7.8 Hz) ppm. ^{13}C NMR (100 MHz, $CDCl_3$) δ: 22.07, 31.82, 52.35, 72.54, 128.42, 128.64, 131.36, 131.96, 132.84, 169.09 ppm. GCMS (EI): calcd for $C_{13}H_{17}BO_4$: 247; found: 247.

1-(2-(5,5-dimethyl-1,3,2-dioxaborinan-2-yl)phenyl)ethanone (**35h**). ^{1}HNMR (400 MHz, $CDCl_3$) δ: 1.13 (6H, s), 2.61 (3H, s), 3.81 (4H, s), 7.41 (2H, d, *J* = 1.2 Hz), 7.54 (2H, d, *J* = 4.8 Hz), 7.82 (1H, d, *J* = 7.6 Hz) ppm. ^{13}C NMR (100 MHz, $CDCl_3$) δ:

22.22, 38.39, 25.61, 31.84, 72.57, 128.40, 128.47, 131.37, 132.67, 140.12, 200.70 ppm. GCMS (EI): calcd for $C_{13}H_{17}BO_3$: 232; found: 232.

2-(5,5-dimethyl-1,3,2-dioxaborinan-2-yl)benzaldehyde (**35m**). ^{1}HNMR (300 MHz, $CDCl_3$) δ: 1.10 (6H, s), 3.83 (4H, s), 7.56 (2H, m), 7.82 (1H, d, *J* = 6.9 Hz), 7.93 (1H, d, *J* = 6.0 Hz), 10.47 (1H, s) ppm. ^{13}C NMR (100 MHz, $CDCl_3$) δ: 22.26, 25.65, 31.89, 72.62, 128.45, 128.53, 131.41, 131.75, 140.39, 200.10 ppm. GCMS (EI): calcd for $C_{12}H_{15}BO_3$: 217; found: 217.

References

1. Fukuda, M., *Cell Surface Carbohydrates and Cell Development*. ed.; CRC Press: Boca Raton, 1992; 'Vol.' p.

2. Fukuda, M.; Hindsgaul, O., *Molecular Glycobiology*. ed.; Oxford University Press: New York, 1994; 'Vol.' p 1-52.

3. Gabius, H.-J.; Gabius, S., *Lectins and Glycobiology*. ed.; Springer-Verlag: New York, 1993; 'Vol.' p.

4. Garegg, P. J.; Lindberg, A. A., *Carbohydrate Antigens*. ed.; American Chemical Society: Washington, D.C., 1993; 'Vol.' p.

5. Hakomori, S., Traveling for the Glycosphingolipid Path. *Glycocon. J.* **2000,** 17, 627-647.

6. Pickup, J. C.; Williams, G., *Textbook of Diabetes*. 2nd ed.; Blackwell Science,: Malden, MA, USA, 1997; 'Vol.' p.

7. Fang, H.; Yan, J.; Wang, B., Boronolectins and Fluorescent Boronolectins-An Examination of the Detailed Chemistry Issues Important for their Design. *Med. Res. Rev.* **2005,** 25, in press.

8. Yang, W.; Gao, X.; Wang, B., Boronic Acid Compounds as Potential Pharmaceutical Agents. *Med. Res. Rev.* **2003,** 23, 346-368.

9. Yang, W.; Gao, S.; Wang, B., Biologically Active Boronic Acid Compounds. In *Organoboronic Acids*, ed.; Hall, D., 'Ed.'^'Eds.' John Wiley and Sons: New York, 2005; 'Vol.' p^pp 481-512.

10. James, T. D.; Sandanayake, K. R. A. S.; Iguchi, R.; Shinkai, S., Novel Saccharide-Photoinduced Electron Transfer Sensors Based on the Interaction of Boronic Acid and Amine. *J. Am. Chem. Soc.* **1995,** 117, 8982-8987.

11. Eggert, H.; Frederiksen, J.; Morin, C.; Norrild, J. C., A New Glucose-selective Fluorescent Bisboronic Acid. First Report of Strong α-Furanose Complexation in Aqueous Solution at Physiological pH. *J. Org. Chem.* **1999,** 64, 3846-3852.

12. Wang, W.; Gao, S.; Wang, B., Building Fluorescent Sensors by Template Polymerization: The Preparation of a Fluorescent Sensor for D-Fructose. *Org. Lett.* **1999,** 1, 1209-1212.

13. Yoon, J.; Czarnik, A. W., Fluorescent Chemosensors of Carbohydrates. A Means of Chemically Communicating the Binding of Polyols in Water Based on Chelation-Enhanced Quenching. *J. Am. Chem. Soc.* **1992,** 114, 5874-5875.

14. Arimori, S.; Bosch, L. I.; Ward, C. J.; James, T. D., Fluorescent Internal Charge Transfer (ICT) Saccharide Sensor. *Tetrahedron Lett.* **2001,** 42, 4553-4555.

15. Yang, W.; He, H.; Drueckhammer, D. G., Computer-Guided Design in Molecular Recognition: Design and Synthesis of a Glucopyranose Receptor. *Angew. Chem. Int. Ed* **2001,** 40, 1714-1718.

16. Wang, W.; Gao, X.; Wang, B., Boronic Acid-based Sensors for Carbohydrates. *Curr. Org. Chem.* **2002,** 6, 1285-1317.

17. Lorand, J. P.; Edwards, J. O., Polyol Complexes and Structure of the Benzeneboronate Ion. *J. Org. Chem.* **1959,** 24, 769.

18. Springsteen, G.; Wang, B., A Detailed Examination of Boronic Acid-Diol Complexation. *Tetrahedron* **2002,** 58, 5291-5300.

19. Yan, J.; Springsteen, G.; Deeter, S.; Wang, B., The Relationship among pKa, pH, and Binding Constants in the Interactions between Boronic Acids and Diols-It is not as Simple as It Appears. *Tetrahedron* **2004**, in press.

20. Arimori, S.; Bell, M. L.; Oh, C. S.; Frimat, K. A.; James, T. D., Modular Fluorescence Sensors for Saccharides. *J. Chem. Soc., Perkin Trans. 1* **2002**, 803-808.

21. Appleton, B.; Gibson, T. D., Detection of total sugar concentration using photoinduced electron transfer materials: development of operationally stable, reusable optical sensors. *Sens. Actuator. B-Chem.* **2000,** 65, 302-304.

22. Karnati, V. V.; Gao, X.; Gao, S.; Yang, W.; Ni, W.; Sankar, S.; Wang, B., A Glucose-Selective Fluorescence Sensor Based on Boronicacid-Diol Recognition. *Bioorg. Med. Chem. Lett.* **2002,** 12, (23), 3373-3377.

23. Cao, H. S.; Heagy, M. D., Fluorescent Chemosensors for Carbohydrates: A decade's worth of Bright Spies for Saccharides in Review. *J. Fluorescence* **2004,** 14, 569-584.

24. Gray Jr., C. W.; Houston, T. A., Boronic Acid Receptors for x-Hydroxycarboxlates: High Affinity of Shinkai's Glucose Receptor for Tartrate. *J. Org. Chem.* **2002,** 67, 5426-5428.

25. Mulla, H. R.; Agard, N. J.; Basu, A., 3-Methoxycarbonyl-5-nitrophenyl boronic acid: high affinity diol recognition at neutral pH. *Bioorg. Med.Chem.Lett* **2004,** 14, 25-27.

26. James, T. D.; Sandanayake, K. R. A. S.; Shinkai, S., Chiral Discrimination of Monosachrides Using a Fluorescent Molecular Sensor. *Nature (London)* **1995,** 374, 345-347.

27. Cao, H.; Diaz, D. I.; DiCesare, D.; Lakowicz, J. R.; Heagy, M. D., Monoboronic Acid Sensor That Displays Anomalous Fluorescence Sensitivity to Glucose. *Org. Lett.* **2002,** 4, 1503 -1505.

28. Rusin, O.; Alpturk, O.; He, M.; Escobedo, J. O.; Jiang, S.; Dawan, F.; Lian, K.; McCarroll, M. E.; Warner, I. M.; Strongin, R. M., Macrocycle-Derived Functional Xanthenes and Progress Towards Concurrent Detection of Glucose and Fructose. *J. Fluorescence* **2004,** 14, 611-615.

29. Cabell, L. A.; Monahan, M.-K.; Anslyn, E. V., A Competition Assay for Determining Glucose-6-phosphate Concentration with a Tris-Boronic Acid Receptor. *Tetrahedron Lett.* **1999,** 40, 7753-7756.

30. Gao, S.; Wang, W.; Wang, B., Building Fluorescent Sensors for Carbohydrates Using Template-directed Polymerizations. *Bioorg. Chem.* **2001,** 29, 308-320.

31. Lavigne, J. J.; Anslyn, E. V., Teaching Old Indicators New Tricks: A Colorimetric Chemosensing Ensemble for Tartrate/Malate in beverages. *Angew. Chem. Int. Ed.* **1999,** 38, 3666-3669.

32. Norrild, J. C.; Eggert, H., Evidence for Mono- and Bisdentate Boronate Complexes of Glucose in the Furanose Form. Application of $^{1}J_{C\text{-}C}$ Coupling Constants as a Structural Probe. *J. Am. Chem. Soc.* **1995,** 117, 1479-1484.

33. Norrild, J. C.; Eggert, H., Boronic Acids as Fructose Sensors. Structure Determination of the Complexes Involved Using $^{1}J_{(CC)}$ Coupling Constants. *J. Chem. Soc. Perkin Trans. 2* **1996**, 2583-2588.

34. Shinkai, S.; Takeuchi, M., Molecular Design of Artificial Sugar Sensing Systems. *Trend in Anal. Chem.* **1996,** 15, 188-193.

35. Wiskur, S. L.; Lavigne, J. L.; Ait-Haddou, H.; Lynch, V.; Chiu, Y. H.; Canary, J. W.; Anslyn, E. V., pKa Valuaes and Geometries of Secondary and Tertiary Amines Complexed to Boronic Acids-Implications for Sensor Design. *Org. Lett.* **2001,** 3, 1311-1314.

36. Yang, W.; Gao, S.; Gao, X.; Karnati, V. R.; Ni, W.; Wang, B.; Hooks, W. B.; Carson, J.; Weston, B., Diboronic Acids as Fluorescent Probes for Cells Expressing Sialyl Lewis X. *Bioorg. Med. Chem. Lett* **2002,** 12, 2175-2177.

37. Paugam, M. F.; Bien, J. T.; Smith, B. D.; Chrisstoffels, L. A. J.; deJong, F.; Reinhoudt, D. N., Facilitated Catecholamine Transport Through Bulk and Polymer-Supported Liquid Membranes. *J. Am. Chem. Soc.* **1996,** 118, 9820-9825.

38. Westmark, P. R.; Gardiner, S. J.; Smith, B., Selective Monosaccharide Transport through Lipid Bilayers Using Boronic Acid Carriers. *J. Am. Chem. Soc.* **1996,** 118, 11093-11100.

39. Riggs, J. A.; Hossler, K. A.; Smith, B. D.; Karpa, M. J.; Griffin, G.; Duggan, P. J., Nucleotide Carrier Mixture with Transport Selectivity for Ribonucleoside-5'-phosphates. *Tetrahedron Lett.* **1996,** 37, 6303-6306.

40. Draffin, S. P.; Duggan, P. J.; Duggan, S. A. M., Highly Fructose Selective Transport Promoted by Boronic Acids Based on a Pentaerythritol Core. *Org. Lett.* **2001,** 3, 917-920.

41. Gardiner, S. J.; Smith, B. D.; Duggan, P. J.; Karpa, M. J.; Griffin, G. J., Selective Fructose Transport Through Supported Liquid Membranes Containing Diboronic Acid or Conjugated Monoboronic Acid- Quaternary Ammonium Carriers. *Tetrahedron* **1999,** 55, (10), 2857-2864.

42. Smith, B. D.; Gardiner, S. J.; Munro, T. A.; Paugam, M. F.; Riggs, J. A., Facilitated Transport of carbohydrates, Catecholamines, and Amino Acids Through Liquid and Plasticized Organic Membranes. *J. Incl. Phenom. Mol. Recogn. Chem.* **1998,** 32, 121-131.

43. Wulff, G.; Vesper, W., Preparation of Chromatographic Sorbents with Chiral Cavities for Racemic Resolution. *J. Chromatography* **1978,** 167, 171-186.

44. Wulff, G., Molecular Recognition in Polymers Prepared by Imprinting with Templates. In *Polymeric Reagents and Catalysis*, ed.; Ford, W. T., 'Ed.'^'Eds.' ACS: Washington, D.C., 1986; 'Vol.' p^pp 186-230.

45. Liu, X.; Hubbard, J.; Scouten, W., Synthesis and structural investigation of two potential boronate affinity chromatography ligands. *Journal of Organometallic Chemistry* **1995,** 493, 91-94.

46. Psotova, J.; Janiczek, O., Boronate Affinity-Chromatography and the Applications. *Chem. Listy* **1995,** 89, 641-648.

47. Singhal, R. P.; Ramamurthy, B.; Govindraj, N.; Sarwar, Y., New Ligands for Boronate Affinity-Chromatography - Synthesis and Properties. *J. Chromatogr.* **1991,** 543, (1), 17-38.

48. Soundararajan, S.; Badawi, M.; Kohlrust, C. M.; Hageman, J. H., Boronic Acids for Affinity-Chromatography - Spectral Methods for Determinations of Ionization and Diol-Binding Constants. *Anal. Biochem.* **1989,** 178, (1), 125-134.

49. Bielecki, M.; Eggert, H.; Norrild, J. C., A Fluorescent Glucose Sensor Binding Covalently to All Five Hydroxy Groups of α-D-Glucose. A Reinvestigation. *J. Chem. Soc., Perkin Trans. 2* **1999**, 449-455.

50. James, T. D.; Sandanayake, K. R. A. S.; Shinkai, S., Novel Photoinduced Electron-transfer Sensor for Saccharides Based on the Interaction of Boronic Acid and Amine. *Chem. Commun.* **1994**, 477-478.

51. Ni, W.; Kaur, G.; Springsteen, G.; Wang, B.; Franzen, S., Regulating the Fluorescence Intensity of an Anthracene Boronic Acid System: A B-N Bond or a Hydrolysis Mechanism? *Bioorgan. Chem.* **2004,** 32, 571-581.

52. Lin, Y.-i.; Lang, S. A.; Seifert, C. M.; Child, R. G.; Morton, G. O.; Fabio, P. F., Aldehyde Syntheses. Study of the Preparation of 9,10-Anthracenedicarboxaldehde. *J. Org. Chem.* **1979,** 44, (25), 4701-4705.

53. Miyaura, N.; Maruoka, K., *Synthesis of Organomettallic Compounds*. ed.; Wiley: New York, 1997; 'Vol.' p.

54. Ishiyama, T.; Murata, M.; Miyaura, N., Palladium(0)-catalyzed cross-coupling reaction of aloxydiboron with haloarenes: a direct procedure for arylboronc esters. *J. Org. Chem.* **1995,** 60, 7508-7510.

55. Ishiyama, T.; Itoh, Y.; Kitano, T.; Miyaura, N., Synthesis of arylboronates via the palladium(0)-catalyzed cross-coupling reaction of tetra(alkoxo)diborons with aryltriflates. *Tetrahedron. Lett.* **1997,** 38, 3447-3450.

56. Murata, M.; Oyama, T.; Watanabe, S.; Masuda, Y., Palladium-catalyzed borylation of aryl halides or triflates with dialkoxyborane: a novel and facile synthetic route to arylboronates. *J. Org. Chem.* **2000,** 65, 164-168.

57. Willis, D. M.; Strongin, R. M., Palladium-catalyzed borylation of aryldiazonium tetrafluoroborate salts. A new synthesis of arylboronic esters. *Tetrahedron. Lett.* **2000,** 41, 8683-8686.

58. Ma, Y.; Song, C.; Jiang, W.; Xue, G.; Cannon, J. F.; Wang, X.; Andrus, M. B., Borylation of Aryldazoium Ions with N-Heterocylclic Carbene-Palladium Catalysts Formed without Added Base. *Org. Lett.* **2003,** 5, 4635-4638.

59. Baudoin, O.; Guenard, D.; Gueritte, F., Palladium-catalyzed borylation of ortho-substituted pheyl halides and application to the one-pot synthesis of 2,2'-disubstituted biphenyls. *J. Org. Chem.* **2000,** 65, 9268-9271.

60. Ishiyama, T.; Miyaura, N., Chemistry of Group 13 element-transition metal linkage-the platinum and palladium-catalyzed reactions of (alkoxo)diborons. *J. Organomet. Chem.* **2000,** 611, 392-402.

61. Ni, W.; Fang, H.; Springsteen, G.; Wang, B., The Design of Boronic Acid Spectroscopic Reporter Compounds by Taking Advantage of the pKa-Lowering Effect of Diol Binding: Nitrophenol-Based Color Reporters for Diols. *J. Org. Chem.* **2004,** 69, 1999-2007.

62. Ishiyama, T.; Ishihara, K.; Miyaura, N., Synthesis of Pinacol Arylboronates via Cross-coupling Reaction of Bis(pinacolato)diboron with Chloroarenes Catalyzed by Palladium(0)-tricylcohexylphosphine Complex. *Tetrahedron. Lett.* **2001,** 57, 9813-9816.

63. Fang, H.; Yan, J.; Wang, B., Biaryl Product Formation from Cross-coupling in Palladiumcatalyzed Borylation of a Boc Protected Aminobromoquinoline Compound. *Molecules* **2004,** 9, 178-184.

64. Li, G. Y., *Angew. Chem. Int. Ed.* **2001,** 40, 1513-1516.

65. Li, G. Y., Highly Active, Air-Stable Palladium Catalysts for the C-C and C-S Bond-Forming Reactions of Vinyl and Aryl Chlorides: Use of Commercially Available [(t-Bu)2P(OH)]2PdCl2, [(t-Bu)2P(OH)PdCl2]2, and [[(t-Bu)2PO-P-(t-Bu)2]PdCl]2 as Catalysts. *J. Org. Chem.* **2002,** 67, 3643-3650.

66. Li, G. Y.; Zheng, G.; Noonan, A. F., Highly Active, Air-Stable Versatile Palladium Catalysts for the C-C, C-N, and C-S Bond Formations via Cross-Coupling Reactions of Aryl Chlorides. *J. Org. Chem.* **2001,** 66, 8677-8681.

67. Han, J. W.; Castro, J. C.; Burgess, K., Microwave-assisted functionalization of bromo-fluorescein and bromorhodamine derivatives. *Tetrahedron. Lett.* **2003,** 44, 9359–9362.

68. Stones, D.; Manku, S.; Lu, X.; Hall, D., Modular Solid-Phase Synthetic Approach to Optimize Structural and Electronic Properties of Oligoboronic Acid Receptors and Sensors for the Aqueous Recognition of Oligosaccharides. *Chem. Eur. J.* **2004,** 10, 92-100.

Chapter 2. Regulating the fluorescence intensity of an anthracene boronic acid System: A B-N bond or a hydrolysis mechanism?

Abstract*:* An anthracene-based fluorescent boronic acid system developed by the Shinkai group as mentioned in Chapter 1 has been widely used for the preparation of fluorescent sensors for carbohydrates. Such application is based on the significant fluorescence intensity increase of this system upon binding with a carbohydrate. The mechanism through which this fluorescence intensity change happens was originally proposed to go through a B-N bond formation mechanism, which masks the nitrogen lone pair electrons. However, our own fluorescence studies suggest a possible alternative mechanism for the fluorescence changes upon the formation of a boronic acid (**1a**) complex with diols. In this new proposed mechanism, complex formation induces solvolysis, which results in the protonation of the amine nitrogen if the reactions are carried out in a protic solvent such as water at physiological pH. This protonation prevents the photoinduced electron transfer, resulting in reduced quenching of the anthracene fluorescence and increased fluorescence. Such a solvolysis mechanism is supported by evidence from various types of experiments and theoretical calculations. This study for the first time establishes a detailed mechanism of the fluorescence intensity changes of the anthracene boronic acid system (**1a**), which has been misunderstood for the last decade.

2.1. Contributions

This chapter includes both theoretical data as well as experimental data for the study. Dr. Weijuan Ni performed and collected theoretical data (section 2.10) and her work has been included in this chapter as further evidence in support of our proposed mechanism (hydrolysis mechanism).

2.2. Introduction

Due to the unique strong interactions between boronic acids and diols through reversible ester formation, there has been a great deal of interest in using boronic acids as the recognition moiety for the development of fluorescent and color sensors,[1-16] carbohydrate transporters,[17-22] and chromatographic stationary materials.[23-26] Various fluorescent boronic acid compounds that show fluorescent intensity/wavelength changes upon binding with diols to varying degrees have been developed. [1, 27-29] Critical to the development of boronic acid-based fluorescent sensors is the availability of fluorescent reporter compounds that change fluorescence intensities upon binding to a diol.[10, 29-31] In this regard, the Shinkai group, based on what was reported by Wulff earlier,[32] has made some of the most important contributions by taking advantage of the fluorescence/color modulation effect of an amino group positioned in a 1,5 relationship to the boron atom of a boronic acid moiety. One specific example is an anthracene-based fluorescent boronic acid compound (**1a**, Scheme 2.1), which shows significant fluorescence intensity changes upon diol binding.[9, 27] It is well known that the nitrogen lone pair electrons can quench anthracene fluorescence through photoelectron transfer (PET). Therefore, compound **1a** is only weakly fluorescent at physiological pH. Due to the proximity of the amine to the

boron atom, a B-N bond can be formed leading to a five-membered ring (**1b**) at neutral pH. Because diol binding often increases the Lewis acidity of the boron atom,[28, 33, 34] carbohydrate binding has been proposed to result in the strengthening of the B-N bond in **2b**, which makes the lone pair electrons less available for fluorescence quenching through PET. The hypothesis was that B-N bond strengthening results in decreased fluorescence quenching and increased fluorescence intensities in **2b**. The same concept has been the inspiration for the development of many other fluorescence or color boronic acid reporter compounds.[10, 31, 35] We have also applied the Shinkai system for the preparation of sensors for mono- and oligosaccharides [17] and studied the effects of B-N bond formation in such systems using density functional theory (DFT) methods. [36]

Although this system (**1a**) has worked very well as a fluorescent reporter compound, there are telltale signs that the mechanism through which such a system works may not have to involve B-N bond formation as originally proposed. For example, available crystal structures actually show a longer B-N bond for the ester than for the acid. The bond lengths of the ester [37] and acid [7] determined by X-ray crystallography are 1.754 Å and 1.669 Å, respectively. Furthermore, James and co-workers have shown that the fluorescence intensity of the sugar-**1b** complex is independent of the intrinsic pK_a of the boronic ester, which contradicts the B-N bond mechanism.[38] Because of the enormous role that molecule (**1a**) has played in the field of boronic acid-based sensor design, there is a need to better understand the mechanism through which the fluorescence intensity change occurs. An understanding of the mechanism will help the future design of improved sensors.

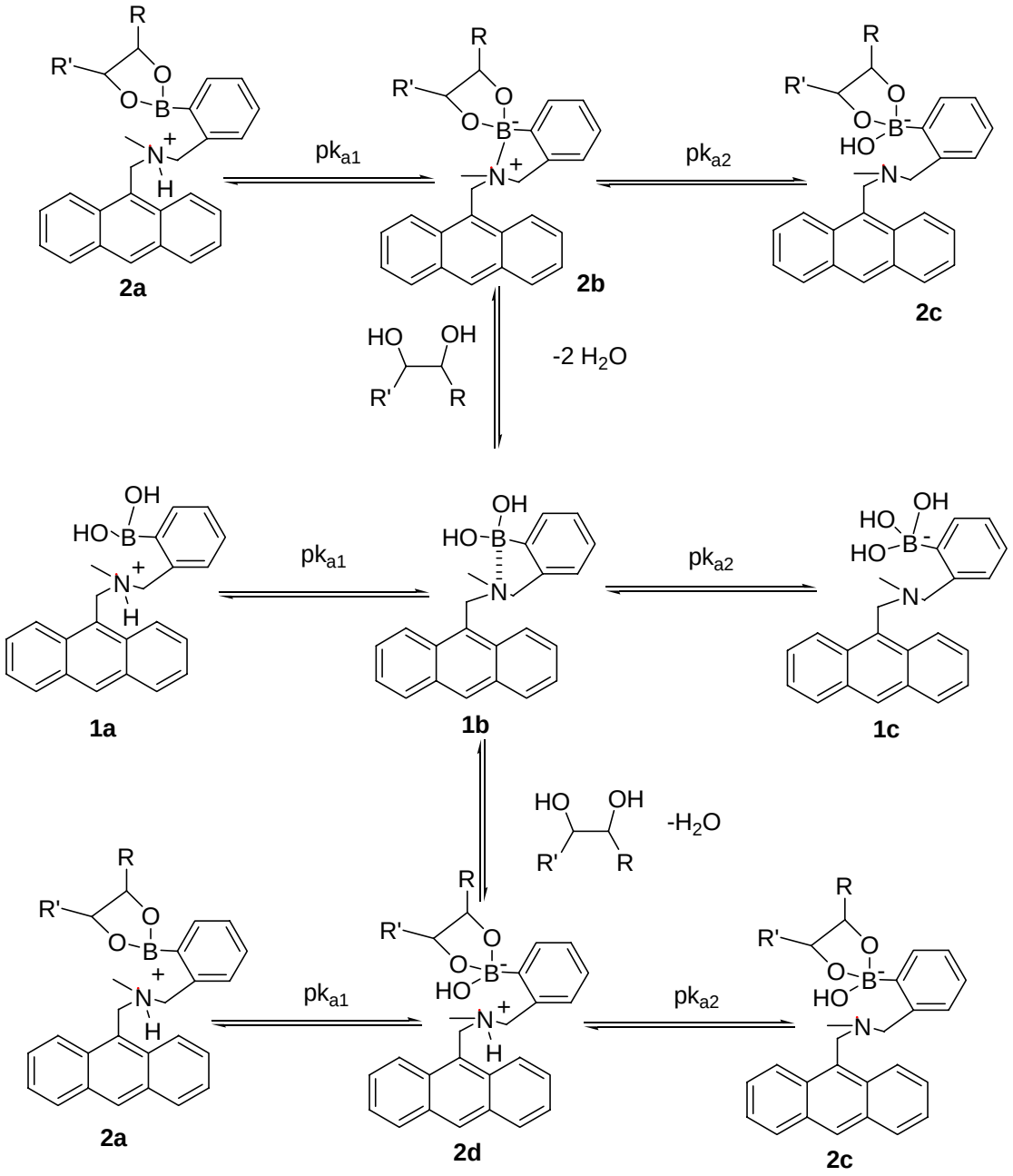

Scheme 2.1. Possible mechanisms for the fluorescence intensity changes

2.3. Experimental

All the reagents were purchased from Aldrich or Fisher/Acros and used as received. Anhydrous tetrahydrofuran (THF) was distilled from Na/benzophenone prior to use. Acetonitrile (CH_3CN) and dichloromethane (CH_2Cl_2) were distilled from CaH_2.

All pH values were determined with an Accumet 1003 Handhold pH/mV/Ion Meter (Fisher Scientific). A Shimadzu RF-5301 PC fluorometer was used for the fluorescence studies. The excitation wavelength was set at 370 nm. A Shimudzu UV-1601 spectrophotometer was used for the UV absorption studies.

Synthesis of model compound **1a** followed literature procedure.[9, 27]

2.4. Experimental Design, Results and Discussions

To analyze the possible mechanisms through which fluorescence intensity changes can occur, one can first write the different possible forms in which the boronic acid and the boronic acid-diol complex can exist. Boronic acid can exist in the protonated form when the pH is below its first pK_a (1a). There are ample literature results proving that the first pK_a is the deprotonation of the amine with the concomitant formation of a B-N bond (1b).[7] The formation of (1b) results in a significant fluorescence intensity decrease relative to (1a) despite the formation of the B-N bond.[9, 27] Such results indicate that B-N bond formation itself is not sufficient to "tie up" the lone pair electrons to prevent PET. With the further increase of the pH, the hydroxide comes in to displace the amino group to give 1c, which no longer has a B-N bond.

With the addition of the diol, there are two possible scenarios, neither of which had been experimentally proven or excluded at present before our studies, although we were the first one proposing the solvolysis mechanism. In the first scenario, pK_{a1} of the ester (2a) is the deprotonation of the amino group and the formation of the B-N bond (2b) as originally proposed by Shinkai and co-workers. The second pK_a is the replacement of the B-N bond by a B-O bond leading to the formation of 2c. In the second scenario, shown in the bottom of Scheme 2.1, the first pK_a is the addition of the hydroxide to the boron atom leading to the formation of 2d. The second pK_a is still the same, leading to the formation of 2c. The key difference between these two mechanisms is that under neutral conditions, addition of a diol will lead to the formation of 2b in one mechanism (referred to as the B-N bond mechanism) or 2d in the other. The latter will be referred to as the hydrolysis mechanism since going from 1b to 2d corresponds to a hydrolysis of the B-N bond as the boron forms a complex with a diol in 2d when the experiments are carried out in an aqueous medium.

In order to analyze existing literature data and to design experiments that can help to elucidate the mechanism, one has to analyze the possible experimental outcome under different experimental conditions for these two possible mechanisms. In Table 2.1, we have listed the expected experimental and/or computational outcomes that correspond to each of the mechanisms.

Table 2.1. Comparison of expected and observed phenomenon for the two different mechanisms in **Scheme 2.1.**

Phenomenon	**Expected results for the B-N bond mechanism**	**Expected results for the hydrolysis mechanism**	**Results observed**
Fluorescence intensity change associated with the first pK_a	Observable for both the acid (**1**) and the ester (**2**)	Observable only for the acid (**1**), not the ester (**2**)	Observable only for the acid (**1**)
Fluorescence intensity change associated with the second pK_a	Observable for both the acid (**1**) and the ester (**2**)	Observable only for the ester (**2**), not the acid (**1**)	Observable only for the ester (**2**)
Fluorescence intensity change in anhydrous solvent	Intensity should increase for ester	Intensity should decrease for ester	Intensity decrease for ester
Magnitude of fluorescence recovery with different sugars	Different	Same	Same
The effect of carbohydrates engaged in trivalent binding	Will not induce fluorescence intensity changes	Will induce fluorescence intensity changes	Fluorescence intensity changes observed
*B-N bond strength difference between the acid (**1**) and the ester (**2**)*	Very large	Small	Small[a]

[a]Computational results.

First, for the B-N bond formation mechanism (going from 2a to 2b to 2c) one would expect to see a significant fluorescence intensity decrease associated with both the first and second pK_a's since the deprotonation of the amino group and breaking the B-N bond are both expected to affect the availability of the lone pair electrons. However, in the hydrolysis mechanism (going from 2a to 2d to 2c) one would only expect to see a

significant fluorescence intensity change associated with the second pK_a since the first pK_a does not affect the protonation state of the amino group, and therefore does not affect the availability of the nitrogen lone pair electrons in the PET process.

Second, since binding with different diols may result in the lowering of the boron pK_a to different degrees,[28, 34] one would expect the B-N bond strength to be different in the boronic acid complexes with different sugars. This difference in B-N strength should be reflected in fluorescence intensity changes observed with addition of sugars if the B-N bond formation mechanism is at work. However, if the hydrolysis mechanism is at work, one would not expect to see a difference in the magnitude of the maximal fluorescence recovery.

Third, binding studies carried out in anhydrous organic solvent would cause fluorescence intensity to increase for the B-N bond mechanism due to formation of complex 2b. If the hydrolysis mechanism is in play, the fluorescence intensity would decrease because the lone pairs on the nitrogen are free to quench the fluorescence via PET.

Fourth, there are some sugars that are known to bind to boronic acid in a trivalent fashion. [5, 39, 40] If the B-N bond formation mechanism is the reason for the observed fluorescence intensity change, one would not expect these trivalent sugars to cause a fluorescence intensity increase because the trivalency prevents the B-N bond formation in the sugar-boronic acid complex (2c).

Fifth, if the strengthening of the B-N bond is the reason for the observed fluorescence intensity changes with this system, one would expect the B-N bond in the boronic acid-diol complex (2b) to be much stronger than in the free boronic acid (1b).

With these expected differences in mind, we examined these factors one by one, through experiments, computation and analysis of literature results. Fluorescent boronic acid **1a** was synthesized following the literature procedure.[27] Density functional theory (DFT) calculations were carried out using Dmol3 as described elsewhere.[36]

2.5. pH profiles of the acid (1a) and various complexes

We first examine the pH profile of 1a. Shinkai's original work has already shown that there is a significant decrease in fluorescence intensity associated with the first pK_a of the boronic acid (1a), but not the second one.[9, 27] We conducted the same experiments under similar conditions, and obtained similar results (Figure 2.1.). This decrease in fluorescence intensity associated with the first pK_a makes sense since it has been experimentally proven using a similar system that the first pK_a is the deprotonation of the amino group accompanied by B-N bond formation.[7] Deprotonation unmasks the nitrogen lone pair electrons and makes them available for PET. It should be noted that the "affinity" of a proton for an amine group has been estimated to be in the range of 200 kcal/mol.[41] This value may vary significantly depending on solvation and pK_a, but even if this "protonation affinity" is half of that number, it is still very strong, comparable to a sigma covalent bond, and higher than the energy required to remove an electron from amine nitrogen. On the other hand, the B-N strength is only a few kcal/mol,[36] which would not be able to "tie up" the nitrogen lone pair electrons nearly as effectively as

protonation does in order to prevent PET. Such reasoning weighs in favor of a key role for protonation of the amine rather than B-N bond formation as the trigger that alters the fluorescence intensity.

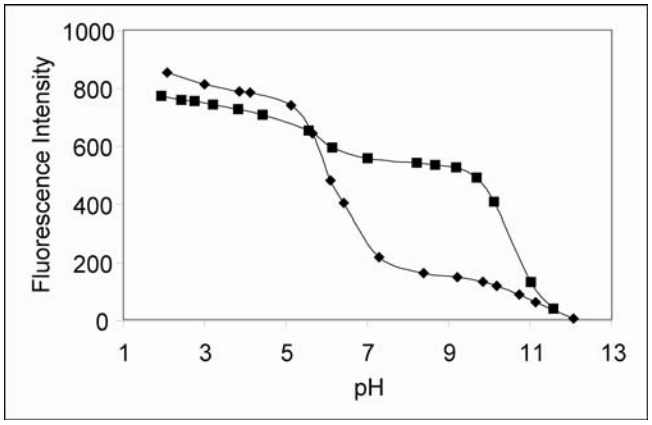

Figure 2.1. pH titration profile of sensor **1a** (2.25×10^{-6} M) at 25 °C in the presence (■) and absence (◆) of D-glucose (0.05 M).

Along these lines, it becomes easy to understand why there is only a very small fluorescence decrease associated with the second pK_a in the case of the free acid (1b) because breaking a ~3.6 kcal/mol B-N bond does not make much of a difference in the PET process. As shown in a previous study, there is only a small effect on the driving force for electron transfer or the reorganization energy. With the addition of a sugar such as glucose, the pH profile of the complex is different.[9, 27] The first pK_a of the complex (2a) is no longer associated with a large decrease in fluorescence intensity. This observation is not in agreement with the B-N bond mechanism since one would expect to see a fluorescence intensity decrease when the amine nitrogen goes from the protonated form to the B-N bond. However, if the hydrolysis mechanism is at work, the

observations can be very easily explained. In the boronic acid-diol complex, going from 2a to 2d does not involve the deprotonation of the amino group. Therefore, one would not expect to see a large fluorescence intensity change associated with the first pK_a of the complex (2a) in the hydrolysis mechanism. With the second pK_a, it is the deprotonation of the amino group that is the reason for the significant decrease in fluorescence intensity. Such a mechanism is also in agreement with the different results observed between the acid (1a) and complex (2a). The B-N interaction itself is not sufficiently strong to tie up the lone pair electrons to prevent PET, which is why the fluorescence intensity changes were observed for the first pK_a of the acid (1a), but not the ester (2a). These observations also agree with DFT calculations that indicate that fluorescence quenching will occur in the neutral B-N forms due to the reduction of the reorganization energy upon B-N bond formation (or strengthening).[36] The hydrolysis hypothesis also explains why fluorescence intensity changes were observed for the second pK_a of the ester (2d) and the first pK_a of the acid (1a) because again it is the deprotonation step that gives rise to fluorescence intensity changes.

2.6. Effect of anhydrous solvent on binding between sugar and 1a

To further study the protonation state of the amine, fluorescence study was conducted in the anhydrous acetonitrile. Since the amino group cannot be protonated in the absence of a protic solvent (the degree of protonation will be diminished, but not completely absence, if there is trace amount of water), experiments in an anhydrous solvent would allow us to probe the B-N bond effect on the fluorescent intensity of the system upon sugar binding. If the hydrolysis mechanism is the reason for fluorescent

intensity changes upon sugar addition in an aqueous environment, the addition of sugar in an anhydrous solvent would be expected to cause the intensity to decrease since the lone pair of electrons on the nitrogen become free upon sugar addition. Indeed, decrease in fluorescence intensity was observed with addition of sugar in the anhydrous condition (Figure 2.2). These results are consistent with the hydrolysis mechanism proposed in Scheme 2.1.

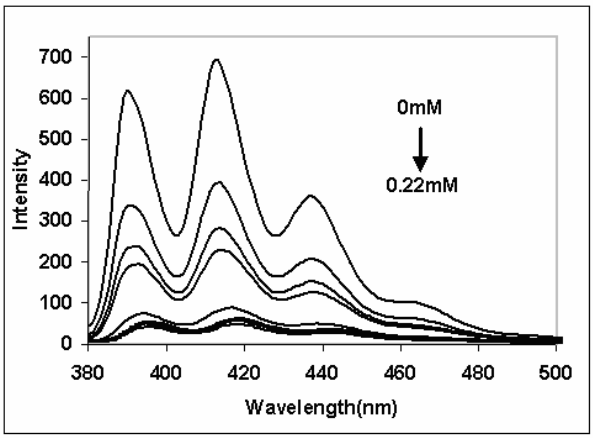

Figure 2.2. Fluorescence intensity changes upon the addition of cyclopentanediol to sensor **1a** (2.0×10^{-5} M) in anhydrous acetonitrile. Cyclopentanediol conc. (mM): 0, 0.007, 0.012, 0.03, 0.045, 0.061, 0.086, 0.113, and 0.225.

2.7. Effect of different sugars on the fluorescence intensity changes of 1a

It has been known for a long time that ester formation (2b) lowers the pK_a of the boron species to different degrees depending on the sugar/diol used.[28, 34] We have recently determined the apparent pK_a values of the phenylboronic acid-diol complex with various sugars/diols, and found that the apparent pK_a drops 2-4 pK_a units upon complexation.[28] For example, the apparent pK_a of phenylboronic acid is about 8.8. The

pK_a values (or more precisely the apparent pK_a's under the experimental conditions) of its fructose and glucose esters are 4.5 and 6.8 respectively. If the B-N bond mechanism is at work, one would expect that the fluorescence intensity of the boronic acid-diol complex to be dependent on the apparent pK_a of the boron. One would also expect to see as much change in fluorescence intensity when adding glucose to the free boronic acid and when replacing the glucose with fructose because their apparent pK_a separations (ΔpK_a) are about the same. In other words, the fluorescence intensity of the glucose complex should be much lower than that of the fructose complex because of the difference in their apparent pK_a. The same is true with the complex with other sugars. Aimed at studying the effect of various sugars on the fluorescence intensity of 1a, we examined the binding between 1a and fructose, glucose, sorbitol, and galactose, and found that these sugars gave about the same maximal fluorescence intensities at saturating concentrations (Figure 2.3). Such results are consistent with those obtained in an earlier study by James and co-workers [38] and cannot be explained by the B-N bond mechanism, but are consistent with the hydrolysis mechanism since the amine is in the same (protonated) state (2d) no matter which sugar/diol is added.

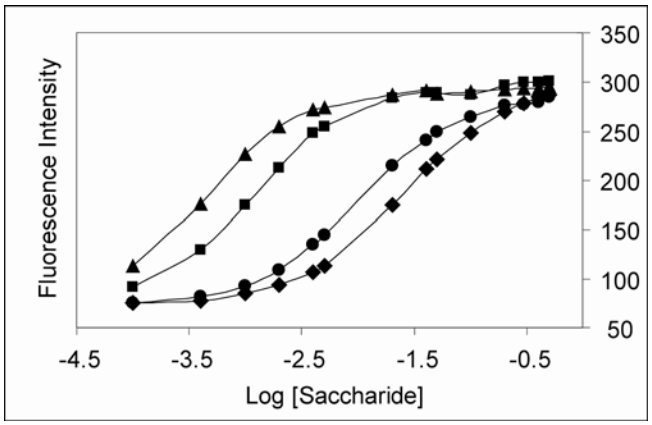

Figure 2.3. The effect of sorbitol (▲), fructose (■), galactose (●), and glucose (◆) on the fluorescence intensity of **1** (2.25×10^{-6} M)**.**

2.8. B-N bond strength

As has been alluded to in the pH profile studies, in order for the B-N to play a role in regulating the PET process two things have to happen.

First, the B-N bond needs to be so strong that it can "tie up" the lone pair electrons. This would mean that the B-N bond strength in the ester (2b) is on the same scale as the energy required transferring one nitrogen lone pair electron. The effect of protonation on the PET process serves as a good reference point. Using mass spectrometry, it has been determined that the proton affinity of an aniline amine is on the order of 215 kcal/mol.[41] However, the B-N bond strength has been estimated to be at about 3.6 kcal/mol using Density Functional Theory,[36] which is far smaller than what is required to tie up the nitrogen lone pair electrons to prevent PET.

Second, the B-N bond strength difference upon diol binding should be large compared to the B-N strength of the free acid (1b) in order to act as an on-off switch. Again, our theoretical calculation indicates that (1) the B-N bond in an ester (2b) is not much different from in the free acid (1b) form and (2) the change in bond strength upon ester formation is probably no more than 2 kcal/mol.[36] The first point would directly contradict a B-N bond mechanism. Even if there is an increase in B-N bond strength upon ester formation, such a small change is not expected to function as an on-off switch as described in a B-N bond mechanism. On the other hand, the computational results and the "proton affinity" experiments[41] are all consistent with the hydrolysis mechanism.

2.9. Experiments with trivalent sugars

There are several carbohydrates, including fructose and sorbitol that are known to bind boronic acids in a trivalent fashion.[28, 34, 40] If the B-N bond mechanism is at work, one would expect that those sugars that complex to boronic acid in a trivalent fashion would not induce a fluorescence intensity change upon binding since B-N bond formation would not be possible. This is also a point raised by Norrild in a crystal structural study.[39] Therefore, we tested the effect of fructose and sorbitol on the fluorescence intensity of 1a. They both induced strong fluorescence intensity increases in a methanol-buffer mixed solvent (Figures 2.4 and 2.5). It should be noted that the effect of fructose has already been tested by Shinkai and co-workers and found to induce as much fluorescence intensity changes as the other sugars tested.[9, 27] This by itself already contradicts the B-N bond mechanism, although the realization of fructose binding in a trivalent fashion came

after the proposed B-N bond mechanism. Such binding results cannot be explained by the B-N bond mechanism, but are consistent with the hydrolysis mechanism.

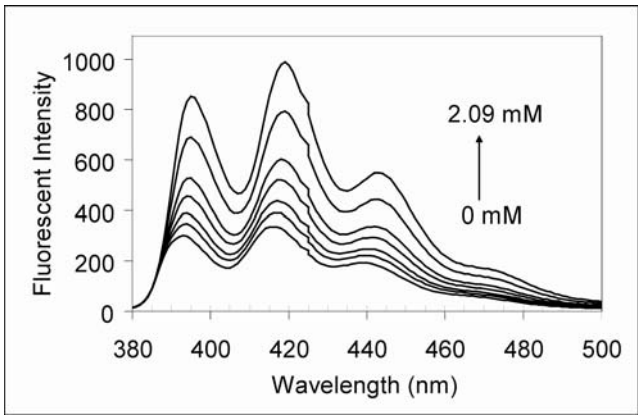

Figure 2.4. Fluorescence intensity changes upon the addition of fructose to sensor **1** (2.81×10^{-6} M) in 1:1 MeOH / 0.1 M aqueous phosphate buffer at pH 7.4. Fructose concentration. (mM): 0, 0.04, 0.09, 0.21, 0.35, 0.88, and 2.09.

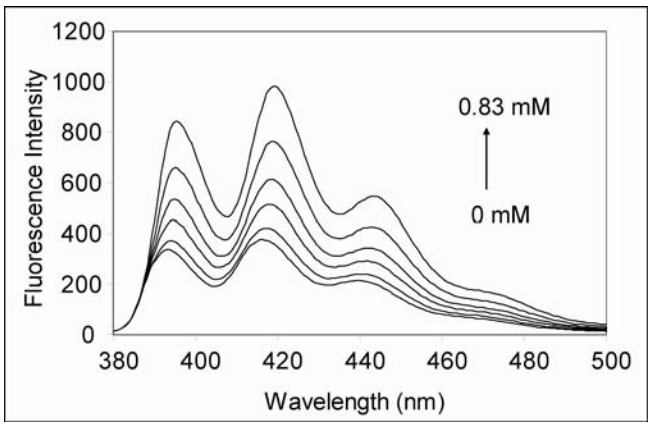

Figure 2.5. Fluorescence intensity change with addition of sorbitol to sensor **1** (2.81×10^{-6} M) in 50% MeOH / 0.1 M aqueous phosphate buffer at pH 7.4. Sorbitol concentration. (mM): 0, 0.03, 0.10, 0.17, 0.39, 0.83.

2.10. Density functional theory (DFT) studies of model systems

We have recently conducted DFT calculations of the B-N bond strength in a variety of adducts including models for those shown in Scheme 2.1 and found that the B-N bond strength to be very weak (< 7.2 kcal/mol) for all boronic acid and boronate ester adducts with geometry observed experimentally and the change in B-N bond strength upon formation of a boronate-ester is < 1 kcal/mol.[36] The effect of the change in boron-nitrogen interaction on the electron transfer rate constant was examined in detail. Estimates of the driving force (energy change for electron transfer) and reorganization energy were obtained. The DFT studies suggest that ester formation will actually decrease the fluorescence yield in aprotic solvents, but will increase the fluorescence yield in protic solvents.

In all the points raised above and the results observed or reported in the literature, any single one is probably not enough to refute the B-N bond mechanism, but putting them all together, it forms a very strong case in support of the hydrolysis mechanism going through **2d** and against the B-N bond mechanism. The hydrolysis mechanism is essentially a pK_a switch mechanism that we have used in the design of spectroscopic and fluorescent boronic acid compounds, which changes spectroscopic and/or fluorescent properties based on the ionization state changes.[29, 42] In such a situation, there are two (or more) ionizable functional groups in the boronic acid compound. In this case, it is an amino and a boronic acid group. In the absence of any diol, the pK_a of the amino group is lower than that of the boronic acid moiety. Therefore, the first pK_a of the free sensor (**1a**) is that of the amino group. However, upon addition of a diol, the intrinsic pK_a of the

boronic acid is decreased, which results in the pK_a of the boronic acid moiety in the complex (**2b**) being lower than that of the amino group. In another words, the pK_a order of these two functional groups is switched with the addition of a diol. With sensor **1a**, this switch results in the protonation of amine nitrogen, which "ties up" the nitrogen lone pair electrons and prevents PET quenching of the anthracene fluorescence.

2.11. Structural evidence of hydrolysis mechanism from other research groups

Recently, based on our proposed hydrolysis mechanism the Anslyn group has further probed the structural and physical properties of different boronic acids and their complex with sugars in understanding the mechanism.[43] They used X-ray crystallography, ^{11}B NMR, and computational analysis as their tools to elucidate the mechanism. X-ray crystal structures of several boronic acids and their boronate forms were obtained from the aprotic and protic solvent. They postualed that the crystals obtained from the aprotic solvent would have the B-N bond whereas boronic acid crystal obtained from the protic solvents would be in the hydrated form. Boronic acid crystal obtained from the aprotic solvent of compound **3** showed B-N bond whereas compound **4** and **5** showed no B-N bond. It was concluded that the B-N bond formation is effected by many forces and crystal lattice packing can play a significant role. Crystal structure of complex **4** with catechol revealed B-N bond formation in anhydrous condition whereas crystal obtain in methanol showed methoxy group of solvent coordinated with the boron. Hence, it was concluded that B-N bond formation in ester depends on the solvent from which the crystal was obtained.

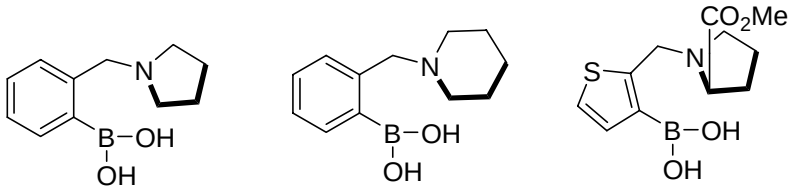

3 **4** **5**

^{11}B NMR studies results coincide with the X-ray crystal structure results where in aprotic solvent boron atom adopts tetrahedral form by coordinating with nitrogen atom to form B-N bond in the free acid and ester form. On the other hand in protic solvent boron atom is fully solvated for both free and complexed boronic acid.

2.12. Conclusions

In organic chemistry in general, it is always hard to prove a mechanism. This is no exception. However, results from the pH profile studies of the free boronic acid and its sugar complex, the effect of different sugars on the fluorescence intensity changes, the effect of trivalent sugar on the fluorescence intensity of the boronic acid, structural studies[43] and the calculated B-N bond strength are all consistent with the hydrolysis mechanism being the reason for the observed fluorescent intensity changes in this system. Therefore, one can say with a high degree of confidence that based on available data, the hydrolysis mechanism proposed is much more probable than the B-N bond mechanism. The understanding of this mechanism helps the future design of more effective boronic acid fluorescent reporter compounds for sensor and other applications as has been demonstrated in some of our own work. [29, 42]

References

1. James, T. D.; Sandanayake, K. R. A. S.; Shinkai, S., *Nature (London)* **1995,** 374, 345-347.

2. Eggert, H.; Frederiksen, J.; Morin, C.; Norrild, J. C., A New Glucose-selective Fluorescent Bisboronic Acid. First Report of Strong α-Furanose Complexation in Aqueous Solution at Physiological pH. *J. Org. Chem.* **1999,** 64, 3846-3852.

3. Norrild, J. C.; Eggert, H., Evidence for Mono- and Bisdentate Boronate Complexes of Glucose in the Furanose Form. Application of $^{1}J_{C\text{-}C}$ Coupling Constants as a Structural Probe. *J. Am. Chem. Soc.* **1995,** 117, 1479-1484.

4. Sandanayake, K. R. A. S.; Nakashima, K.; Shinkai, S., Specific Recognition of Disaccharides by trans-3,3'-Stilbenediboronic Acid: Rigidification and Fluorescence Enhancement of the Stilbene Skeleton upon Formation of a Sugar-Stilbene Macrocycle. *J. Chem. Soc., Chem. Commun.* **1994**, 1621-1622.

5. Norrild, J. C.; Eggert, H., Boronic Acids as Fructose Sensors. Structure Determination of the Complexes Involved Using $^{1}J_{(CC)}$ Coupling Constants. *J. Chem. Soc. Perkin Trans. 2* **1996**, 2583-2588.

6. Shinkai, S.; Takeuchi, M., Molecular Design of Artificial Sugar Sensing Systems. *Trend in Anal. Chem.* **1996,** 15, 188-193.

7. Wiskur, S. L.; Lavigne, J. L.; Ait-Haddou, H.; Lynch, V.; Chiu, Y. H.; Canary, J. W.; Anslyn, E. V., pKa Valuaes and Geometries of Secondary and Tertiary Amines Complexed to Boronic Acids-Implications for Sensor Design. *Org. Lett.* **2001,** 3, 1311-1314.

8. Yang, W.; He, H.; Drueckhammer, D. G., Computer-Guided Design in Molecular Recognition: Design and Synthesis of a Glucopyranose Receptor. *Angew. Chem. Int. Ed* **2001,** 40, 1714-1718.

9. James, T. D.; Sandanayake, K. R. A. S.; Shinkai, S., Novel Photoinduced Electron-transfer Sensor for Saccharides Based on the Interaction of Boronic Acid and Amine. *Chem. Commun.* **1994**, 477-478.

10. Wang, W.; Gao, X.; Wang, B., Boronic Acid-based Sensors for Carbohydrates. *Curr. Org. Chem.* **2002,** 6, 1285-1317.

11. Lavigne, J. J.; Anslyn, E. V., Teaching Old Indicators New Tricks: A Colorimetric Chemosensing Ensemble for Tartrate/Malate in beverages. *Angew. Chem. Int. Ed.* **1999,** 38, 3666-3669.

12. Cabell, L. A.; Monahan, M.-K.; Anslyn, E. V., A Competition Assay for Determining Glucose-6-phosphate Concentration with a Tris-Boronic Acid Receptor. *Tetrahedron Lett.* **1999,** 40, 7753-7756.

13. Gao, S.; Wang, W.; Wang, B., Building Fluorescent Sensors for Carbohydrates Using Template-directed Polymerizations. *Bioorg. Chem.* **2001,** 29, 308-320.

14. Wang, W.; Gao, S.; Wang, B., Building Fluorescent Sensors by Template Polymerization: The Preparation of a Fluorescent Sensor for D-Fructose. *Org. Lett.* **1999,** 1, 1209-1212.

15. Yang, W.; Gao, S.; Gao, X.; Karnati, V. R.; Ni, W.; Wang, B.; Hooks, W. B.; Carson, J.; Weston, B., Diboronic Acids as Fluorescent Probes for Cells Expressing Sialyl Lewis X. *Bioorg. Med. Chem. Lett* **2002,** 12, 2175-2177.

16. Yoon, J.; Czarnik, A. W., Fluorescent Chemosensors of Carbohydrates. A Means of Chemically Communicating the Binding of Polyols in Water Based on Chelation-Enhanced Quenching. *J. Am. Chem. Soc.* **1992,** 114, 5874-5875.

17. Paugam, M. F.; Bien, J. T.; Smith, B. D.; Chrisstoffels, L. A. J.; deJong, F.; Reinhoudt, D. N., Facilitated Catecholamine Transport Through Bulk and Polymer-Supported Liquid Membranes. *J. Am. Chem. Soc.* **1996,** 118, 9820-9825.

18. Westmark, P. R.; Gardiner, S. J.; Smith, B., Selective Monosaccharide Transport through Lipid Bilayers Using Boronic Acid Carriers. *J. Am. Chem. Soc.* **1996,** 118, 11093-11100.

19. Riggs, J. A.; Hossler, K. A.; Smith, B. D.; Karpa, M. J.; Griffin, G.; Duggan, P. J., Nucleotide Carrier Mixture with Transport Selectivity for Ribonucleoside-5'-phosphates. *Tetrahedron Lett.* **1996,** 37, 6303-6306.

20. Draffin, S. P.; Duggan, P. J.; Duggan, S. A. M., Highly Fructose Selective Transport Promoted by Boronic Acids Based on a Pentaerythritol Core. *Org. Lett.* **2001,** 3, 917-920.

21. Gardiner, S. J.; Smith, B. D.; Duggan, P. J.; Karpa, M. J.; Griffin, G. J., Selective Fructose Transport Through Supported Liquid Membranes Containing Diboronic Acid or Conjugated Monoboronic Acid- Quaternary Ammonium Carriers. *Tetrahedron* **1999,** 55, (10), 2857-2864.

22. Smith, B. D.; Gardiner, S. J.; Munro, T. A.; Paugam, M. F.; Riggs, J. A., Facilitated Transport of carbohydrates, Catecholamines, and Amino Acids Through Liquid and Plasticized Organic Membranes. *J. Incl. Phenom. Mol. Recogn. Chem.* **1998,** 32, 121-131.

23. Singhal, R. P.; Ramamurthy, B.; Govindraj, N.; Sarwar, Y., New Ligands for Boronate Affinity-Chromatography - Synthesis and Properties. *J. Chromatogr.* **1991,** 543, (1), 17-38.

24. Psotova, J.; Janiczek, O., Boronate Affinity-Chromatography and the Applications. *Chem. Listy* **1995,** 89, 641-648.

25. Soundararajan, S.; Badawi, M.; Kohlrust, C. M.; Hageman, J. H., Boronic Acids for Affinity-Chromatography - Spectral Methods for Determinations of Ionization and Diol-Binding Constants. *Anal. Biochem.* **1989,** 178, (1), 125-134.

26. Wulff, G.; Vesper, W., Preparation of Chromatographic Sorbents with Chiral Cavities for Racemic Resolution. *J. Chromatography* **1978,** 167, 171-186.

27. James, T. D.; Sandanayake, K. R. A. S.; Iguchi, R.; Shinkai, S., Novel Saccharide-Photoinduced Electron Transfer Sensors Based on the Interaction of Boronic Acid and Amine. *J. Am. Chem. Soc.* **1995,** 117, 8982-8987.

28. Springsteen, G.; Deeter, S.; Gao, X.; Wang, B., The Optiml pH for Boronic Acid-Diol Binding. *Tetrahedron* **2002,** 58, 5291-5300.

29. Gao, X.; Zhang, Y.; Wang, B., New Boronic Acid Fluorescent Reporter Compounds II. A Naphthalene-based Sensor Functional at Physiological pH. *Org. Lett.* **2003,** 5, 4615-4618.

30. Yang, W.; Springsteen, G.; Yan, J.; Deeter, S.; Wang, B., A Novel Type of Fluorescent Boronic Acid that Shows Large Fluorescence Intensity Changes upon Binding with a Diol in Aqueous Solution at Physiological pH. *Bioorg. Med. Chem. Lett.* **2003,** 13, 1019 - 1022.

31. James, T. D.; Shinkai, S., Artificial Receptors as Chemosensors for Carbohydrates. *Top. Curr. Chem.* **2002,** 218, 159-200.

32. Burgemeister, T.; Grobe-Einsler, R.; Grotstollen, R.; Mannschreck, A.; Wulff, G., Fast Thermal Breaking and Formation of a B-N Bond in 2-(aminomethyl)benzene Boronates. *Chem. Ber.* **1981,** 114, 3403-3411.

33. Springsteen, G.; Wang, B., Alizarin Red as a General Fluorescent Reporter for Studying the Binding of Boronic Acids and Carbohydrates. *Chem. Commun.* **2001**, 1608-1609.

34. Lorand, J. P.; Edwards, J. O., Polyol Complexes and Structure of the Benzeneboronate Ion. *J. Org. Chem.* **1959,** 24, 769.

35. James, T. D.; Linnane, P.; Shinkai, S., Fluorescent Saccharide Receptors: A Sweet Solution to the Design, Assembly and Evaluation of Boronic Acid Derived PET Sensors. *Chem. Commun.* **1996**, 281-288.

36. Franzen, S.; Ni, W.; Wang, B., A Study of the Mechanism of Electron Transfer Quenching by Boron-Nitrogen Adducts in Fluorescent Sensors. *J. Phys. Chem. B* **2003,** 107, 12942-12948.

37. Toyota, S.; Futawaka, T.; Asakura, M.; Ikeda, H.; Oki, M., Experimental and Theoretical Evidence of an S_N2-Type Mechnaism for Dissociation of B-N Coordination Bonds in 2,6-Bis((dimethylamino)methyl)phenylborane Derivatives. *Organometallics* **1998,** 17, 4155-4163.

38. Cooper, C. R.; James, T. D., Selective Fluorescence Signalling of Saccharides in Their Furanose Form. *Chem. Lett.* **1998**, 883-884.

39. Norrild, J. C.; Sotofte, I., Crystal Structures of 2-(*N,N*-Dimethylaminoalkyl)ferroceneboronic Acids and Their Diol Derivatives. The Quest for a B-N Intramolecular Bond in the Solid State. *J. Chem.Sco. Perkin Trans. 2* **2001**, 727-732.

40. Norrild, J. C., An Illusive Chiral Aminoalkylferroceneboronic Acid. Structural Assignment of a Atrong 1 : 1 Sorbitol Complex and New Insight into Boronate-polyol Interactions. *J. Chem. Soc. Perkin Trans. 2* **2001**, 719-726.

41. Hahn, I. S.; Wesdemiotis, C., Protonation Thermochemistry of Beta-alanine - An Evaluation of Proton Affinities and Entropies Determined by the Extended Kinetic Method. *Int. J. Mass Spectromet.* **2003,** 222, 465-479.

42. Ni, W.; Fang, H.; Springsteen, G.; Wang, B., Design of Boronic Acid Spectroscopic Reporter Compounds by Taking Advantage of the pKa-Lowering Effect of Diol-binding: Nitrophenol-based Color Reporters for Diols. *J. Org. Chem.* **2004,** 69, 1999-2007.

43. Zhu, L.; Shabbir, S.; Gray, M.; Lynch, V.; Sorey, S.; Anslyn, E. V., A Structural Investigation of the N-B Interaction in an *o*-(N,N-Dialkylaminomethyl)arylboronate System. *J. Am. Chem. Soc.* **2006,** 128, (4), 1222-1232.

Chapter 3. Design and synthesis of boronic acid based sensors for sialic acid for anti-influenza therapy

Abstract: A new series of fluorescent boronic acid based sensors for sialic acid were designed and synthesized as potential anti-influenza agents. Three sensors were designed on "two point" interaction. Two interactions points were: boronic acid group and different amine based groups (amino/guandino/benzlyamine). Compounds (**13**, **15**, **19**) were synthesized via [2+3] Huisgen cyloaddition reaction and were fluorescent at micromolar range. Compounds **13** and **19** did not show significant fluorescence change upon binding with sialic acid whereas the guanidine based compound (**15**) showed significant spectroscopic change upon addition of sialic acid with binding affinity (*Ka*) of 8 M^{-1}.

3.1. Introduction

3.1.1. Sialic acid structure

Sialic acids (SA) are nine carbon α-keto acids with many biological functions. Sialic acid exits in many forms, main core structure is 2-keto-3-deoxy-D-glycero-D-galacto-nonulosonic acid (**1**).[1] Common modifications that occur in nature of SA are: 5-amino group is either acetylated or glycolylated while all non-glycosidic hydroxyl group at position 4, 7, 8, and 9 have been substituted with acetates, sulfates, phosphates, and methyl ethers. Usually mono *O*-acetylation (**3**) occurs but di- or tri- acetylation in one SA has also been reported. Such modifications can interfere with cell's mode of action. For example *O*-acetylation prevents the monosaccharide to be a counter-receptor for influenza virus A and B whereas it is more susceptible to the binding of influenza virus C.[2] The most common form of sialic acid and almost only form found in humans is the N-acetylneuraminic acid (**2**).[3] Sialic acids rarely occur free in nature and are usually found on the terminal ends of the cell surface glycoconjugates in mamals. They are found in various linkages with the complex carbohydrates but mainly to galactose as *N*-acetylgalactosamine.[1] Sialic acid are also found in sialy Lewis a and x tetrasaccharides which have been associated with development and progression of certain types of cancer.[4] Due to their location at the terminal end and the negative charge of the carboxylate functional group, sialic acids plays important role in mediating cellular recognition and adhesion processes. Bacteria on the other hand do not normally produce sialic acids on their own but some pathogenic strains can and they exhibit sialic acid on their cell surface to mimic mammalian cells and evade the host's immune system. [1]

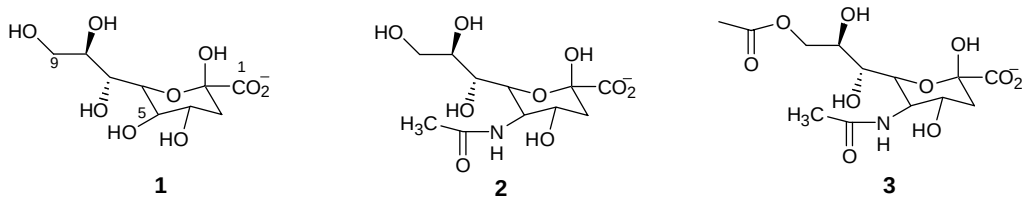

Figure 3.1. Common sialic acid forms: 2-keto-3-deoxy-D-glycero-D-galacto-nonulosonic acid (**1**), N-acetylneuraminic acid (**2**), and *N*-acetyl-9-*O*-acetylneuraminic acid (**3**)

3.1.2. Role of sialic acid in biological funtions and diseases

Mammals, including human beings and other various microorganisms have the ability to produce sialic acids in a series of reaction from a simple precrursor, glucose.[5] Mammailian nervous system contains the highest amount of sialic acid in the form of gangliosides (65%), glycoproteins (32%) and the rest is in free form. However, in humans the gangliosides are not present evenly; they are mainly concentrated in the brain compared to other organs such as liver, lung, and spleen. Thus sialic acid moieties of gangliosides and glycoproteins play a role in structural and functional roles of celluar events such as cell recoginition, cell-to-cell contact, receptor binding, and other biosignal transduction. [6] High content of sailic acid has also been found in human milk. Aside from this property of cellular recognition and adhesion processes, the extent of outer surface celluar sialyation has been related to the tumorogenesis and metatasis of certain cancers. The *N*-glycolyneuraminic acid form of sialic acid is found mainly in animal species but it has also been found in certain human cancers.[3] It has also been reported that the levels of circulating sialic acid are higher in Type II diabetic patients than in nondiabetic patients.[7]

3.1.3. Sialic acid: a key recognition molecule for influenza viral infection

Cell surface SA receptors has been considered to be critical for the influenza virus.[8] There are three types of influenza viruses: influenza B and C are human viruses and influenza A virus is found in wide range of avian and mammalian hosts. Entry of the virus into the host occurs through the glycoproteins present on the viral surface. In specific, glycoproteins haemagglutinin (type A and B) and haemagglutinin esterase (type C) attaches to host cell-surface molecules containing sialic acid. The process is followed by endocytosis and fusion of viral membrane with the endosomal membrane which leads to the entry of the virus.[8, 9] Studies have indicated that sialylcells are main celluar targets for the virus attachment to the host, in specific the *N*-acetyl-9-*O*-acetylneuraminic acid (**3**) has been the key determinant in this process. Recent outburst of H5N1 avian influenza flu or better known "bird flu" studies have also indicated haemagglutinin as a key receptor on the virus surface for cellular attachment. As in other influenza infection studies, the hemaggluctinin H5N1 also attaches to sialic acid receptors, specifically to sialic acid linked to galactose in α2,3 (**4**) or α2,6 (**5**) fashion (Figure 3.2). Different linkages have been important determinant for prefential binding of virus as well the spread of the virus among species. Human influenza prefers to bind to sialic acid attached to galactose in α2,6 linkage (SA- α-2,6-Gal) whereas avian influenza binds in α2,3 linkage (SA- α-2,3-Gal), thus the ability of virus to spread from avain to human is difficult due to linkage barrier.[10]

Since sialic acid is a key component for the influenza infection, we were interested in designing boronic acid based sensors for the sialic acid as potential sensors or drug targets for influenza therapy.

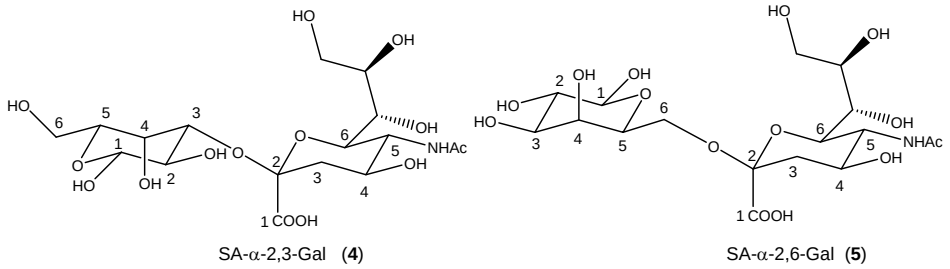

Figure 3.2. Chemical structures of SA-α-2,3-Gal (**4**) and SA-α-2,6-Gal (**5**)

3.2. Design of boronic acid based sensors for sialic acid

Boronic acids are known for their strong interaction with cis diols containing compounds and such interactions has been employed in the design of sensors for cell surface carbohydrates (chapter 1).[4, 11, 12] As mentioned in chapter 1 a selective sensor consist of three components: a) proper functional groups that afford strong intermolecular interaction, b) a 'reporting' event/moiety that allows the binding event to be recognized, and c) the appropriate three-dimensional scaffold that allow for necessary complementarity in terms of size, shape, and functional group orientation. Taking in account of all the essential components for a selective sensor, potential sensors for sialic acid were designed using computer molecular modeling. Sialic acid bears a pair of cis diols at positions 8 and 9 which make it a perfect substrate for boronic acid based sensor design. Aside from having a pair of cis diols SA also has a carboxylate anion and sensors

based on "two-point" interaction taking in account both the cis diol and carboxylate ionic interactions have been reported. Shinkai *et al* reported the first PET (see Chapters 1 and 2) based chemosensors for sialic acid based on two-point interaction.[13] Their design included 1,10-phenanothroline-Zn(II) complex linked to aminomethylphenyl boronic acid (Figure 3.3). The metal complex served as carboxylate binding site and boronic acid group for diol binding. The receptor showed binding affinity (Ka) of 200 M^{-1} in an aqueous methanol solution at pH of 8.0. A similar system based on two-point interaction was reported by Takeuchi group where they designed surface plasmon resonance sensor for detection of sialic acid.[14] In there design *p*-vinylbenzeneboronic acid group interacted with the cis diols and *N*,*N*,*N*-trimethylaminoethyl methacrylate interacted with carboxylate group of the sialic acid. In a combinatorial effort, Bradley Smith and coworkers have also worked on developing sialic acid sensors with limited success.[15] They designed there scaffold on a polymer chain with two recognition domains: conserved and variable. An anthracene based boronic acid acted as fluorophore and conserved recognition domain. It was attached to a poly(allylamine) (PAA) chain with 50 free amines sites. After the attachment of the boronic acid moiety, the PAA chain was futher derivatized to give several cationic sites on the chain that acted as variable recognition domain. Several libraries were designed and tested with sialic acid, fructose, and glucose. Fluorescence enhancement of 2-3 fold was seen among the libraries tested but with low selectivity among the sugars.

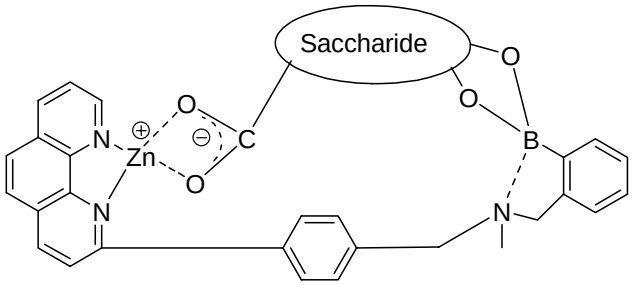

6

Figure 3.3. Complex structure of 1,10-phenanothroline-Zn(II) with sialic acid

As of today only limted examples of boronic acid based sensors are known for the sialic acid detection, which only have moderate affinity and selectivity. The above three examples of sensors for sialic acid have certains limitation. In Shinkai's case, the receptor was only soluble in high concentration of methanol and high pH (8.0) was required to measure the fluorescence intensity changes. Such factors prevent them from being employed in normal physiological conditions where aqueous media rather than organic solvent are desired. To further enhance the solubility, binding affinity, and selectivity at physiological pH of sensors for the sialic acid, we designed several potential sialic acid sensors. Our designed also included two-point interactions where boronic acid unit would interact with the diols and an amino/guandino/amidino unit will interact with the carboxylate via hydrogen bonding and/or ionic interactions at physiological pH. Two units (boronic acid and amine) in the sensor were set apart in a distance equivalent to that between the cis diols and carboxylate anion in SA as shown in Figure 3.4. Three triazole ring based sensors were designed and synthesized with different pKa values for the amine units substituted to promote protonation at physiological pH (Figure 3.4 a vs Figure 3.4

b). The boronic acid (blue) was overlap with its complex (pink) with sialic acid to study the sturctural difference between their free and complex form. The overlay indicates that the sensor substituted with guanidine moiety has similar conformation when compared between its free and complex form whereas aniline substituted sensor has poor overlap. Such poor overlap translates into improper orientation of functional groups which are necessary for the higher binding affinity of sensor for its substrate. Table 3.1 lists the distance measured for the sensors and their complex. Their binding constants with sialic acid were also determined (Table 3.2).

A B

Figure 3.4. a) Structure of sensor **13** (blue) with its complex (pink) with sialic acid; b) **15** (blue) overlap with its complex (pink) sialic acid

Table 3.1. Measurements of bond lengths between boronic acid (BA) and amine (NH)

Sensor	Sensor (BA-NH) distance (A^o)	Complex (BA-NH) distance (A^o)	-H bond Length (A^o)
13	9.362	8.005	2.126, 2.602
15	8.750	8.351	2.169, 1.900
19	8.364	7.774	2.108, 1.878

3.3. Synthesis of triazole based sialic acid sensors

Synthesis of aniline, benzyl amine, and guanidine based sensors were accomplished with [2+3] Huisgen cycloaddition or "click chemistry" of an arylboronic acid bearing a terminal alkyne group and arylazide. The building blocks, alkyne[16] and azide[17], were synthesized by literature procedures. Briefly, the ethynylarylboronic ester (**10**) was synthesised with the Sonogashira coupling using the 3-bromoarylboronic acid. For the ease of purification, 3-bromophenhylboronic acid was first protected with pinacol to give its ester (**8**) in 66 % yield. The Sonogashira coupling under microwave irridation at 120 ^oC for 25 min gave the Sonogashira coupling product (**9**) in 78%. The trimethylsilyl group was removed in presence of K_2CO_3 in methanol to give terminal free ethynylbrononic ester in 97% yield (Scheme 3.1). Arylazides were prepared with Ullmann type coupling of arylhalides in the presence of CuI. Azidoaniline (**12**) was prepared by refluxing 3-bromoaniline with sodium azide in the presence of CuI to give the desired azide in 97% yield. The 3-bromobenzylamine was first protected with di-*tert*-

butyldicarbonate in methanol in the presence of triethyl amine (TEA) and then its azide was prepared with similar procedure as in the aniline case to give the desired product in 58% yield (Scheme 3.1). The guanidinoazide (**14**) was synthesized by reacting aniline azide with the guanylating agent which was prepared by reacting 1H-pyrazole-1-carboxamidine with di-*tert*-butyl dicarbonate in presence of 3 equivalents of lithium hydride.[18] Final triazole based compounds were obtained via copper catalyzed Huisgen cycloaddition[19] of amidoazide and alkyne in the presence sodium ascorbate to give boronic ester and free boronic acid of respective amine . In the case of benzylamine (**19**) and guanidine (**15**), the Boc protecting group was removed with trifluoroacetic acid to give free amino groups (Scheme 3.1).

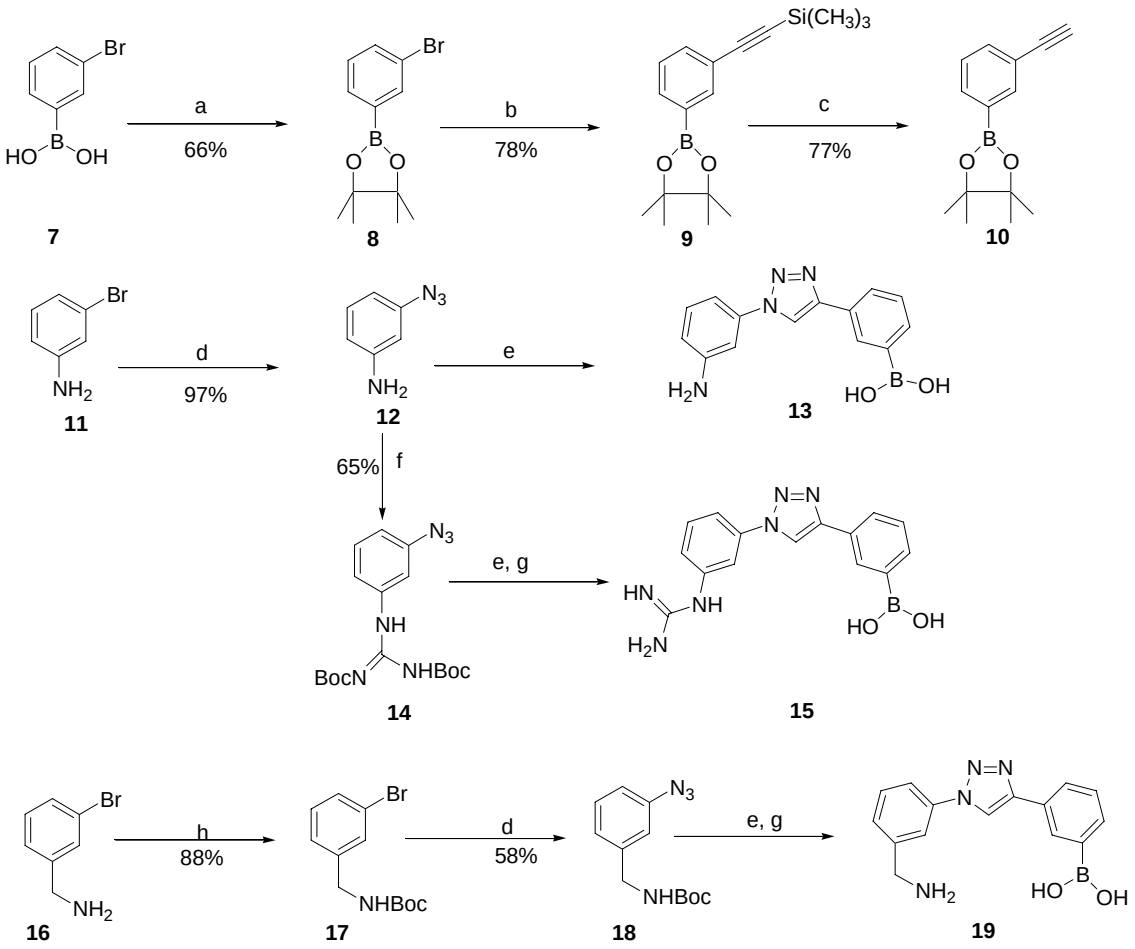

Scheme 3.1. a) Pinacol, toluene, 120 ^{o}C; b) $(CH_3)_3SiCCH$, $Pd(PPh_3)_3Cl_2$, CuI, PPh_3, diethylamine, DMF, 120 ^{o}C, MW; c) K_2CO_3, MeOH; d) NaN_3, CuI, sodium ascorbate, *N*,*N*-diethylethane-1,2-diamine, EtOH/H_2O (7:3), reflux, N_2; e) **10**, $CuSO_4.5H_2O$, sodium ascorbate, *t*-butanol/H_2O(1:1); f) 1-H-Pyrazole-1-(*N*,*N*'-bis(*tert*-butoxycarbonyl)carboxamidine, MeCN; g) TFA(50%), DCM; h) di-*tert*-butyl dicarbonate, MeOH, TEA

3.4. Binding studies

The fluorescence experiments were conducted to determine the appropriate binding constants of **13, 15,** and **19** with sialic acid. Guandino based sensor (**15**) was

completely soluble in phosphate buffer (pH 7.4) with a sensor concentration of 2×10^{-4} M. The aniline based sensor required 16% methanol and benzylaine required 8% methanol for there complete solubility. The binding constants were determined with sialic acid. Upon sugar addition, guanidine substituted sialic acid sensor analogs (**15**) showed increased in fluorescence intensity whereas aniline and benzylamine substituted did not show much change in fluorescence intensity. Figure 3.6 shows two sets of fluorescent spectral changes upon sugar addition using compound **13** and **15** as examples.

The guanidino-substituted compound **15** showed the highest change in fluorescence intensity with a 3-fold increase upon SA addition. It also showed the highest binding affinity with an apparent binding constant (K_a) of 8 M^{-1} (Table 3.2). As predicted the aniline-substitued (**13**) showed very weak binding due to presence of only one binding unit (boronic acid) since aniline with a low pka was not protanated at physiological pH and probably did not interacted with carboxylate group of the SA. The benzylamine- substituted compound **19** did not show significant change in fluorescence intensity to determine the binding constant.

a)

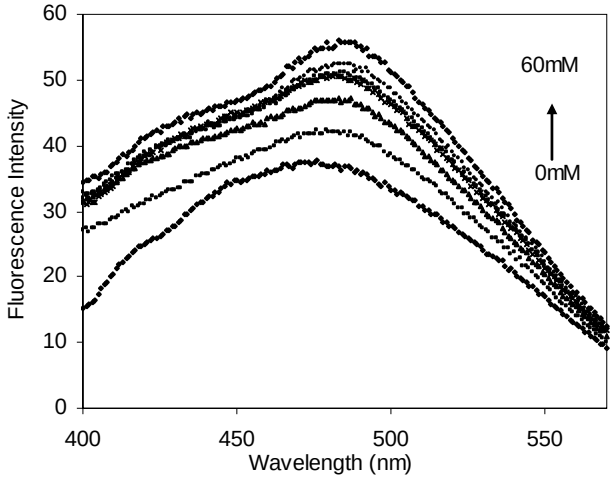
60
50
40
30
20
10
0
Fluorescence Intensity
400
450
500
550
Wavelength (nm)
60mM
0mM

b)

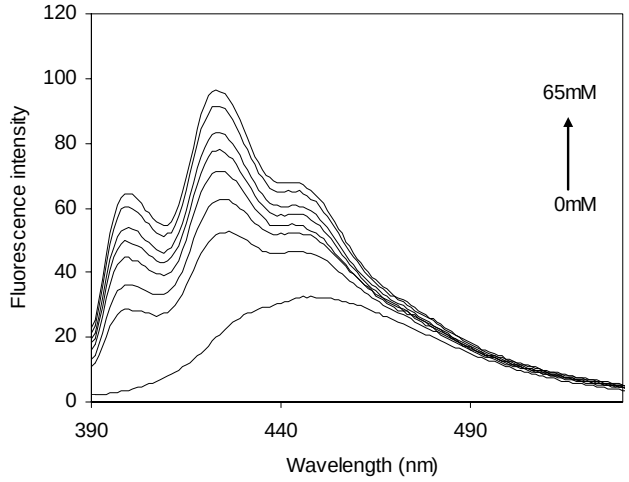
120
100
80
60
40
20
0
Fluorescence intensity
390
440
490
Wavelength (nm)
65mM
0mM

c)

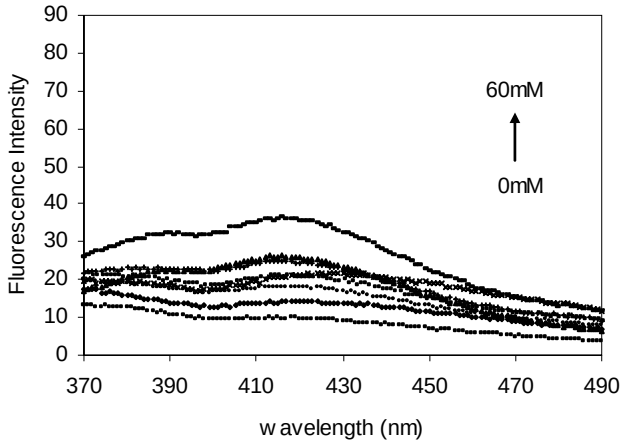

Figure 3.6. a) Fluorescence spectra of **13** (1.0×10^{-4} M) with sialic acid (0 mM-60 mM) at 25 ^{o}C in 16% MeOH/0.1 M aqueous phosphate buffer at pH 7.4: λ_{ex} = 300 nm. b) Fluorescence spectra of **15** (1.0×10^{-4} M) with sialic acid (0 mM-65 mM) at 25 ^{o}C in 0.1 M aqueous phosphate buffer at pH 7.4: λ_{ex} = 375 nm. c) Fluorescence spectra of **19** (1.0×10^{-4} M) with sialic acid (0 mM-60 mM) at 25 ^{o}C in 8% MeOH/0.1 M aqueous phosphate buffer at pH 7.4: λ_{ex} = 288 nm

Table 3.2. Binding Constant (K_a) for compounds **13, 15, and 19** with sialic acid

Compound	K_a (M^{-1})	Fluorescence intensity change
13	4.0	1-fold increase
15	8.0	3-fold increase
19	a	b

a: binding constant (*K*a) could not be determined
b: no change in fluorescence intensity

3.5. Conclusions

Three new fluorescent triazole-based boronic sensors (**13, 15,** and **19**) were synthesized. Guanidine based sensor (**15**) had higher apparent binding constant for sialic acid (K 8 M^{-1}) under physiological conditions. On the other hand aniline and beznylamine based boronic acids did not show binding affinity towards sialic acid. Premiliary results indicate that guanidine based sensor is a potential target which can be futher optimized to give better induce fit model to futher enhance the binding affinity.

3.6. Future Prespective

Among the design sensors, the guanidine based sensor showed a low affinity toward sialic acid but it is a potential target for further optimization. The design optimization include

3.7. Experimental

3.7.1. General Procedures

All air- and water-sensitive reactions were performed under dry nitrogen which was passed through dryrite in oven-dried glassware. Commercially available reagents were used without additional purification unless otherwise indicated. Dichloromethane was distilled from CaH_2. THF was distilled from sodium and benzophenone.

Analytical thin layer chromatography (TLC) was performed with Scientific Adsorbents plastic-backed TLC silica gel 60 F hard layer plates. TLC plates were visualized with UV light (254 nm) or with 5% (w/v) solution of phosphomolybidic acid in ethanol. Flash column chromatography was performed with Scientific Adsorbents silica gel (flash 32-63 nm).

Mass spectrometry (MS) analyses were performed by the Mass Spectrometry Facilities of Georgia State University. ^{1}H and ^{13}C NMR spectra were recorded at 400 MHz and 100 MHz. Chemical shifts (δ) are given in ppm relative to TMS for ^{1}H spectra and residual solvents for ^{13}C spectra.

3.7.2. Procedures for Fluorescence Binding Studies

A Shimadzu RF-5301PC fluorometer was used for all the fluorescent studies. For a typical fluorescent measurement, a 140 μL of sensor (2.0×10^{-4} M) stock solution in methanol/ 0.1 M phosphate buffer was mixed with 140 μL of saccharide solution in 0.1 M of phosphate buffer (pH 7.4) at various concentrations. The apparent pH was checked with pH meter and corrected if necessary. The mixture was allowed to mix for 10 min and fluorescence intensity was recorded. Triplicate measurements were taken for each sugar. The correlation coefficients for all determinations in fitting the 1:1 model were over 0.98. The binding constants were determined by procedure as described in section 1.7.

2-(3-Bromophenyl)-4,4,5,5-tetramethyl-1,3,2-dioxaborolane (**8**). A mixture of 3-bromophenyl boronic acid **7** (14.9 mmol) and pinacol (17.9 mmol) was stirred in refluxing toluene equipped with a Dean-Stark trap for about 24 h until evolution of water ceased, then the solvent was removed on a rota-evaporator. The crude product was purified by flash chromatography to give **8** in 66%. ^{1}H NMR (400 MHz, $CDCl_3$): 1.38 (12H, s), 7.28 (1H, t, J = 7.2 Hz), 7.61 (1H, d, J = 7.6 Hz), 7.74 (1H, d, J = 7.2 Hz), 7.95 (1H, s) ppm. ^{13}C NMR (100 MHz, $CDCl_3$): 24.86, 84.16, 122.46, 129.50, 133.09, 134.19, 137.48 ppm. MS-EI: calcd for $C_{11}H_{13}BBrO_2$: 282; found: 282.

Trimethyl(3-(4,4,5,5-tetramethyl-1,3,2-dioxaborolan-2-yl)phenyl)ethynyl)silane (**9**). A mixture of aryl bromide (**8**) (0.9 mmol), $Pd(PPh_3)Cl_2$ (0.05 mmol), CuI (0.05 mmol), triphenylphosphine (0.18 mmol), trimethylsilylacetylene (1 mmol), and diethylamine (13.6 mmol) in dimethylformamide (DMF, 0.5 mL) was irradiated with microwave with temperature maintained at 120 ºC for 20 ~ 25min in a heavy-walled glass vial sealed with Teflon septum. Then the reaction mixture was filtered and washed with dichloromethane. The filtrate was concentrated under reduced pressure and the residue was purified by flash chromatography to give **9** in 78%. ^{1}H NMR (400 MHz, $CDCl_3$): 0.23 (9H, *J* = 3.2 Hz) 1.34 (12H, s), 7.30 (1H, t, *J* = 7.6 Hz), 7.52-7.55 (1H, tt, *J* = 1.2,1.2 Hz), 7.72-7.74 (1H, dd, *J* = 1.2, 1.2 Hz), 7.93 (1H, s) ppm. ^{13}C NMR (100 MHz, $CDCl_3$): 0.01, 24.87, 83.99, 94.06, 105.07, 122.68, 127.58, 133.09, 134.58, 138.47 ppm. MS-EI: calcd for $C_{17}H_{25}BO_2Si$: 300; found: 300.

2-(3-Ethynylphenyl)-4,4,5,5-tetramethyl-1,3,2-dioxaborolane (**10**) A mixture of trimethylsilylethynylaryl boronate **9** (0.5 mmol) and potassium carbonate (2 mmol) in methanol (10 mL) was stirred at room temperature for 0.5 h ~ 2 h. Then the reaction mixture was filtered, and the filtrate was concentrated under reduced pressure to give a residue, which was purified by flash chromatography to give **10** in 77%. ^{1}H NMR (400 MHz, $CDCl_3$): 1.34 (12H, s), 3.04 (1H, s), 7.32 (1H, t, *J* = 7.6 Hz), 7.58 (1H, d, *J* = 7.6 Hz), 7.78 (1H, d, *J* = 7.2 Hz), 7.95 (1H, s) ppm. ^{13}C NMR (100 MHz, $CDCl_3$): 24.86, 83.60, 84.02, 121.68, 127.66, 134.64, 134.89, 138.52 ppm. MS-EI: calcd for $C_{14}H_{17}BO_2$: 228; found: 228.

3.7.3 General procedure for the synthesis of azides

In a 2-neck flask, aryl bromide (1 mmol), NaN_3 (2 mmol), sodium ascorbate (0.05 mmol), CuI (0.1 mmol), *N*,*N*-dimethylethylamine (0.15mmol), and 4 mL of EtOH-H_2O (7:3) were added. The flask was degassed and backfill with nitrogen, the reaction was stirred under reflux condition and reaction was monitored by TLC. Upon completion of reaction, the reaction was cooled down to room temperature. Reaction mixture was diluted with water and aqeous layer was extracted with ethyl acetate (2 X 30 mL). Organic layers were combined together and dried over $MgSO_4$ and solvent was evaporated. Crude mixture was purified by flash chromatography to give the desired aryl azide.

3-Azidoaniline (**12**). Reaction was completed in 40 min to give **12** in 97% yield. ^{1}H NMR (400 MHz, $CDCl_3$): 3.73 (2H, s), 6.31 (1H, s), 6.45 (1H, d, J = 8.0 Hz), 7.11 (2H, t, J = 7.6 Hz) ppm. ^{13}C NMR (100 MHz, $CDCl_3$): 105.40, 109.02, 111.93, 130.61, 140.99, 148.10 ppm. MS-EI: calcd for $C_6H_6N_4$: 134; found: 134.

***tert*-Butyl (3-azidophenylamino)-(tert-butoxycarbonylamino)methylenecarbamate** (**14**). In a flask equipped with a stir bar, 1H-pyrazole-1-carboxamidine with di-*tert*-butyl dicarbonate and 8 mL of CH_3CN were mixed at room temperature until completely dissolved. To the flask was added **12** and mixture was refluxed for 8 hrs. Solvent was evaporated and crude reaction mixture was purified with flash chromatorgraphy giving **14** in 35% yield. ^{1}H NMR (400 MHz, $CDCl_3$): 1.51 (9H, s), 1.54 (9H, s), 6.76 (1H, s, J = 3.6 Hz), 7.27 (2H, s), 7.61 (1H, s), 10.38 (1H, s), 11.60 (1H, s) ppm. ^{13}C NMR (100

MHz, $CDCl_3$): 28.15, 28.08, 79.81, 83.98, 112.64, 115.17, 118.16, 129.97, 138.39, 140.72, 153.30, 163.29 ppm. MALDI (M+H): calcd for $C_{17}H_{24}N_6O_4$: 377; found: 377.

***tert*-Butyl 3-bromobenzylcarbamate** (**17**). In a flask commerically available 3-bromobenzylamine and di-*tert*-butyl dicarbonate were dissolved in methanol (10 mL). To the flask TEA was added dropwise and reaction mixture was stirred for 12 hrs. Solvent was evaporated and crude reaction mixture was purified with flash chromatorgraphy giving **17** in 88% yield. ^{1}H NMR (400 MHz, $CDCl_3$): 1.46 (9H, s), 4.29 (2H, d, J = 5.6 Hz), 4.85 (1H, s), 7.21 (2H, m), 7.40 (1H, m), 7.42 (1H, s) ppm. ^{13}C NMR (100 MHz, $CDCl_3$): 28.38, 122.66, 125.97, 130.15, 130.40, 141.38 ppm. MS-EI: calcd for $C_{12}H_{16}BrNO_2$: 286; found: 286.

***tert*-Butyl 3-azidobenzylcarbamate** (**18**). General procedure for azide synthesis was used to obtain **18** (58% yield). ^{1}H NMR (400 MHz, $CDCl_3$): 1.46 (9H, s), 4.30 (2H, d, J = 5.6 Hz), 4.96 (1H, s), 6.90 (1H, s), 6.93 (1H, s), 7.05 (1H, d, J = 7.6 Hz), 7.29 (1H, t, J = 8.4 Hz) ppm. ^{13}C NMR (100 MHz, $CDCl_3$): 28.39, 44.24, 79.71, 117.78, 117.89, 123.83, 129.96, 140.32, 141.19, 155.92 ppm. MS-EI: calcd for $C_{12}H_{16}N_4O_2$: 248; found: 248.

3.7.4. General procedure for the synthesis of trizole ring based boronic acids

Compound **10** (1 mmol) and respective azide (1 mmol) was suspended in a 1:1 mixture of water: tert-butanol in a flask. To the flask was added sodium ascorbate (0.3 mmol, dissolved in 0.05 mL water) followed by copper (II) sulfate pentahydrate (0.03 mmol, dissolved in 5 µL water). The hetergoneous mixture was stirred at 80 ^{o}C until the reaction went to completion. The reaction mixture was diluted with water and aqeous layer was

extracted with ethyl acetate. Organic layers were combined together and dried over $MgSO_4$ and solvent was evaporated. The crude mixture was purified with flash chormatorgraphy to give the desired boronic ester and boronic acid.

3-(1-(3-Aminophenyl)-1-*H*-1,2,3-triazol-4-yl)boronic acid (13). The reaction was stirred for 24 hr and yield boronic ester 17 % and boronic acid in 9.6 %. Boronic ester: ^{1}H NMR (400 MHz, $CDCl_3$): 1.37 (12H, s), 3.94 (N-H, 2H, s), 6.71-6.74 (1H, dd, *J* = 2.4, 5.6 Hz), 7.05-7.08 (1H, dd, *J* = 2.0, 6.0 Hz), 7.19 (1H, t, *J* = 2.0 Hz), 7.28 (2H, t, *J* = 8.0 Hz), 7.48 (1H, t, *J* = 7.6 Hz), 7.81 (1H, d, *J* = 7.6 Hz), 8.12-8.14 (1H, tt, *J* = 1.6 Hz), 8.21 (1H, s) ppm. ^{13}C NMR (100 MHz, $CDCl_3$): 24.87 (d), 83.98, 106.91, 109.95, 115.08, 117.78, 128.39, 128.68, 129.75, 130.51, 132.07, 134.72, 147.85, 148.12 ppm. HRMS (ESI+): calcd for $C_{20}H_{23}BN_4O_2$: 363.1914; found: 363.1992. Boronic acid: ^{1}H NMR (400 MHz, $CDCl_3$) δ: 6.78-6.82 (2H, m), 7.06-7.09 (1H, m), 7.18 (1H, t, *J* = 2.4 Hz), 7.23-7.28 (2H, m), 7.33-7.35 (2H, m) ppm. ^{13}C NMR (100 MHz, $CDCl_3$) δ: 107.74, 110.31, 113.67, 116.73, 118.33, 131.33, 131.60, 132.70, 139.24, 149.47, 150.93, 159.09 ppm. Under mass spectrometery conditions the boronic acid was oxidized. MS (ESI-): $C_{14}H_{12}N_4O$: 252; found: 252.

3-(1-(3-Guanidinophenyl)-1*H*-1,2,3-triazol-4-yl)boronic acid (**15**). The reaction was stirred for 48 hr and yield boronic ester 8.2% and Boc protected boronic acid in 8.5%. Boronic ester: ^{1}H NMR (400 MHz, $CDCl_3$): 1.37 (12H, s), 1.53 (9H, s), 1.56 (9H, s), 7.48 (2H, t, *J* = 7.6 Hz), 7.62 (2H, t, *J* = 6.0 Hz), 7.82 (1H, t, *J* = 7.2 Hz), 8.14 (1H, d, *J* = 7.6 Hz), 8.24 (1H, s), 8.30 (2H, d, *J* = 4.0 Hz) ppm. ^{13}C NMR (100 MHz, $CDCl_3$): 24.86 (d), 28.09 (d), 83.95, 84.20, 113.87, 116.33, 117.79, 121.66, 128.36, 128.69, 129.68, 130.18,

132.03, 134.78, 137.38, 138.34, 148.29, 153.48, 163.19 ppm. MS (ESI+): calcd for $C_{31}H_{41}BN_6O_6$: 605.5; found: 605.5. Boronic acid: ^{1}H NMR (400 MHz, $CDCl_3$): 6.80-6.83 (1H, qq, *J* = 0.8, 1.6 Hz), 7.28 (1H, t, *J* = 8.0 Hz), 7.35-7.37 (2H, m), 7.40-7.42 (1H, tt, *J* = 1.2 Hz), 7.69 (1H, t, *J* = 8.0 Hz), 7.89-7.93 (2H, m) ppm. ^{13}C NMR (100 MHz, $CDCl_3$): 112.21, 115.28, 116.71, 118.50, 118.85, 124.92, 129.75, 131.02, 131.15, 136.57, 138.10, 148.49, 156.69, 157.79 ppm. Under mass spectrometery conditions the boronic acid was oxidized. MS (ESI-): calcd for $C_{15}H_{14}N_6O$: 295.3; found: 295.2.

3-(1-(3-Aminomethyl)phenyl)-1H-1,2,3-triazol-4-yl)boronic acid (**19**). The reaction was stirred for 24 hr and yield Boc protected boronic acid in 7.5% and upon deprotection of Boc group with TFA gave the final boronic acid (**19**). ^{1}H NMR (400 MHz, $CDCl_3$): 4.28 (2H, s), 6.85 (2H, d, *J* = 7.6 Hz), 7.28 (1H, t, *J* = 8.0 Hz), 7.39 (2H, d, *J* = 6.8 Hz), 7.61-7.67 (2H, m), 7.98 (1H, d, *J* = 7.2 Hz), 8.08 (1H, s), 8.86 (1H, s) ppm. ^{13}C NMR (100 MHz, $CDCl_3$): 42.44, 107.74, 110.31, 113.67, 116.73, 118.33, 131.33, 131.60, 132.70, 139.24, 149.47, 150.93, 159.09 ppm. MALDI (M+H): calcd for $C_{15}H_{14}N_4O$: 267.3; found: 267.0.

References

1. Tanner, M., The enzymes of sialic acid biosynthesis. *Bioorg. Chem.* **2005,** 33, 216-228.

2. Schauer, R., Origin and biological role of the great chemical diversity of natural sialic acids. *Trends. Gylcosci. Glyc.* **1997,** 9, (48), 315-330.

3. Wang, B.; Brand-miller, J., The role and potential of sialic acid in human nutrition. *Eur. J. Clin. Nutr.* **2003,** 57, 1351-1369.

4. Karnati, V. V.; Gao, X.; Gao, S.; Yang, W.; Ni, W.; Sankar, S.; Wang, B., A glucose-selective fluorescence sensor based on boronicacid-diol recognition. *Bioorg. Med. Chem. Lett.* **2002,** 12, (23), 3373-3377.

5. Dickson, J.; Messer, M., Intestinal neuraminidase activity of suckling rats and other mammals. Relationship to the sialic acid content of milk. *Biochem. J.* **1978,** 170, 407-413.

6. Brunngraber, E.; Witting, L.; Haberland, C.; Brown, B., Glycoproteins in Tay-sachs disease: isolation and carbohydrate composition of glycopeptides *Brain. Res.* **1972,** 38, 151-162.

7. Crook, M.; Tutt, P.; Simpson, H.; Pickup, J., Serum sialic acid and acute phase proteins in type 1 and type 2 diabetes mellitus. *Clin. Chim. Acta.* **1996,** 219, 131-138.

8. Pedroso de Lima, M.; Ramlho-Santos, J.; Flasher, D.; Slepushkin, V.; Nir, S.; Duzgunes, N., Target cell membrane sialic acid modulates both binding and fusion activity of influenza virus. *Biochim. Biophys. Acta.* **1995,** 1236, 323-330.

9. Matrosovich, M.; Klenk, H.-D., Natural and synthetic sailic acid-containing inhibitors of influenza virus receptor binding. *Rev. Med. Virol.* **2003,** 13, 85-97.

10. Minyong, L.; Binghe, W., Computational studies of H5N1 hemagglutinin binding with SA-[alpha]-2, 3-Gal and SA-[alpha]-2, 6-Gal. *BBRC.* **2006,** 347, (3), 662-668.

11. James, T. D.; Sandanayake, K. R. A. S.; Iguchi, R.; Shinkai, S., Novel saccharide-photoinduced electron transfer sensors based on the interaction of boronic acid and amine. *J. Am. Chem. Soc.* **1995,** 117, 8982-8987.

12. Eggert, H.; Frederiksen, J.; Morin, C.; Norrild, J. C., A new glucose-selective fluorescent bisboronic acid. First report of strong α-furanose complexation in aqueous solution at physiological pH. *J. Org. Chem.* **1999,** 64, 3846-3852.

13. Yamamoto, M.; Takeuchi, M.; Shinkai, S., Molecular design of a PET-based chemosensor for uronic acids and sialic acids utilizing a cooperative action of boronic acid and metal chelate. *Tetrahedron.* **1998,** 54, 3125-3140.

14. Kugimiya, A.; Takeuchi, T., Surface plasmon resonance sensor using molecularly imprinted polymer for detection of sialic acid. *Biosens. Bioelectron.* **2001,** 16, 1059-1062.

15. Patterson, S.; Bradley, S.; Taylor, R., Tuning the affinity of a synthetic sialic acid receptor using combinatorial chemistry. *Tetrahedron Lett.* **1998,** 39, 3111-3114.

16. Shi-Long, Z.; Reid, S.; Lin, N.; Wang, B., Microwave-assisted synthesis of ethynylarylboronates for the construction of boronic acid-based fluorescent sensors for carbohydrates. *Tetrahedron.* **2006,** 47, 2331-2335.

17. Andersen, J.; Madsen, U.; Bjorkling, F.; Liang, X., Rapid Synthesis of aryl azides from aryl halides under mild condition. *Synlett.* **2005,** 14, 2209-2213.

18. Drake, B.; Patek, M.; Lebl, M., Convenient of monosubstituted N,N'-di(Boc)-protected guanidines. *Synthesis.* **1994**, 579-582.

19. Rostovtsez, V.; Green, L.; Fokin, V.; Sharpless, K. B., A stepwise Huisgen cycloaddition process: Copper(I)-catalyzed regioselective "ligation" of azide and terminal alkynes. *Angew.Chem. Int. Ed.* **2002,** 41, (14), 2596-2599.

Chapter 4. Synthesis and Structure-activity Relationship and NMR Studies of a Series of Phenyl Alkyl ketone Analogs as Highly Potent and Selective PDE4D2 Inhibitors

Abstract: A new series of the phenyl alkyl ketones as PDE4D2 inhibitors were investigated. Seven compounds were identified to have sub-micromolar IC_{50} values. Among them, the most potent compounds **5q**, **5l**, and **5g** have IC_{50} values of 83, 170, and 200 nM respectively. Compound **5a** showed lower inhibition activity of 45 μM, but better selectivity (22 fold) over other PDE families (PDE9A2, HisPDE2A3, and PDE5A1) except for PDE7A1 when compared to genistein**.** Compound **5b** had similar inhibition activity as genistein but showed preference for PDE4D2 with selectivity of 285, 285, 142, and 42-fold over PDE7A1, PDE9A2, HisPDE2A3 and PDE5A1 respectively. Transfer NOESY studies indicated that the free **5e** and the bound inhibitor with PDE4D2 may have the same conformation.

4.1. Contributions

The goal of this project was to synthesize a new class of PDE4 enzyme inhibitors. Earlier designed PDE4 enzyme inhibitors have shown promising results but have therapeutic limitations due to their does-limiting side effects such as nausea and emesis. Such limitations arise from their poor selectivity among the different PDE families. Herein we have focused on the design and synthesis of novel enzyme inhibitors to target the subfamily of PDE4, i.e. PDE4D to enhance selectivity among families and reduce the side effects. Totally, 41 inhibitors were synthesized, among which 23 were synthesized by Dr. Shilong Zheng. Compounds that I have synthesized will be described further with their synthesis and inhibition activity and selectivity.

Dr. Ke at University of North Carolina carried out the inhibition assays and calculated the IC_{50} values. NMR studies were carried out by Dr. James Prestegard at University of Georgia. Molecular modeling on binding profile of inhibitors was carried by Dr. Minyong Li.

4.2. Introduction

Four decades ago, Sutherland and Rall first reported the hydrolytic activities of cyclic nucleotide phosphodiesterases (PDEs). They reported that PDEs can hydrolyze adenosine and guanosine 3′, 5′-cyclic monophosphates (cAMP and cGMP) to 5′-AMP and 5'-GMP in a variety of tissues[1] (Figure. 4.1). The second messengers cAMP and cGMP mediate the response of cells to a wide variety of hormones and neurotransmitters, and modulate many biological and metabolic processes, such as cardiac and smooth muscle contraction, platelet aggregation, secretion, apoptosis, and growth control.[2-8]

Intracellular cAMP and cGMP are synthesized respectively by adenylyl cyclase and guanylyl cyclase, [6] and hydrolyzed by PDEs.

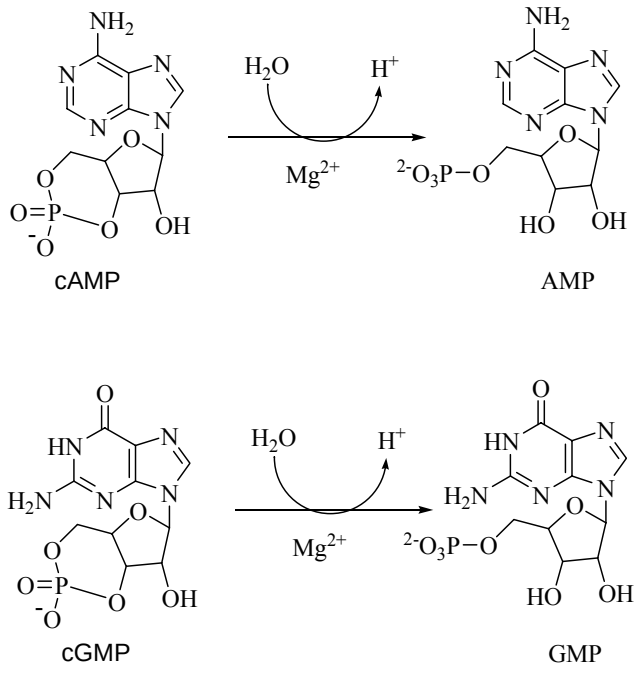

Figure 4.1. PDE- catalyzed hydrolysis of cAMP and cGMP

The human genome encodes twenty one PDE genes that are categorized into eleven families and subdivided into over sixty PDE isoforms. The discovery of PDEs families was first made during a study conducted from the crude tissue extracts eluted from the anion exchange column. Different fractions collected from the column indicated at least one kinetically distinct PDE and more significantly the amounts of PDE differ among various tissues.[9] Such a discovery led to the proposal of developing new selective inhibitors that could target specific diseases. Theophylline (**1**), a non selective PDE inhibitor, has been used for the treatment of asthma and other pulmonary diseases. The non-selective nature of theophylline not only produces side effects but also limits its use

in selectively inhibiting particular PDE in target tissues.[1] With the discovery of PDE families and some twenty crystal structures of PDEs available,[10] selective inhibitors of PDEs have been synthesized and studied as therapeutics for treatment of various human diseases. Successful examples include PDE5 (PDE family 5) inhibitors sildenafil (Viagra™), vardenafil (Levitra™), and tadalafil (Cialis™) for treatment of erectile dysfunction. PDE4 inhibitors have shown great potential for treatment of asthma and chronic obstructive pulmonary disease, but side effects such as emesis prevent their practical applications. It is generally believed and hypothesized that side effects of PDE4 inhibitors arise from inhibition of non-targeted PDE families or lack of selectivity against subfamilies PDE4A, B, C, and D. However, the molecular basis for family and subfamily selectivity of PDE4 inhibitors is poorly understood. This study was aimed at the design and synthesis therapeutically useful PDE4 subfamily inhibitors.

The nomenclature of the PDE families is as follow: Most families include more than one gene and sometimes numerous splice variants. Nomenclature of PDEs includes gene family designation (PDE isozyme 4) followed by the gene product (PDE4**D**) and lastly the splice variant (PDE4D**2**)

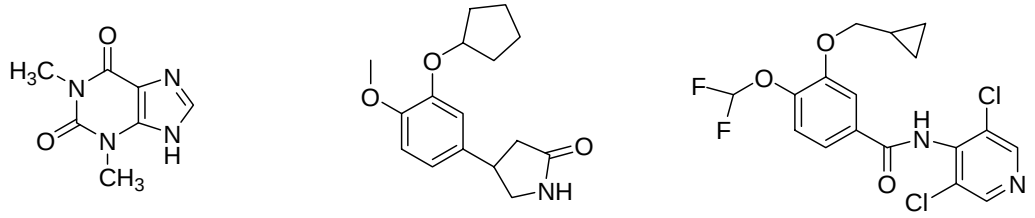

Theophylline (**1**) **Rolipram** (**2**) **Roflumilast** (**3**)

Figure 4.2. PDE4 Inhibitors

4.3. Substrate Selectivity

The homology of PDEs is categorized into three regions: conserved catalytic domain, the N-terminal, and the C-terminal region (Figure 4.3). The catalytic domain of all 11 families of PDE shares about 30 to 50% of amino acids. The C-terminal domain functions are unclear however the N-terminal region regulates various functions in PDEs. For example, in PDE2, the N-terminal contains the cGMP binding site whereas it has phosphorylation sites for various protein kinases in PDE1, PDE3, PDE4, and PDE5.[1] All PDEs contain a conserved catalytic domain, but each family possesses different substrate specificities and selective inhibitors. PDE 4, 7, and 8 prefer to hydrolyze cAMP while PDE 5, 6, and 9 are cGMP-specific. PDE 1, 2, 3, 10, and 11 enzymes show activity toward both nucleotides.[10] The conservation of the catalytic domain among the families predicts that the families would also share the same inhibitors. Indeed it has been reported that a selective inhibitor of PDE5, Viagra, has IC_{50} of 3.5 nM and it also shows inhibition for PDE4 with IC_{50} of 7.7 μM.[11]

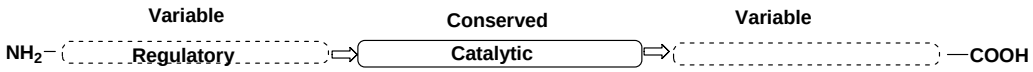

Figure 4.3. Different domains of PDEs[1]

4.4.1. Crystallographic data of PDEs

Crystal structures of PDEs typically contain a compact arrangement of 16 α helices which are arranged in three subdomains. An example of PDE crystal structure is shown in Figure 4.4, where the binding site domains are shown in blue and green colors.[12] The active site of enzyme consists of deep hydrophobic pocket located at the intersection of the three subdomains. The binding site domain consists of four regions: a) metal binding site (M), b) core pocket (Q), c) hydrophobic pocket (H), and d) lid region.[10] At the time of writing crystal structures of five families have been reported: PDEs 1, 3, 4, 5, and 9. Since the focus of this study is on PDE4, only crystal structures of PDE4 subfamilies will be discussed. The crystal structure of PDE4D shows a tetrameric formation, however a dimer for PDE4D has been proposed as the catalytic form based on crystal structure of PDE4D with zardavarine (PDED 4 inhibitor).[12] While PDE4B catalytic domain is a monomer, PDE4A have various oligomerization states from monomer, dimer, to tetramer. Aside from their distinct conformational states, the subtypes of PDE4 have distinct tissue and cellular distribution as well. Several studies have shown that the PDE4C is abundant in the neuronal tissue but absent in the inflammatory and immune cells.[13, 14] PDE4A has been shown to be distributed evenly in tissues[1] and PDE4B is expressed in heart, brain, skeletal muscle, and lung.[15] The *N*-terminal of PDE4A also

influences inhibitor potency for some of the PDE4 inhibitors. For example, a careful examination of PDE4A4 has shown that it coexists in two conformational states and rolipram (**2**), a known PDE4 inhibitor, prefers to bind one conformer over the other. Upon deletion of *N*-terminus the potency of rolipram is reduced by 10- to 30-fold.[16-18] In a similar example, the *N* terminal of PDE4D3 is a site for phosphorylation. The phosphorylation activates one conformer over the other of PDE4D3 and studies have indicated that rolipram binds to the phosphorylated conformer with higher affinity than the non phosphorylated conformer.[18, 19]

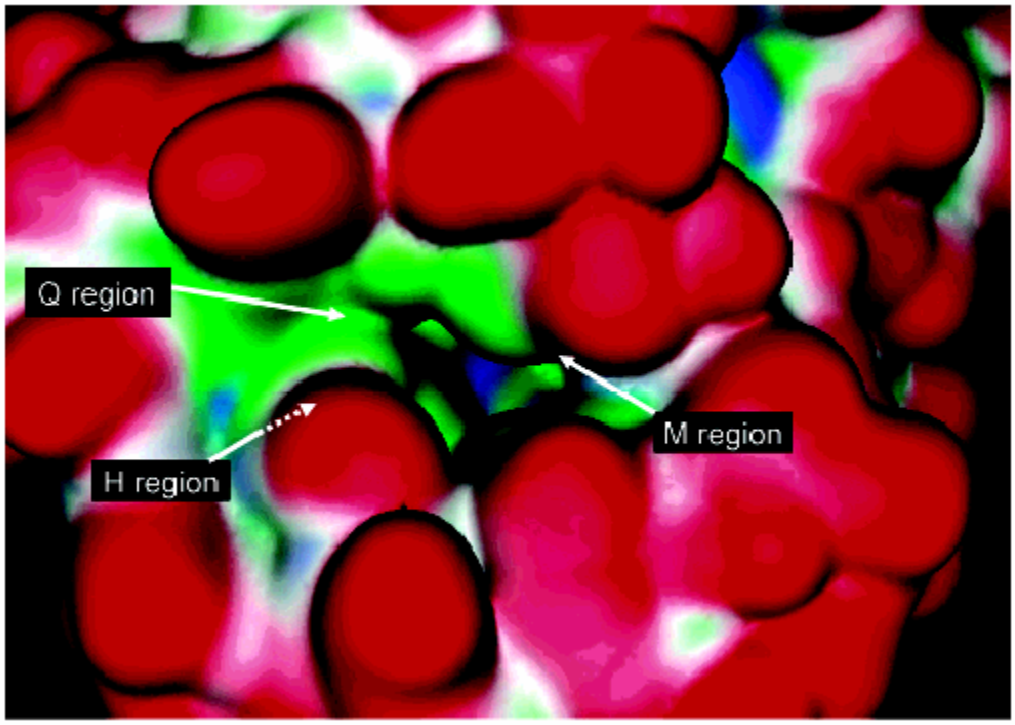

Figure 4.4. Surface plot of the crystal structure of PDE4D2. Blue indicates binding pocket hydrophilic areas and green hydrophobic areas. Binding subdomains are: core region (Q), metal region (M), and hydrophobic region (H).[10]

4.4.2. Design of new PDE4 inhibitors based on crystallographic data of rolipram

The complex structure of PDE4D2-rolipram showed that the binding residues for PDE4 inhibitor rolipram is absolutely conserved in the PDE4 subfamilies, thus suggesting that the subfamily selectivity is largely dependent on their conformational states.[12] The derivatives of rolipram account for a large percentage of the PDE4 inhibitors known and show encouraging results in clinical trials for treatment of asthma and chronic obstructive pulmonary disease (COPD). Roflumilast (**3**) is the best representative of these compounds and has been filed for Investigative New Drug application (IND) as a drug for COPD and asthma. Thus we synthesized our general-PDE4 selective inhibitors based on the rolipram core. Co-crystallized structure of the rolipram (**2**) with enzyme reveals that it forms two hydrogen bonds with the side chain of Gln369 and many hydrophobic interactions with the active site (Figure 4.5). The cyclopentyloxy group of rolipram occupies the hydrophobic pocket thus hydrophobic substitution can be made with groups such as a cyclopentane ring in new inhibitor design. The phenylmethoxy ring sits in the ditch shaped pocket. Thus only a planar ring can be used for the new PDE4 inhibitor. The methoxy group of the phenylmethoxy occupies the opening space. This open space has a little extra space for a slightly bigger group either polar or nonpolar to be substituted. The pyrrolidone ring does not make any significant interactions with the catalytic site; rather it is open to the adjacent metal pocket. Thus dramatic changes can be made to the pyrrolidone ring.[12]

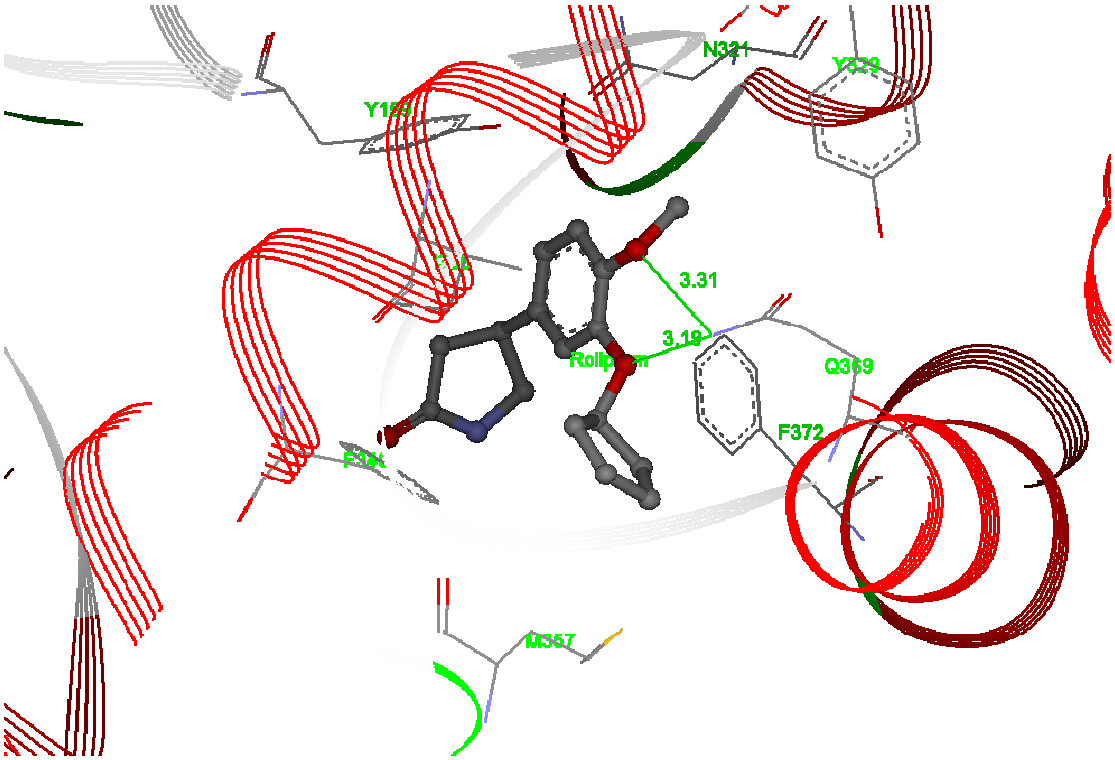

Figure 4.5. The key residues in the binding site of Rolipram to PDE4D2 X-ray model (PDB entry: 1OYN). The residues are represented as line and rolipram is shown in stick and ball. H-bond is represented as green line and distance (Å). The hydrogen atoms were removed for clarity.

4.5. Chemical synthesis of novel PDE4 inhibitors

Earlier studies have indicated that the alkoxy group in both 3 and 4 position are needed.[20] So in our designed analogs, various heteroatom based alkoxy groups were substituted on the 3-position via alkylation of **1** and **2a-2b** (Scheme 4.1). Alkylation of 3,4-dihydroxybenzaldehyde using chlorodifluoroacetate in the presence of $CsCO_3$ provided 4-difluoromethoxy-3-hydroxy benzaldehyde **2a** in 50% and 3,4-bis(difluoromethoxy)benzaldehyde **2b** as side product. The commercially available 3-hydroxy-4-methoxybenzaldehyde **2c** and 4-difluoromethoxy-3-hydroxy-benzaldehyde **2a** were reacted with various racemic alcohols (R_2OH) in THF via Mitsunobu reaction to

give racemic aldehydes **3a-e** in 38-40% yield. Treatment of aldehydes (**3a-e**) with either *n*-butyllithium, *t*-butyllithium or Grignard reagent gave the corresponding diastereomeric mixture of alcohols **4a-o**. The oxidization of the alcohol with PCC afforded the corresponding ketones **5a-o.**

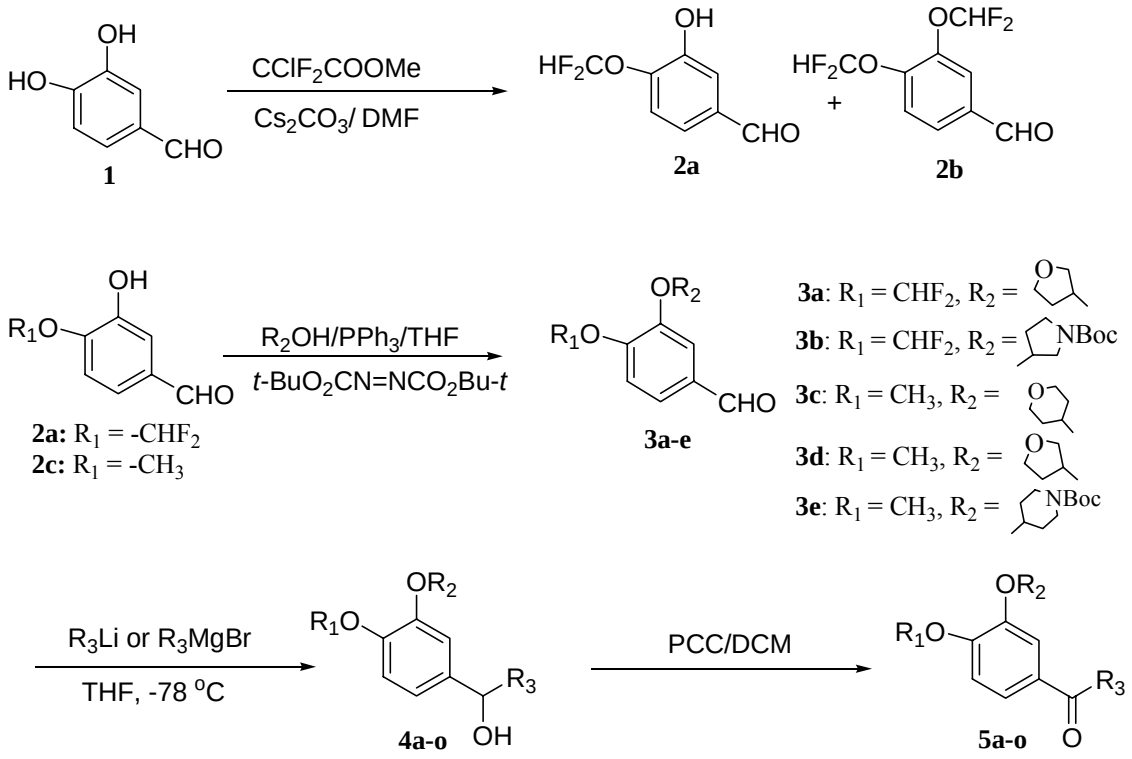

Scheme 4.1. Synthesis route to phenyl alkyl ketones

4.6. Structure activity relationship (SAR) of PDE4D inhibitors

The enzyme inhibitory activities of the synthesized compounds were evaluated against human PDE4D2 which had been cloned and expressed in *E. coli* strain BL21 (Codonplus). The results are summarized in Table 4.1 and 4.2. Table 4.1 also includes compounds (entries 1-4) that were synthesized by Dr. Shilong Zheng for comparison purposes and for the discussion of SAR

In Table 4.1, a few of the intermediates were tested along with the final compounds for their inhibition activity and it was found that the phenyl alkyl methanols (entries 1-2, 4) were 2 ~150 folds less potent than the corresponding phenyl alkyl ketones (entries 5-25). The 3-methoxy substituted phenyl compounds (entry 4) were 20 ~ 150 fold more potent than the corresponding 4-methoxy substituted compounds (entries 1-3). From the initial SAR results it was concluded that the new series of compounds should be substituted with 3-methoxy substitutent and that the ketones have higher inhibition activity than their corresponding alcohols (entry 2 and 3)

Table 4.1. IC_{50} (μM) values of PDE4D2 phenyl alkyl methanols and phenyl alkyl ketones inhibitors

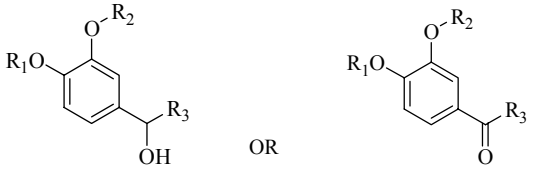

Entry	Compd		R_1	R_2	R_3	IC_{50} (μM)
1	4a	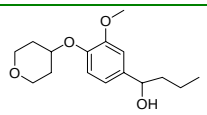		-CH_3	*n*-Pr	1500
2	4b	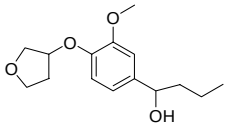		-CH_3	*n*-Pr	520
3	4c	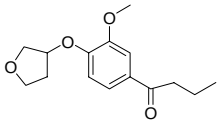		-CH_3	*n*-Pr	24
4	4d	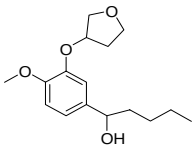	-CH_3		*n*-Bu	10

Table 4.2 shows the new series of compounds that were synthesized after the initial round of testing. The tetrahydrofuran-3-yloxy substituted phenyl compounds (entries 12-13) have 1.3 ~ 8.5 fold better activity than the corresponding tetrahydropyran-3-yloxy substituted phenyl compounds (entries 8-9). Upon chaging the tetrahydropyran ring to piperidine ring, both compounds **5d** and **5e**, the Boc protected piperidi-4-nyl (IC_{50} 4.8 μM) and the deprotected piperidi-4-nyl substituted (IC_{50} 102 μM) (entries 10 and 11) lost their activity and were 2 fold less active than the corresponding tetrahydropyran-3-

yloxy substituted phenyl compounds. Compared to the Boc protected compound (**5d**) the deprotected compound **5e** has lower inhibition activity.

In the series of the 4-methoxy-3-tetrahydrofuran-3-yloxy phenyl ketones (entries 12-20), the ketone with *i*-butyl side chain has the best activity (IC_{50} 176 nM) and the ketone (entry 13) with the *n*-butyl side chain has the second best activity (IC_{50} 200 nM). Upon increasing the side chain length for **5m**, the activity was lost (IC_{50} 380 nM). The activity of ketones (entries 16 and 17) with a cyclohexylalkyl chain and a phenylalkyl chain (entries 14 and 15) consistently showed the weakest activity. The replacement of tetrahydrofuran ring with the Boc protected tetrahydropyrrol (entries 21 and 22) decreased the activity to 380 nM and 30 μM, respectively. Again, among the Boc protected terahydropyrrol compounds (entries 21 and 23), the compound with *i*-butyl side chain had better activity (IC_{50} 380 nM) compared to its analog with *n*-butyl side chain (IC_{50} 30 μM). Upon deprotecting the Boc group, the n-butyl side chain analog of tetrahydropyrrol series had better activity (IC_{50} 1 μM, entry 22). However the acetyl protected tetrahydropyrrol gave the best activity with IC_{50} of 83 nM.

From the above SAR studies, ketones with alkyl chains and 3-tetrahydrofuran-3-yloxy group gave good activity. However upon substituting the 3-tetrahydrofuran-3-yloxy group with 3- acetyl protected tetrahydropyrrol the inhibition activity improved with IC_{50} of 83 nM which turned out to be the best inhibitor among the series of compounds synthesized.

Table 4.2. IC_{50} (μM) values of PDE4D2 phenyl alkyl ketones inhibitors

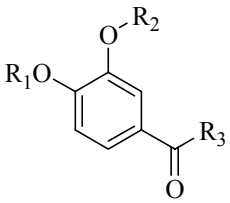

Entry	Compd		R_1	R_2	R_3	IC_{50} (μM)
7	5a	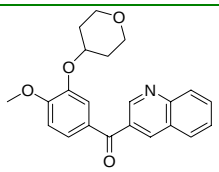	-CH_3		3-quinoline	45
8	5b	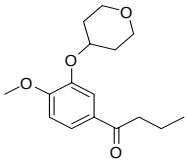	-CH_3		*n*-Pr	3.5
9	5c	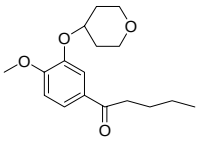	-CH_3		*n*-Bu	0.72
10	5d	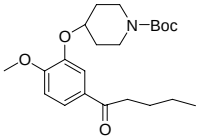	-CH_3	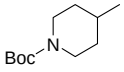	*n*-Bu	4.8
11	5e	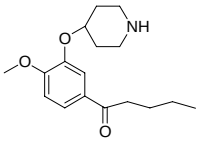	-CH_3	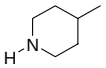	*n*-Bu	102
12	5f	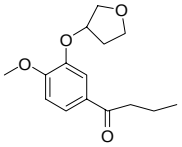	-CH_3		*n*-Pr	0.4

13	5g	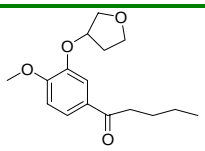	$-CH_3$		*n*-Bu	0.2
14	5h	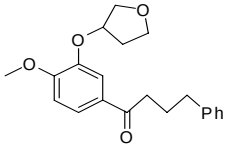	$-CH_3$		$-(CH_2)_3Ph$	2.3
15	5i	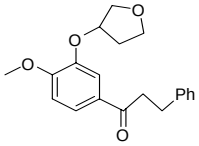	$-CH_3$		$-(CH_2)_2Ph$	2.6
16	5j	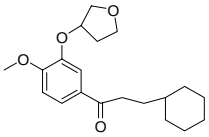	$-CH_3$		$(CH_2)_2$cyclohexyl	1.9
17	5k	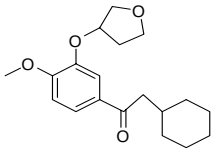	$-CH_3$		$-CH_2$-cyclohexyl	2.6
18	5l	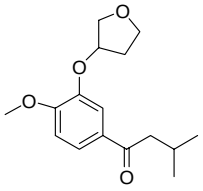	$-CH_3$		*i*-Bu	0.176
19	5m	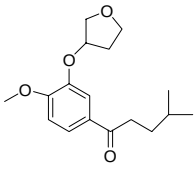	$-CH_3$		*i*-pen	0.380
20	5n	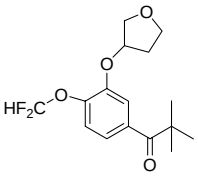	$-CHF_2$		*t*-Bu	0.410

21	5o	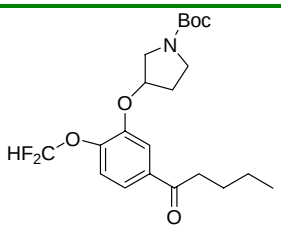	-CHF_2	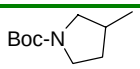	*n*-Bu	30
22	5p	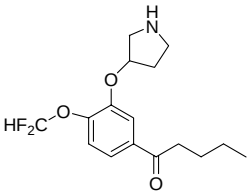	-CHF_2	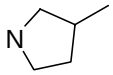	*n*-Bu	1.0
23	5q	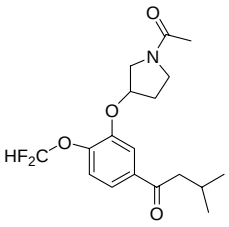	-CHF_2	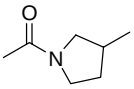	*i*-Bu	0.083

Two representatives of the found PDE4D2 inhibitors were tested in human PDE7A1, 9A2, 2A3 and 5A1 subtypes , which had been cloned and expressed in *E. coli* strain BL21(Codonplus) (Table 4.3). Compared with the low selectivity of Genistein, most of our compounds showed interesting PDE4D2 subtype specificities. For example, **5a** had lower inhibition activity but showed preference for PDE4D2 with selectivity of 11, 22, 22, and 22 fold over PDE7A1, PDE9A2, HisPDE2A3 and PDE5A1 respectively. Compound **5b** had similar PDE4D2 inhibitory activities (IC_{50} 3.5 μM) compared with Genistein (IC_{50} 3.2 μM), however, its selectivity over PDE7A1, PDE9A2, HisPDE2A3 and PDE5A1 was 14, 14, 12, and 5-fold higher than that of genistein, respectively.

Table 4.3. IC_{50} values (μM) of selected inhibitors with various PDEs

	PDE4D2 (79-438)	PDE7A1 (130-482)	PDE9A2 (181-506)	His-PDE2A3 (580-941)	PDE5A1 (535-860)
Genistein	3.2	70	70	40	30
5a	45	500	1000	1000	1000
5b	3.5	1000	1000	500	150

IC_{50}(μM) is about 1000 μM means no less of activity with 100 μM inhibitors

Among the 23 inhibitors that were synthesized, 7 inhibitors had better activity than rolipram (1μM). Selective inhibitors (**5m**, **5n**, and **5q**) were overlayed with rolipram (Figure 4.6) in the active site of the enzyme to study the conformation of inhibitors to the rolipram. All the three inhibitors **5m** (yellow), **5n** (green), and **5q** (blue) occupied the same binding pockets compared to rolipram (red) but with different conformation. Compared to the rolipram the three inhibitors had the alkyl chains extending towards the metal pocket compared to pyrrolidone ring of the rolipram, the closer proximity of the new inhibitors towards the metal pocket could have led to enhanced inhibition activity of the inhibitors.

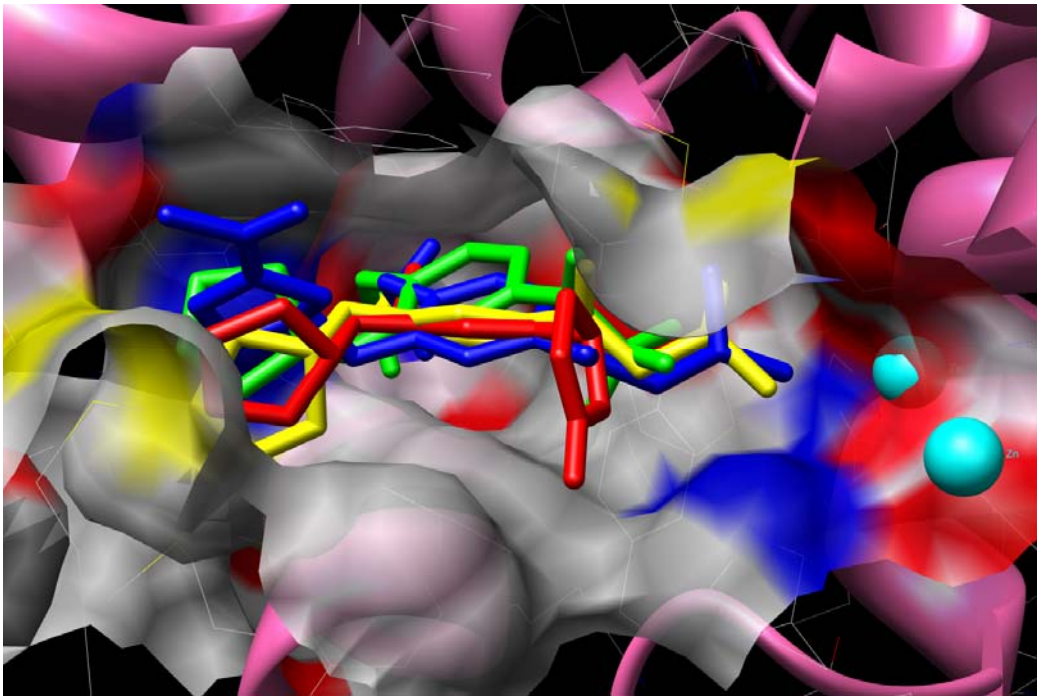

Figure 4.6. Overlay of the inhibitors **5m** (yellow), **5n** (green), and **5q** (blue) with rolipram into the PDE4D2 crystal

4.7. NMR study of the interaction of 5e with PDE4D2 protein

The interactions of inhibitor **5e** with PDE4D2 were studied with NMR. Saturation transfer difference (STD) and transfer nuclear Overhauser effect (trNOE) experiments were performed to demonstrate binding between PDE4D2 and the inhibitor **5e**. The binding epitope of the inhibitor was also determined. The solubility of **5e** up to 800 μM in D_2O was confirmed by NMR. A reference ^1H spectrum allowed assignment of resonances as indicated in Figure 4.7. A 2D NOESY spectrum was also obtained for the **5e** (Figure 4.8).

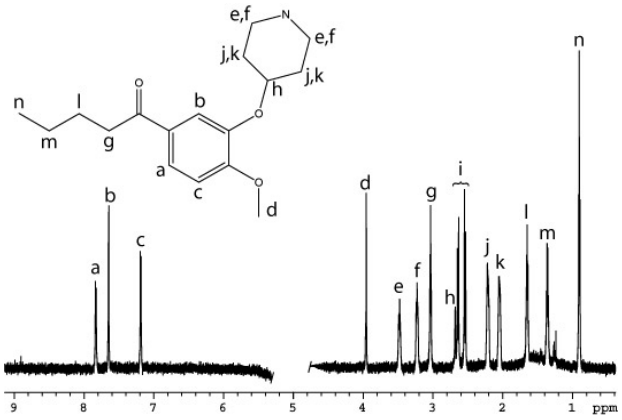

Figure 4.7. A reference and assignment of ^{1}H spectrum of 400 μM **5e**. The water peak in the center of the spectrum was removed for clarity. Note: Peak 'i' was not assigned and is believed to be a contaminant.

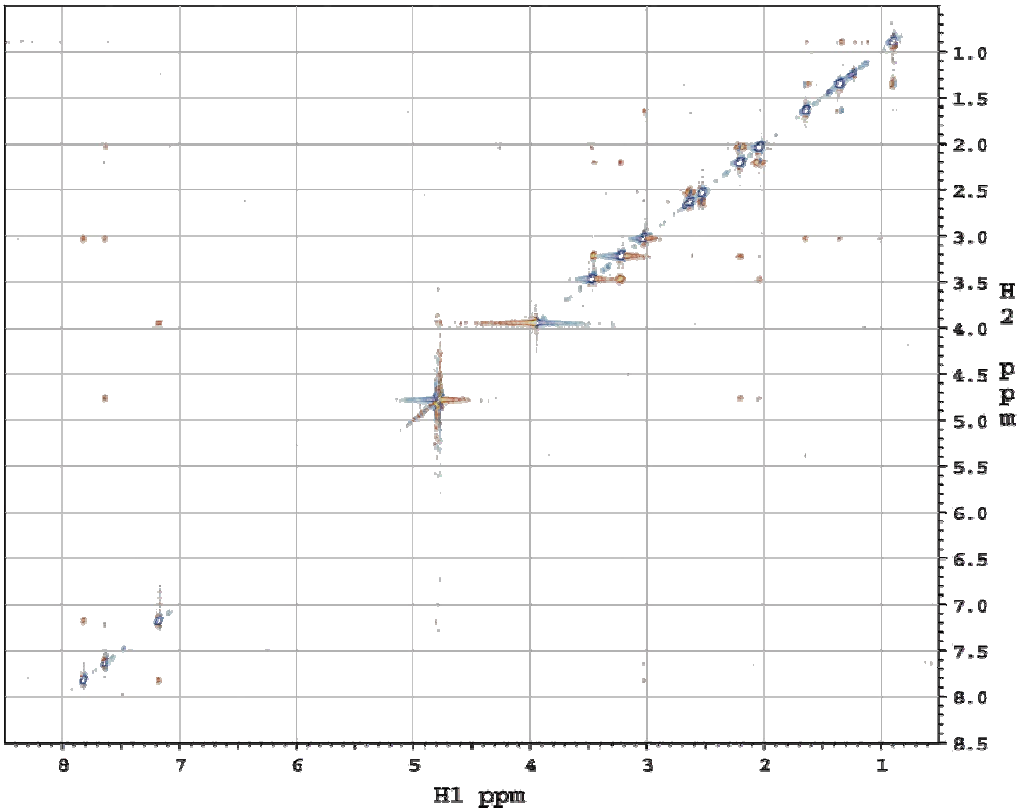

Figure 4.8. A 2D NOESY spectrum of 400 μM **5e** with 500 ms mixing time. Blue indicates positive peaks and red indicates negative peaks. The crosspeak intensities are negative indicating positive NOE's typical of small molecules free in solution.

The 800 μM STD spectrum of **5e** with the PDE4D2 shows changes in the spectrum (Figure 4.9). The different distribution of peak intensities can be seen as compared to the reference spectrum. For example, peak 'd' is depressed and peak 'n' enhanced relative to other peaks. This is due to close contact of protons assigned to these peaks with protons of the protein.

The trNOEsy spectra obtained are shown in Figure 4.10. The changes in signs were observed for the cross peaks relative to those in the reference NOESY spectra. This is indicative of dominance by the slowly tumbling bound form of the inhibitor. The appearance of similar cross peak sets to those seen in the reference NOESY spectrum is indicative of some similarity in the bound form as compared to the solution form of the inhibitor.

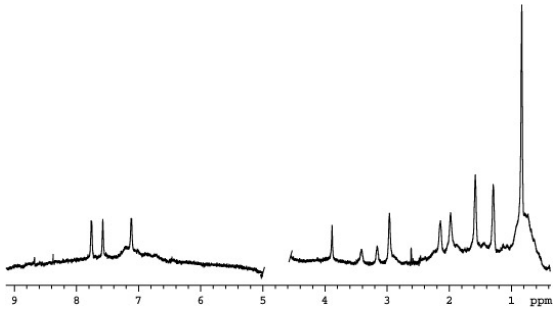

Figure 4.9. A STD spectrum of 800 μM **5e** and 10 μM PDE4D2. The protein was selectively saturated at 0.5 ppm with 250 ms of saturation. The protein background was not subtracted or suppressed. The water peak was removed for clarity.

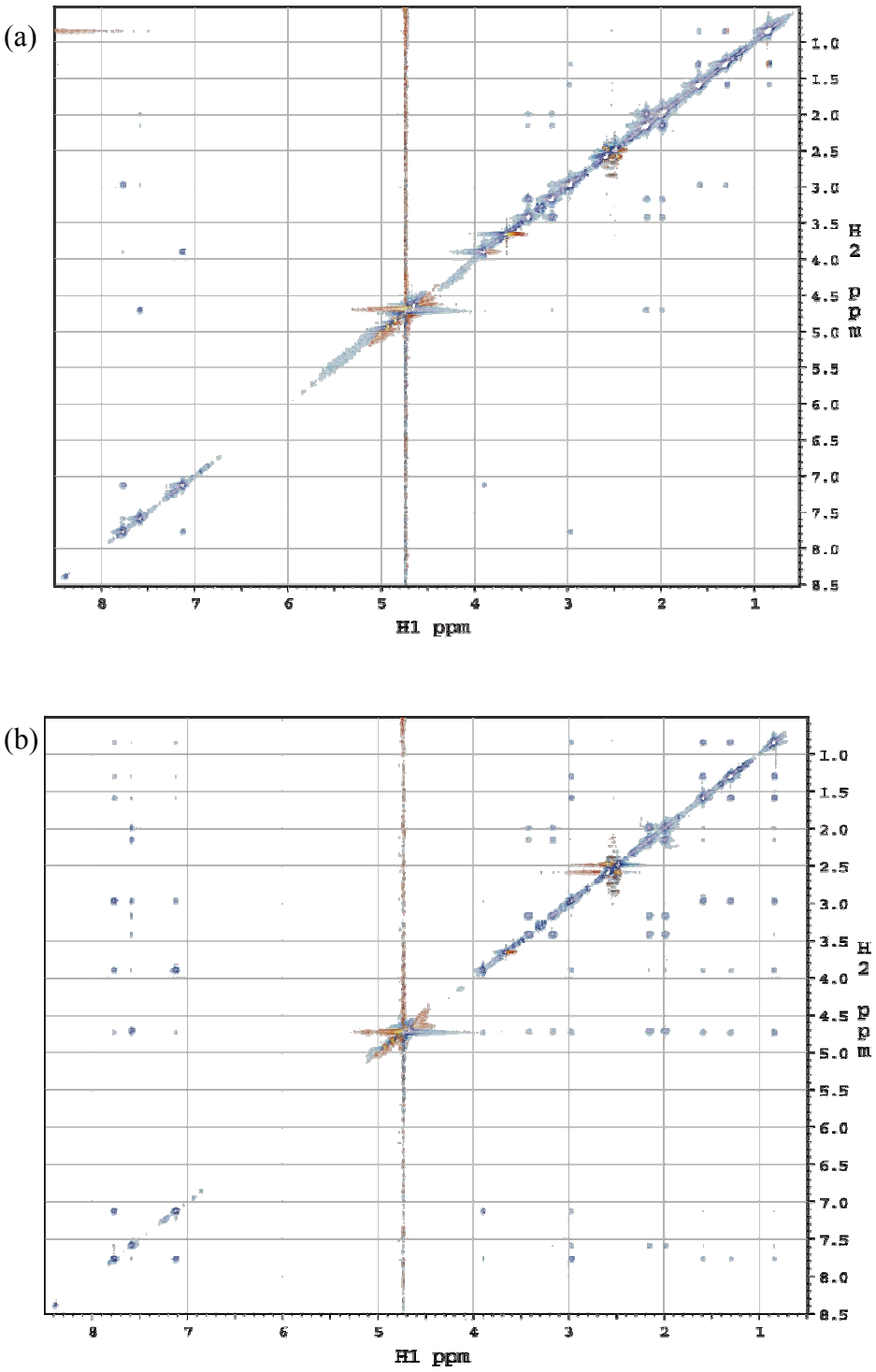

Figure 4.10. 2D NOESY spectra of 800 µM **5e** and 10 µM PDE4D2 with (a) 50 ms and (b) 300 ms mixing times. The crosspeaks have positive intensities (i.e. negative NOE's) which indicate that **5k** is binding PDE4D2.

Compound **5e** and PDE4D2 provide a near ideal system for the NMR study. The solubility of **5e** was high enough to prepare a sample for NMR detection, and the exchange rate with the protein was fast enough to perform STD and trNOE experiments. The binding epitope and interesting NOE's were observed. The peaks for **5e** in STD and NOESY spectra were assigned using the ^{1}H reference spectrum. The peak integrals from the reference and STD spectrum were compared and normalized to give a STD percentage for each proton (Figure 4.11). The STD percentages give an indication of which protons of bound **5e** are close to the protein, i.e. an epitope map. For **5e**, peak 'i' was not observed in the STD indicating that it does not bind PDE4D2 providing evidence that it is a contaminant. Non-specific binding was not observed for **5e** at the concentrations studied as evidenced by the STD of the diluted sample which showed a similar pattern of enhancements (data not shown).

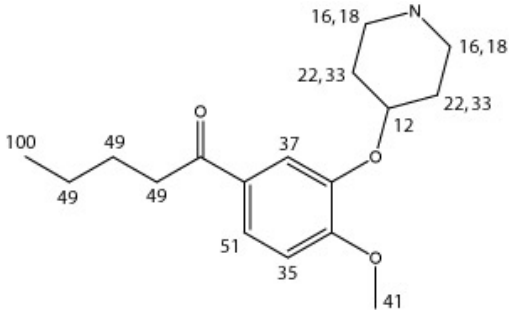

Figure 4.11. The STD percentage for each proton is shown for the **5e**.

NOESY spectra also gave useful information about the binding and structural conformation of small molecules. When compared to the reference NOESY spectrum of the inhibitor, the transferred NOESY spectrum of the inhibitor in the presence of the protein can indicate binding. Small molecules exhibit positive NOE's and large

molecules have negative NOE's. When a small molecule binds to a large molecule, such as a protein, its properties change and negative NOE's are observed. For **5e**, positive NOE's are observed for the sample of the inhibitor alone (Figure 4.8) and negative NOE's are observed for the samples in the presence of PDE4D2 (Figure 4.10). These results corroborate the STD results that **5e** binds to PDE4D2. Moreover, transferred NOESY spectra can provide information about the conformation of the bound inhibitor. The relative intensities of the NOESY crosspeaks can be used to calculate distances between protons. Qualitative information can be readily determined by looking at crosspeaks in the 50 ms transferred NOESY spectrum of **5e** in the presence of PDE4D2 (Figure 4.10a). For example, the crosspeaks observed from the aromatic protons show that peaks 'a' and 'b' are close in space to the methylene group, 'g', and peak 'c' is close to the methyl group, 'd'. In addition, peak 'b' is close to peaks 'j' and 'k' and to water. All of these interactions are also observed in the NOESY spectrum of the free inhibitor (Figure 4.8) indicating that the free and bound conformation may be the same. The NOE to the water molecule in the transferred NOESY spectrum indicates that water is accessible to the inhibitor in the bound state, demonstrating that water is in the binding pocket with the inhibitor or the bound state inhibitor is solvent-accessible on the side of the molecule.

4.8. Conclusions

A new series of the phenyl alkyl ketones as PDE4D inhibitors were investigated. Seven compounds were identified as having sub-micromolar IC_{50} values. Among them,

the most potent compounds **5q**, **5l**, and **5g** have IC_{50} values of 83, 170, and 200 nM, respectively. Compound **5a** showed lower inhibition activity of 45 μM, but better selectivity (22 fold) over other PDE families (PDE9A2, HisPDE2A3, and PDE5A1) except for PDE7A1 when compared to genistein**.** Compound **5b** had similar inhibition activity as to genistein but showed preference for PDE4D2 with selectivity of 285, 285, 142, and 42-fold over PDE7A1, PDE9A2, HisPDE2A3 and PDE5A1 respectively. Comparison of STD experiments of both free and bound inhibitor indicated that the methyl group of the butyl side chain was in close contact with the protein. Also the intensity of the methyl of methoxy group decreased in the bound form indicating binding to the protein. Transferred NOESY studies indicated that free **5e** and the bound inhibitor with PDE4D2 may have the same conformation, since the cross peaks observed from the aromatic protons matched the cross peaks observed in the free inhibitor. Cross peaks observed also showed that α methylene group and methoxy group were closer to the aromatic protons. It was also indicated that one of the aromatic proton was accessible to the water molecule in the binding pocket.

4.9. Experimental

4.9.1. General chemistry

All reagents were purchased from Acros and Aldrich. N-(*t*-butoxycarbonyl)-4-piperidinol was synthesized according to the procedure[1]. Microwave heating was performed in the single-mode microwave cavity of a Discover Synthesis System (CEM Co.), and all microwave-irradiated reactions were conducted in a heavy-walled glass vials sealed with Teflon septa. ^{1}H-NMR and ^{13}C-NMR were recorded at 400 and 100 MHz,

respectively, on a Bruker 400 NMR spectrometer. Combustion analyses and mass spectra were performed by the analytical and the mass spectrometry facilities at Georgia State University. Molecular modeling on binding profile of inhibitors was carried by Dr. Minyong Li. The inhibition constants (IC_{50}), the inhibitor concentration that produces 50% enzyme inhibition in the presence of substrate [S], were determined by Dr. Hingming Ke at University of Chapel Hill.

4.9.2. Determing Inhibiton Constants (IC_{50})

The inhibition constants (IC_{50}), the inhibitor concentration that produces 50% enzyme inhibition in the presence of substrate [S], were determined by equation 1. The activity of the substrates, cAMP and cGMP, were measured at eight different concentration and each measurement was repeated three times. V_{max} and K_m values were calculated by linear plot of Eadie-Hofstee (V/[S] vs. V) where V is velocity of reaction and [S] is concentration of substrate. In the linear plot the y intercept is equivalent to V_{max} and slope is equal to $-K_m$. The apparent inhibition constants (Kapp) were measured with LineWeaver-Burt plot in the presence of the inhibitors. The Ki values of the inhibitors were obtained form the plot of Kapp versus inhibitor concentration.

$$IC_{50} = (1+ [S]/K_m) K_i \qquad \text{Equation 1}$$

4.9.3. Preparation of 4-Difluoromethoxy-3-hydroxybenzaldehyde (2a) and 3,4-Bisdifluoromethoxybenzaldehyde (2b)

A mixture of 3,4-dihydroxybenzaldehyde (1.38 g, 0.01 mol), methyl chlorofluoroacetate (1.87 g, 0.013 mol) and cesium carbonate (4.24 g, 0.013 mol) in DMF (20 mL) was stirred at 65 °C for 3 h under an nitrogen atmosphere, then DMF was removed *in vacuo* and the residue was portioned between aqueous 3N HCl and ether. The aqueous layer was extracted three times with ether. The combined organic solution was washed with water and brine, dried over $MgSO_4$, filtered and evaporated. The residue was purified by flash chromatography to afford **2a** as a white solid (0.85 g, 45%) and **2b** as a yellowish liquid (0.48 g, 20%). (**2a**). ^{1}H NMR (400 MHz, $CDCl_3$): 6.17 (1H, s, br), 6.67 (1H, t, J = 72.8 Hz), 7.28 (1H, d, J = 8.4 Hz), 7.45 (1H, dd, J = 4.0 and 8.4 Hz), 7.55 (1H, d, J = 4.0 Hz), 9.92 (1H, s) ppm. ^{13}C NMR ($CDCl_3$): 115.6 (triplet, J = 262 Hz, d), 117.1 (d), 119.3 (d), 123.2 (d), 134.5, 143.0, 147.8, 191.1 (d) ppm. MS (EI): calcd for $C_8H_6F_2O_3$ (M^+): 188; found 188. (**2b**). ^{1}H NMR (400 MHz, $CDCl_3$): 6.63 (1H, t, J = 72.8 Hz), 6.68 (1H, t, J = 72.4 Hz), 7.43 (1H, dd, J = 8.8 Hz), 7.79 ~7.77 (2H, m), 9.95 (1H, s) ppm. ^{13}C NMR (100 MHz, $CDCl_3$): 115.3 ((d)t, J = 262 Hz), 115.5 ((d)t, J = 263 Hz), 121.4 (d), 128.7 (d), 134.1, 142.3, 147.1, 190.1 (d) ppm. MS (EI): calcd for $C_9H_6F_4O_3$ (M^+): 238; found 238.

4.9.4. General Procedure for the Synthesis of 3 by Mitsunobu Reaction of 2a and 2c with R_2OH

To the mixture of compounds **2** (1 mmol), R_2OH (1.1 mmol) and di-*tert*-butyl azodicarboxylate (1.2 mmol) in THF (5 mL), was added dropwise triphenylphosphine

(1.2 mmol) in THF (5 mL) at 0 °C. The resulting solution was stirred until the compound **2** consumed completely (usually for 24 h). The solvent was removed *in vacuo* and the residue was purified by flash chromatography to afford the product **3**.

4-Difluoromethoxy-3-(tetrohydro-furan-4-yloxy)-benzaldehyde (3a) Yield: 84%. ^{1}H NMR (400 MHz, $CDCl_3$): 2.19 (1H, m), 2.30 (1H, m), 3.91-4.06 (4H, m), 5.07 (1H, m), 6.67 (1H, t, J = 74.4 Hz), 7.33 (1H, d, J = 8.4 Hz), 7.44 (1H, d, J = 1.6 Hz), 7.48 (1H, dd, J = 1.6 and 8.4 Hz) 9.93 (1H, s) ppm. ^{13}C NMR ($CDCl_3$): 32.7 (t), 67.0 (t), 72.5 (t), 78.8 (d), 112.9 (d), 115.5 ((d) t, J = 260 Hz), 122.2 (d), 125.2 (d), 134.3, 145.6, 149.4, 190.5 (d) ppm. MS (EI): calcd for $C_{12}H_{12}F_2O_4$ (M^+):258; found 258.

***tert*-Butyl 3-(2-(difuloromethoxy)-5-formylphenoxy)pyrrolidine-1-carboxylate (3b)**. Yield: 26%. ^{1}H NMR (400 MHz, $CDCl_3$): 1.46 (9H, s), 2.20 (2H, d, J = 7.6 Hz), 3.65-3.49 (4H, m), 5.01 (1H, s), 6.59 (1H, (d)t, J = 74 Hz), 7.32 (1H, s), 7.45 (1H, s), 7.49 (1H, d, J = 8.4 Hz), 9.26 (1H, s) ppm. ^{13}C NMR (100 MHz, $CDCl_3$): 28.46, 31.53 (d), 44.00 (d), 51.47 (d), 79.72 (d), 113.54 (d), 122.53 (d), 125.64, 154.54, 190.55 ppm. HRMS (ESI+): calcd for $C_{13}H_{13}F_2NO_5$ (M^+-*t*-butyl) : 302.0840; found: 302.0823.

4-Methoxy-3-(tetrahydro-pyran-4-yloxy)-benzaldehyde (**3c**). Yield: 52%. ^{1}H NMR (400 MHz, $CDCl_3$): 1.84 – 1.86 (2H, q, J = 4.4, 4.4 Hz), 2.06 (2H, d, J = 8.8 Hz), 3.57 (2H, t, J = 9.2 Hz), 3.95 (3H, s), 4.05 (2H, m), 4.51 (1H, m), 7.01 (1H, d, J = 8.4 Hz), 7.44 (1H, s), 7.47 – 7.49 (1H, q, J = 1.6, 6.4 Hz) 9.84 (1H, s) ppm. ^{13}C NMR (100 MHz, $CDCl_3$): 31.86, 56.16, 65.31, 73.49, 111.25, 113.92, 127.15, 129.99, 147.09, 156.06, 190.80 ppm. HRMS (ESI+): calcd for $C_{13}H_{16}O_4$: 237.1127; found: 237.1121.

4- Methyoxy-3-(tetrahydro-furan-3-yloxy-benzaldehye (**3d**)**.** Yield: 40%. ^{1}H NMR (400 MHz, $CDCl_3$): 2.25 (2H, q, *J* = 6.0, 8.0 Hz), 3.94 (4H, d, *J* = 12 Hz), 4.04 (3H, d, *J* = 2.4 Hz), 5.02 (1H, s), 7.00 (1H, d, *J* = 8.0 Hz), 7.35 (1H, s), 7.48 (1H, q, *J* = 2.0, 6.4 Hz), 9.84 (1H, s) ppm. ^{13}C NMR (100 MHz, $CDCl_3$): 32.98, 56.16, 67.72, 72.91, 78.67, 111.07, 112.18, 127.21, 129.96, 147.58, 155.56, 190.73 ppm. HRMS (ESI+): calcd for $C_{12}H_{14}O_4$: 223.0970; found: 223.0965.

4-(5-Formyl-2-methoxy-phenoxy)-piperidine-1-carboxylic acid-*tert*-butyl ester (**3e**). Yield: 53%. ^{1}H NMR (400 MHz, $CDCl_3$): 1.47 (9H, s), 1.80 (2H, q, *J* = 3.2, 3.6 Hz), 1.95(2H, q, *J* = 4.0, 4.8 Hz), 3.30 (2H, m), 3.80 (2H, s), 3.94 (3H, s), 4.52 (1H, s), 7.01 (1H, d, *J* = 8.0 Hz), 7.44 (1H, s), 7.49 (1H, d, *J* = 8.0 Hz), 9.84 (1H, s) ppm. ^{13}C NMR (100 MHz, $CDCl_3$): 28.45, 30.61, 56.17, 74.20, 79.62, 111.26, 114.11, 127.21, 130.04, 147.16, 154.78, 156.13, 190.79 ppm. HRMS (ESI+): calcd for $C_{18}H_{25}NO_5$: 336.1811; found: 336.1814.

4.9.5. General Procedure for the Synthesis of 4 by Nucleophilic Addition to the Aldehydes 3

To aldehyde **3** (1 mmol) in THF (5 mL), was added dropwise the n-butyllithium or Grignard reagent at -78 °C. The resulting mixture was stirred overnight at -78 °C to rt and quenched with water. The aqueous layer was extracted three times with ethyl acetate. The combined organic solution was dried over $MgSO_4$, filtered and evaporated. The residue was purified by flash chromatography to afford **4**

.**1-[4-Methoxy-3-(tetrahydro-pyran-4 yloxy)-phenyl]-butan-1-ol** (**4b**). Yield 60%. ^{1}H NMR (400 MHz, $CDCl_3$): 0.92 (3H, t, *J* = 7.6 Hz), 1.44 (3H, m), 1.68 (1H, m), 1.87 (4H,

m), 2.01 (2H, m), 3.56-3.51 (2H, dd, *J* = 2.4, 8.8 Hz), 3.84 (3H, s), 4.03 (2H, m), 4.44 (1H, m), 4.59 (1H, s), 6.86 (1H, d, *J* = 8.4 Hz), 6.92 (1H, d, *J* = 8.4 Hz), 6.95(1H, s) ppm. ^{13}C NMR (100 MHz, $CDCl_3$): 13.97, 19.10, 32.12, 41.24, 56.05, 65.38, 73.80, 73.96, 112.10, 115.34, 119.66, 137.75, 146.40, 150.28 ppm. HRMS (ESI+): calcd for $C_{16}H_{22}O_3$ -H_2O: 263.1647; found: 263.1645.

1-[4-Methoxy-3-(tetrahydro-pyran-4-yloxy)-phenyl]-pentan-1-ol (**4c**). Yield 72%. ^{1}H NMR (400 MHz, $CDCl_3$): 0.88 (3H, t, *J* = 6.8 Hz), 1.25 (1.32 (3H, m), 1.65 (1H, m), 1.85 (4H, m), 2.01 (2H, s), 3.53 (2H, t, *J* = 8.8 Hz), 3.84 (3H, s), 4.01 (2H, t, *J* = 5.6 Hz), 4.43 (1H, d, *J* = 4.0 Hz), 4.57 (1H, s), 6.86 (1H, d, *J* = 8.4 Hz), 6.92 (1H, d, *J* = 8.4 Hz), 6.95 (1H, s) ppm. ^{13}C NMR (100 MHz, $CDCl_3$): 14.03, 22.58, 28.05, 32.10, 38.81, 56.02, 65.34, 73.76, 74.14, 112.09, 115.40, 119.69, 137.83, 146.35, 150.24 ppm. HRMS (ESI+): calcd for $C_{17}H_{27}O_4$– H_2O: 277.1804; found: 277.1795.

4-[5-(1-Hydroxy-pentyl)-2-methoxy-phenoxy]-piperidine-1-carboxylic acid *tert*-butyl ester (**4d**). Yield 84%. ^{1}H NMR (400 MHz, $CDCl_3$): 0.95 (3H, t, *J* = 7.2 Hz), 1.44 (2H, q, *J* = 7.2, 7.6 Hz), 1.47 (9H, s) 1.69 (4H, m), 1.73 (2H, s), 1.92-1.96 (2H, m), 2.91 (2H, t, *J* = 7.2 Hz), 3.23-3.29 (2H, m), 3.80 (2H, m), 4.63 (1H, s), 3.91 (3H, s), 4.50-4.51 (1H, m), 4.70-4.72 (1H, s), 6.92 (1H, d, *J* = 8.4 Hz), 7.57 (1H, d, *J* = 2 Hz), 7.60-7.63 (1H, dd, *J* = 2, 6.4 Hz) ppm. ^{13}C NMR (100 MHz, $CDCl_3$): 14.03, 22.59, 28.06, 28.45, 30.83, 38.79, 56.04, 74.28, 74.53, 79.52, 112.13, 115.49, 119.75, 137.72, 146.47, 150.37, 154.84 ppm. HRMS (ESI+): calcd for $C_{18}H_{25}NO_4$ - (H_2O+ *t*-butyl): 320.1862 found: 320.1882

1-[4-Methoxy-3-(tetrahydro-furan-3-yloxy)-phenyl]-butan-1-ol (**4e**)**.** Yield 40%. ^{1}H NMR (400 MHz, $CDCl_3$): 0.92 (3H, t, *J* = 7.2 Hz), 1.30 (1H, dd, *J* = 6.4, 9.6 Hz), 1.42 (1H, d, *J* = 7.2 Hz), 1.63 (1H, s), 1.81 (2H, bs), 2.19 (2H, m), 3.84 (2H, s), 3.90 (2H, s), 4.00 (3H, s), 4.60 (1H, s), 4.97 (1H, s), 6.89 (3H, m) ppm. ^{13}C NMR (100 MHz, $CDCl_3$): 13.97, 19.08, 33.07, 41.24, 56.08, 67.22, 73.01, 74.07, 78.88, 112.05, 113.66, 119.33, 137.68, 146.89, 149.70 ppm. HRMS (ESI+): calcd for $C_{15}H_{23}O_4$– H_2O: 249.1491; found: 249.1480.

1-[4-Methoxy-3-(tetrahydro-furan-3-yloxy)-phenyl]-pentan-1-ol (**4f**). Yield 41%. ^{1}H NMR (400 MHz, $CDCl_3$): 0.88 (3H, t, *J* = 6.4 Hz), 1.22-1.35 (4H, m), 1.65-1.77 (2H, m), 1.86 (1H, s), 2.18 (2H, d, *J* = 5.6 Hz), 3.84 (2H, s), 3.89-3.92 (1H, m), 4.00 (3H, s), 4.58 (1H, s), 4.96 (1H, s), 6.84-6.91 (3H, m) ppm. ^{13}C NMR (100 MHz, $CDCl_3$): 14.03, 22.59, 28.03, 33.04, 38.80, 56.05, 67.19, 72.98, 74.26, 78.83, 112.02, 113.65, 119.35, 137.76, 146.83, 149.62 ppm. HRMS (ESI+): calcd for $C_{16}H_{25}O_4$ – H_2O: 263.1647; found: 263.1643.

1-[4-Methoxy-3-(tetrahydro-furan-3-yloxy)-phenyl]-4-phenyl-butan-1-ol (**4g**)**.** Yield 20%. ^{1}H NMR (400 MHz, $CDCl_3$): 1.60 (1H, m), 1.74 (2H, m), 1.85 (2H, m), 2.18 (2H, m), 2.64 (2H,t, *J* = 6.4 Hz), 3.83 (3H, s), 3.90 (2H, m), 4.04 (3H, s), 4.60 (1H, m), 4.95 (1H, m), 6.83 (1H, d, *J* = 2 Hz), 6.84 (1H, s), 6.87-6.89 (1H, dd, *J* = 1.6, 1.6 Hz), 7.15 (3H, m), 7.25 (2H, d, *J* = 6.8 Hz) ppm. ^{13}C NMR (100 MHz, $CDCl_3$): 27.61, 33.07, 35.72, 38.51, 56.06, 67.22, 73.02, 74.17, 78.84, 112.01, 113.49, 119.36, 125.77, 128.30, 128.42, 137.39, 142.22, 146.92,149.73 ppm. HRMS (ESI+): calcd for $C_{21}H_{27}O_4$ – H_2O: 325.1804; found: 325.1792.

1-[4-Methoxy-3-(tetrahydro-furan-3-yloxy)-phenyl]-3-phenyl-propan-1-ol (**4h**). Yield 99%. ^{1}H NMR (400 MHz, $CDCl_3$): 1.96-2.00 (1H, m), 2.09 (1H, s), 2.11-2.18 (2H, m), 2.63-2.72 (2H, m), 3.83 (3H, s), 3.82 (3H, m), 3.85-3.90 (1H, m), 3.94-4.03 (3H, m), 4.59 (1H, t, *J* = 7.2 Hz), 4.93-4.95 (1H, m), 6.83 (1H, s), 6.85 (1H,s), 6.91 (1H, d, *J* = 8.4 Hz), 7.17 (3H, t, *J* = 4.4 Hz), 7.25-7.29 (2H, dd, *J* = 7.2, 7.6 Hz) ppm. ^{13}C NMR (100 MHz, $CDCl_3$): 32.14, 33.07, 40.49, 56.07, 67.22, 73.00, 73.49, 78.86, 112.08, 113.63, 119.41, 125.89, 128.42, 128.44, 137.35, 141.79, 146.92, 149.76 ppm. HRMS (ESI+): calcd for $C_{20}H_{25}O_4 - H_2O$: 311.1647; found: 311.1639. Anal. Calcd for $C_{20}H_{24}O_4$: C, 73.15; H, 7.37; found: C, 73.25; H, 7.56.

3-Cyclohexyl-1-[4-methoxy-3-(tetrahydro-furan-3-yloxy)-phenyl]-propan-1-ol (**4i**). Yield 70%**.** ^{1}H NMR (400 MHz, $CDCl_3$): 0.86 (2H, t, *J* = 12 Hz), 1.09-1.30 (7H, m), 1.61-1.69 (6H, m), 1.74-1.77 (2H, m), 2.16-2.20 (2H, m), 3.84 (3H, d, *J* = 2.8 Hz), 3.88-3.91 (1H, m), 4.54 (1H, d, *J* = 6.8 Hz), 4.96 (1H, s), 6.83-6.85 (2H, dd, *J* = 2.8,5.2 Hz), 6.70 (1H, d, *J* = 7.6 Hz) ppm. ^{13}C NMR (100 MHz, $CDCl_3$): 26.36, 26.65, 33.06, 33.35, 33.53, 36.43, 37.64, 56.06, 67.22, 73.01, 74.67, 78.84, 112.00, 113.60, 119.37, 137.67, 146.85, 149.66 ppm. HRMS (ESI+): calcd for $C_{20}H_{31}O_4 - H_2O$: 317.2117; found: 317.2112. Anal. calcd for $C_{20}H_{30}O_4$: C, 71.82; H, 9.04; Found: C, 71.92 ; H, 9.10.

2-Cyclohexyl-1-[4-methoxy-3-(tetrahydro-furan-3-yloxy)-phenyl]-ethanol (**4j**). Yield 55%. ^{1}H NMR (400 MHz, $CDCl_3$): 0.94 (2H, m), 1.20 (2H, m), 1.36 (1H, m), 1.48 (1H, m), 1.69 (7H, m), 2.18 (2H, m), 3.84 (3H, s), 3.90 (1H, m), 4.00 (2H, m), 4.71 (1H, s), 4.96 (1H, s), 6.83 (1H, s), 6.85 (1H, s), 6.92 – 6.89 (1H, q, *J* = 2.0, 6.0 Hz) ppm. ^{13}C NMR (100 MHz, $CDCl_3$): 26.17, 26.29, 26.56, 33.03, 33.07, 33.91, 34.29, 46.97, 56.07,

67.23, 71.79, 73.01, 78.86, 112.06, 113.59, 113.63, 119.27, 138.03, 146.88, 149.68 ppm. HRMS (ESI+): calcd for $C_{19}H_{28}O_4$-H_2O: 303.1960; found: 303.1975.

1-[4-Methoxy-3-(tetrahydro-furan-3-yloxy)-phenyl]-3-methyl-butan-1-ol (**4k**). Yield 34%. ^{1}H NMR (400 MHz, $CDCl_3$): 0.91-0.94 (6H, q, *J* = 4.4, 2.0 Hz), 1.24 (1H, s), 1.44-1.49 (1H, m), 1.64-1.72 (2H, m), 1.92 (1H, bs, O-H), 2.16-2.19 (2H, m), 3.83 (3H, s), 3.86-3.91 (1H, m), 3.97-4.02 (3H, m), 4.64-4.67 (1H, q, *J* = 5.6, 2.0 Hz), 4.94-4.97 (1H, m), 6.84 (1H, d, *J* = 8.4Hz), 6.86 (1H, *J* = 2 Hz), 6.91-6.89 (1H, dd, *J* = 2, 6.4 Hz) ppm. ^{13}C NMR (100 MHz, $CDCl_3$): 22.34, 23.09, 24.84, 33.04, 48.28, 56.06, 67.21, 72.41, 72.99, 78.85, 112.04, 113.62, 119.32, 137.96, 146.89, 149.68 ppm. HRMS (ESI+): calcd for $C_{16}H_{22}O_3$– H_2O: 263.1647; found: 263.1648.

1-(4-Methoxy-3-(tetrahydrofuran-3-yloxy)phenyl-4-methylpentan-1-ol (**4l**). Yield 68%. ^{1}H NMR (400 MHz, $CDCl_3$): 0.85-0.88 (6H, dd, *J* = 2.0, 4.4 Hz), 1.08-1.14 (1H, m), 1.25-1.33 (1H, m), 1.51-1.57 (1H, m), 1.62-1.81 (2H, m), 1.82 (1H, b, s), 2.15-2.20 (2H, m), 3.84 (3H, s), 3.87-3.93 (1H, m), 3.99-4.05 (3H, m), 4.56 (1H, t, *J* = 6.8 Hz), 4.95-4.99 (1H, m), 6.84-6.87 (2H, m), 6.89-6.92 (1H, dd, *J* = 6.0, 2.0 Hz) ppm. ^{13}C NMR (100 MHz, $CDCl_3$): 22.57, 27.99, 33.05, 33.07, 34.99, 36.93, 56.06, 67.22, 73.01, 74.66 78.85, 112.0, 113.57, 113.60, 119.37, 137.63, 146.87, 149.69 ppm. HRMS (ESI+): calcd for $C_{17}H_{26}O_4$-H_2O: 276.1801; found: 277.1797.

1-[4-Difluoromethoxy-3-(tetrahydro-furan-3-ylxoy)-phenyl]-2,2-dimethyl-propan-1-ol(**4m**). Yield 8.6%. ^{1}H NMR (400 MHz, $CDCl_3$): 0.92 (9H, d, *J* = 0.8 Hz), 1.95 (1H, s), 2.16-2.20 (2H, m), 3.90-3.92 (1H, m), 3.98-4.00 (3H, m), 4.36 (1H, s), 4.96 (1H, d, *J* = 2.0 Hz), 6.52 (1H, (d) t, *J* = 75.2 Hz), 6.85-6.87 (1H, dd, *J* = 2.0, 6.0 Hz), 6.89-6.91

(1H, dd, *J* = 2.0, 2.4 Hz), 7.11 (1H, d, *J* = 8.0 Hz) ppm. ^{13}C NMR (100 MHz, $CDCl_3$): 25.88, 29.71, 32.98, 33.02, 35.71, 67.16, 72.80, 72.83, 78.72, 81.73, 114.69 (t, *J* = 160 Hz), 120.96, 121.93, 140.05, 140.88, 148.17 ppm. MS (EI+): calcd for $C_{16}H_{22}F_2O_4$: 316; found: 316.

3[2-Difluoromethoxy-5-91-hydroxy-3-methyl-butyl)-phenoxy]-pyrrolidine-1-carboxylic acid *tert*-butyl ester (**4n**). Yield 14%. ^{1}H NMR (400 MHz, $CDCl_3$): 0.96 (6H, d, *J* = 6.4 Hz), 1.46 (9H, s), 1.69 (2H, m), 1.90 (1H, d, *J* = 2.8 Hz), 2.20 (2H, m), 3.57 (4H, m), 4.71 (1H, s), 4.94 (1H, s), 6.65 (1H, d(t), *J* = 75.2 Hz), 6.92 (1H, d, *J* = 6.8 Hz), 6.97 (1H, d, *J* = 1.2 Hz), 7.12 (1H, d, *J* = 6.4 Hz) ppm. ^{13}C NMR (100 MHz, $CDCl_3$): 14.1 (d), 22.6, 24.7, 28.4, 31.5, 43.6 (d), 48.5, 51.5 (d), 60.3, 72.1, 79.60, 113.5 (d, *J* = 14 Hz), 119.4, 122.9, 140.3 ppm. HRMS (ESI+): calcd for $C_{17}H_{21}F_2NO_4$- (H_2O + t-butyl) : 342.1515; found: 342.1159.

3-[2-Difluoromethoxy-5-(1-hydroxy-pentyl)-phenoxy]-pyrrolidine-1-carboxylic acid *tert*-butyl ester (**4o**). Yield 25%**.** ^{1}H NMR (400 MHz, $CDCl_3$): 0.89 (3H, t, *J* = 6.8 Hz), 1.36 (4H, m), 1.46 (9H, s), 1.73 (2H, m), 1.95 (1H, d, *J* = 2.8 Hz), 2.20 (2H, m), 3.67 (4H, m), 4.63 (1H, s), 4.93 (1H, s), 6.65 (1H, t, *J* = 75.2 Hz), 6.91 (1H, s), 6.96 (1H, d, *J* = 1.6 Hz), 7.12 (1H, d, *J* = 6.8 Hz) ppm. ^{13}C NMR (100 MHz, $CDCl_3$): 14.0, 22.55, 27.9, 28.47, 29.72, 30.82, 31.67, 39.02, 44.07, 51.08, 51.57, 74.02, 78.11, 79.61, 113.4, 119.4, 122.89 ppm. HRMS (ESI+): calcd for $C_{21}H_{31}F_2NO_5$: 416.2248; found: 416.2247.

4.9.6. General Procedure for the Synthesis of 5 by Oxidization of the Alcohols with PCC

To the solution of alcohol **4** (1 mmol) in dichloromethane (5 mL) was added PCC in portions. The resulting mixture was stirred at rt for 2 h. The solvent was removed *in vacuo* and the residue was purified by flash chromatography to afford **5**.

4-Methoxy-3-(tetrahydro-pyran-4-yloxy-phenyl]-quinolin-3-yl-methanone (**5a**). Yield 88%. ^{1}H NMR (400 MHz, $CDCl_3$): 1.85-1.92 (2H, m), 2.04 – 2.10 (2H, m), 3.53-3.59 (2H, m), 3.97 (3H, s), 4.02 (2H, t, *J* = 6.0 Hz), 4.00-4.05 (2H, m), 4.56 (1H, m), 6.97 (2H, d, *J* = 8.4 Hz), 7.45-7.47 (1H, dd, *J* = 2.0, 6.4 Hz), 7.58 (1H, d, *J* = 1.6 Hz), 7.65 (1H, t, *J* = 7.2 Hz), 7.86 (1H, t, *J* = 6.8 Hz), 8.21 (1H, d, *J* = 8.4 Hz), 8.54 (1H, d, *J* = 2.0 Hz), 9.27 (1H, d, *J* = 2.0 Hz) ppm.^{13}C NMR (100 MHz, $CDCl_3$): 29.72, 31.95, 56.19, 65.34, 73.75, 110.89, 117.15, 126.71, 127.60, 129.02, 129.51, 131.65, 138.27, 146.75, 150.27 ppm. MS (ESI+): calcd for $C_{22}H_{21}NO_4$: 363.1; found: 363.

1-[4-Methoxy-3-(tetrahydro-pyran-4-yloxy)-phenyl]-butan-1-one (**5b**). Yield 63%. ^{1}H NMR (400 MHz, $CDCl_3$): 1.02 (3H, t, *J* = 7.2 Hz), 1.78 - 1.73 (2H, q, *J* = 7.6, 6.4 Hz), 1.85 (2H, m), 2.05 (2H, d, *J* = 10.8 Hz), 2.89 (2H, t, *J* = 7.2 Hz), 3.55 (2H, t, *J* = 10 Hz), 3.92 (3H, s), 4.02 (2H, t, *J* = 6.0 Hz), 4.51 (1H, s), 6.91 (1H, d, *J* = 8.0 Hz), 7.57 (1H, s), 7.62 (1H, d, *J* = 8.4 Hz) ppm. ^{13}C NMR (100 MHz, $CDCl_3$): 13.95, 18.10, 32.00, 40.08, 56.07, 65.41, 73.70, 110.87, 115.63, 123.46, 130.33, 146.44, 154.84, 199.14 ppm. HRMS (ESI+): calcd for $C_{16}H_{22}O_4$: 279.1596; found: 279.1606.

1-[4-Methoxy-3-(tetrahydro-pyran-4-yloxy)-phenyl]-pentan-1-one (**5c**). Yield 75%. ^{1}H NMR (400 MHz, $CDCl_3$): 0.95 (3H, t, *J* = 7.2 Hz), 1.41 (2H, q, *J* = 7.2, 7.2 Hz), 1.72

(2H, q, *J* = 7.2, 7.2 Hz), 1.84 (2H, t, *J* = 4.4 Hz), 2.05 (2H, d, *J* = 10.0 Hz), 2.90 (2H, t, *J* = 7.2 Hz), 3.55 (2H, t, *J* = 9.2 Hz), 3.92 (3H, s), 4.03 (2H, d, *J* = 11.2 Hz), 4.52 (1H, s), 6.91 (1H, d, *J* = 8.0 Hz), 7.57 (1H, s), 7.62 (1H, d, *J* = 8.4 Hz) ppm. ^{13}C NMR (100 MHz, $CDCl_3$): 13.95, 22.52, 26.83, 31.99, 37.86, 56.04, 65.37, 73.68, 110.87, 115.67, 123.48, 130.27, 146.42, 154.83, 199.14 ppm. HRMS (ESI+): calcd for $C_{17}H_{25}O_4$: 293.1753; found: 293.1754. Anal. Calcd for $C_{17}H_{24}O_4.1/8\ H_2O$: C, 69.24; H, 8.23; found: C, 69.27; H, 8.61.

4-(2-Methoxy-5-pentanoyl-phenoxy)-piperidine-1-carboxylic acid *tert*-butyl ester (**5d**). Yield 75%.^{1}H NMR (400 MHz, $CDCl_3$): 0.95 (3H, t, *J* = 7.2 Hz), 1.42 (2H, q, *J* = 7.2, 7.6 Hz), 1.47 (9H, s), 1.69 -1.80 (4H, m), (1.94 (2H, m), 2.91 (2H, t, *J* = 7.6 Hz), 3.29 (2H, m), 3.82 (2H, m), 3.91 (3H, s), 4.51 (1H, m), 6.92 (1H, d, *J* = 8.4 Hz), 7.57 (1H, d, *J* = 2 Hz), 7.60 (1H, dd, *J* = 2, 6.4 Hz) ppm. ^{13}C NMR (100 MHz, $CDCl_3$): 13.95, 22.52, 26.83, 28.44, 30.69, 37.88, 56.03, 74.39, 79.55, 110.91, 115.90, 123.54, 130.30, 146.47, 154.79, 154.90, 199.15 ppm. HRMS (ESI+): calcd for $C_{22}H_{33}NO_5$: 392.2437; found: 392.2434.

1-[4-Methoxy-3-(piperidin-4-yloxy)-phenyl]-pentan-1-one (**5e**). Yield 96%. ^{1}H NMR (400 MHz, $CDCl_3$): 0.93 (3H, t, *J* = 7.2 Hz), 1.36-1.43 (2H, m), 2.15 (4H, d, *J* = 3.6 Hz), 2.91 (2H, t, *J* = 7.6 Hz), 3.33 (2H, d, *J* = 12 Hz), 3.53 (2H, s), 3.91 (3H, s), 4.66 (1H, t, *J* = 3.2 Hz), 6.95 (1H, d, *J* = 8.4 Hz), 7.56 (1H, d, *J* = 2 Hz), 7.66-7.69 (1H, dd, *J* = 2, 6.4 Hz) ppm. ^{13}C NMR (100 MHz, $CDCl_3$): 13.82, 22.43, 26.97 (d), 37.96, 40.48, 55.91, 70.00, 111.28, 113.98, 116.83, 117.24, 125.08, 129.99, 145.59, 155.60, 161.29 (d), 200.65 ppm. HRMS (ESI+): calcd for $C_{17}H_{26}NO_3$: 292.1913; found: 292.1900.

1-[4-Methoxy-3-(tetrahydro-furan-3-yloxy)-phenyl]-pentan-1-one (**5f**). Yield 92%.^{1}H NMR (400 MHz, $CDCl_3$): 0.95 (3H, t, *J* = 7.2 Hz), 1.43 (2H, q, *J* = 6.8, 7.2 Hz), 1.72 (2H, t, *J* = 6.8 Hz), 2.24 (2H, m), 2.91 (2H, t, *J* = 6.8 Hz), 3.92 (4H, s), 4.03 (3H, s), 5.03 (1H, s), 6.90 (1H, d, *J* = 7.6 Hz), 7.48 (1H, s), 7.61 (1H, d, *J* = 8 Hz) ppm. ^{13}C NMR (100 MHz, $CDCl_3$): 13.96, 22.54, 26.84, 33.01, 37.86, 56.07, 67.23, 72.97, 78.74, 110.72, 113.90, 123.30, 130.22, 146.90, 154.24, 199.10 ppm. HRMS (ESI+): calcd for $C_{16}H_{23}O_4$: 279.1596; found: 279.1598.

1-[4-Methoxy-3-(tetrahydro-furan-3-yloxy)-phenyl]-butan-1-one (**5g**). Yield 64%.^{1}H NMR (400 MHz, $CDCl_3$): 1.00 (3H, t, *J* = 7.2 Hz), 1.75 (2H, m), 2.24 (2H, m), 2.91 (2H, t, *J* = 7.2 Hz), 3.91 (4H, s), 4.06 (3H, s), 5.02 (1H, s), 6.91 (1H, d, *J* = 8.4 Hz), 7.48 (1H, s), 7.61 (1H, d, *J* = 8.4 Hz) ppm. ^{13}C NMR (100 MHz, $CDCl_3$): 13.98, 18.12, 33.03 (d), 40.08, 56.07, 67.25 (d), 72.99 (d), 78.77, 110.76 (d), 113.92, 123.31, 130.27 (d), 146.92, 154.28 (d), 198.95 ppm. HRMS (ESI+): calcd for $C_{15}H_{21}O_4$: 265.1440; found: 265.1436.

1-[4-Methoxy-3-(tetrahydro-furan-3-yloxy)-phenyl]-4-phenyl-butan-1-one (**5h**). Yield 80%. ^{1}H NMR (400 MHz, $CDCl_3$): 2.11(2H, d, *J* = 7.6 Hz), 2.24 (2H, d, *J* = 5.2 Hz), 2.76 (2H, t, *J* = 7.6 Hz), 2.96 (2H, t, *J* = 7.6 Hz), 3.94 (4H, s), 4.06 (3H, s), 6.92 (1H, d, *J* = 8.4 Hz), 7.26 (3H, d, *J* = 7.2 Hz), 7.30-7.35 (2H, q, *J* = 7.6, 4.8 Hz), 7.50 (1H, s), 7.60 (1H, d, *J* = 8 Hz) ppm. ^{13}C NMR (100 MHz, $CDCl_3$): 26.08, 33.00, 35.27, 37.22, 56.08, 67.24, 72.97, 78.71, 110.72, 113.77, 123.27, 125.95, 128.40, 128.54, 130.11, 141.75, 146.90, 154.30, 198.63 ppm. HRMS (ESI+): calcd for $C_{21}H_{25}O_4$: 341.1753; found: 341.1748.

1-[4-Methoxy-3-(tetrahydro-furan-3-yloxy)-phenyl]-3-phenyl-propan-1-one (**5i**). 98%.^{1}H NMR (400 MHz, $CDCl_3$): 2.21 (2H, s), 3.06 (2H, s), 3.25 (2H, s), 3.91 (4H, s), 4.02 (3H, s), 5.01 (1H, s), 6.89 (1H, d, *J* = 7.6 Hz), 7.21-7.30 (5H, m), 7.48 (1H, s), 7.60 (1H, d, *J* = 6.8 Hz) ppm. ^{13}C NMR (100 MHz, $CDCl_3$): 30.42, 33.00, 39.99, 56.08, 67.24, 72.96, 78.73, 110.74, 113.80, 123.27, 126.14, 128.45, 128.54, 129.98, 141.41, 146.93, 154.40, 197.72 ppm. HRMS (ESI+): calcd for $C_{20}H_{23}O_4$: 327.1596; found: 327.1609. Anal. Calcd for $C_{20}H_{22}O_4$: C, 73.60; H, 6.79; found: C, 73.57; H, 7.09.

3-Cyclohexyl-1-[4-methoxy-3-(tetrahydro-furan-3-yloxy)-phenyl]-propan-1-one (**5j**). Yield 95%. ^{1}H NMR (400 MHz, $CDCl_3$): 0.88-0.97 (2H, q, *J* = 11.6, 10 Hz),1.31 (4H, m), 1.76 (7H, m), 2.20 (2H, m), 2.90 (2H, t, *J* = 7.6 Hz), 3.90 (4H, s), 4.02 (3H, s), 5.01 (1H, s), 6.89 (1H, d, *J* = 8.4 Hz), 7.47 (1H, s), 7.60 (1H, d, *J* = 7.6 Hz) ppm. ^{13}C NMR (100 MHz, $CDCl_3$): 26.29, 26.58, 32.18, 33.01, 33.23, 35.69, 37.48, 56.07, 67.24, 72.98, 78.72, 110.71, 113.89, 123.29, 130.16, 146.89, 154.22, 199.38 ppm. HRMS (ESI+): calcd for $C_{20}H_{29}O_4$: 333.2066; found: 333.2067. Anal. Calcd for $C_{20}H_{28}O_4$: C, 72.26; H, 8.49; found: C, 71.95; H, 8.76.

2-Cyclohexyl-1-[4-methoxy-3-(tetrahydro-furan-3-yloxy)-phenyl]-ethanone (**5k**). Yield 78%. ^{1}H NMR (400 MHz, $CDCl_3$): 1.02 (2H, m), 1.29 (3H, m), 1.76 (5H, m), 1.96 (1H, m), 2.22 (2H, m), 2.76 (2H, d, *J* = 6.8 Hz), 3.91(1H, s), 4.03 (3H, s), 5.02 (1H, s), 6.90 (1H, d, *J* = 8.4 Hz), 7.47 (1H, d, *J* = 2.0 Hz), 7.60 (1H, q, *J* = 2.0, 6.4 Hz) ppm. ^{13}C NMR (100 MHz, $CDCl_3$): 26.18, 26.27, 33.01, 33.50, 34.96, 45.73, 56.08, 67.24, 72.99, 78.72, 110.68, 113.89, 123.45, 130.62, 146.88, 154.24, 198.76 ppm. HRMS (ESI+): calcd for $C_{19}H_{26}O_4$: 319.1909; found: 319.1911

1-[4-Methoxy-3-(tetrahydro-furan-3-yloxy)-phenyl]-3-methyl-butan-1-one (**5l**)**.** Yield 93%. ^{1}H NMR (400 MHz, $CDCl_3$): 0.99 (6H, d, *J* = 6.4 Hz), 2.19-2.28 (3H, m), 2.77 (3H, d, *J* = 6.8 Hz), 3.90 (4H, d, *J* = 4.8 Hz), 4.02 (3H, t, *J* = 3.6 Hz), 5.02 (1H, d, *J* = 3.2 Hz), 6.89 (1H, d, *J* = 8.4 Hz), 7.47 (1H, d, *J* = 1.6 Hz), 7.57-7.59 (1H, dd, *J* = 2.0, 1.6 Hz) ppm. ^{13}C NMR (100 MHz, $CDCl_3$): 22.82, 25.48, 29.70, 33.00, 47.01, 56.05, 67.23, 72.97, 78.72, 110.67, 113.87, 123.39, 130.54, 146.90, 154.24, 198.73 ppm. MS (EI+): calcd for $C_{16}H_{22}O_4$: 278; found: 278

1-[4-Methoxy-3-(tetrahydro-furan-3-yloxy)-phenyl]-4-methyl-pentan-1-one (**5m**)**.** Yield 93%. ^{1}H NMR (400 MHz, $CDCl_3$): 0.95 (6H, d, *J* = 6.0 Hz), 1.59-1.64 (3H, m), 2.19-2.25 (2H, m), 2.90 (2H, t, *J* = 7.6 Hz), 3.88-3.94 (4H, m), 4.02-4.06 (3H, m), 5.01-5.03 (1H, q, *J* = 2.4, 2.8 Hz), 6.91 (1H, d, *J* = 8.4 Hz), 7.48 (1H, d, *J* = 1.6 Hz), 7.59-7.62 (1H, dd, *J* = 6.8, 1.6 Hz) ppm. ^{13}C NMR (100 MHz, $CDCl_3$): 22.46, 27.90, 29.70, 33.00, 33.64, 36.16, 56.05, 67.22, 72.97, 78.72, 110.71, 113.88, 123.29, 130.15, 146.90, 154.23, 199.28 ppm. MS (EI+): calcd for $C_{17}H_{24}O_4$: 292; found: 292.

1-[4-Difluoromethoxy-3-(tetrahydro-furan-3-yloxy0-phenyl]-2,2-dimethyl-propan-1-one (**5n**). Yield 81%. ^{1}H NMR (400 MHz, $CDCl_3$): 1.36 (9H, s), 2.19-2.25 (2H, m), 3.91-3.95 (1H, m), 3.99-4.03 (3H, m), 5.00 (1H, s), 6.59 (1H, t, *J* = 74.8 Hz), 7.18 (1H, d, *J* = 8.4 Hz), 7.30 (1H, d, *J* = 2.0 Hz), 7.40-7.42 (1H, dd, *J* = 2.0, 1.6 Hz) ppm. ^{13}C NMR (100 MHz, $CDCl_3$): 28.15, 29.71, 32.96, 44.22, 67.16, 72.81, 78.94, 115.84 (d, *J* = 36 Hz), 121.77 (d), 136.04, 148.72, 206.85 ppm. MS (EI+): calcd for $C_{16}H_{20}F_2O_4$: 314; found: 314

3-(2-Difluoromethoxy-5-pentanoyl-phenoxy)-pyrrolidine-1-carboxylic acid *tert*-butyl ester (**5o**)**.** Yield 96%. ^{1}H NMR (400 MHz, $CDCl_3$): 0.95 (3H, t, J = 7.2 Hz), 1.46 (9H, s), 1.58-1.71 (3H, m), 2.20 (3H, m), 2.90 (2H, s), 3.54-3.62 (4H, m), 5.01 (1H, s), 6.62 (1H, t, J = 74.4 Hz), 7.23 (1H, s), 7.56 (2H, s) ppm. ^{13}C NMR (100 MHz, $CDCl_3$): 14.00, 22.55, 27.90, 28.47, 30.82 (t), 39.02, 44.07(d), 51.57(d), 74.02, 78.11, 79.61, 113.87 (d, J = 272 Hz), 119.40, 122.89, 130.54, 146.90, 154.24, 198.73 ppm. HRMS (ESI+): calcd for $C_{16}H_{21}F_2NO_3$ – (*t*-butyl): 314.1567; found: 314.1758

1-[3-(1-Acetyl-pyrrolidin-3-yloxy)-4-difluoromethoxy-phenyl]-3-methyl-butan-1-one (**5q**). Yield 46%. ^{1}H NMR (400 MHz, $CDCl_3$): 0.99 (6H, d, J = 5.2 Hz), 2.10 (3H, s), 2.19 (1H, s), 2.26 (2H, s), 2.79 (2H, s), 3.60-3.88 (4H, m), 5.01 (1H, s), 6.53 (1H, (d)t, J = 74.0 Hz), 7.22 (1H, d, J = 8.4 Hz), 7.57 (2H, d, J = 8.0 Hz) ppm. ^{13}C NMR (100 MHz, $CDCl_3$): 22.19 (d), 22.65, 25.22, 30.33 (t), 45.32 (t), 52.80 (d), 78.50, 89.64, 100.83, 115.87 (d, J = 272 Hz), 121.98 (d), 122.82 (d), 135.85, 171.15, 198.29 ppm. MS-EI: calcd for $C_{18}H_{23}F_2NO_4$: 355; found: 356

References

1. Torphy, T. J., Phosphodiesterase Isozymes Molecular Targets for the Novel Antiasthma Agents. *Am J Respir Crit Care Med* **1998,** 157, 351-370.

2. Houslay, M. D.; Schafer, P.; Zhang, K. Y. J., Phosphodiesterase-4 as a therapeutic target. *Drug Discovery Today* **2005,** 10, (22), 1503-1519.

3. Pelligrino, D.; Wang, Q., Cyclic nucleotide crosstalk and the regulation of cerebral vasodilation. *Prog Neurobiol* **1998,** 56, 1-18.

4. Antoni, F., Molecular Diversity of cyclic AMP Signaling. *Front. Neuroendocrin* **2000,** 21, 103-132.

5. Carvajal, J.; Germain, A.; Huidobro-Toro, J.; Weiner, C., Molecular Mechanism of cGMP-Mediated Smooth Relaxation. *J. Cell. Physiol* **2000,** 184, 409-420.

6. Lucas, K.; Pitari, G.; Kazerounian, S.; Ruiz-Stewart, I.; Park, J.; Schulz, S.; Chepenik, K.; Waldman, S., Guanylyl Cyclases and Signaling by Cyclic GMP. *Pharmacol. Rev* **2000,** 52, 375-414.

7. Klein, C., Nitric oxide and the other cyclic nucleotide. *Cell Signaling* **2002,** 14, 493-498.

8. Chin, K.; Yang, W.; Ravatn, R.; Kita, T.; Reitman, E.; Vettori, D.; Cvijic, M.; Shin, M.; Iacono, L., Reinventing the Wheel of Cyclic AMP: Novel Mechanism of cAMP signaling. *Ann N Y Acad Sci* **2002,** 968, 49-64.

9. Appleman, M. M.; Thompson, W. J.; Russell, T. R., *Cyclic Nucleotide Phosphodiesterases.* ed.; Raven Press: New York, 1973; 'Vol.' p 65-96.

10. Manallack, D. T.; Hughes, R. A.; Thompson, P. E., The next generation of phosphodiesterase inhibitors: structural clues to ligand and substrate selectivity of phosphodiesterases. *J. Med. Chem.* **2005,** 48, (10), 3449-3462.

11. Corbin, J. D.; Francis, S. H., Pharmacology of Phosphodiesterase-5 inhibitors. *Int. J. Clin. Pract* **2002,** 56, 453-459.

12. Huai, Q.; Wang, H.; Sun, Y.; Kim, H.-Y.; liu, Y.; Ke, H., Three- Dimensional Structures of PDE4D in Complex with Roliprams and Implication on Inhibitor Selectivity. *Structure* **2003,** 11, 865-873.

13. Sullivan, E.; Muller, T.; Lubbert, H., Molecular cloning and functional expression in yeast of a human cAMP-specific phosphodiesterase subtypes (PDE IV-C). *FEBS Lett* **1995,** 358, 305-310.

14. Fichtel, E.; Lubbert, H., Expression and regulation of human and rat phosphodiesterase type IV isogenes. *FEBS Lett* **1994,** 350, (291-295).

15. McLaughlin, M. M.; Cieslinski, L. B.; Burman, M.; Torphy, T. J.; Livi, G. P., A low-K_m rolipram-sensitive, cyclic AMP-specific phosphodiesteraase from human brain: cloning and expression of cDNA, preliminary biochemical characterization and tissue distribution of mRNA. *J.Biol.Chem* **1993,** 268, 6460-6476.

16. Muller, E.; Fozard, J. R., Subtypes of the Type 4 cAMP Phoshpodiesterases: Structure, Regulation and Selective Inhibitor. *Trends Pharm. Sci* **1996,** 17, 294-298.

17. Jacobitz, S.; McLaughlin, M. M.; Livi, G. P.; Burman, M.; Torphy, T. J., Mapping the Functional Domains of Human Recombinant Phosphodiesterase 4A: Structural Requirments for Catalytic Activity and Rolipram Binding. *Mol. Pharmacol* **1996,** 50, 891-899.

18. Sette, C.; Conti, M., Phosphorylation and Activation of a cAMP-Specific Phosphodiesterase by the cAMP-Dependent Protein Kinase: Involvment of Serine 54 in the enzyme activation. *J.Biol.Chem* **1996,** 271, 16526-16534.

19. Sette, C.; Vicini, E.; Conti, M., The Short-term activation of a rolipram-sensitive, cAMP-specific Phosphodiesterase by Thyroid-Stimulating Hormone in Thyroid FRTL-5 Cells in Mediated by a cAMP- Dependent Phosphorylation. *J. Biol.Chem* **1994,** 269, 9245-9252.

20. Marivet, M.; Bourguignon, J.; Lugnier, C.; Mann, A.; Stoclet, J.; Wermuth, C., Inhibition of cyclic Adenosine-3',5' -monophophate Phosphodiesterase from Vasular Smooth Muscle by Rolipram Analogues. *J. Med. Chem.* **1989,** 32, 1450-1457.

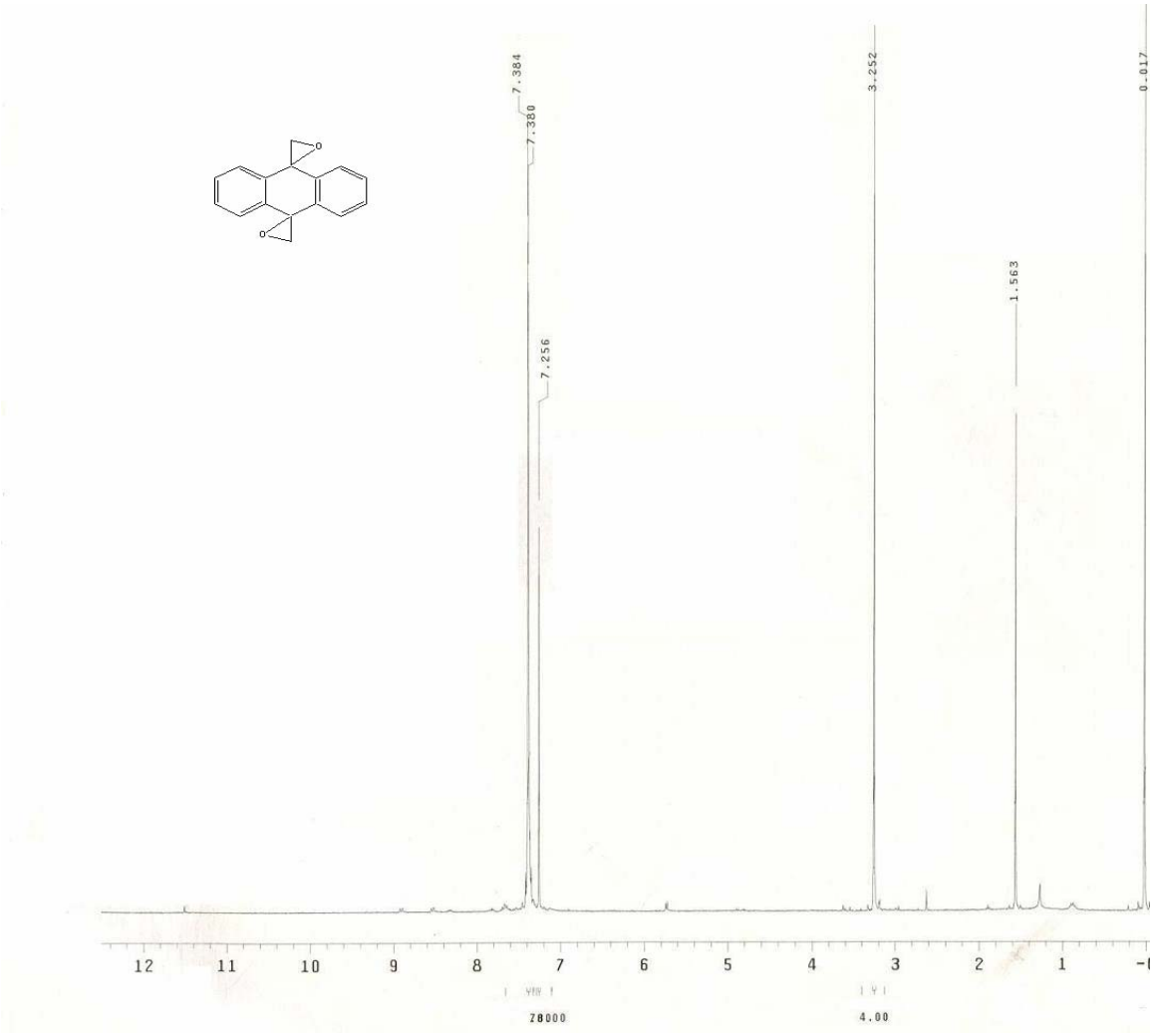
7.384
7.380
7.256
3.252
1.563
0.017
12
11
10
9
8
7
6
5
4
3
2
1
28000
4.00

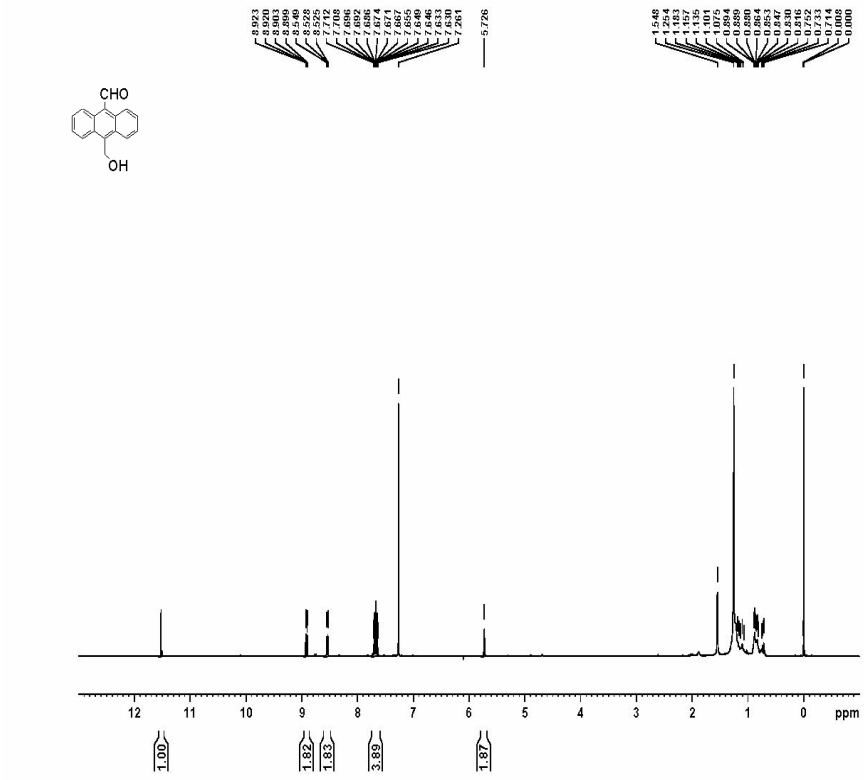
8.923
8.920
8.903
8.899
8.549
8.526
8.525
7.712
7.708
7.698
7.692
7.686
7.674
7.671
7.867
7.855
7.649
7.646
7.633
7.630
7.261
5.726
1.548
1.254
1.183
1.157
1.135
1.101
1.075
0.894
0.889
0.880
0.864
0.853
0.847
0.530
0.516
0.753
0.733
0.714
0.000
0.000
CHO
OH
12
11
10
9
8
7
6
5
4
3
2
1
0
ppm
1.00
1.82
1.83
3.89
1.87

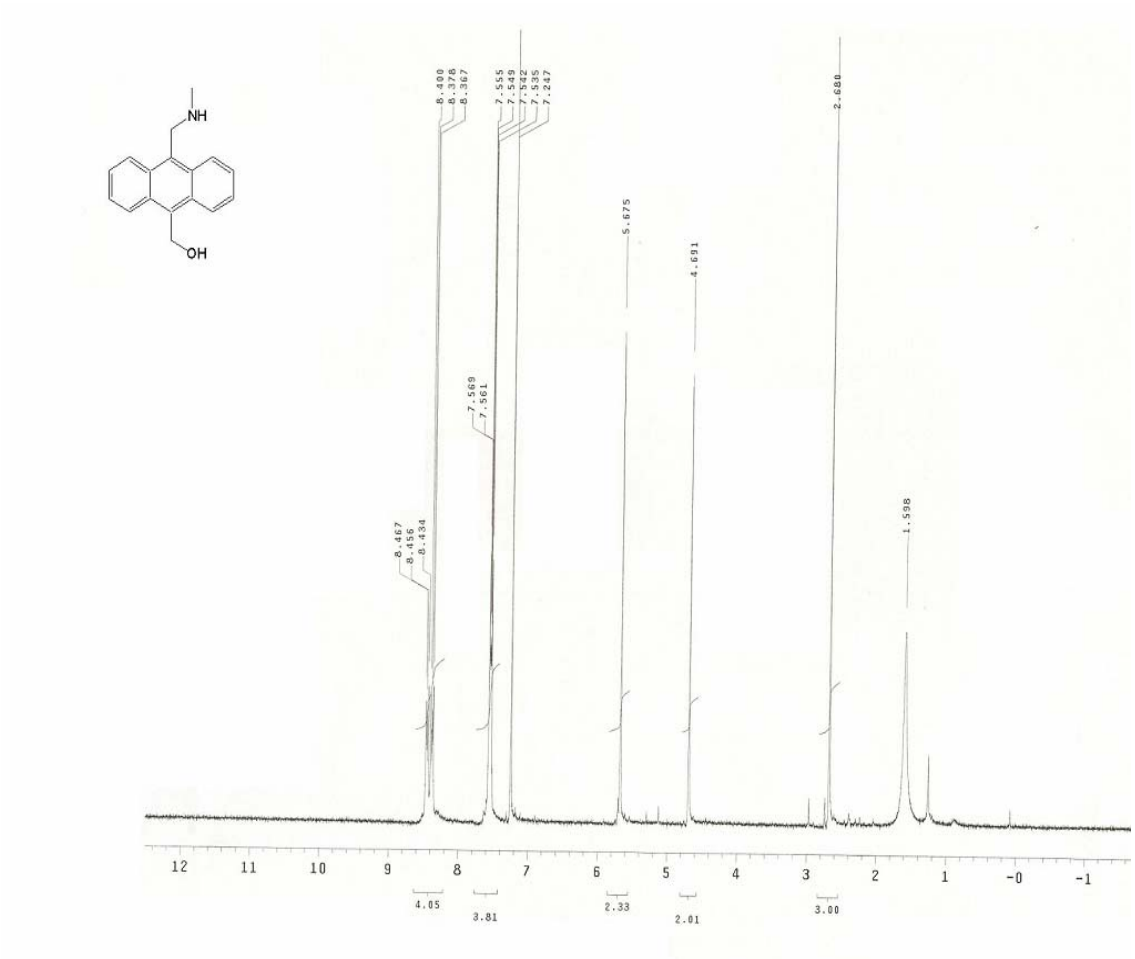
NH
OH
8.490
8.378
8.367
7.555
7.549
7.542
7.535
7.247
2.680
5.675
4.691
7.569
7.561
8.467
8.456
8.434
1.598
12
11
10
9
8
7
6
5
4
3
2
1
-0
-1
4.05
3.81
2.33
2.01
3.00

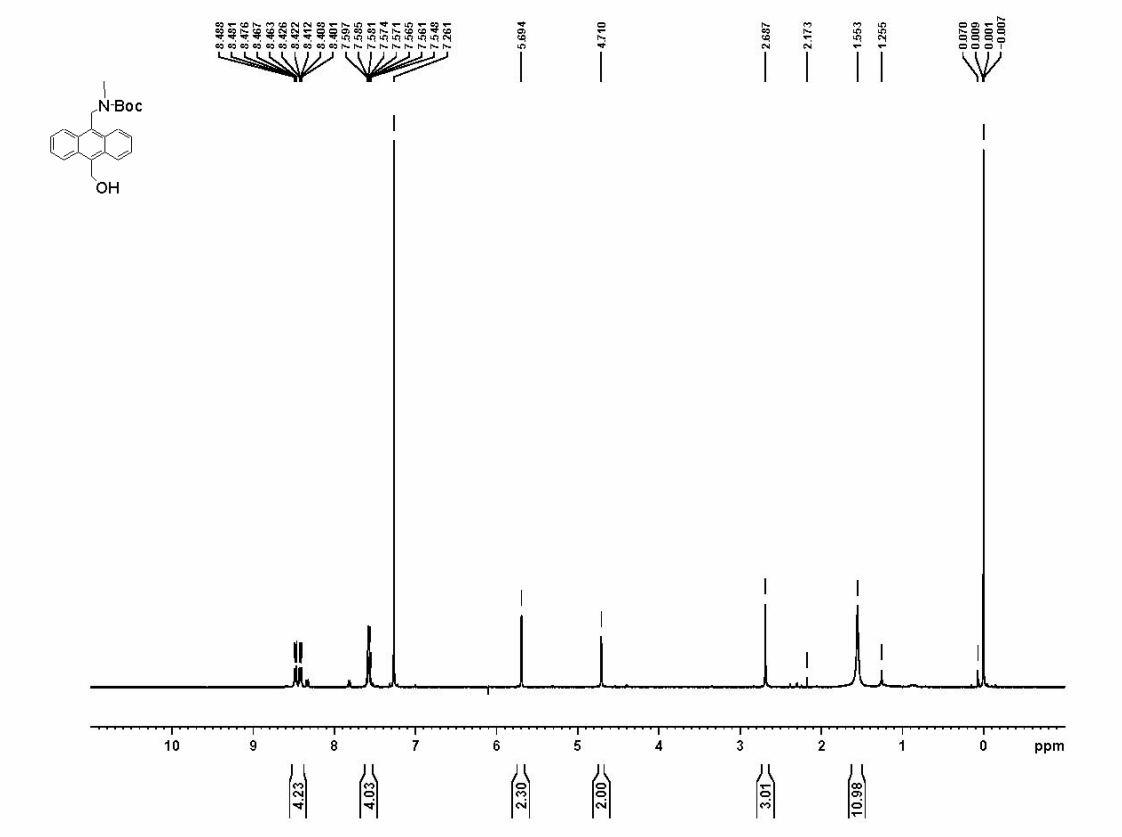
8.488
8.481
8.476
8.467
8.463
8.426
8.422
8.412
8.408
8.401
7.597
7.585
7.581
7.574
7.571
7.565
7.561
7.548
7.261
5.694
4.710
2.687
2.173
1.553
1.255
0.070
0.009
0.001
-0.007
N-Boc
OH
10
9
8
7
6
5
4
3
2
1
0
ppm
4.23
4.03
2.30
2.00
3.01
10.98

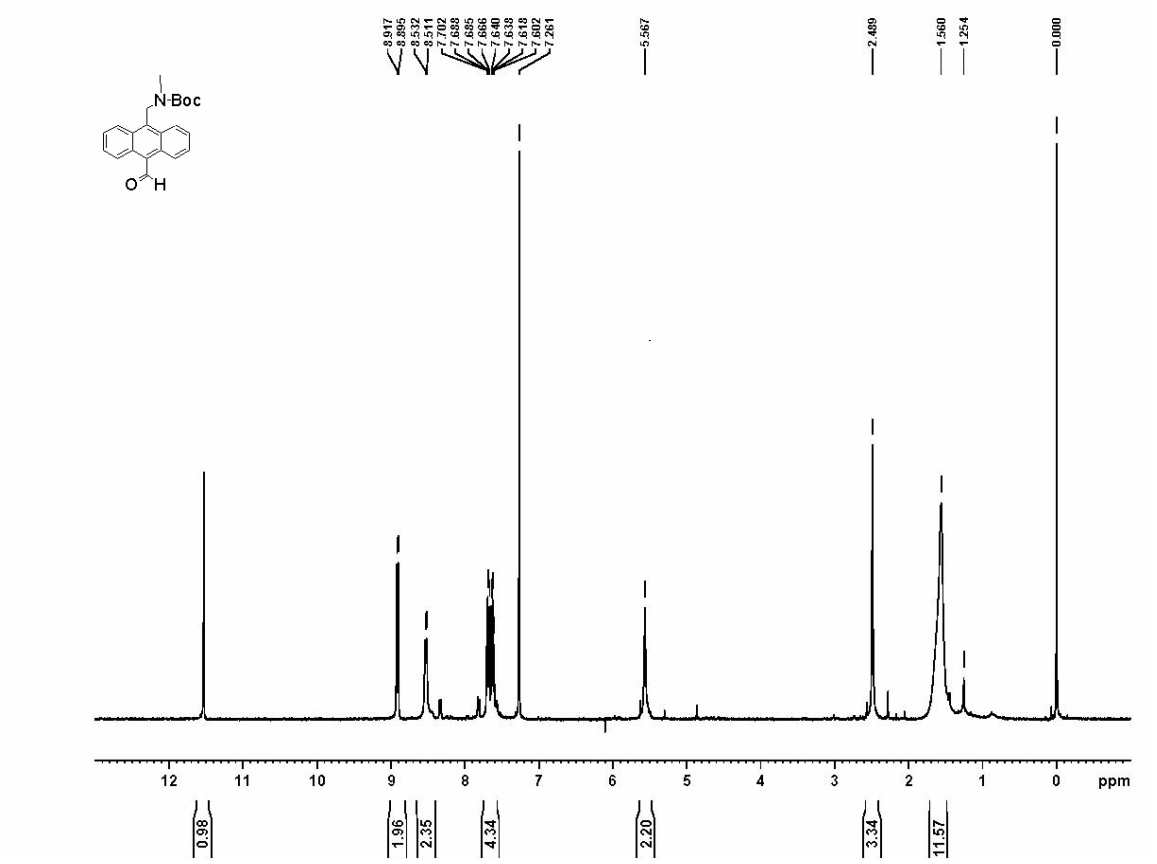
8.917
8.895
8.532
8.511
7.702
7.688
7.685
7.666
7.640
7.638
7.618
7.602
7.261
5.567
2.489
1.560
1.254
0.000
N-Boc
O
H
12
11
10
9
8
7
6
5
4
3
2
1
0
ppm
0.98
1.96
2.35
4.34
2.20
3.34
11.57

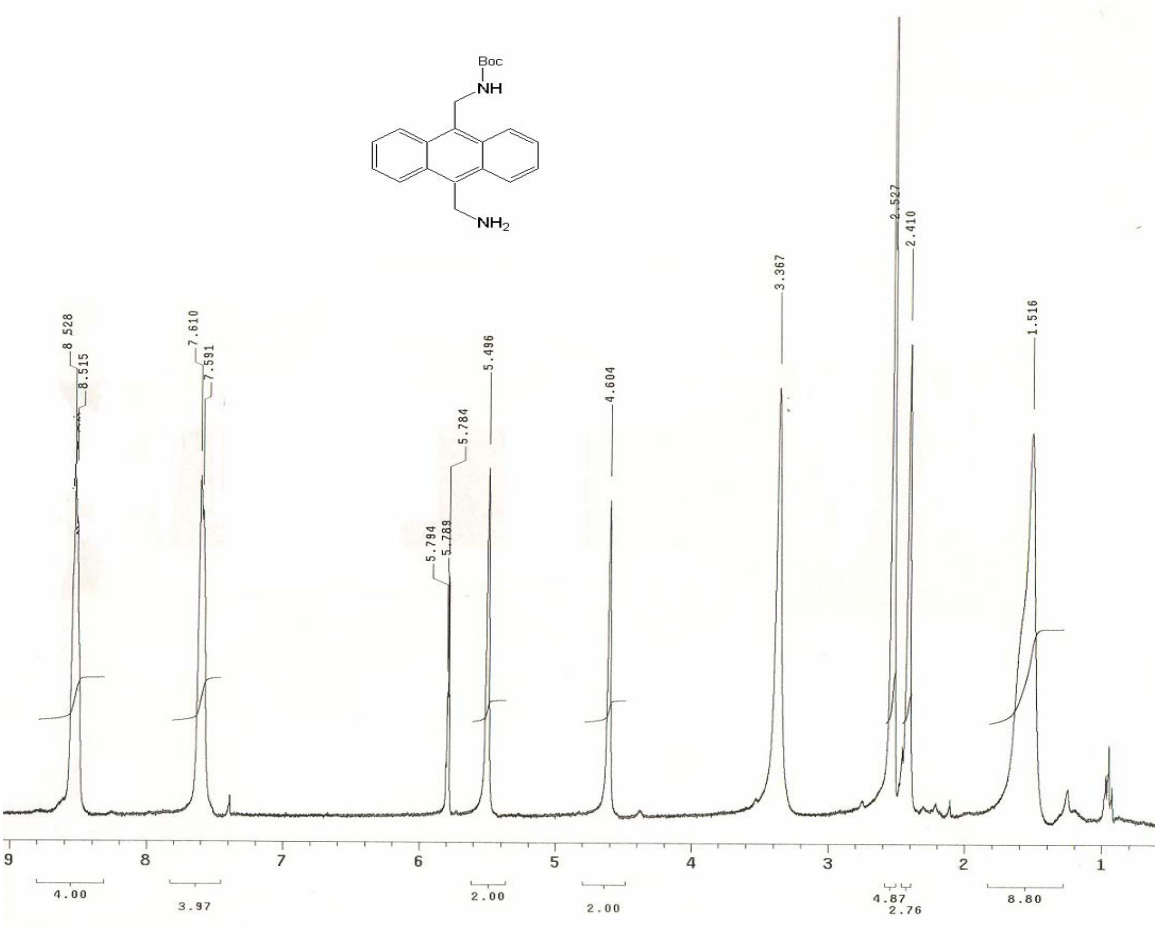
Boc
NH
NH2
8.528
8.515
7.610
7.591
5.794
5.789
5.784
5.496
4.604
3.367
2.527
2.410
1.516
9
8
7
6
5
4
3
2
1
4.00
3.97
2.00
2.00
4.87
2.76
8.80

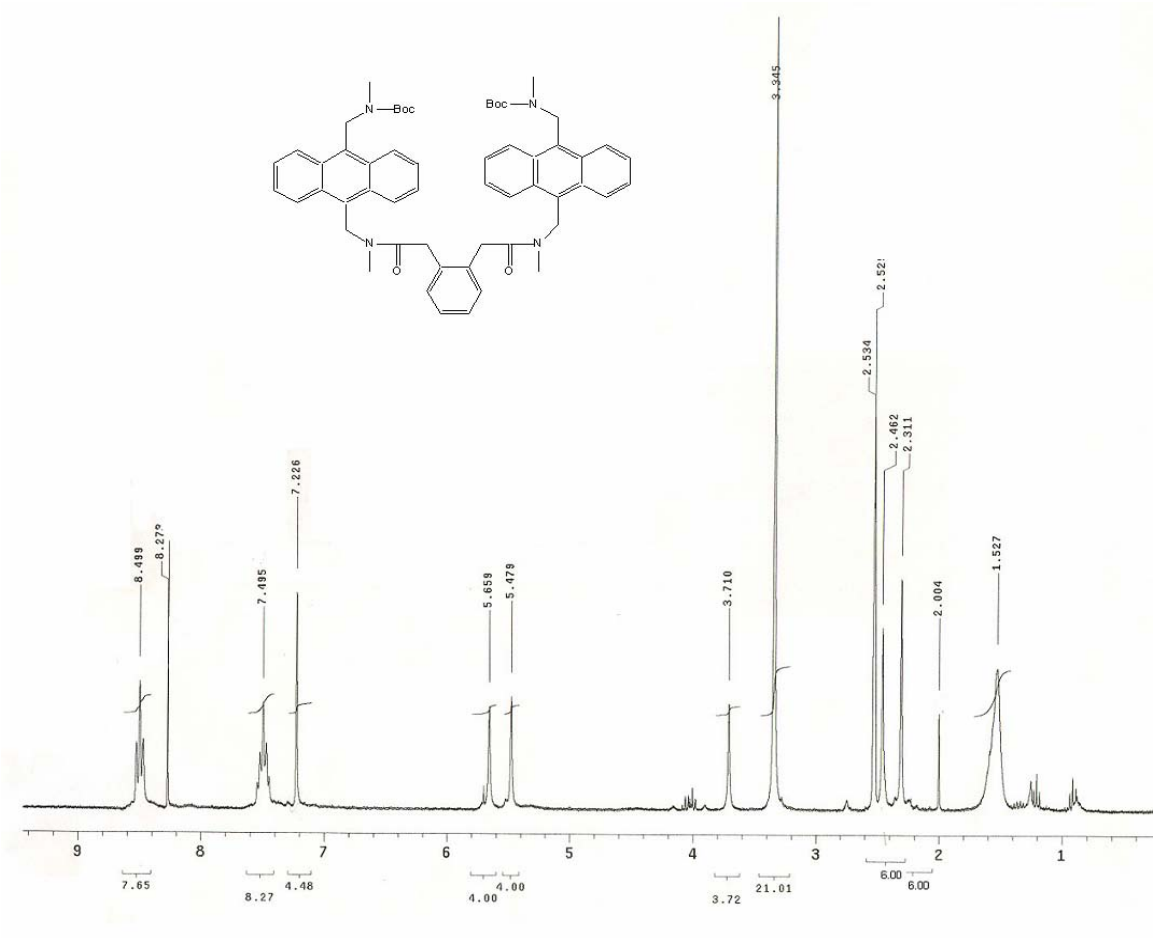
N—Boc
Boc—N
N
O
8.499
8.279
7.495
7.226
5.659
5.479
3.710
3.345
2.534
2.462
2.311
2.004
1.527
9
8
7
6
5
4
3
2
1
7.65
8.27
4.48
4.00
4.00
3.72
21.01
6.00
6.00

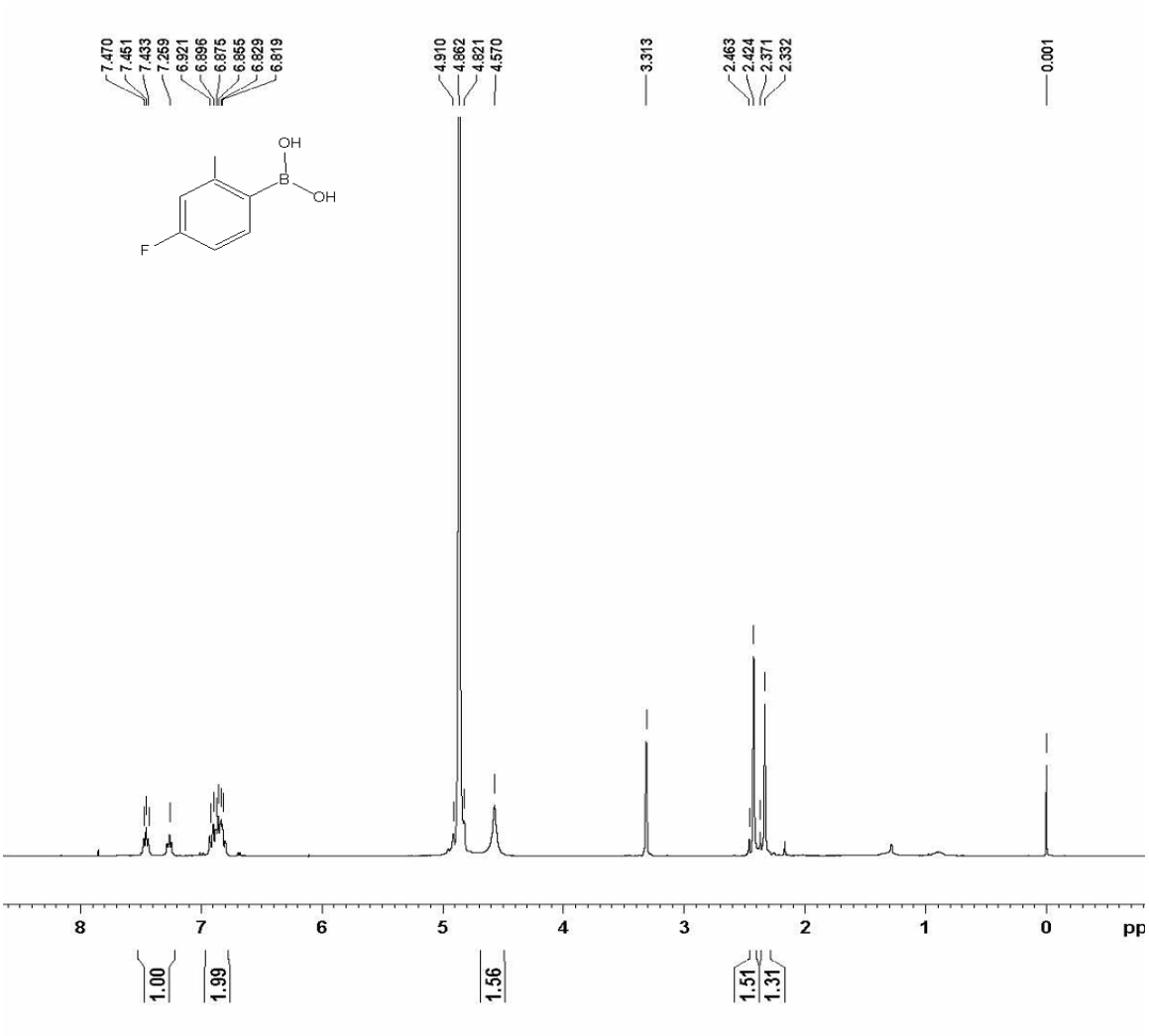
7.470
7.461
7.433
7.269
6.921
6.896
6.875
6.865
6.829
6.819
4.910
4.862
4.821
4.570
3.313
2.463
2.424
2.371
2.332
0.001
OH
B
OH
F
8
7
6
5
4
3
2
1
0
ppm
1.00
1.99
1.56
1.51
1.31

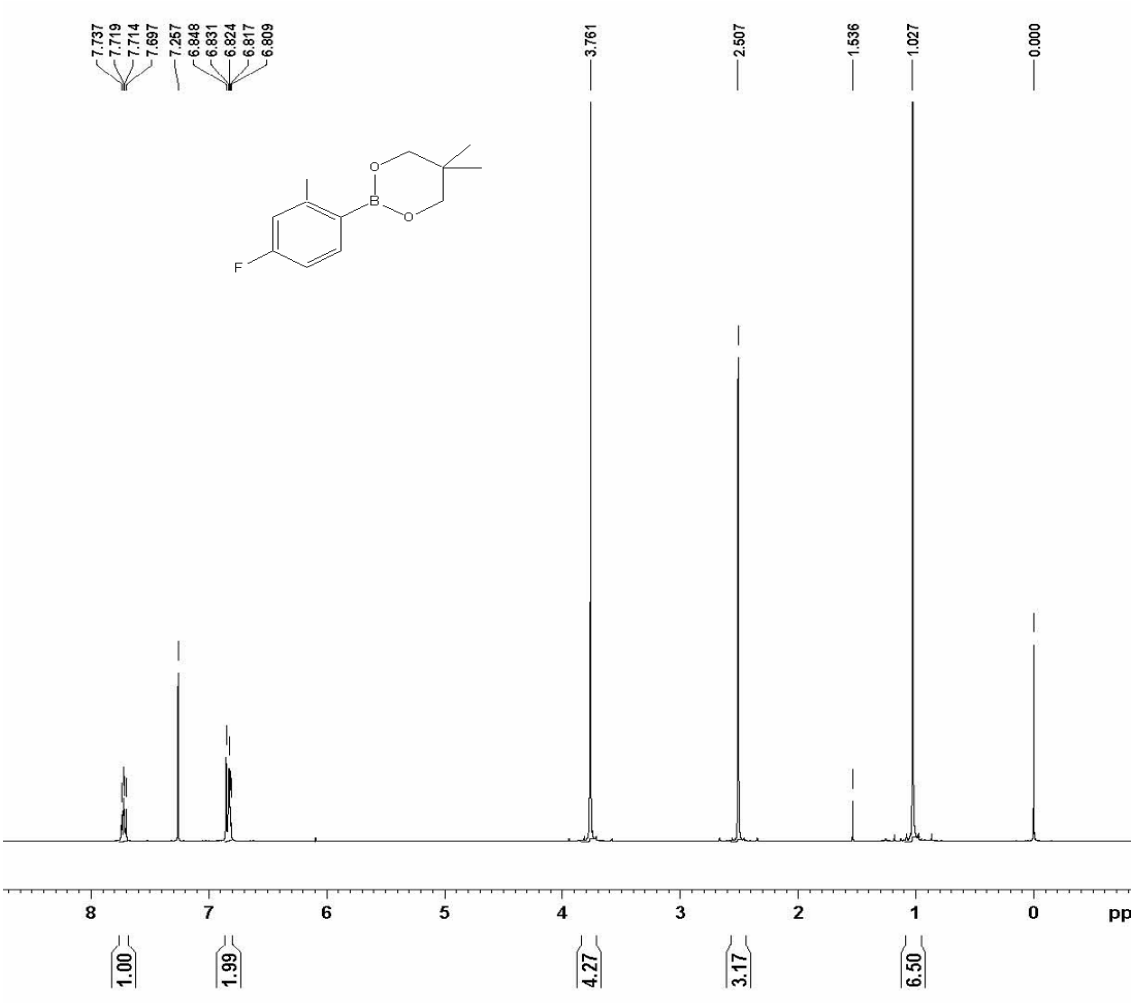
7.737
7.719
7.714
7.697
7.267
6.848
6.831
6.824
6.817
6.809
3.761
2.507
1.536
1.027
0.000
O
B
O
F
8
7
6
5
4
3
2
1
0
ppm
1.00
1.99
4.27
3.17
6.50

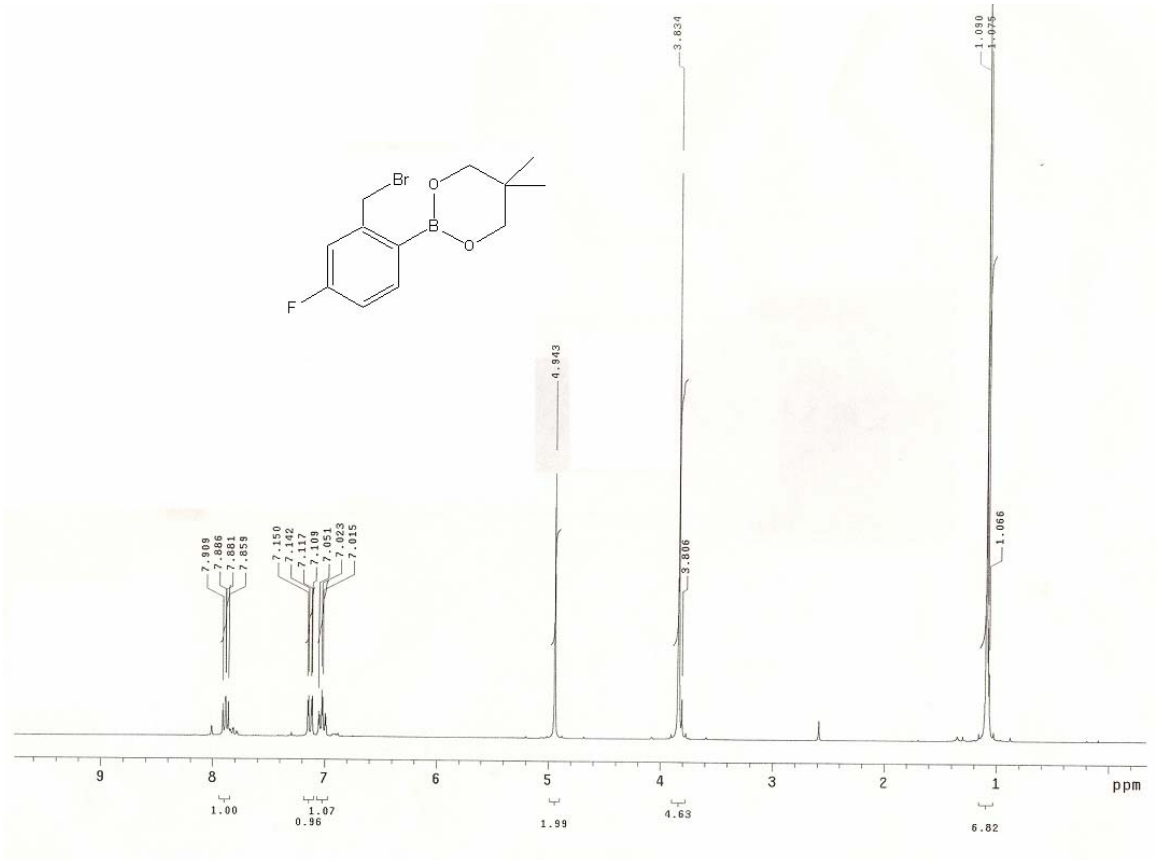
Br
O
B
O
F
7.909
7.886
7.881
7.859
7.150
7.142
7.117
7.109
7.051
7.023
7.015
4.943
3.834
3.806
1.090
1.075
1.066
9
8
7
6
5
4
3
2
1
ppm
1.00
1.07
0.96
1.99
4.63
6.82

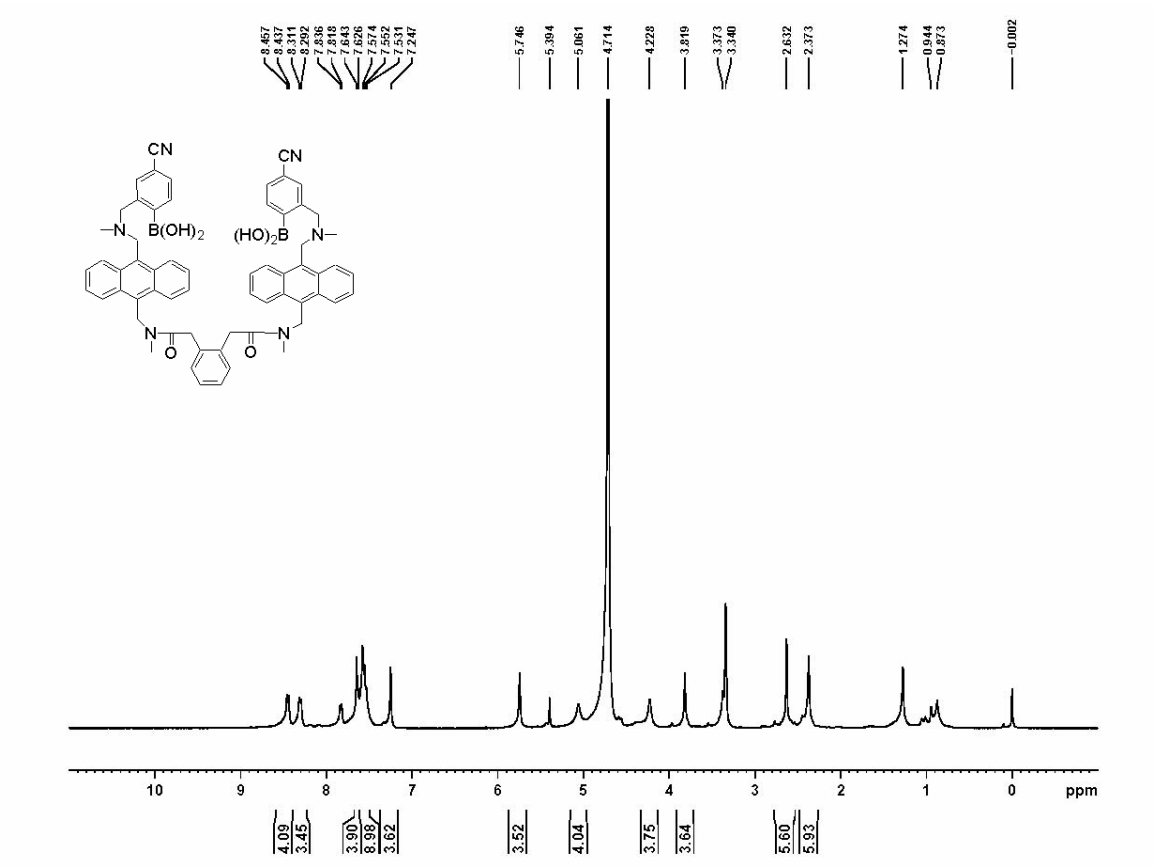
8.457
8.437
8.311
8.292
7.836
7.818
7.643
7.626
7.574
7.552
7.531
7.247
5.746
5.394
5.061
4.714
4.228
3.819
3.373
3.340
2.632
2.373
1.274
0.944
0.873
0.002
CN
B(OH)2
(HO)2B
N
O
10
9
8
7
6
5
4
3
2
1
0
ppm
4.09
3.45
3.90
8.98
3.62
3.52
4.04
3.75
3.64
5.60
5.93

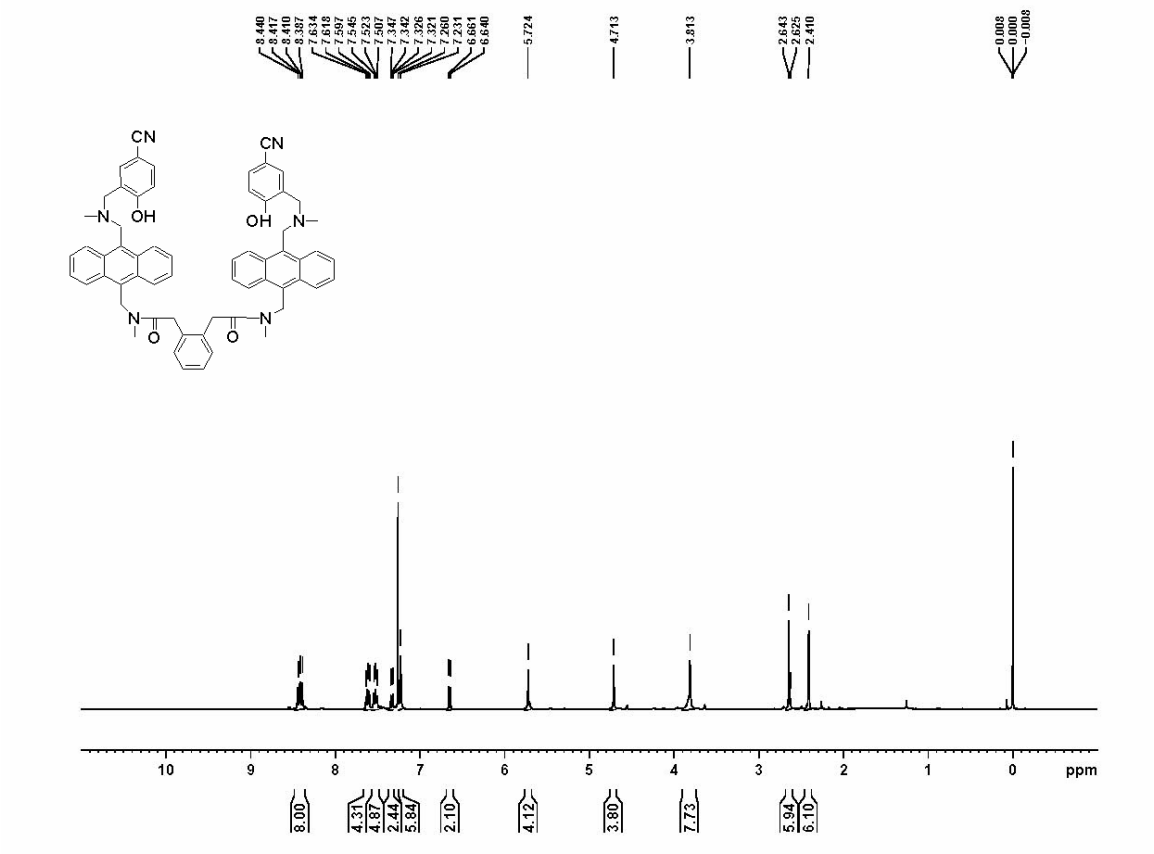
8.440
8.417
8.410
8.387
7.634
7.618
7.597
7.545
7.523
7.507
7.347
7.342
7.326
7.321
7.260
7.231
6.661
6.640
5.724
4.713
3.813
2.643
2.625
2.410
0.008
0.000
-0.008
CN
OH
N
O
10
9
8
7
6
5
4
3
2
1
0
ppm
8.00
4.31
4.87
2.44
5.84
2.10
4.12
3.80
7.73
5.94
6.10

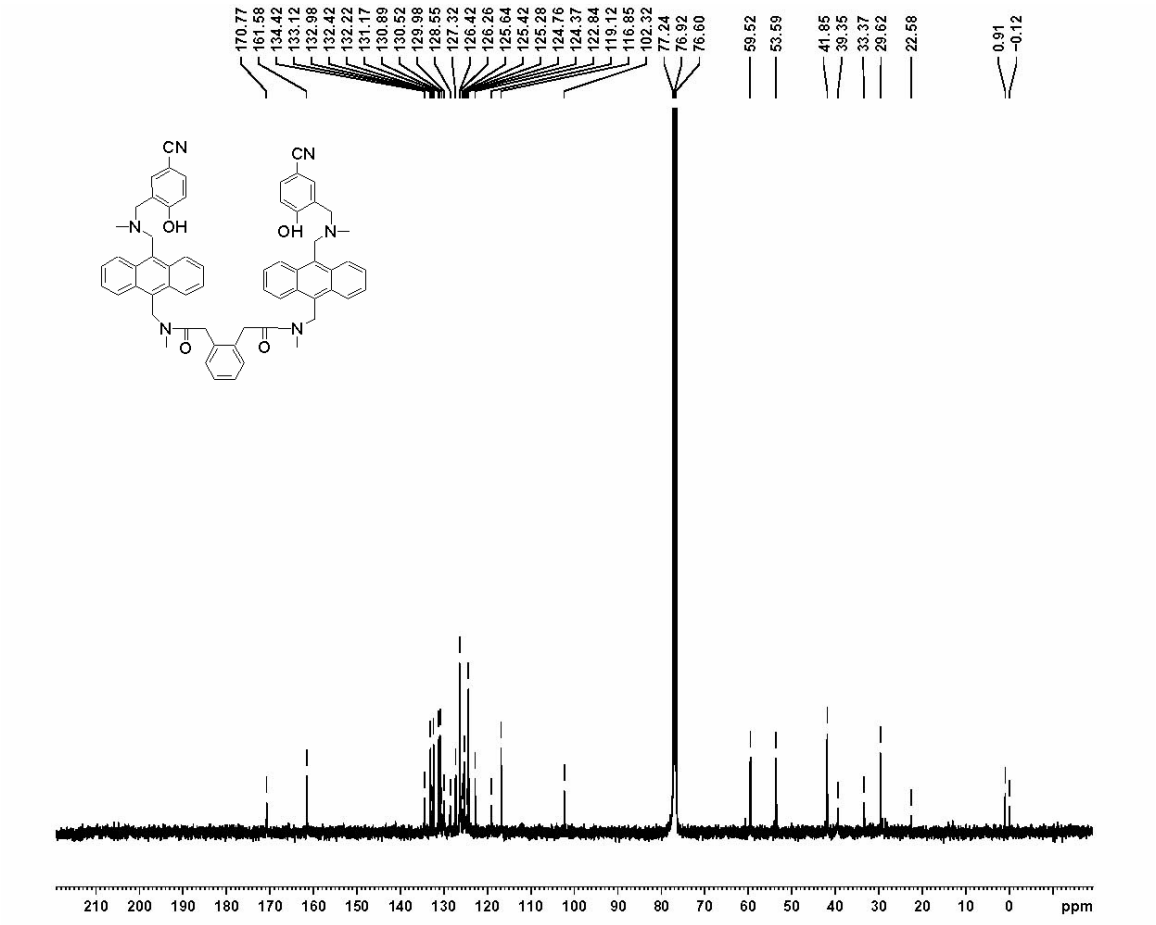
170.77
161.58
134.42
133.12
132.98
132.42
132.22
131.17
130.89
130.52
129.98
128.55
127.32
126.42
126.26
125.64
125.42
125.28
124.76
124.37
122.84
119.12
116.85
102.32
77.24
76.92
76.60
59.52
53.59
41.85
39.35
33.37
29.62
22.58
0.91
-0.12
CN
OH
N
O
210 200 190 180 170 160 150 140 130 120 110 100 90 80 70 60 50 40 30 20 10 0 ppm

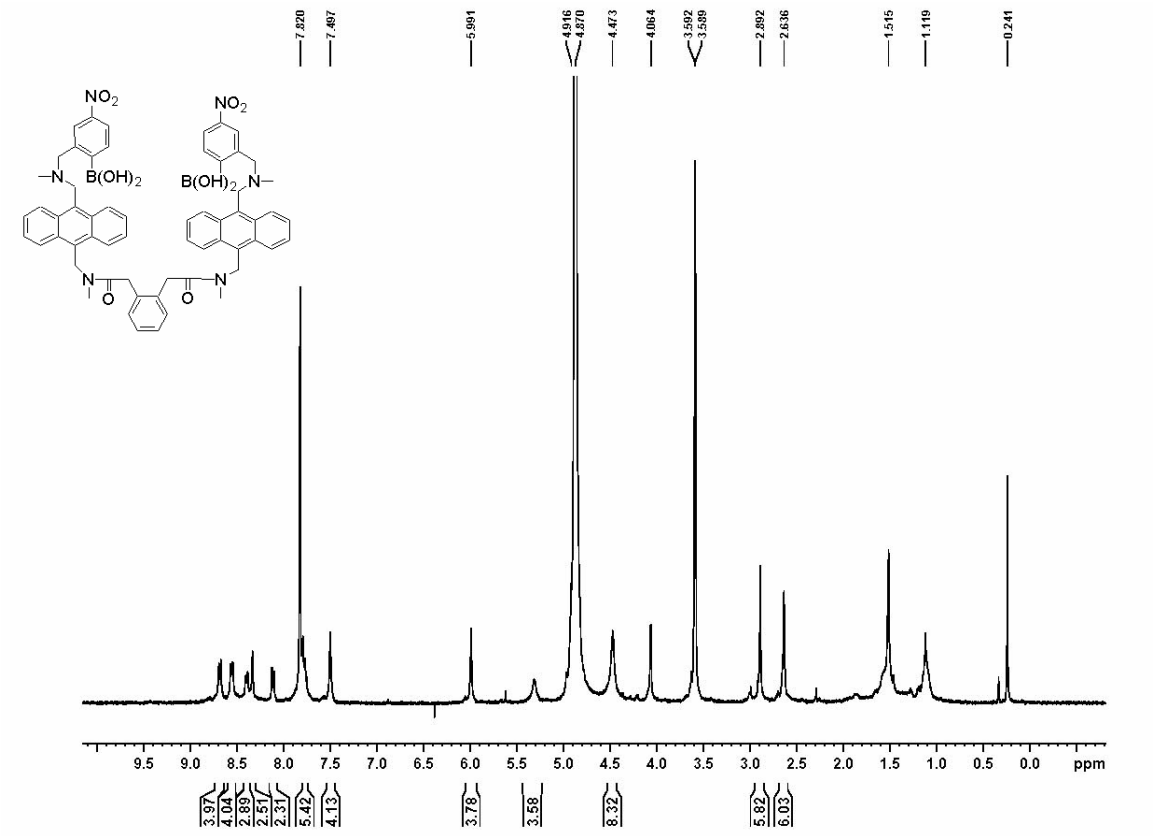
7.820
7.497
5.991
4.916
4.870
4.473
4.064
3.592
3.589
2.892
2.636
1.515
1.119
0.241
NO2
B(OH)2
9.5 9.0 8.5 8.0 7.5 7.0 6.5 6.0 5.5 5.0 4.5 4.0 3.5 3.0 2.5 2.0 1.5 1.0 0.5 0.0 ppm
3.97
4.04
2.89
2.51
2.31
5.42
4.13
3.78
3.58
8.32
5.82
6.03

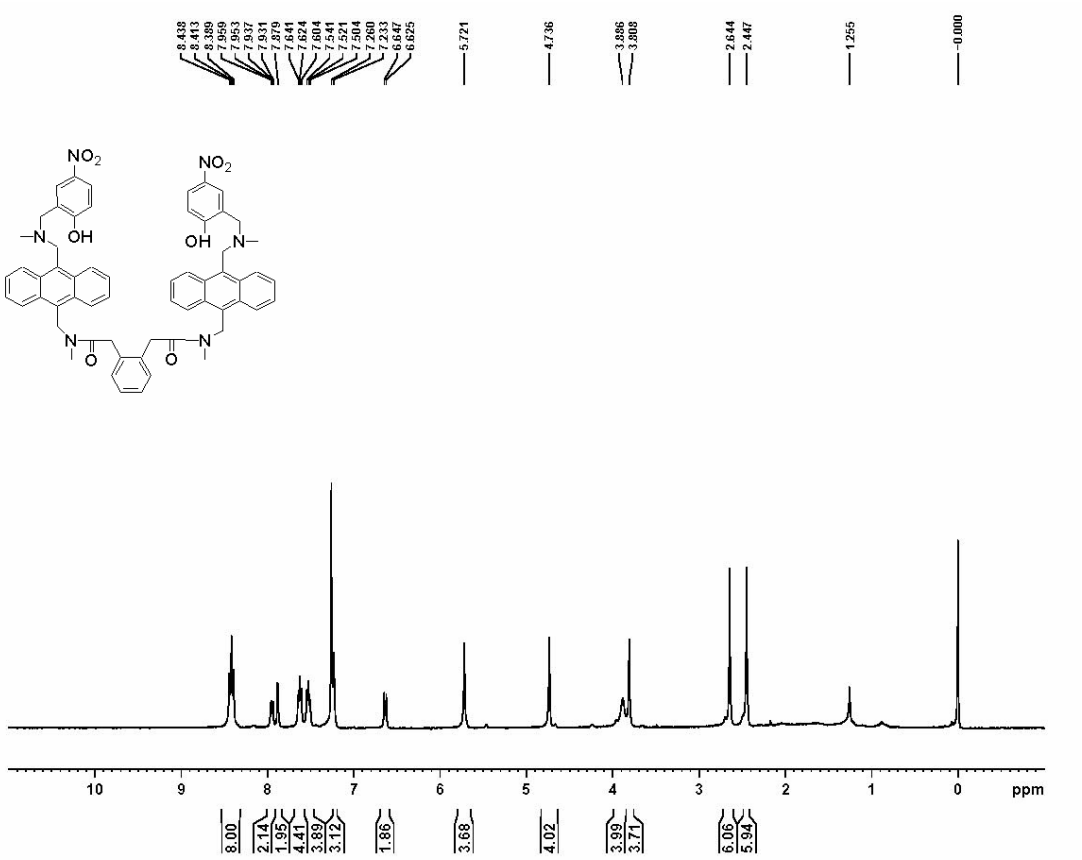
8.438
8.413
8.389
7.959
7.953
7.937
7.931
7.909
7.841
7.824
7.604
7.541
7.521
7.504
7.260
7.233
6.647
6.625
5.721
4.736
3.886
3.808
2.644
2.447
1.255
0.000
NO2
OH
N
O
10
9
8
7
6
5
4
3
2
1
0
ppm
8.00
2.14
1.95
4.41
3.89
3.12
1.86
3.68
4.02
3.99
3.71
6.06
5.94

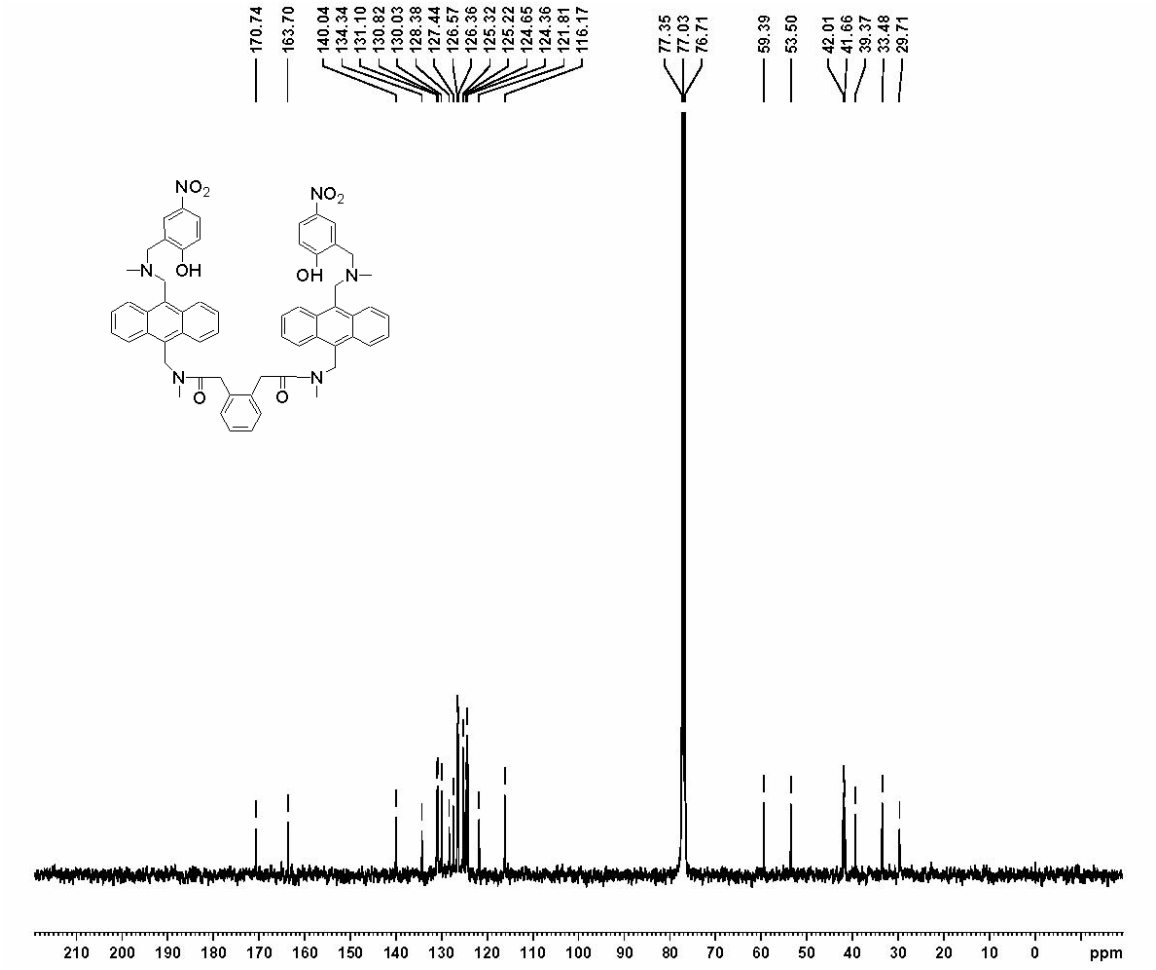
170.74
163.70
140.04
134.34
131.10
130.82
130.03
128.38
127.44
126.57
126.36
125.32
125.22
124.65
124.36
121.81
116.17
77.35
77.03
76.71
59.39
53.50
42.01
41.66
39.37
33.48
29.71
NO2
OH
N
O
210 200 190 180 170 160 150 140 130 120 110 100 90 80 70 60 50 40 30 20 10 0 ppm

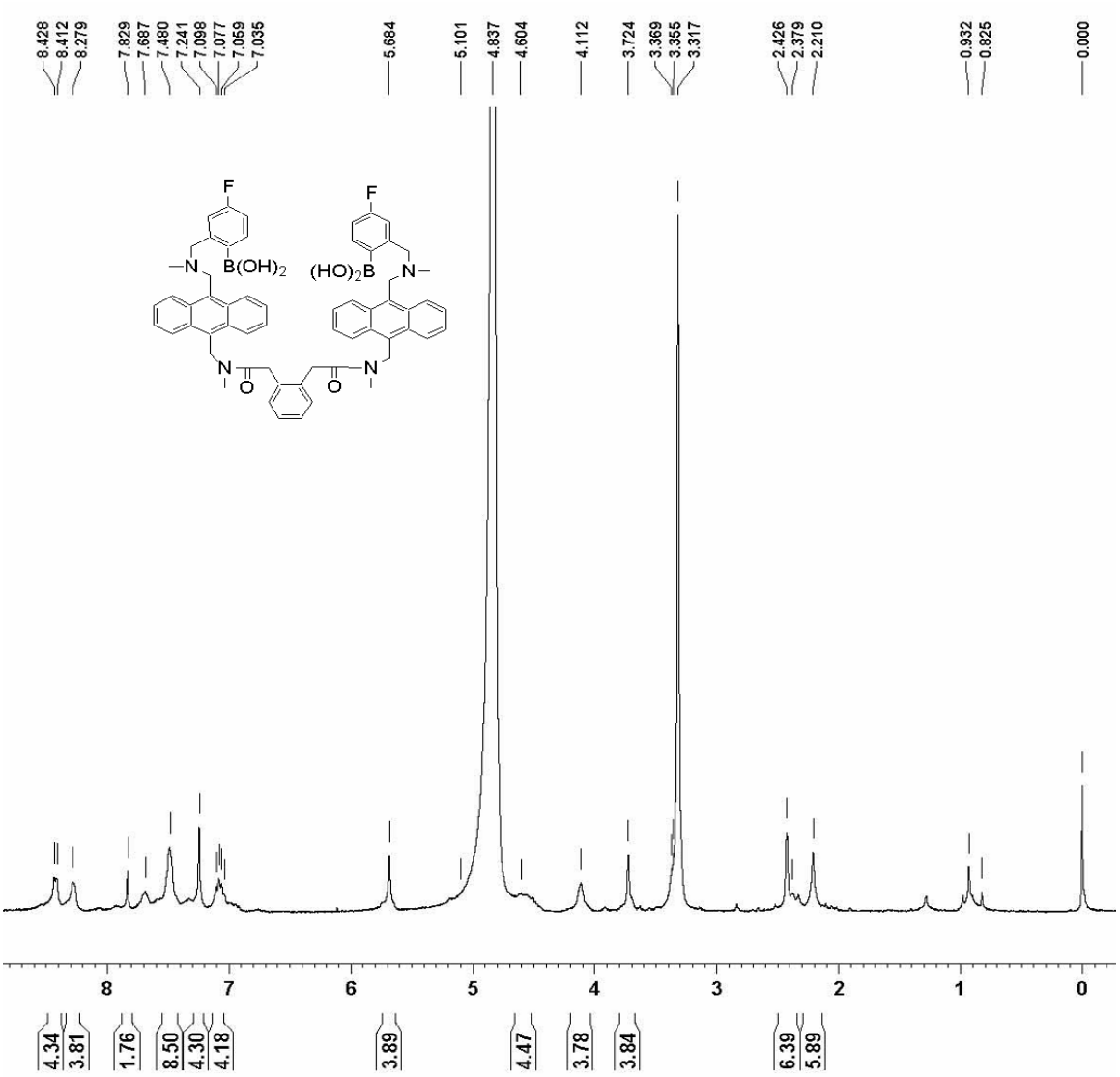
8.428
8.412
8.279
7.829
7.687
7.480
7.241
7.098
7.077
7.059
7.035
5.684
5.101
4.837
4.604
4.112
3.724
3.369
3.355
3.317
2.426
2.379
2.210
0.932
0.825
0.000
F
B(OH)2
(HO)2B
N
O
8
7
6
5
4
3
2
1
0
4.34
3.81
1.76
8.50
4.30
4.18
3.89
4.47
3.78
3.84
6.39
5.89

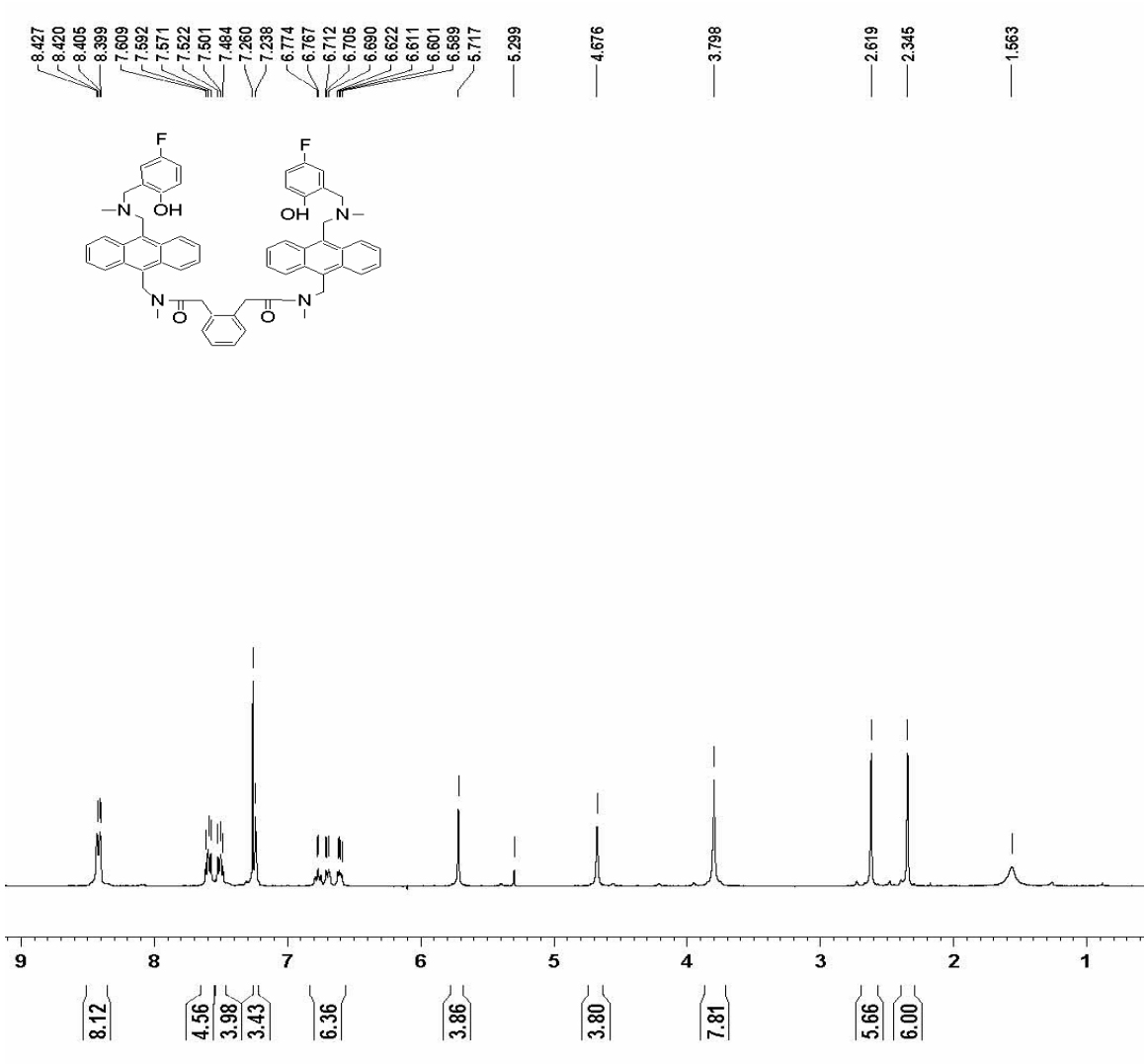
8.427
8.420
8.405
8.399
7.609
7.592
7.571
7.522
7.501
7.484
7.260
7.238
6.774
6.767
6.712
6.705
6.690
6.622
6.611
6.601
6.589
5.717
5.299
4.676
3.798
2.619
2.345
1.563
F
OH
N
O
9
8
7
6
5
4
3
2
1
8.12
4.56
3.98
3.43
6.36
3.86
3.80
7.81
5.66
6.00

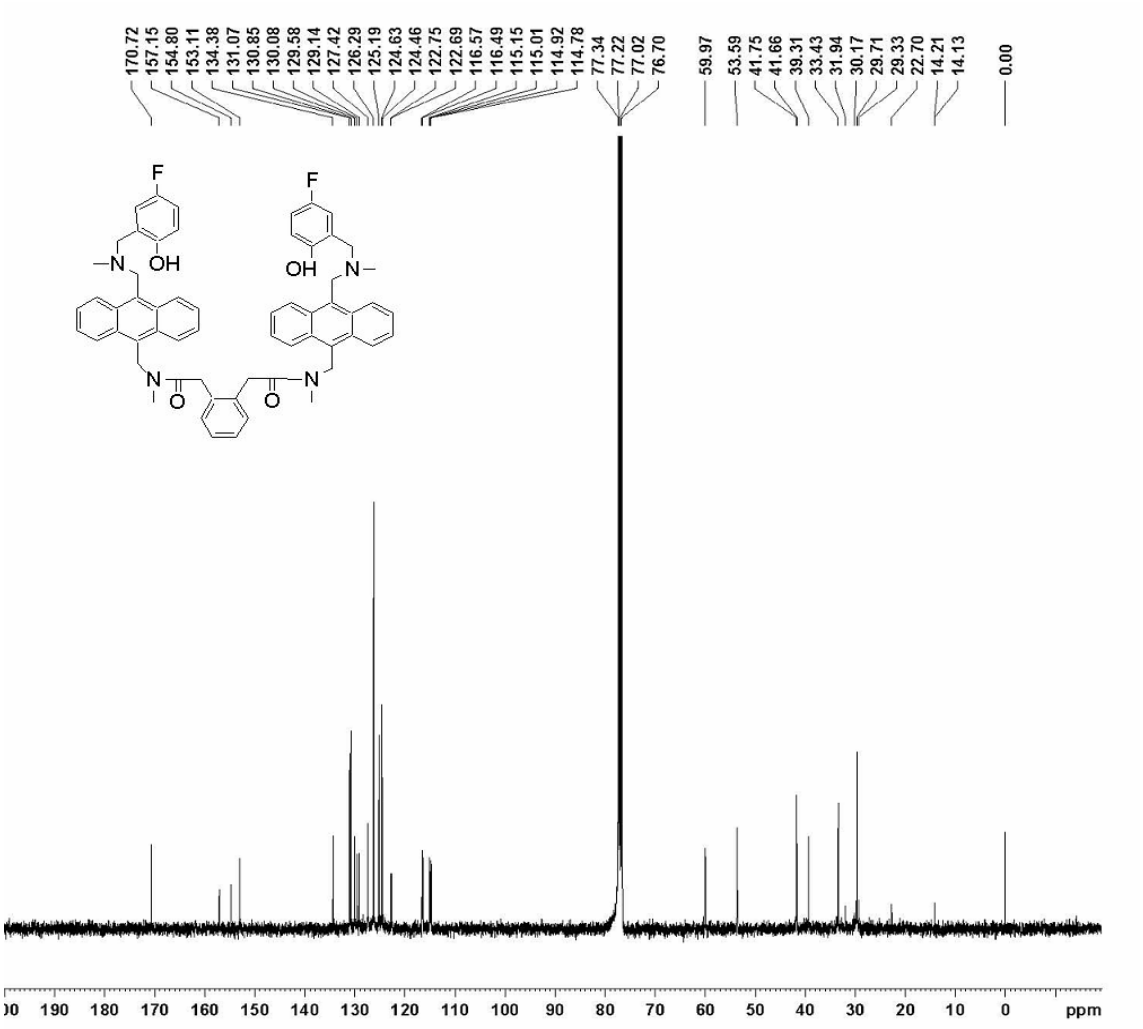
170.72
157.15
154.80
153.11
134.38
131.07
130.85
130.08
129.58
129.14
127.42
126.29
125.19
124.63
124.46
122.75
122.69
116.57
116.49
115.15
115.01
114.92
114.78
77.34
77.22
77.02
76.70
59.97
53.59
41.75
41.66
39.31
33.43
31.94
30.17
29.71
29.33
22.70
14.21
14.13
0.00
F
OH
N
O
ppm

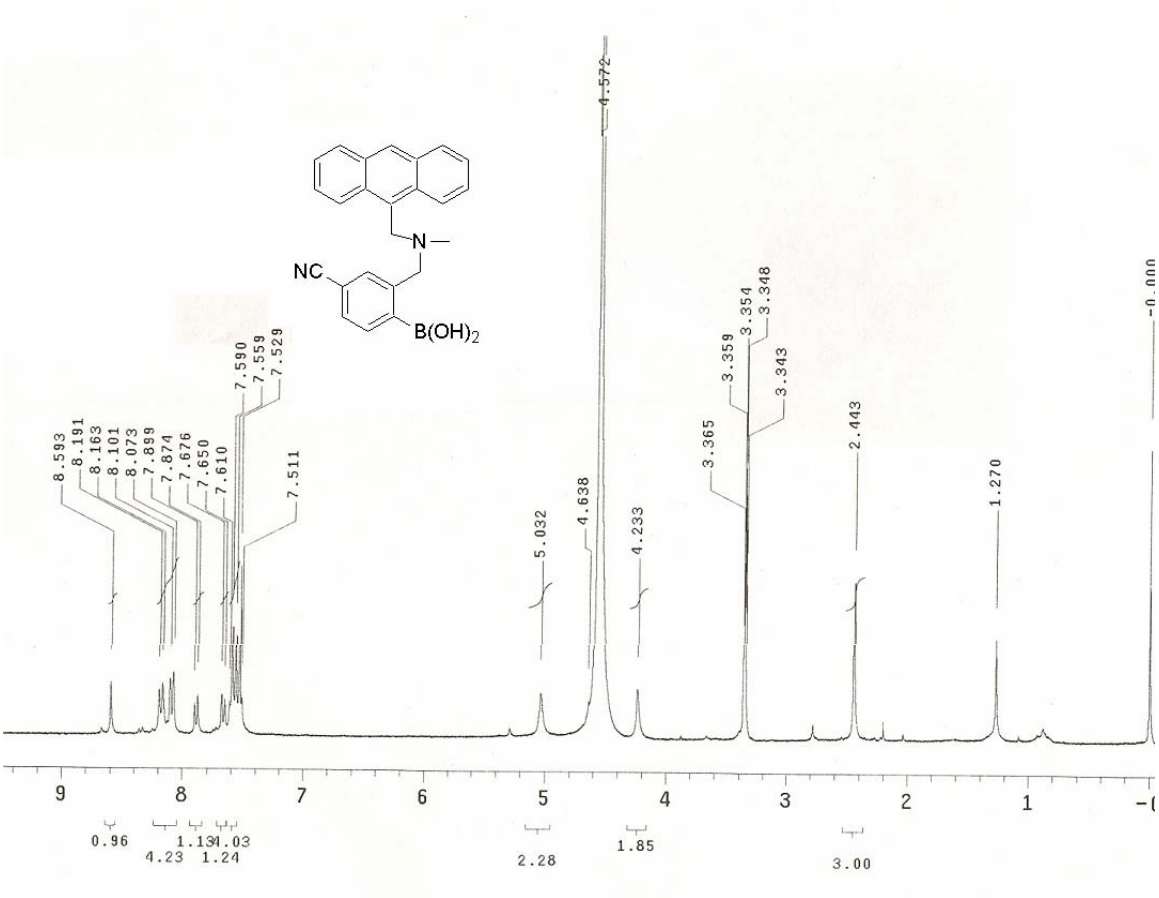
NC
N
B(OH)2
8.593
8.191
8.163
8.101
8.073
7.899
7.874
7.676
7.650
7.610
7.590
7.559
7.529
7.511
5.032
4.638
4.572
4.233
3.365
3.359
3.354
3.348
3.343
2.443
1.270
0.000
9
8
7
6
5
4
3
2
1
0.96
4.23
1.13
1.24
1.03
2.28
1.85
3.00

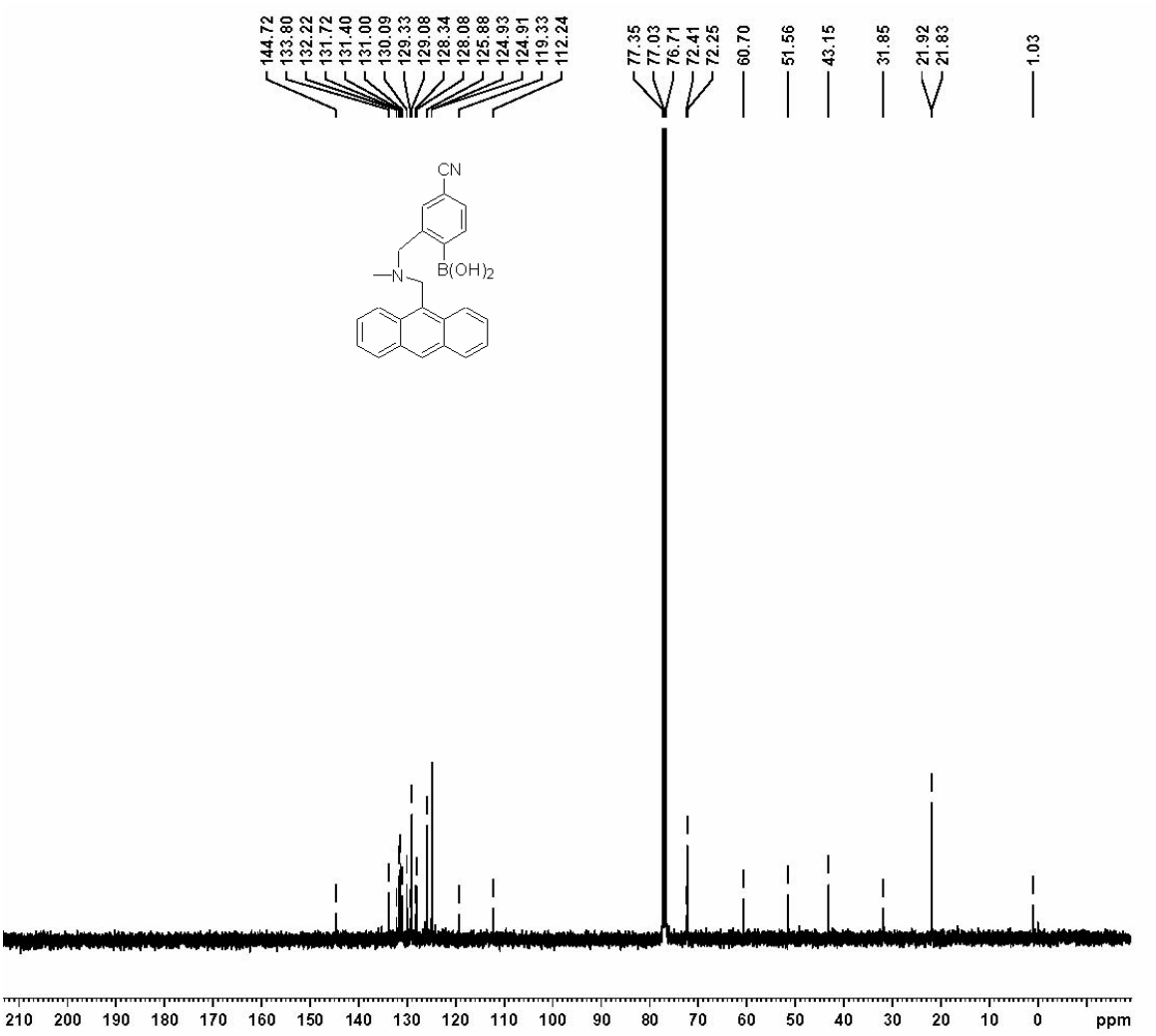
144.72
133.80
132.22
131.72
131.40
131.00
130.09
129.33
129.08
128.34
128.08
125.88
124.93
124.91
119.33
112.24
77.35
77.03
76.71
72.41
72.25
60.70
51.56
43.15
31.85
21.92
21.83
1.03
CN
B(OH)2
N
210 200 190 180 170 160 150 140 130 120 110 100 90 80 70 60 50 40 30 20 10 0 ppm

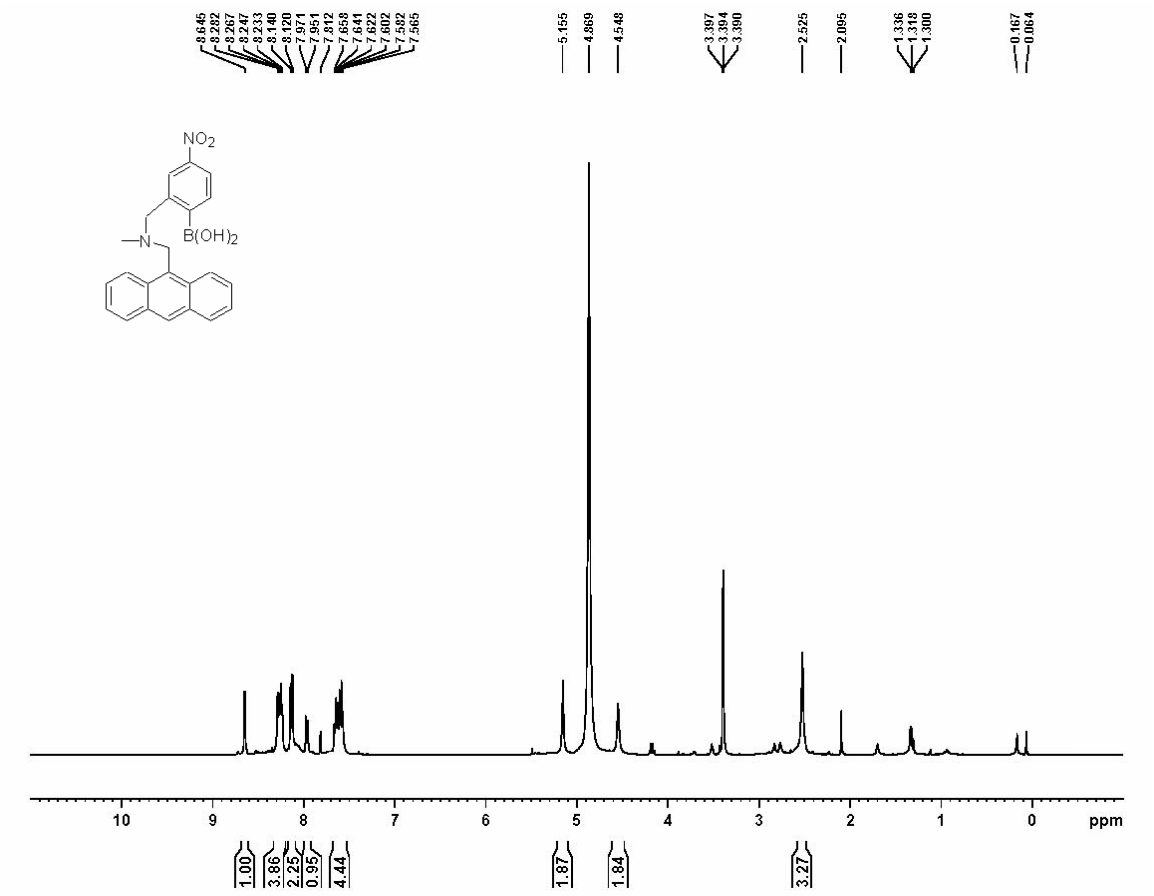
8.645
8.292
8.267
8.247
8.233
8.140
8.120
7.971
7.951
7.912
7.858
7.641
7.622
7.602
7.582
7.565
5.155
4.869
4.548
3.397
3.394
3.390
2.525
2.095
1.336
1.318
1.300
0.167
0.064
NO2
B(OH)2
N
10
9
8
7
6
5
4
3
2
1
0
ppm
1.00
3.86
2.25
0.95
4.44
1.87
1.84
3.27

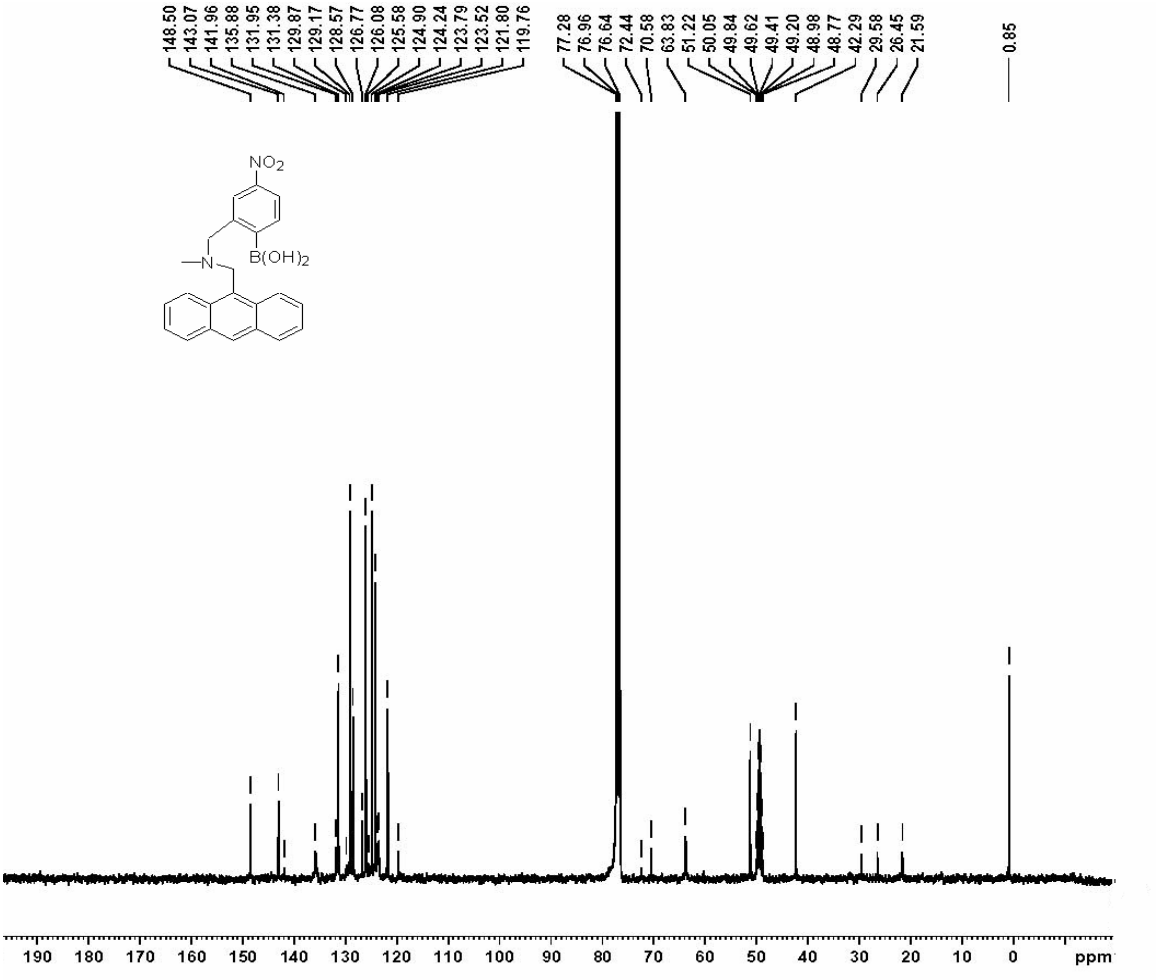
148.50
143.07
141.96
135.88
131.95
131.38
129.87
129.17
128.57
126.77
126.08
125.58
124.90
124.24
123.79
123.52
121.80
119.76
77.28
76.96
76.64
72.44
70.58
63.83
51.22
50.05
49.84
49.62
49.41
49.20
48.98
48.77
42.29
29.58
26.45
21.59
0.85
NO2
B(OH)2
N
190 180 170 160 150 140 130 120 110 100 90 80 70 60 50 40 30 20 10 0 ppm

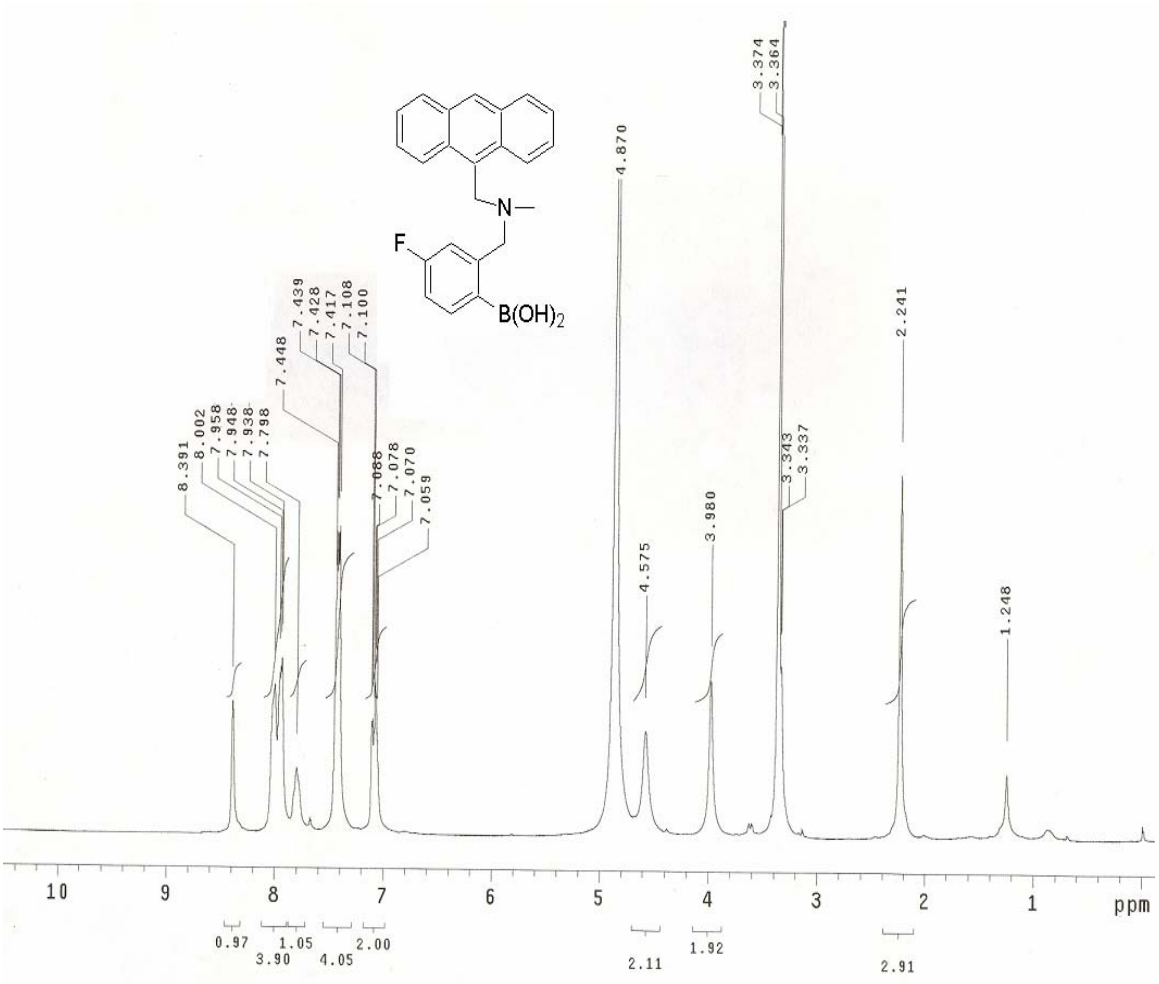
8.391
8.002
7.958
7.948
7.938
7.798
7.448
7.439
7.428
7.417
7.108
7.100
7.088
7.078
7.070
7.059
4.870
4.575
3.980
3.374
3.364
3.343
3.337
2.241
1.248
F
N
B(OH)2
10
9
8
7
6
5
4
3
2
1
ppm
0.97
1.05
3.90
4.05
2.00
2.11
1.92
2.91

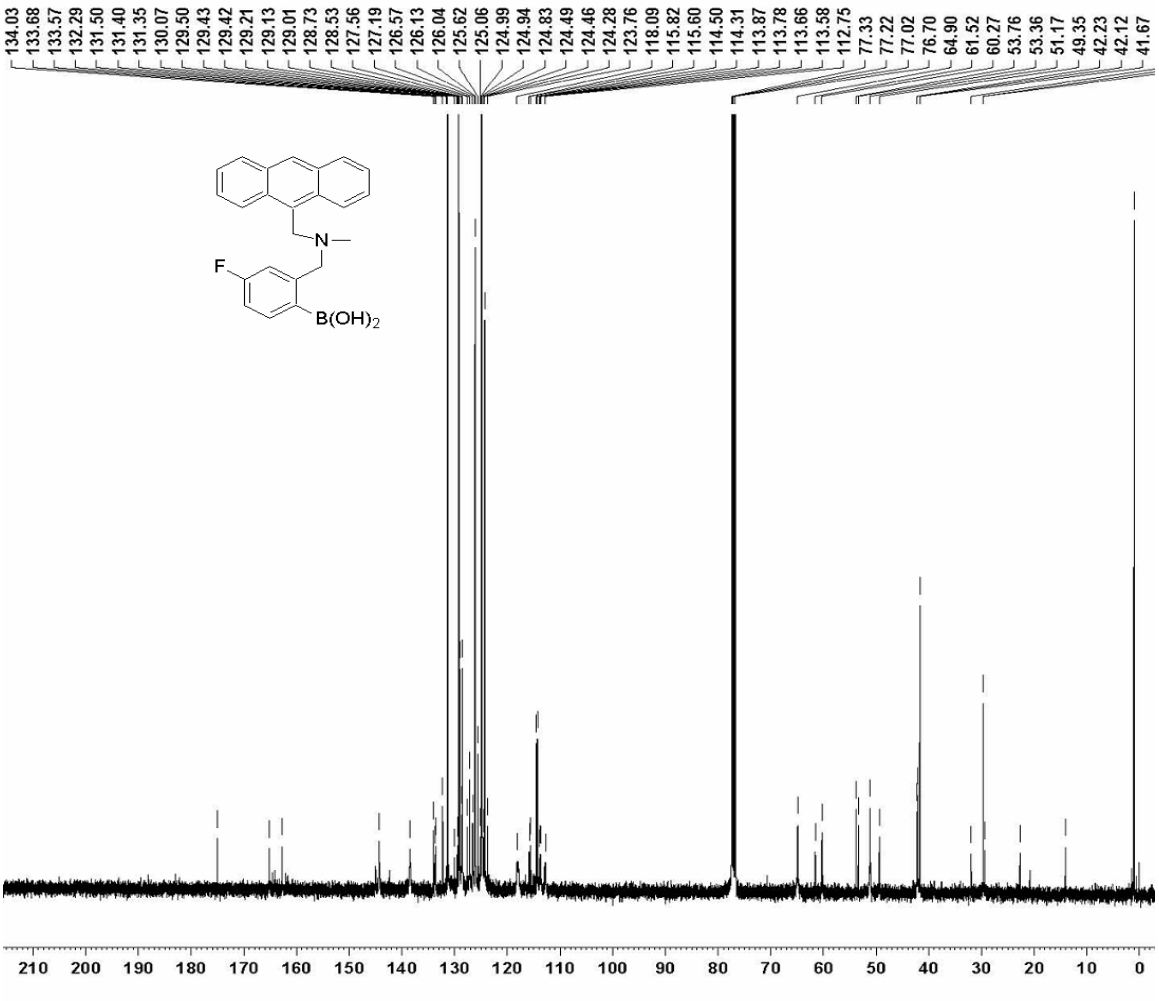
134.03
133.68
133.57
132.29
131.50
131.40
131.35
130.07
129.50
129.43
129.42
129.21
129.13
129.01
128.73
128.53
127.56
127.19
126.57
126.13
126.04
125.62
125.06
124.99
124.94
124.83
124.49
124.46
124.28
123.76
118.09
115.82
115.60
114.50
114.31
113.87
113.78
113.66
113.58
112.75
77.33
77.22
77.02
76.70
64.90
61.52
60.27
53.76
53.36
51.17
49.35
42.23
42.12
41.67
N
F
B(OH)2
210
200
190
180
170
160
150
140
130
120
110
100
90
80
70
60
50
40
30
20
10
0

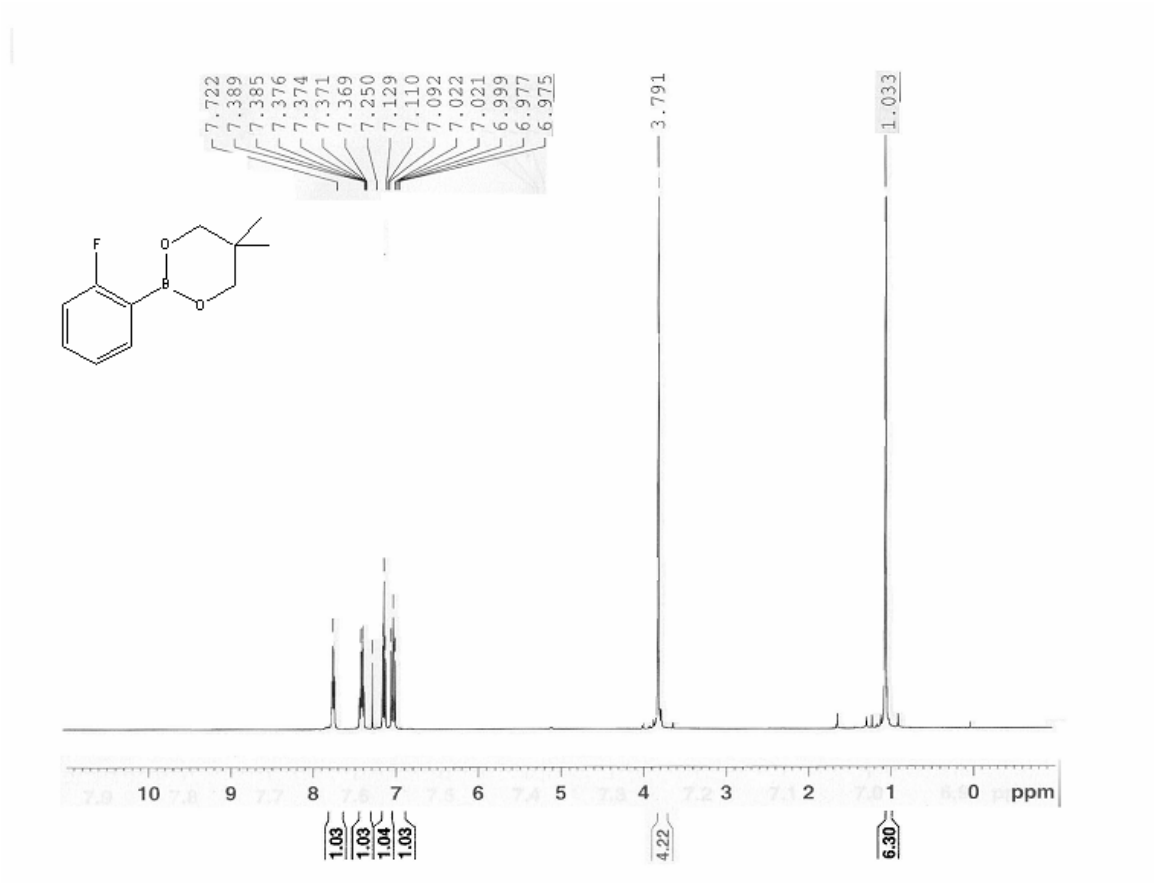
7.722
7.389
7.385
7.376
7.374
7.371
7.369
7.250
7.129
7.110
7.092
7.022
7.021
6.999
6.977
6.975
3.791
1.033
F
O
B
O
10
9
8
7
6
5
4
3
2
1
0
ppm
1.03
1.03
1.04
1.03
4.22
6.30

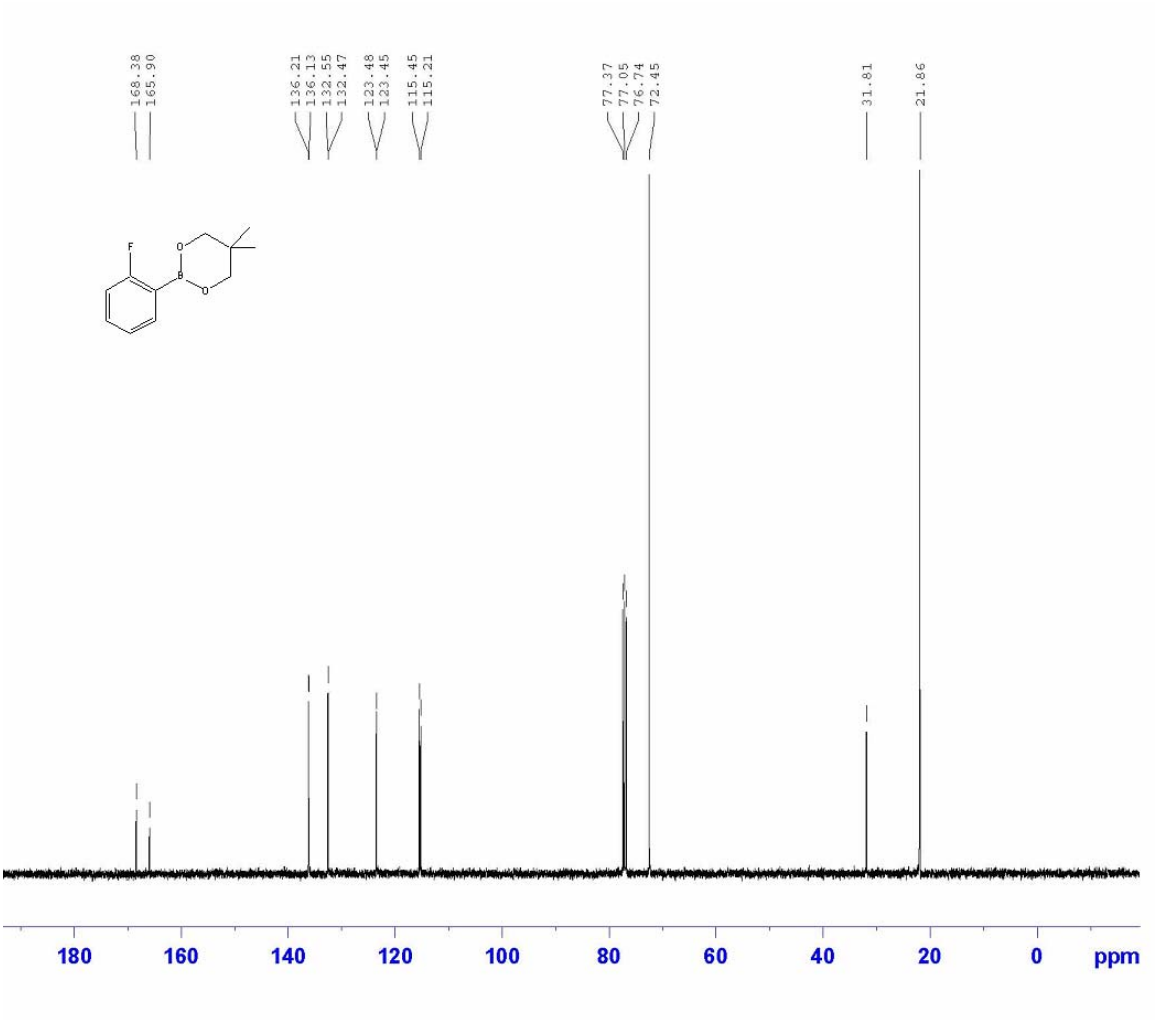
168.38
165.90
136.21
136.13
132.55
132.47
123.48
123.45
115.45
115.21
77.37
77.05
76.74
72.45
31.81
21.86
F
O
B
O
180
160
140
120
100
80
60
40
20
0
ppm

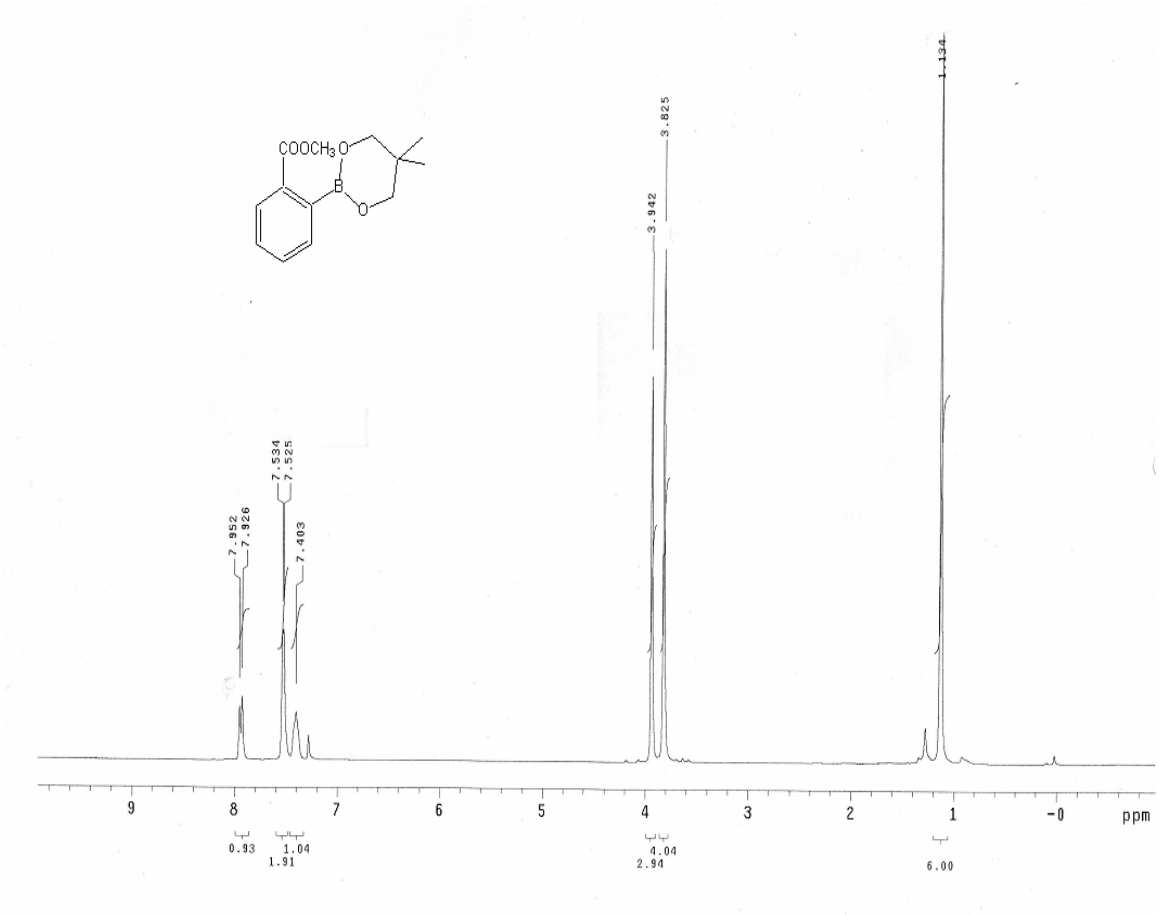
COOCH3
O
B
O
7.952
7.926
7.534
7.525
7.403
3.942
3.825
1.134
9
8
7
6
5
4
3
2
1
-0
ppm
0.93
1.04
1.91
4.04
2.94
6.00

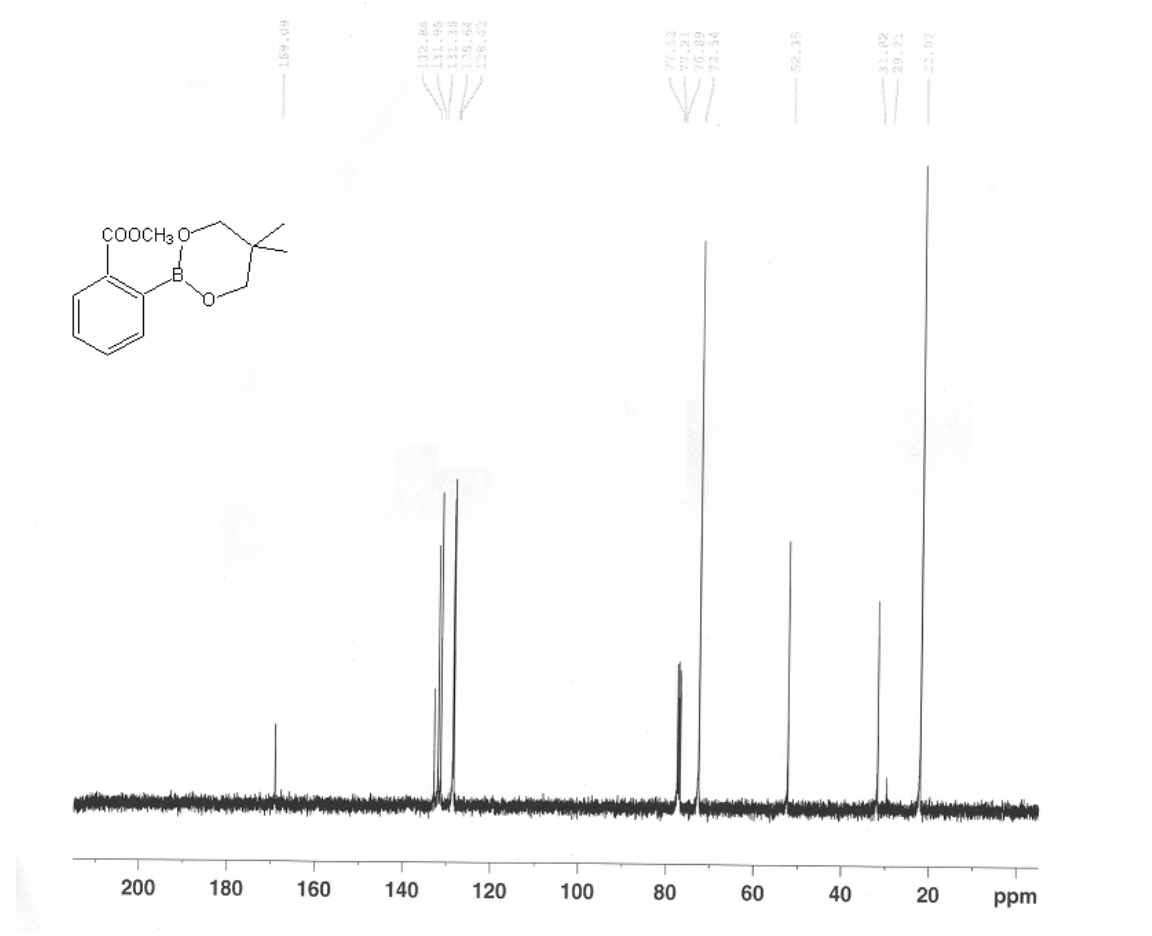
169.09
132.64
131.95
131.16
128.64
128.42
77.32
77.21
76.89
72.54
52.35
31.82
29.71
23.07
COOCH3
O
B
O
200
180
160
140
120
100
80
60
40
20
ppm

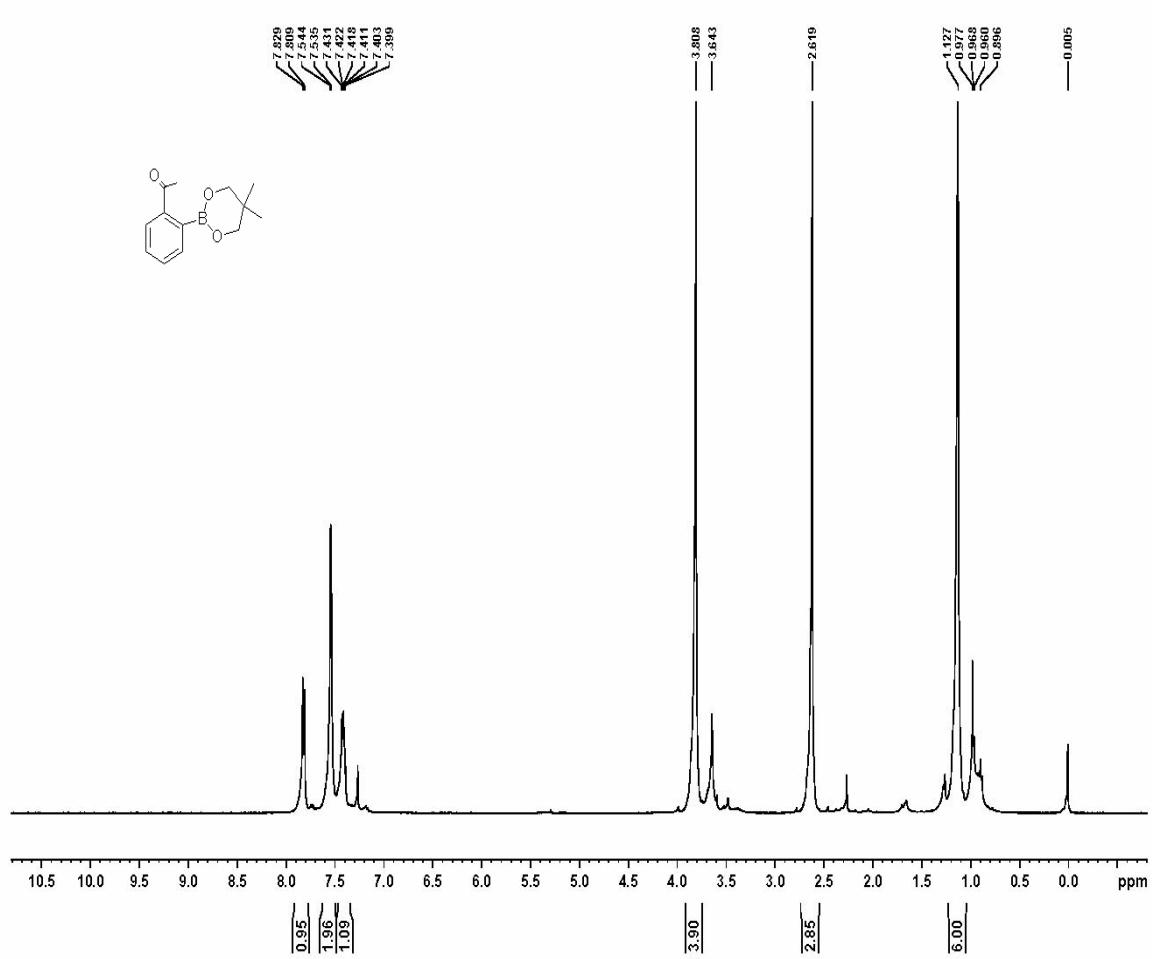
7.829
7.809
7.544
7.535
7.431
7.422
7.418
7.411
7.403
7.399
3.808
3.643
2.619
1.127
1.077
0.968
0.960
0.896
0.005
10.5 10.0 9.5 9.0 8.5 8.0 7.5 7.0 6.5 6.0 5.5 5.0 4.5 4.0 3.5 3.0 2.5 2.0 1.5 1.0 0.5 0.0 ppm
0.95
1.96
1.09
3.90
2.85
6.00

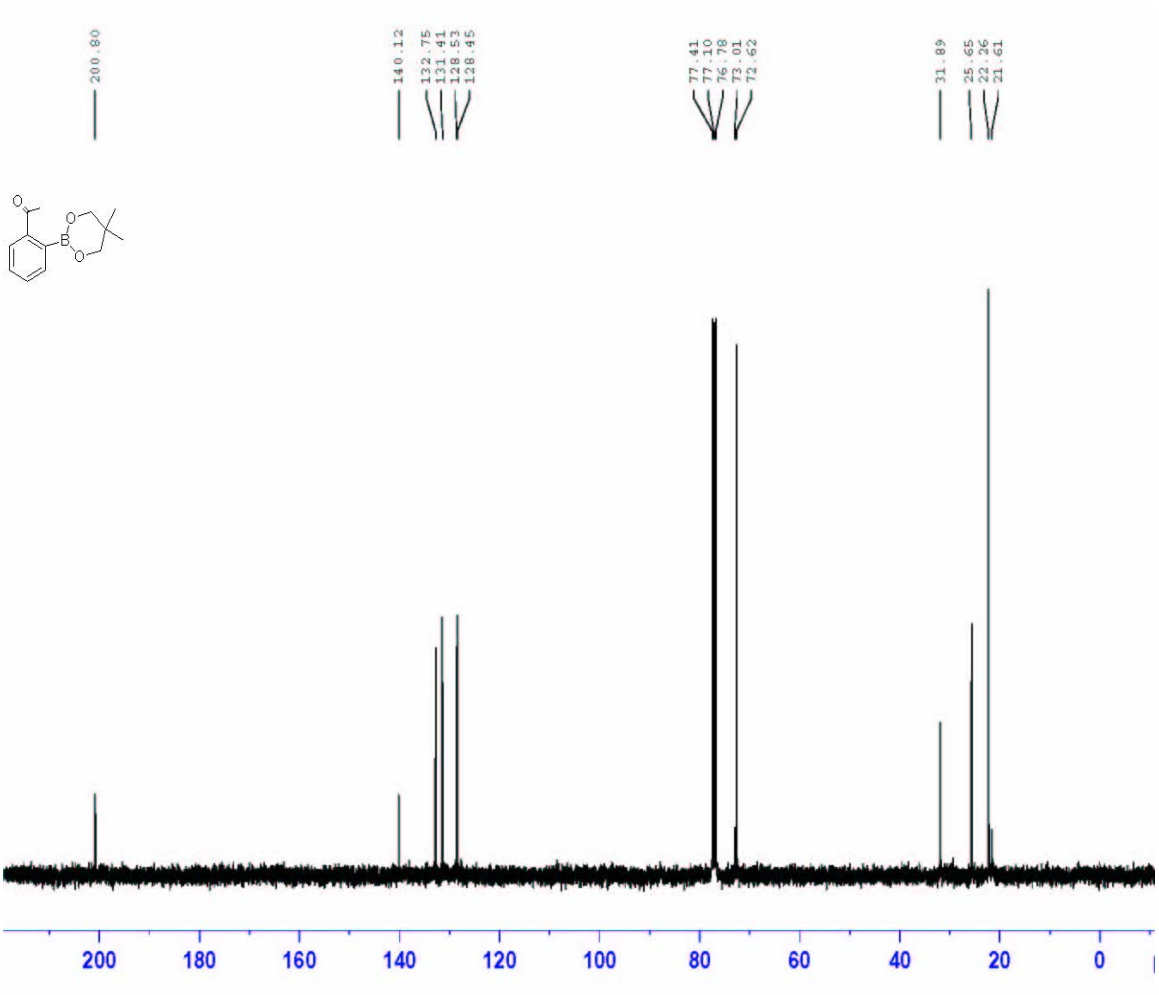
200.80
140.12
132.75
131.41
128.53
128.45
77.41
77.10
76.78
73.01
72.62
31.89
25.65
22.26
21.61
200
180
160
140
120
100
80
60
40
20
0

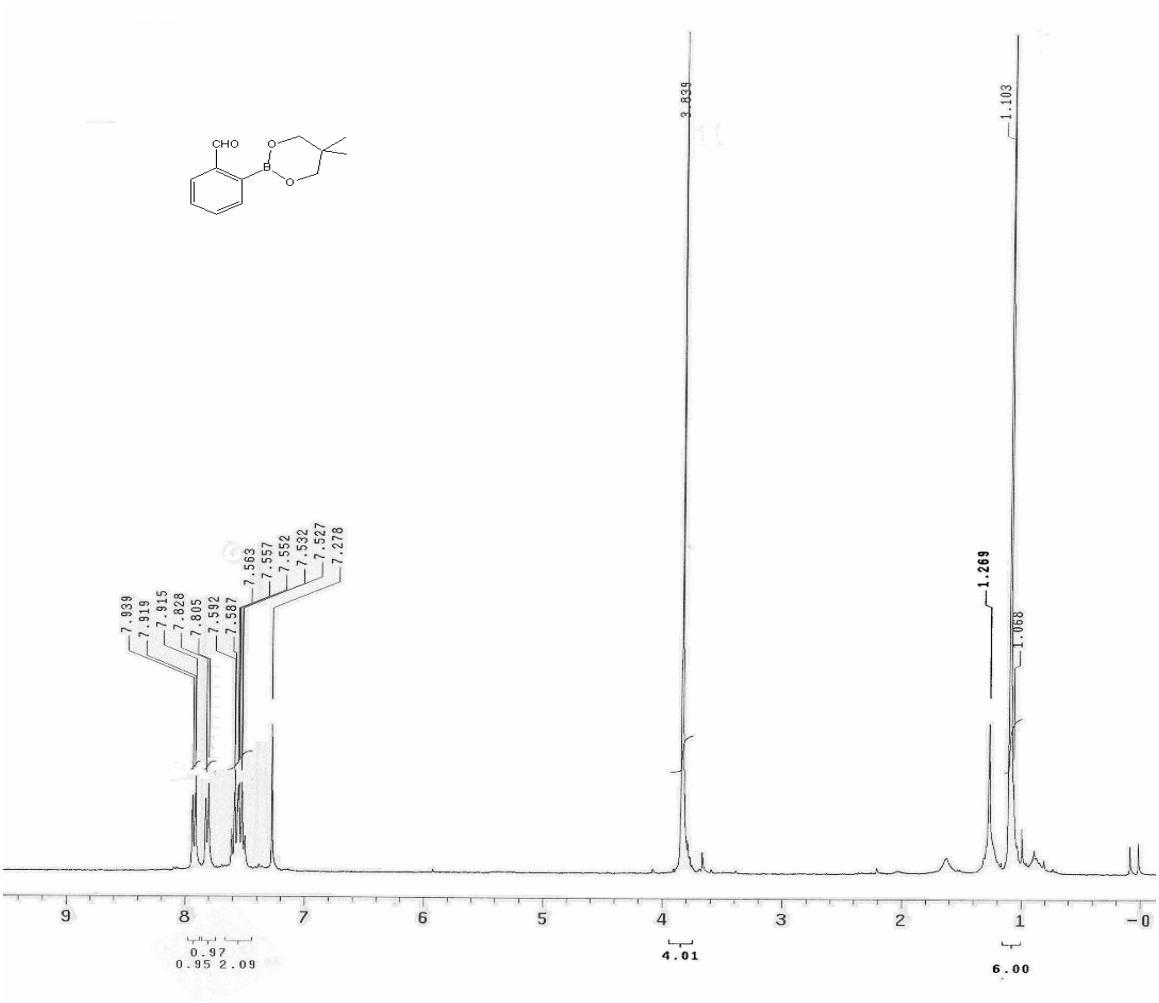
CHO
O
B
O
3.839
1.103
1.269
1.068
7.939
7.919
7.915
7.828
7.805
7.592
7.587
7.563
7.557
7.552
7.532
7.527
7.278
9
8
7
6
5
4
3
2
1
0
0.97
0.95 2.09
4.01
6.00

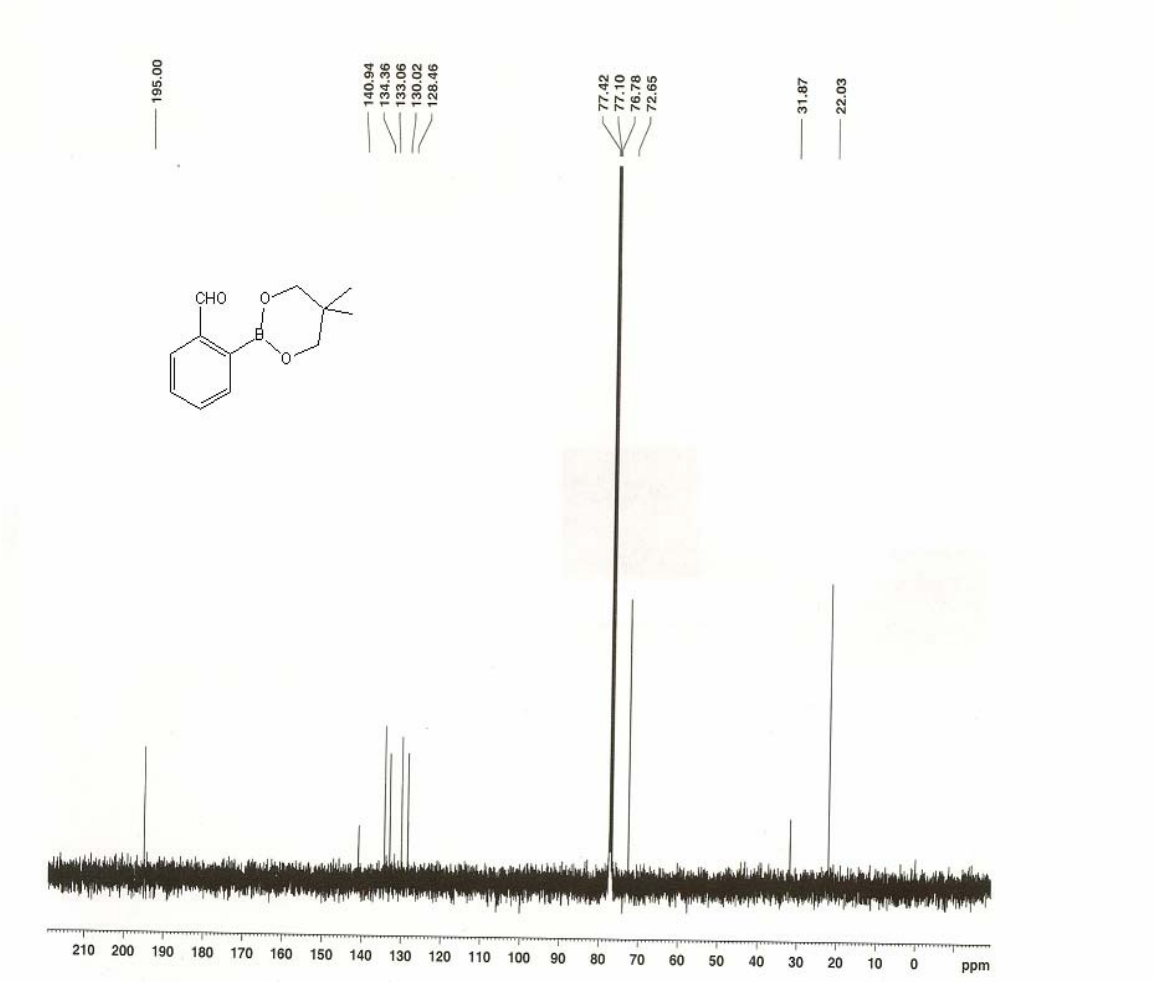
195.00
140.94
134.36
133.06
130.02
128.46
77.42
77.10
76.78
72.65
31.87
22.03
CHO
O
B
O
210 200 190 180 170 160 150 140 130 120 110 100 90 80 70 60 50 40 30 20 10 0
ppm

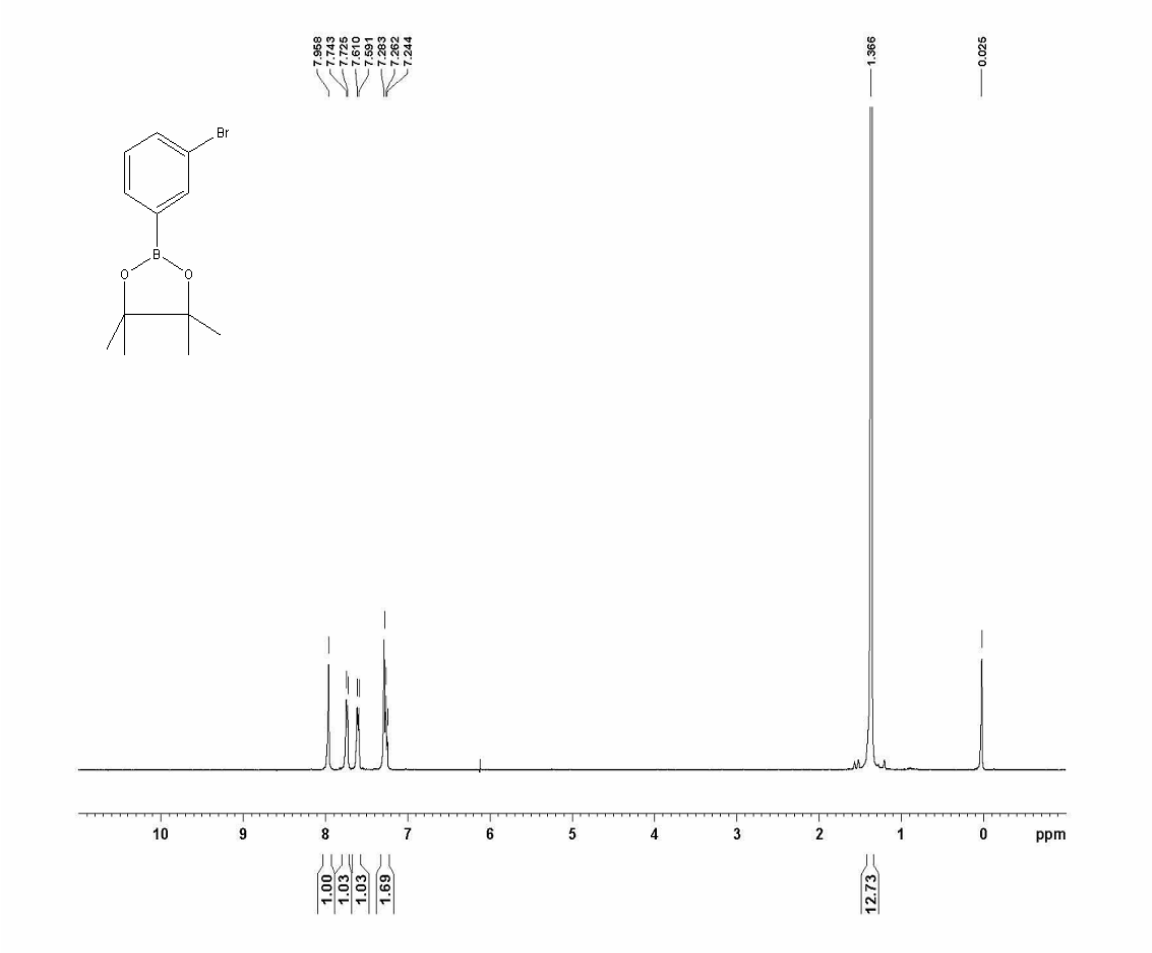
7.998
7.743
7.725
7.610
7.591
7.283
7.262
7.244
1.366
0.025
Br
B
O
O
10
9
8
7
6
5
4
3
2
1
0
ppm
1.00
1.03
1.03
1.69
12.73

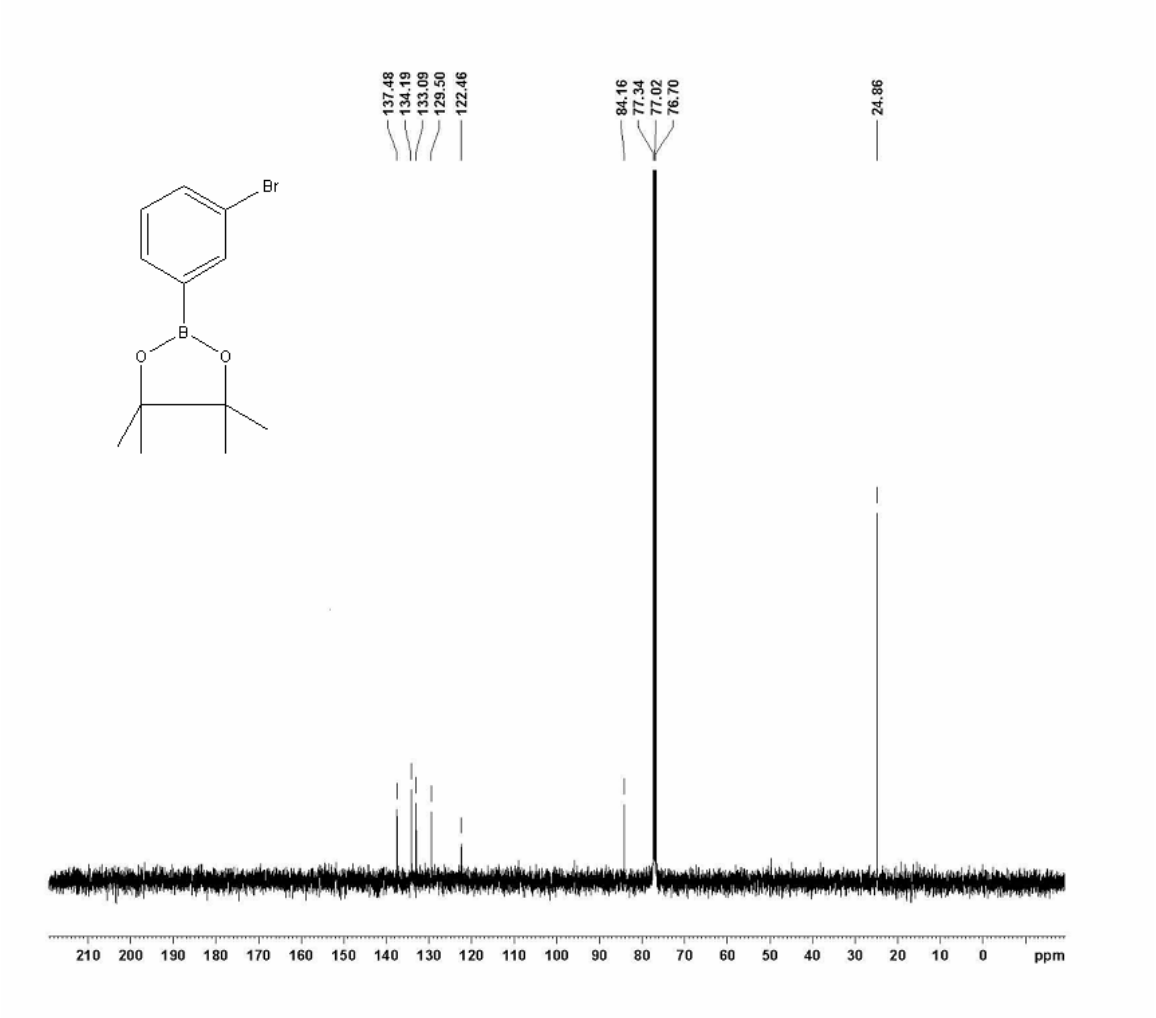
137.48
134.19
133.09
129.50
122.46
84.16
77.34
77.02
76.70
24.86
Br
B
O
O
210 200 190 180 170 160 150 140 130 120 110 100 90 80 70 60 50 40 30 20 10 0 ppm

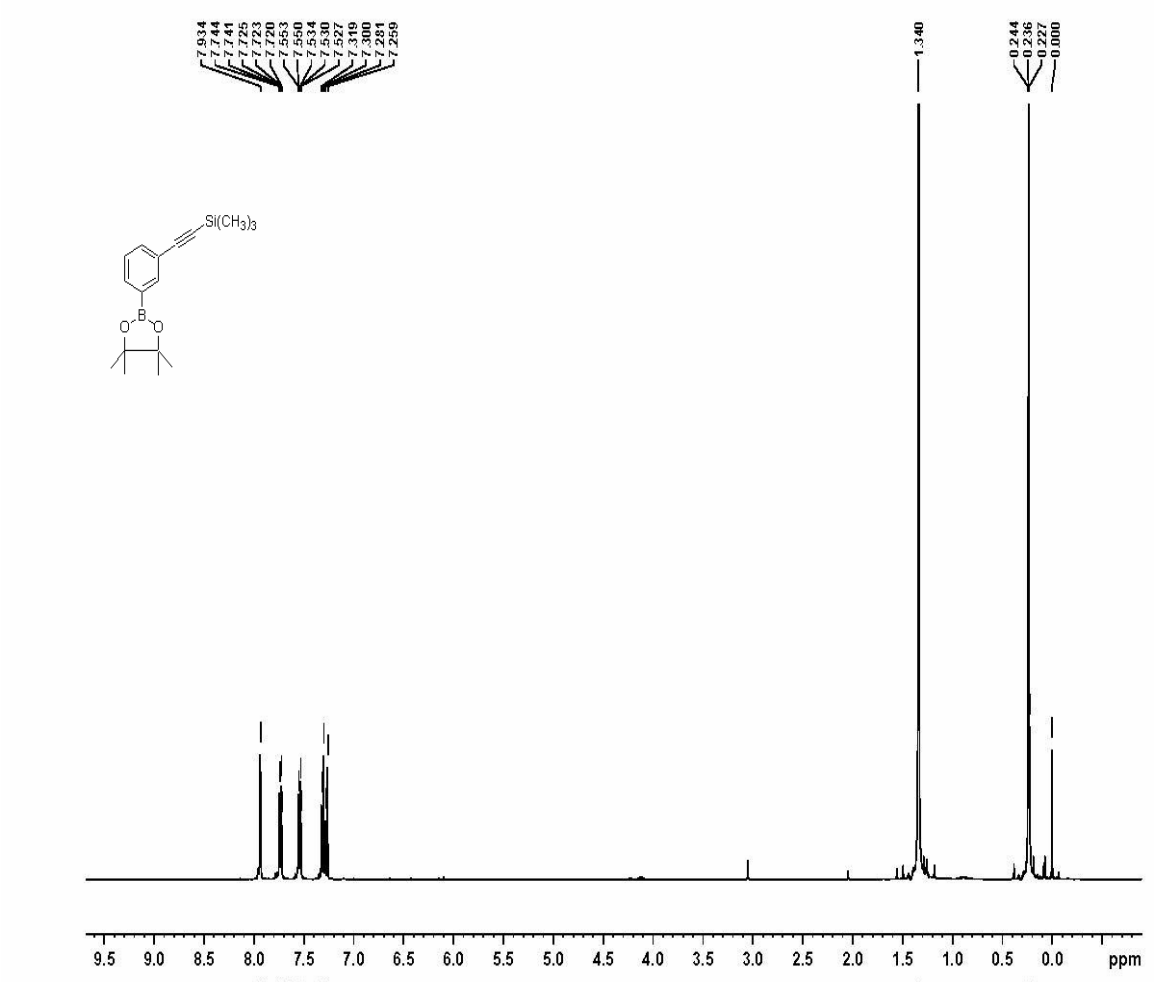
7.934
7.744
7.741
7.725
7.723
7.720
7.553
7.550
7.534
7.530
7.527
7.319
7.300
7.281
7.259
1.340
0.244
0.236
0.227
0.000
Si(CH3)3
B
O
O
9.5 9.0 8.5 8.0 7.5 7.0 6.5 6.0 5.5 5.0 4.5 4.0 3.5 3.0 2.5 2.0 1.5 1.0 0.5 0.0 ppm

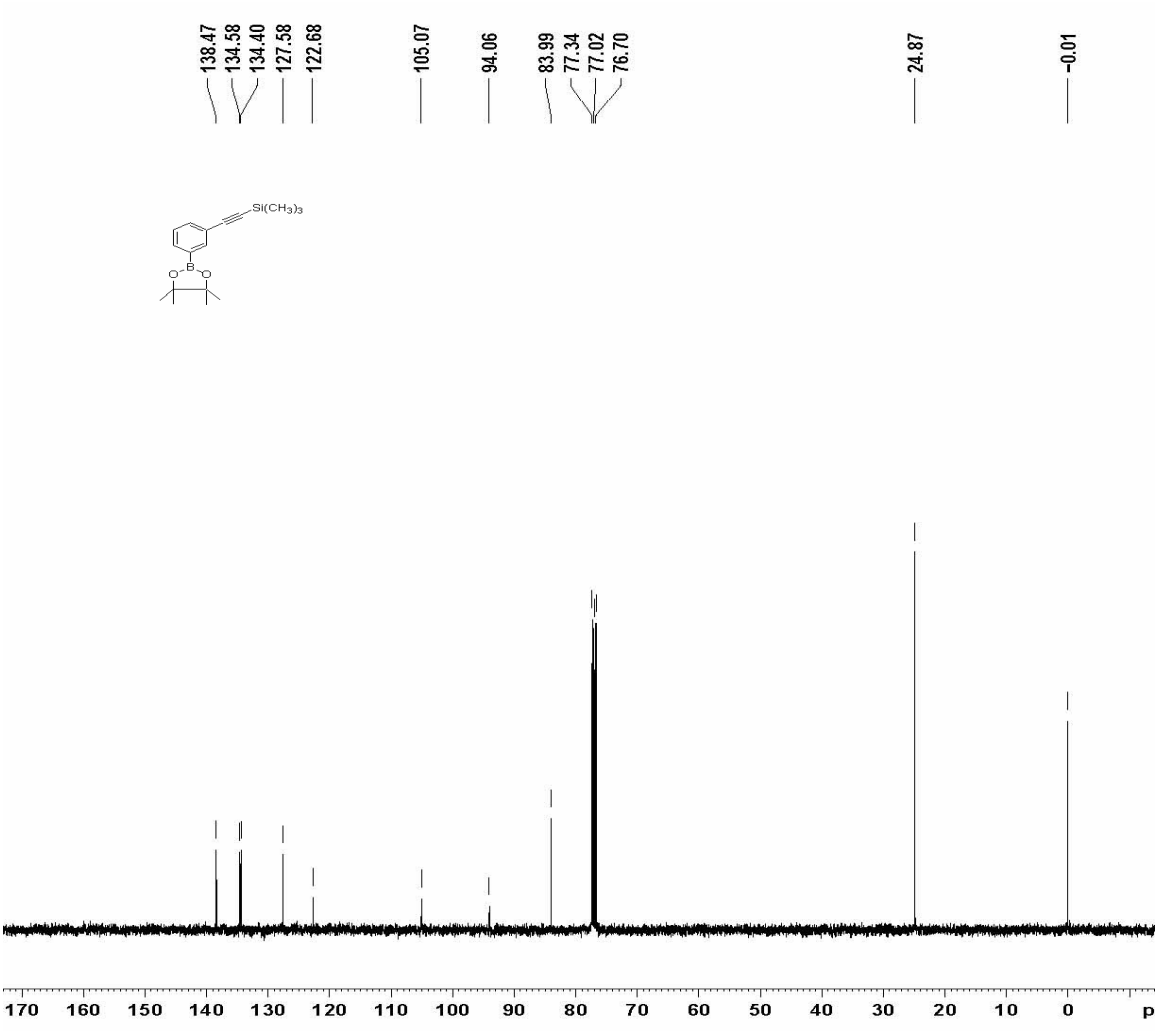
138.47
134.58
134.40
127.58
122.68
105.07
94.06
83.99
77.34
77.02
76.70
24.87
-0.01
Si(CH3)3
B
O
O
170
160
150
140
130
120
110
100
90
80
70
60
50
40
30
20
10
0
p

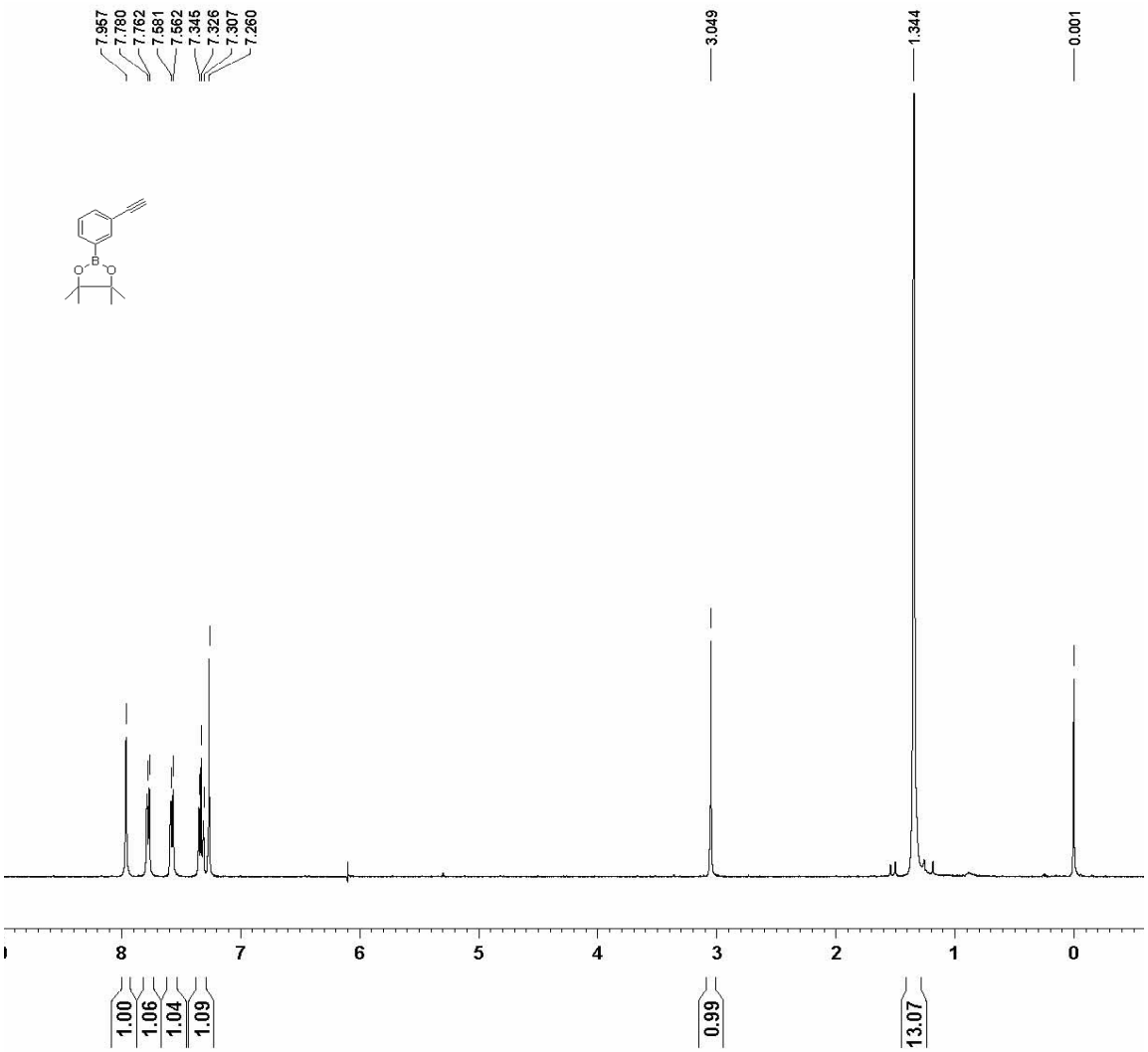
7.957
7.780
7.762
7.681
7.562
7.345
7.326
7.307
7.260
3.049
1.344
0.001
8
7
6
5
4
3
2
1
0
1.00
1.06
1.04
1.09
0.99
13.07

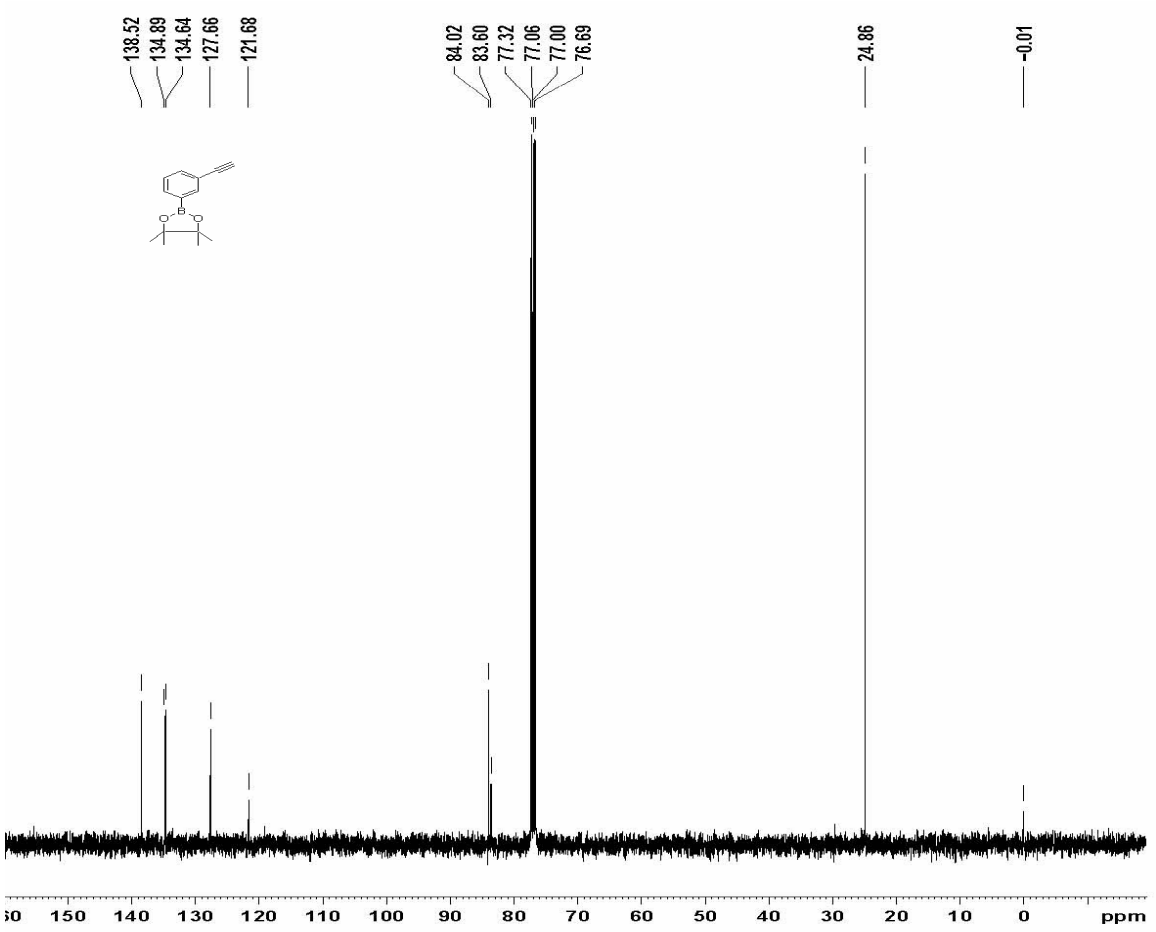
138.52
134.89
134.64
127.66
121.68
84.02
83.60
77.32
77.06
77.00
76.69
24.86
-0.01
150
140
130
120
110
100
90
80
70
60
50
40
30
20
10
0
ppm

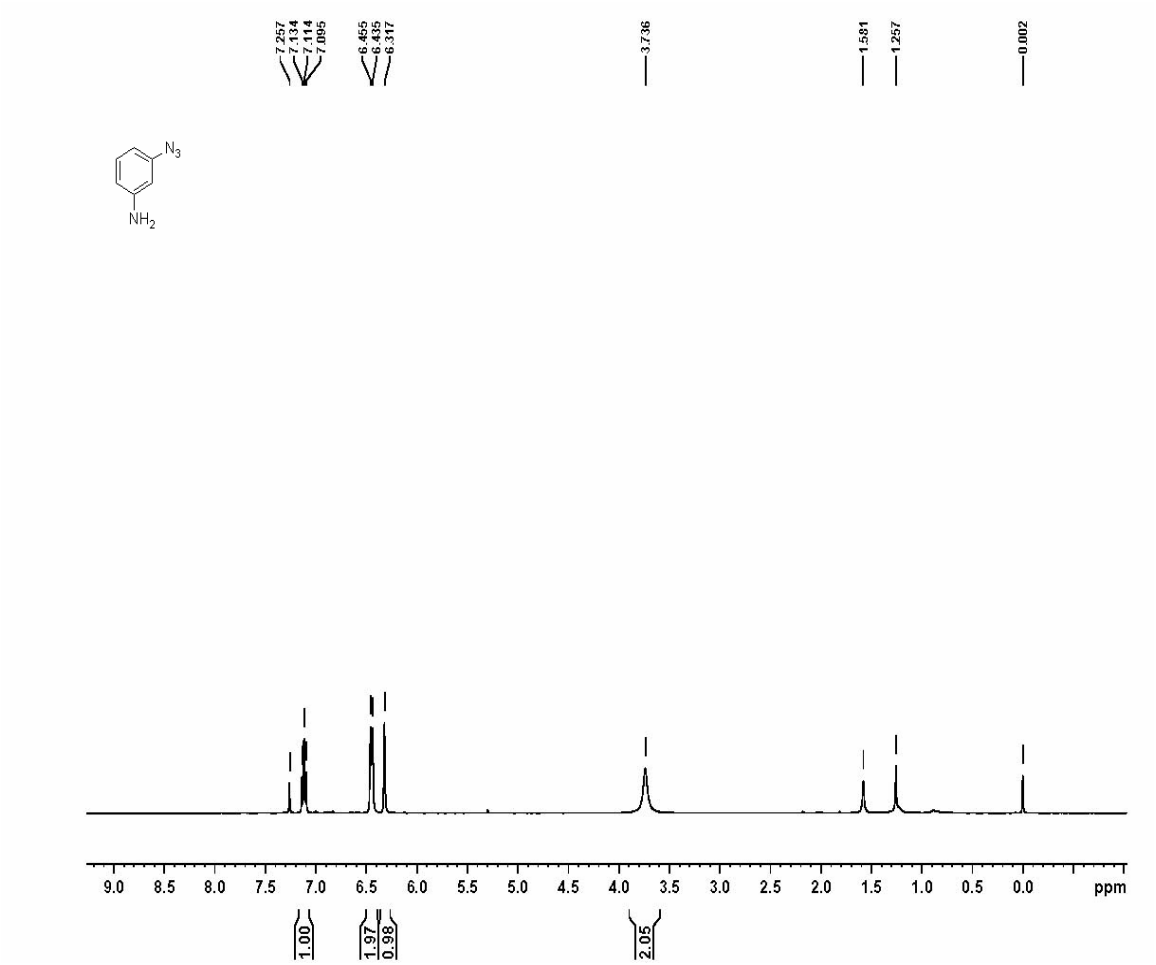
7.257
7.134
7.114
7.095
6.455
6.435
6.317
3.736
1.581
1.257
0.002
N3
NH2
9.0
8.5
8.0
7.5
7.0
6.5
6.0
5.5
5.0
4.5
4.0
3.5
3.0
2.5
2.0
1.5
1.0
0.5
0.0
ppm
1.00
1.97
0.98
2.05

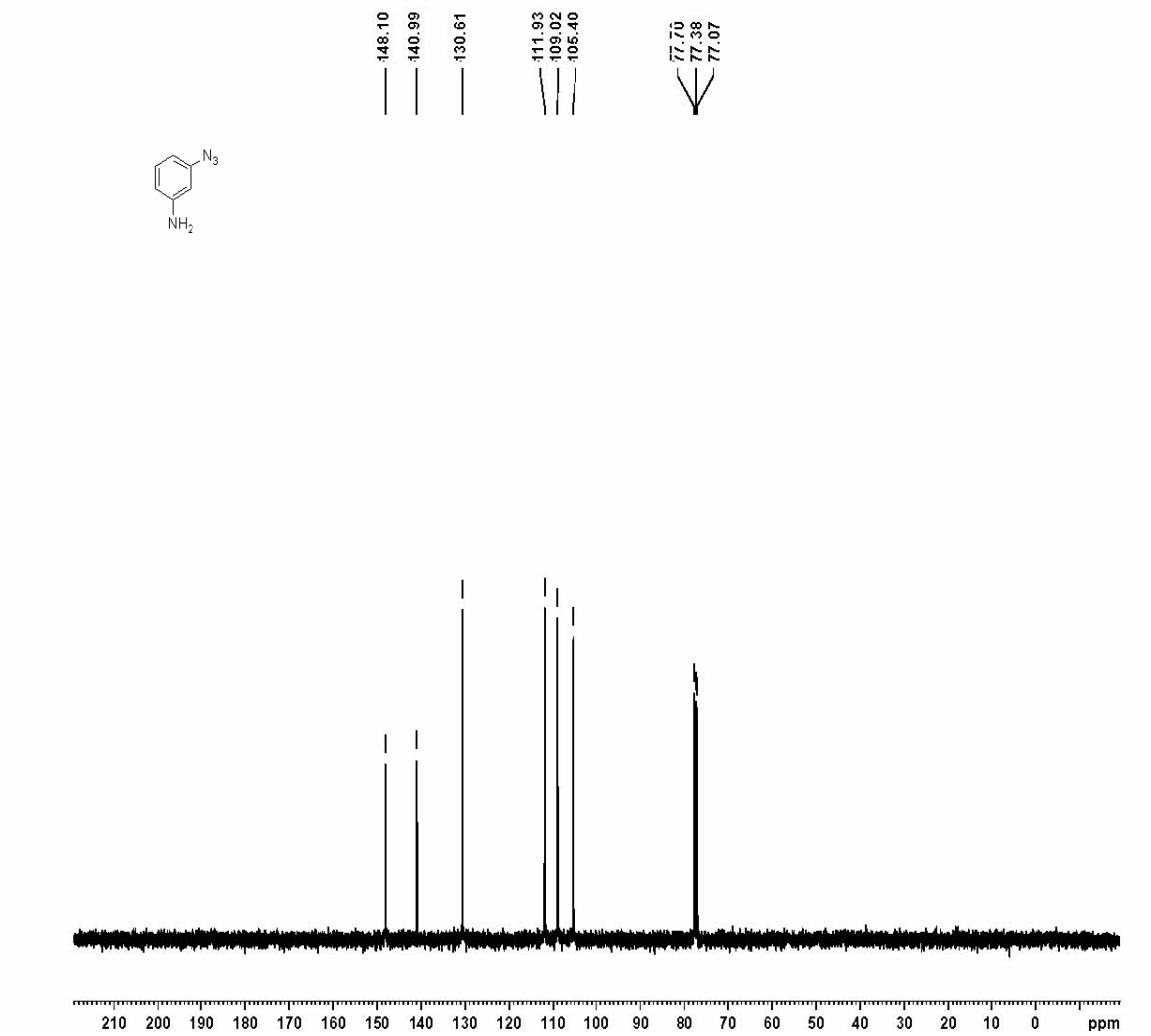
148.10
140.99
130.61
111.93
109.02
105.40
77.70
77.38
77.07
N3
NH2
210 200 190 180 170 160 150 140 130 120 110 100 90 80 70 60 50 40 30 20 10 0 ppm

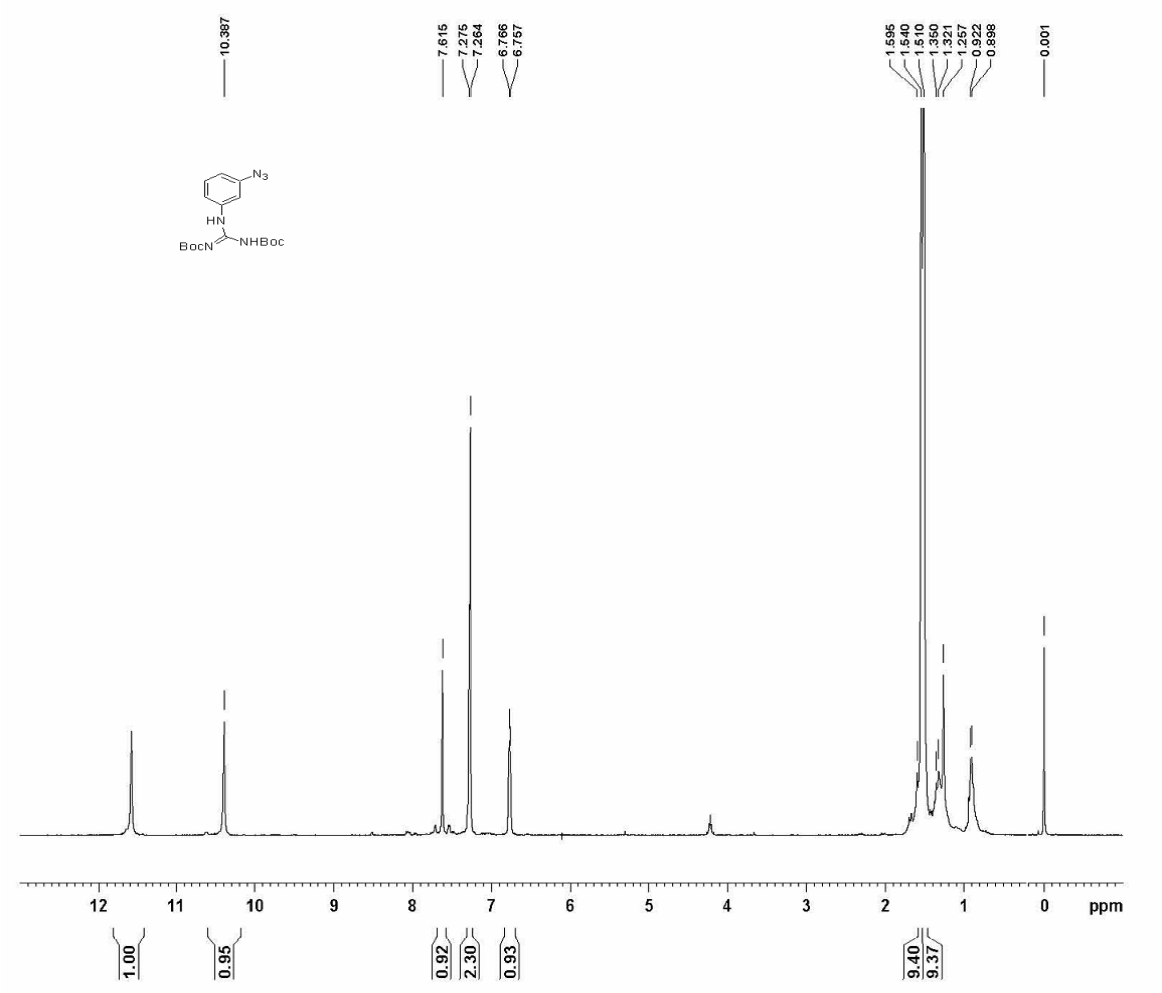
10.387
7.615
7.275
7.264
6.766
6.757
1.595
1.540
1.510
1.350
1.321
1.257
0.922
0.898
0.001
N3
HN
BocN
NHBoc
12
11
10
9
8
7
6
5
4
3
2
1
0
ppm
1.00
0.95
0.92
2.30
0.93
9.40
9.37

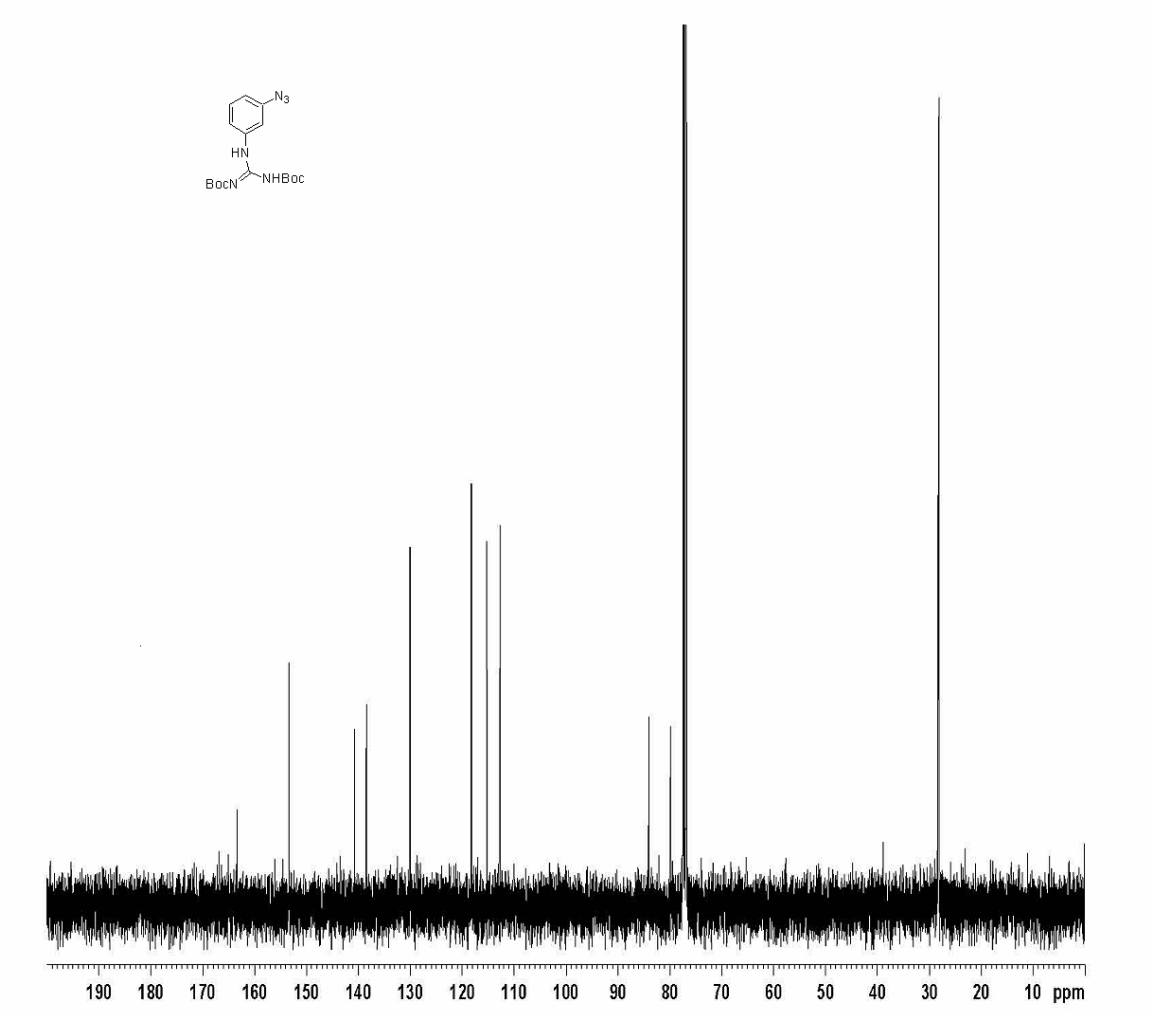
N3
HN
BocN
NHBoc
190 180 170 160 150 140 130 120 110 100 90 80 70 60 50 40 30 20 10 ppm

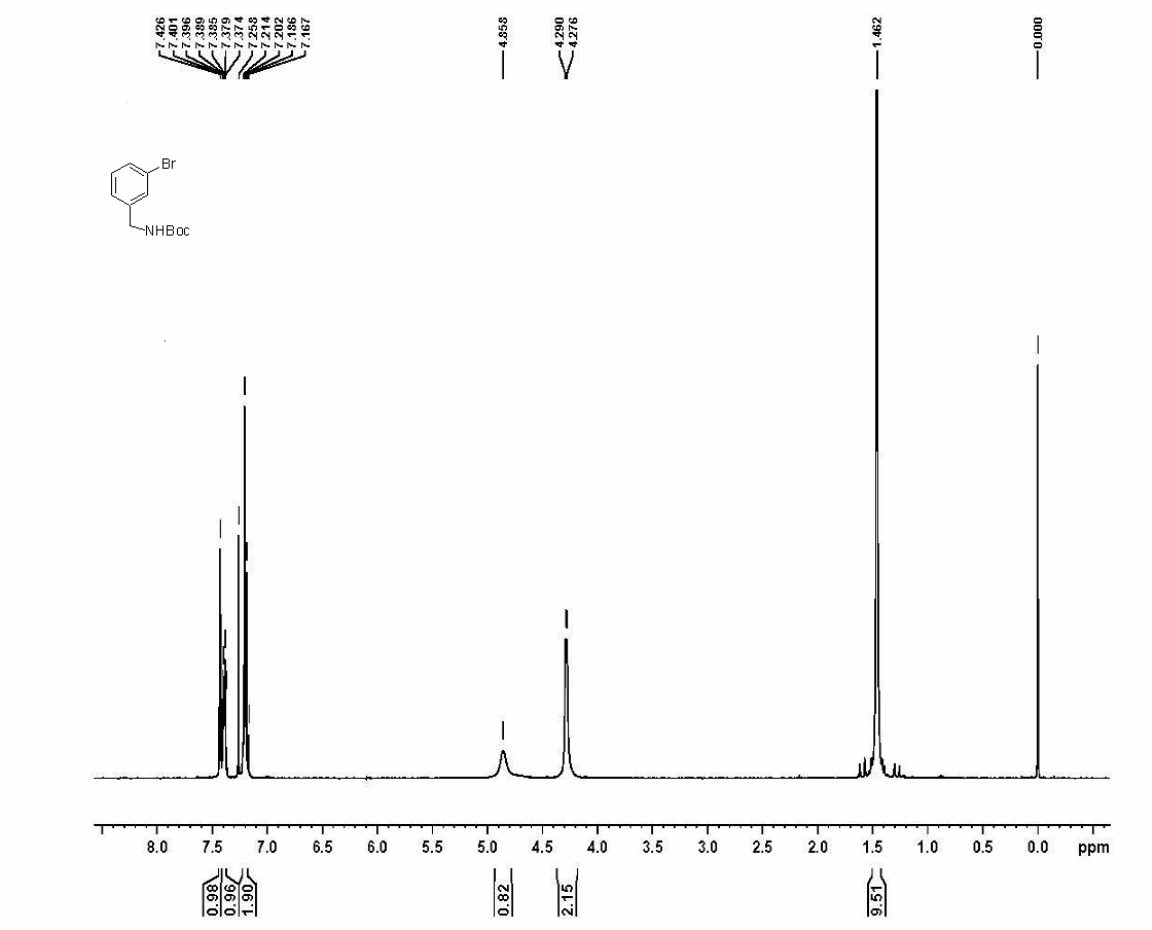
7.426
7.401
7.396
7.389
7.385
7.379
7.374
7.258
7.214
7.202
7.186
7.167
4.858
4.290
4.276
1.462
0.000
Br
NHBoc
8.0
7.5
7.0
6.5
6.0
5.5
5.0
4.5
4.0
3.5
3.0
2.5
2.0
1.5
1.0
0.5
0.0
ppm
0.98
0.96
1.90
0.82
2.15
9.51

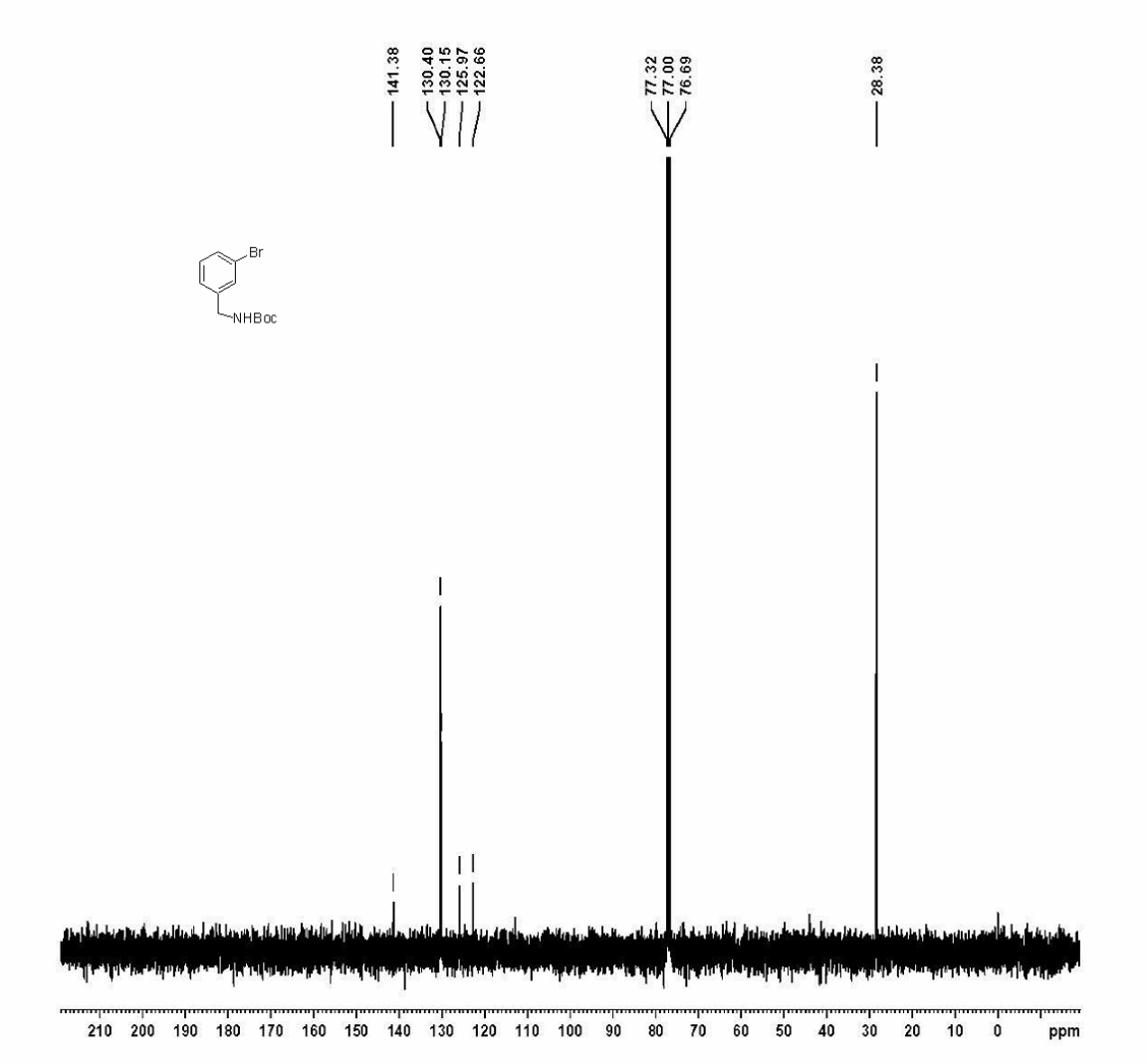
141.38
130.40
130.15
125.97
122.66
77.32
77.00
76.69
28.38
Br
NHBoc
210 200 190 180 170 160 150 140 130 120 110 100 90 80 70 60 50 40 30 20 10 0 ppm

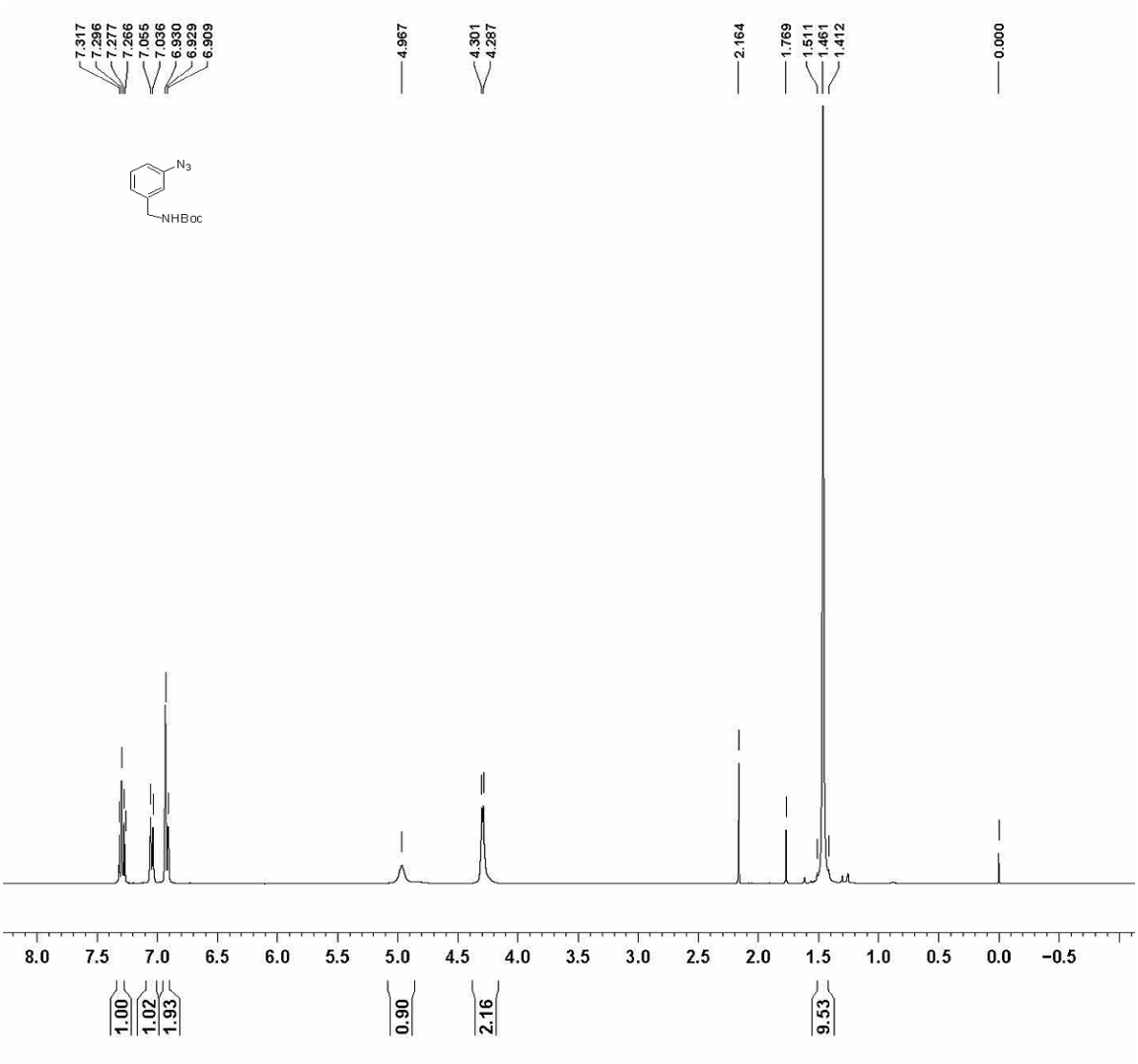
7.317
7.296
7.277
7.266
7.055
7.036
6.930
6.929
6.909
4.967
4.301
4.287
2.164
1.769
1.511
1.461
1.412
0.000
N3
NHBoc
8.0
7.5
7.0
6.5
6.0
5.5
5.0
4.5
4.0
3.5
3.0
2.5
2.0
1.5
1.0
0.5
0.0
−0.5
1.00
1.02
1.93
0.90
2.16
9.53

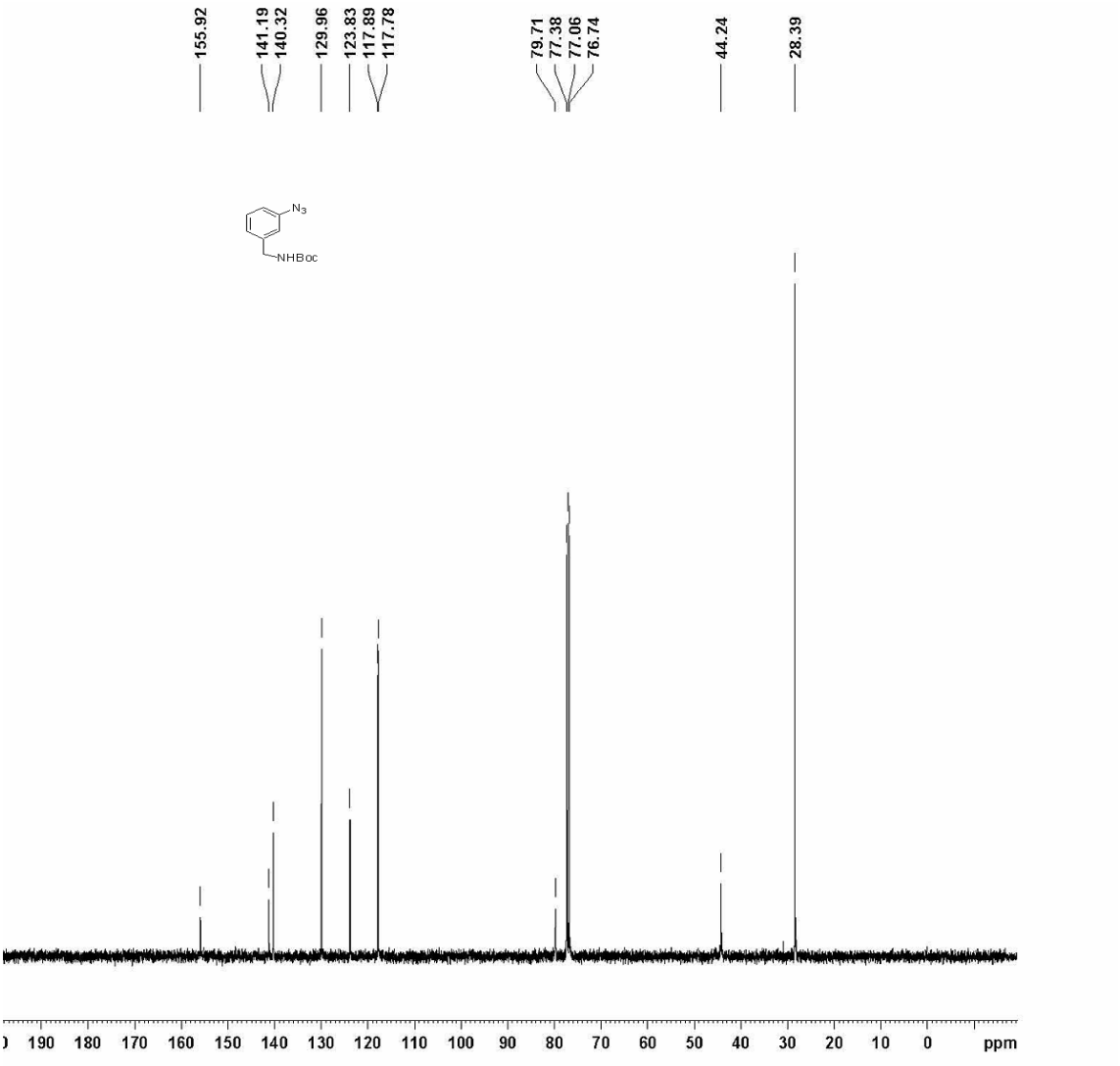
155.92
141.19
140.32
129.96
123.83
117.89
117.78
79.71
77.38
77.06
76.74
44.24
28.39
N3
NHBoc
190 180 170 160 150 140 130 120 110 100 90 80 70 60 50 40 30 20 10 0 ppm

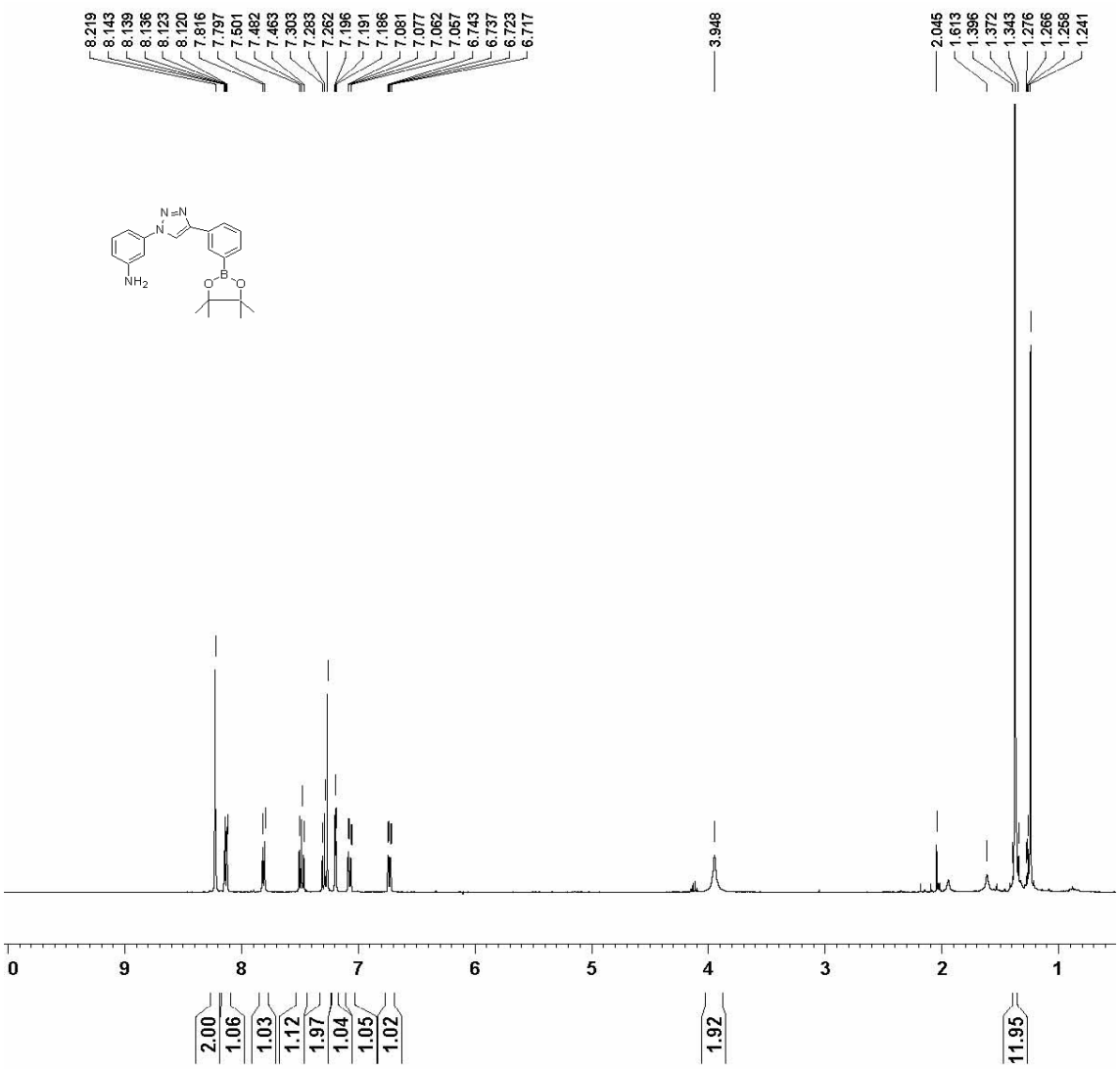
8.219
8.143
8.139
8.136
8.123
8.120
7.816
7.797
7.501
7.482
7.463
7.303
7.283
7.262
7.196
7.191
7.186
7.081
7.077
7.062
7.057
6.743
6.737
6.723
6.717
3.948
2.045
1.613
1.396
1.372
1.343
1.276
1.266
1.258
1.241
NH2
0
9
8
7
6
5
4
3
2
1
2.00
1.06
1.03
1.12
1.97
1.04
1.05
1.02
1.92
11.95

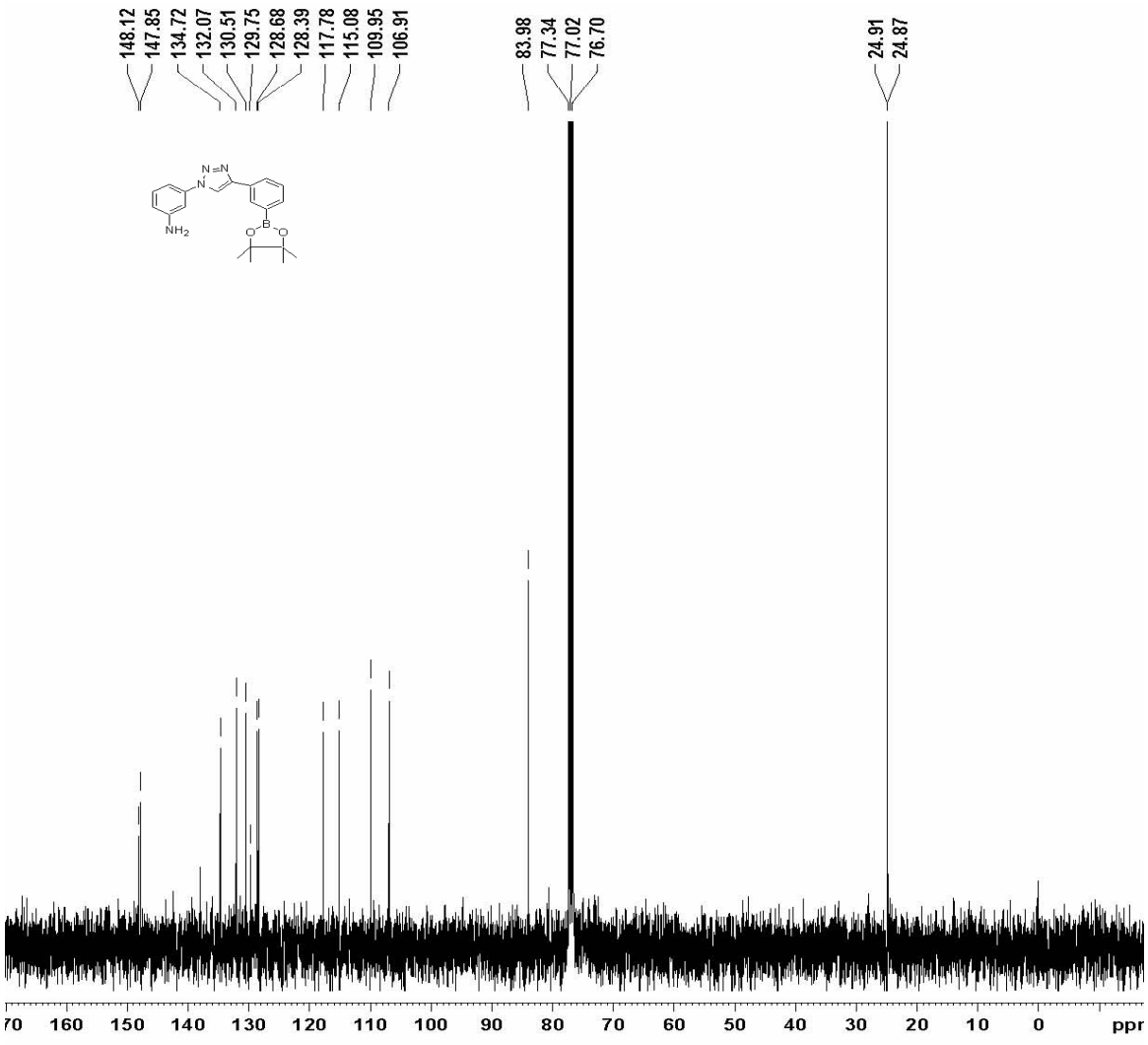
148.12
147.85
134.72
132.07
130.51
129.75
128.68
128.39
117.78
115.08
109.95
106.91
83.98
77.34
77.02
76.70
24.91
24.87
NH2
B
O
O
N=N
N
70
160
150
140
130
120
110
100
90
80
70
60
50
40
30
20
10
0
ppr

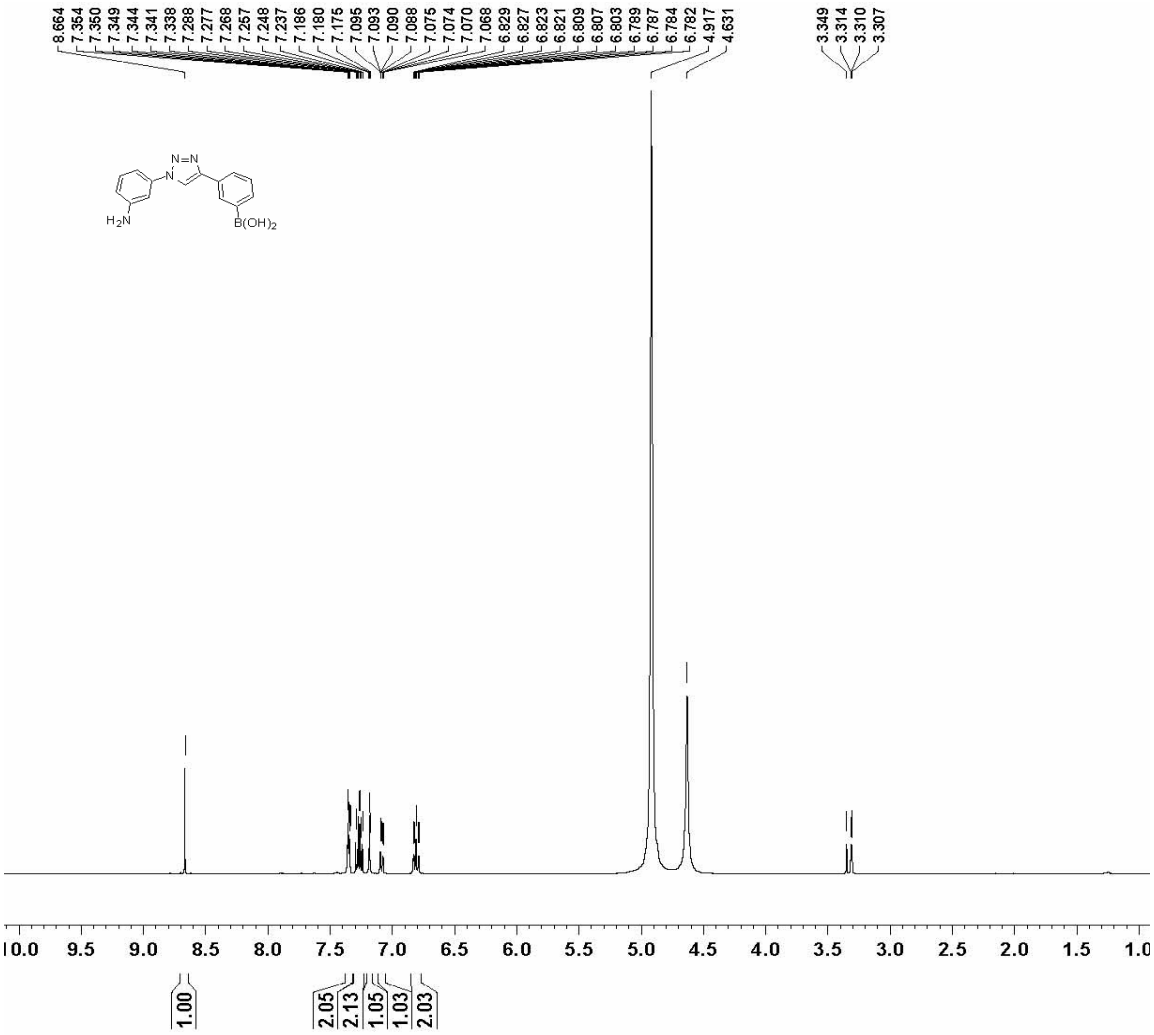
8.664
7.354
7.350
7.349
7.344
7.341
7.338
7.288
7.277
7.268
7.257
7.248
7.237
7.186
7.180
7.175
7.095
7.093
7.090
7.088
7.075
7.074
7.070
7.068
6.829
6.827
6.823
6.821
6.809
6.807
6.803
6.789
6.787
6.784
6.782
4.917
4.631
3.349
3.314
3.310
3.307
N=N
N
H2N
B(OH)2
10.0
9.5
9.0
8.5
8.0
7.5
7.0
6.5
6.0
5.5
5.0
4.5
4.0
3.5
3.0
2.5
2.0
1.5
1.0
1.00
2.05
2.13
1.05
1.03
2.03

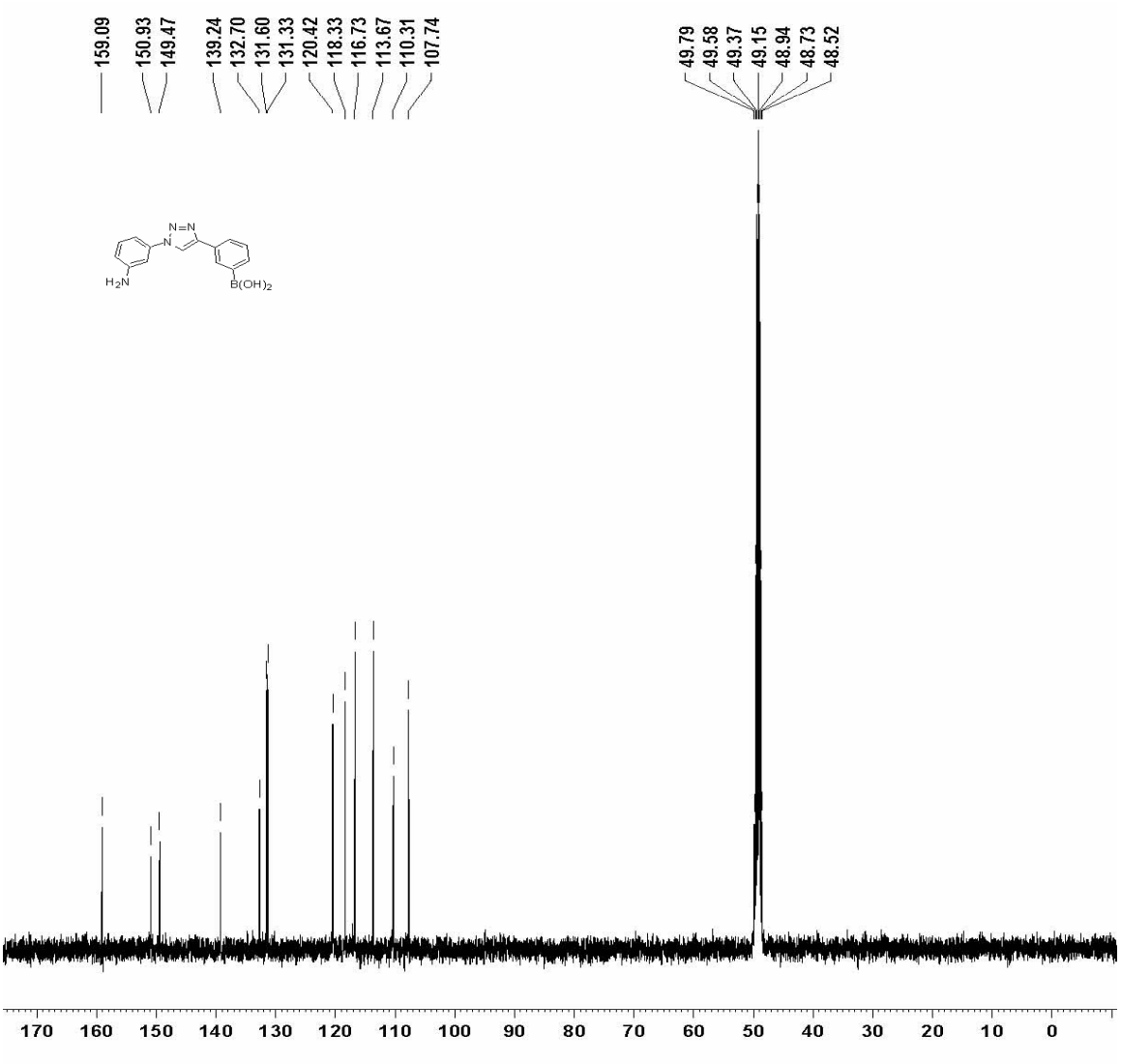
159.09
150.93
149.47
139.24
132.70
131.60
131.33
120.42
118.33
116.73
113.67
110.31
107.74
49.79
49.58
49.37
49.15
48.94
48.73
48.52
N=N
N
H2N
B(OH)2
170
160
150
140
130
120
110
100
90
80
70
60
50
40
30
20
10
0

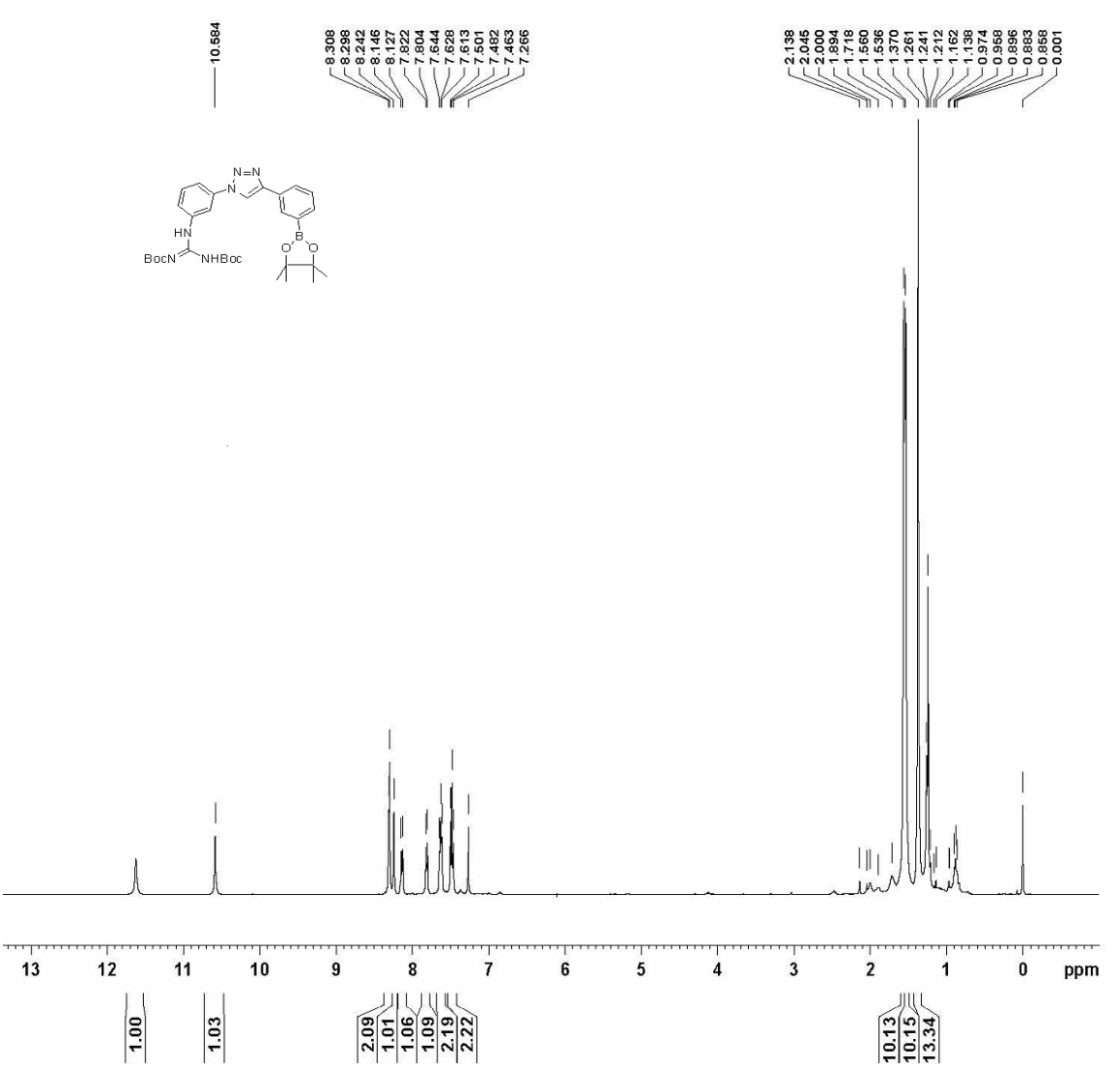
10.584
8.308
8.298
8.242
8.146
8.127
7.822
7.804
7.644
7.628
7.613
7.501
7.482
7.463
7.266
2.138
2.045
2.000
1.894
1.718
1.560
1.536
1.370
1.261
1.241
1.212
1.162
1.138
0.974
0.958
0.896
0.883
0.858
0.001
HN
BocN
NHBoc
13
12
11
10
9
8
7
6
5
4
3
2
1
0
ppm
1.00
1.03
2.09
1.01
1.06
1.09
2.19
2.22
10.13
10.15
13.34

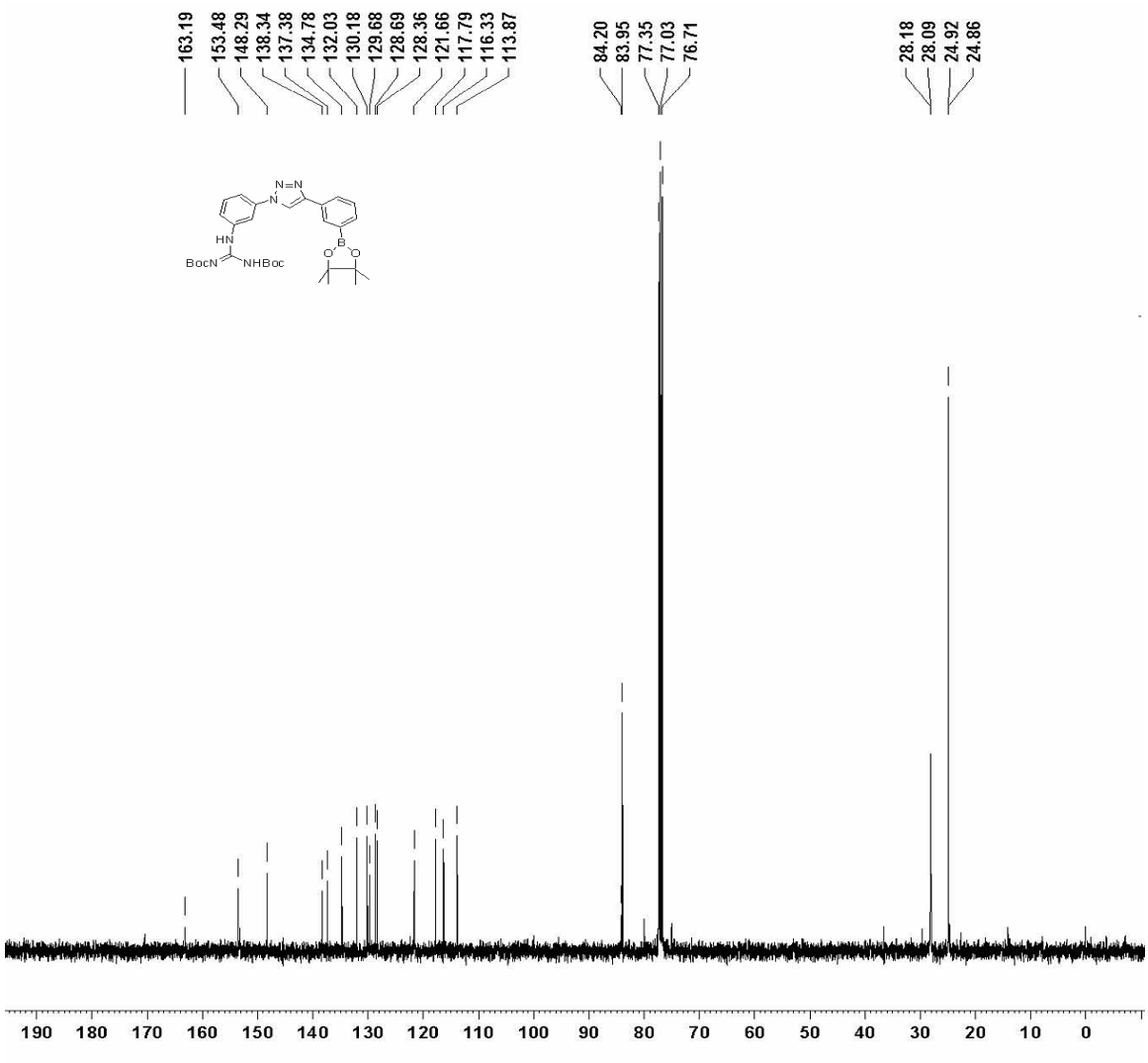
163.19
153.48
148.29
138.34
137.38
134.78
132.03
130.18
129.68
128.69
128.36
121.66
117.79
116.33
113.87
84.20
83.95
77.35
77.03
76.71
28.18
28.09
24.92
24.86
N=N
N
HN
BocN
NHBoc
B
O
O
190
180
170
160
150
140
130
120
110
100
90
80
70
60
50
40
30
20
10
0

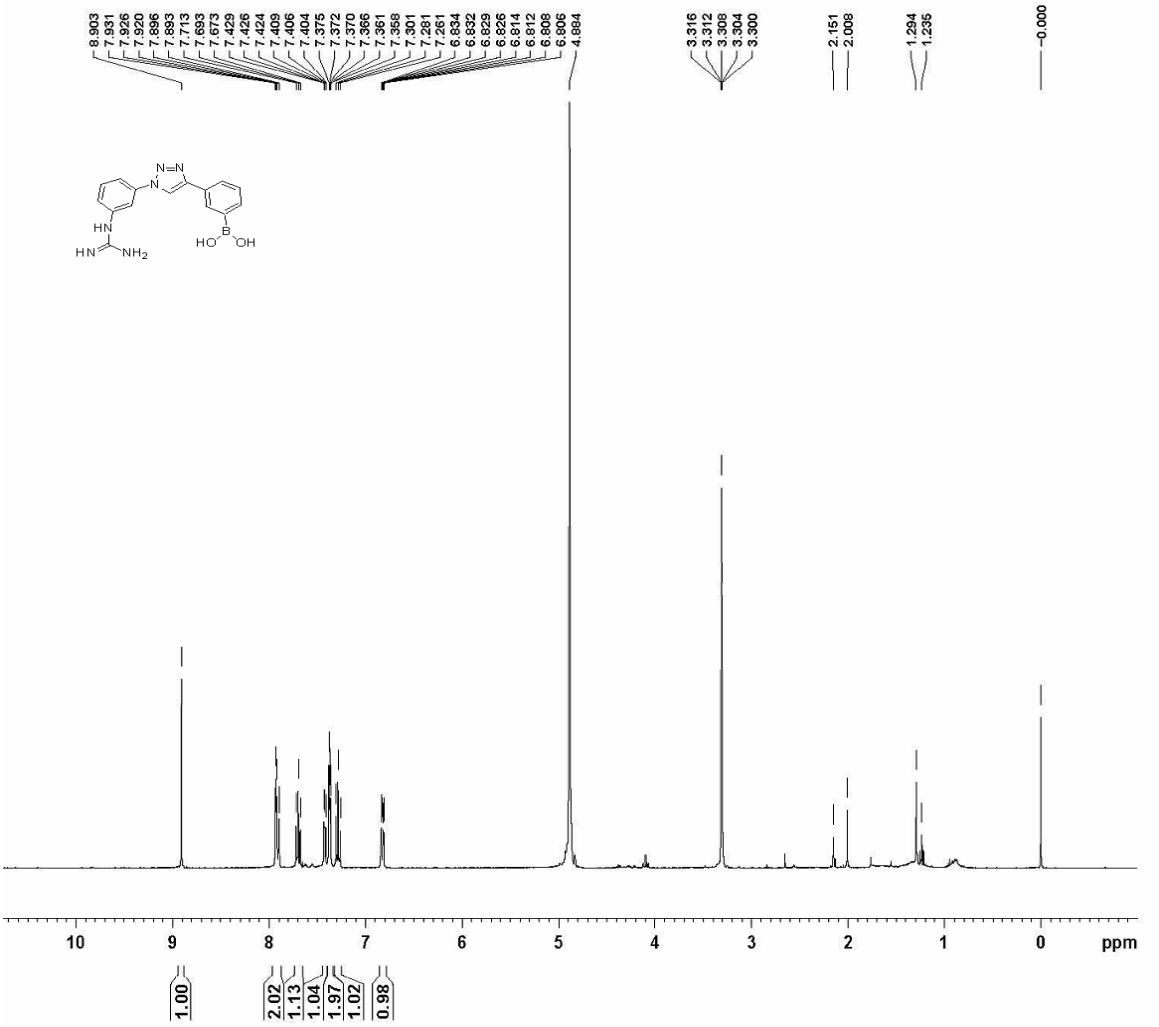
8.903
7.931
7.926
7.920
7.896
7.893
7.713
7.693
7.673
7.429
7.426
7.424
7.409
7.406
7.404
7.375
7.372
7.370
7.366
7.361
7.358
7.301
7.281
7.261
6.834
6.832
6.829
6.826
6.814
6.812
6.808
6.806
4.884
3.316
3.312
3.308
3.304
3.300
2.151
2.008
1.294
1.235
0.000
HN
HN
NH2
N=N
N
B
HO
OH
10
9
8
7
6
5
4
3
2
1
0
ppm
1.00
2.02
1.13
1.04
1.97
1.02
0.98

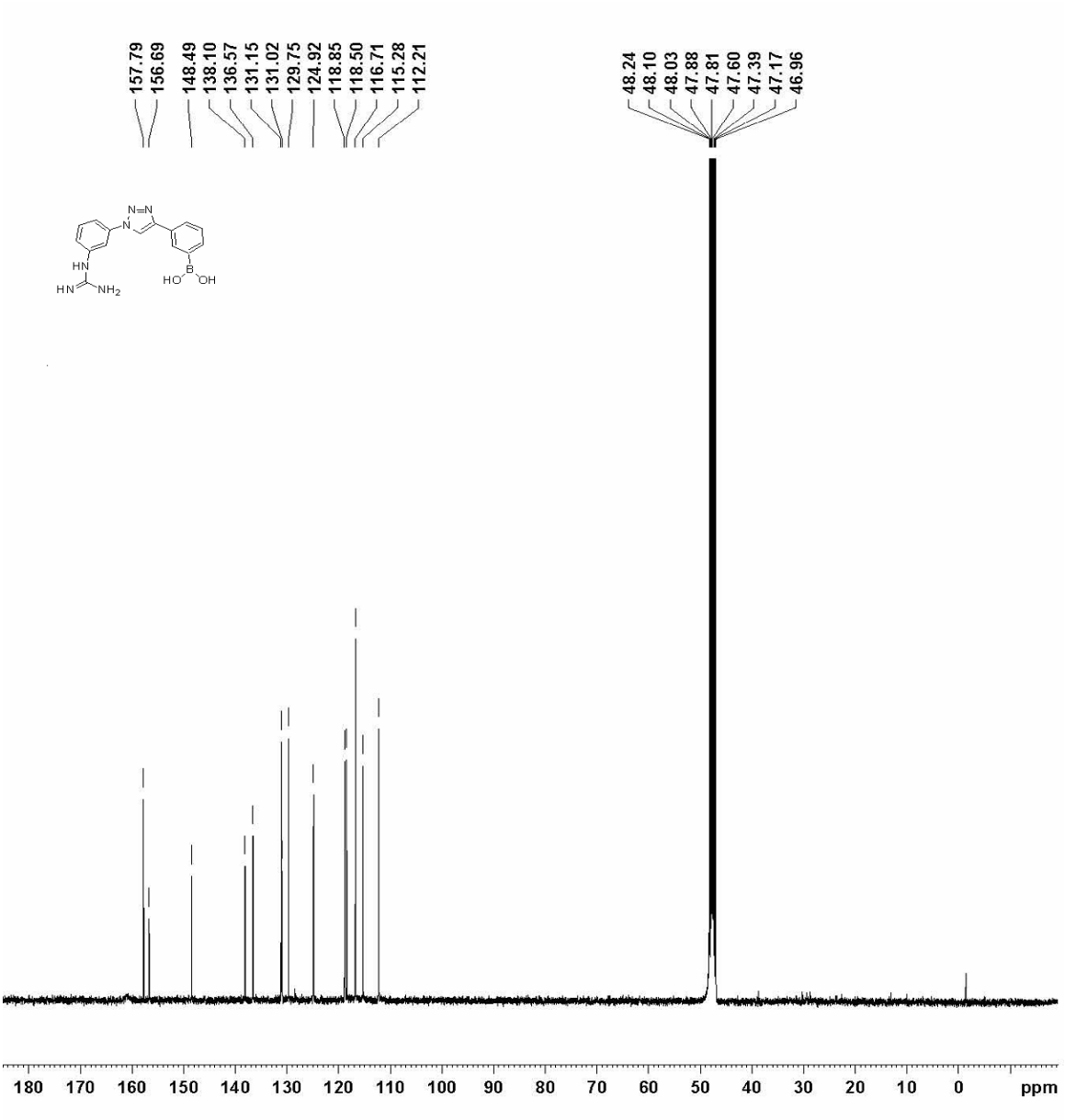
157.79
156.69
148.49
138.10
136.57
131.15
131.02
129.75
124.92
118.85
118.50
116.71
115.28
112.21
48.24
48.10
48.03
47.88
47.81
47.60
47.39
47.17
46.96
N=N
N
HN
HN
NH2
B
HO
OH
180
170
160
150
140
130
120
110
100
90
80
70
60
50
40
30
20
10
0
ppm

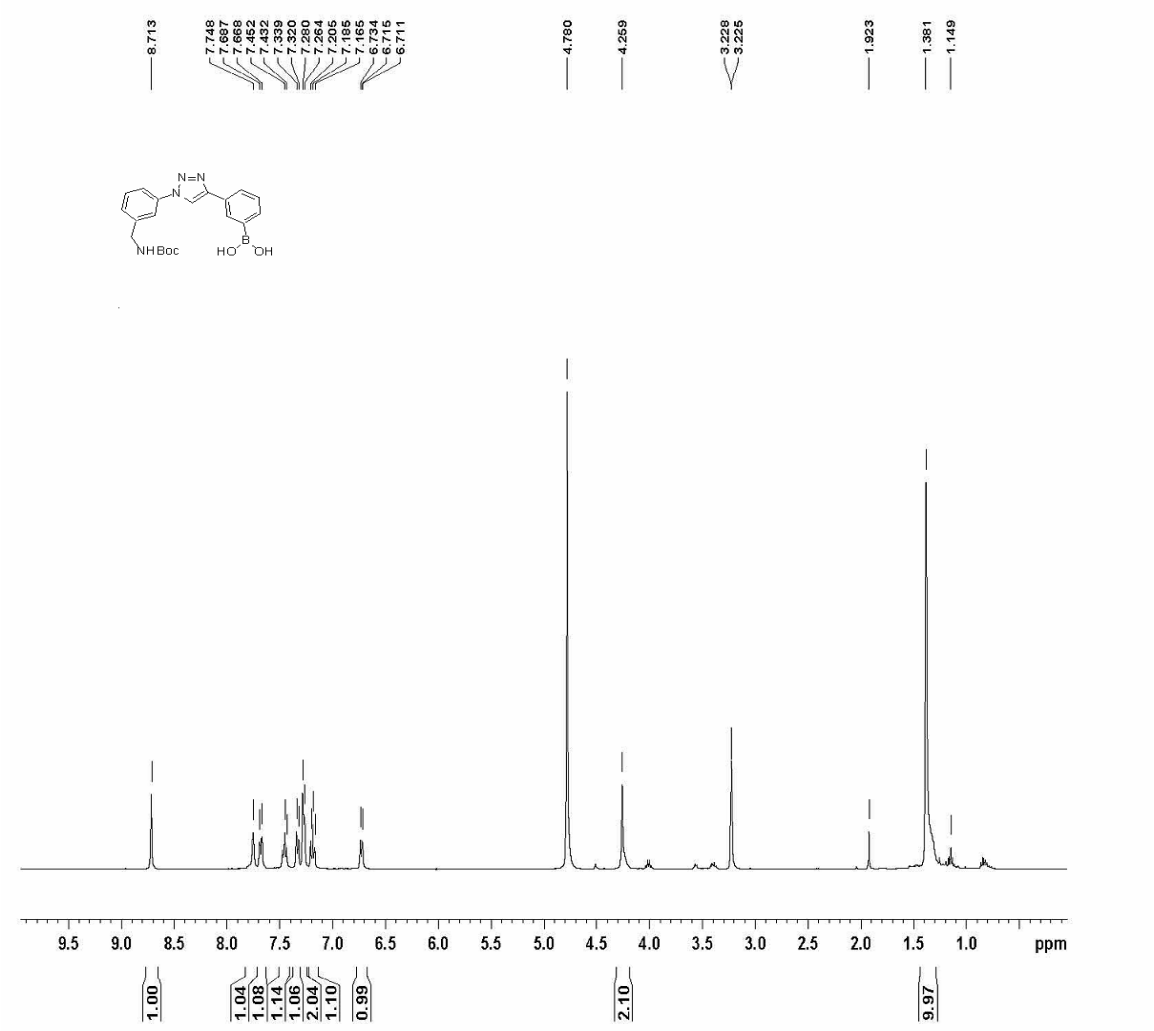
8.713
7.748
7.687
7.668
7.452
7.432
7.339
7.320
7.280
7.264
7.205
7.186
7.165
6.734
6.715
6.711
4.790
4.259
3.228
3.225
1.923
1.381
1.149
N=N
NHBoc
B
HO
OH
9.5
9.0
8.5
8.0
7.5
7.0
6.5
6.0
5.5
5.0
4.5
4.0
3.5
3.0
2.5
2.0
1.5
1.0
ppm
1.00
1.04
1.08
1.14
1.06
2.04
1.10
0.99
2.10
9.97

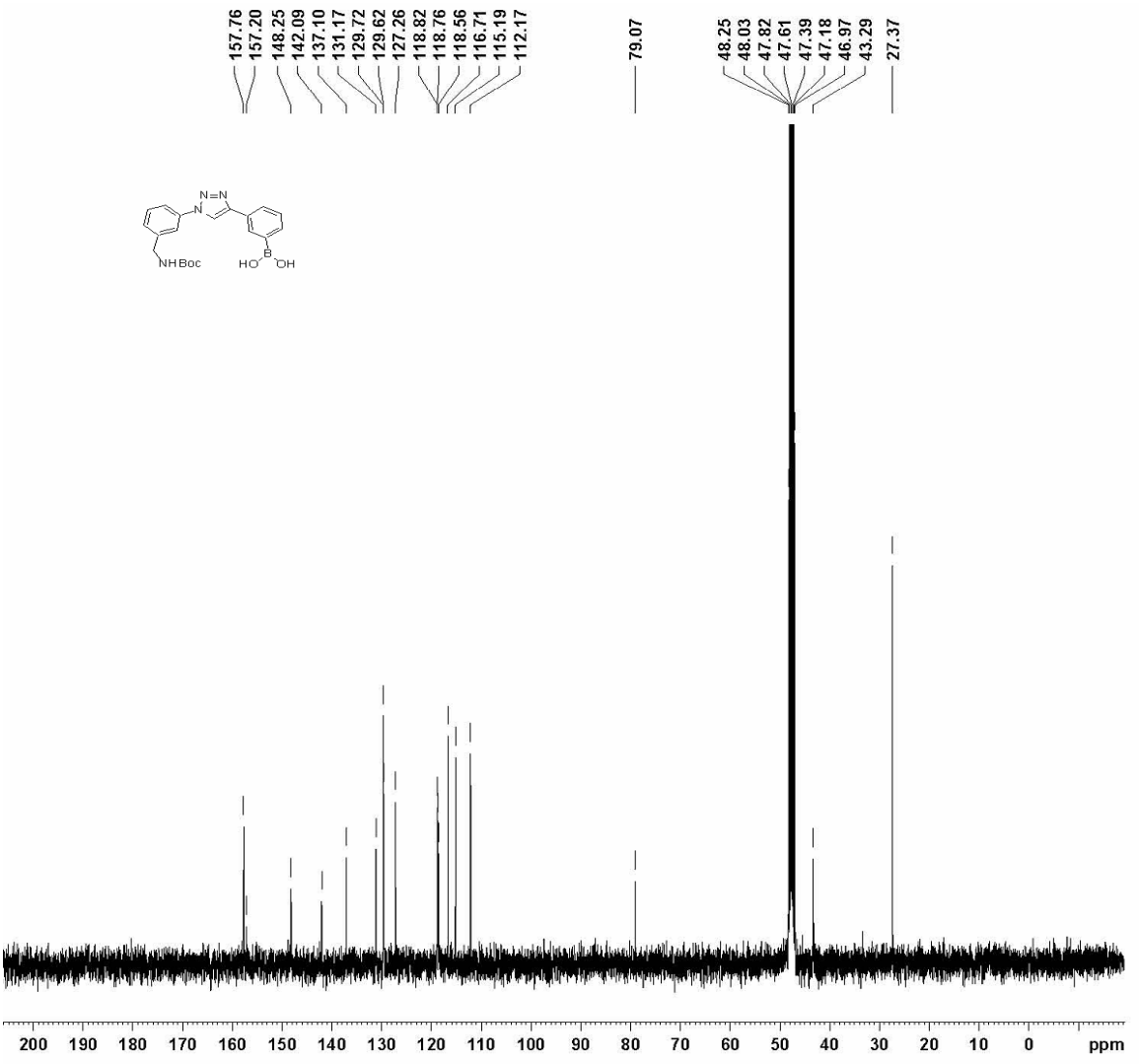
157.76
157.20
148.25
142.09
137.10
131.17
129.72
129.62
127.26
118.82
118.76
118.56
116.71
115.19
112.17
79.07
48.25
48.03
47.82
47.61
47.39
47.18
46.97
43.29
27.37
N=N
N
NHBoc
B
HO
OH
200
190
180
170
160
150
140
130
120
110
100
90
80
70
60
50
40
30
20
10
0
ppm

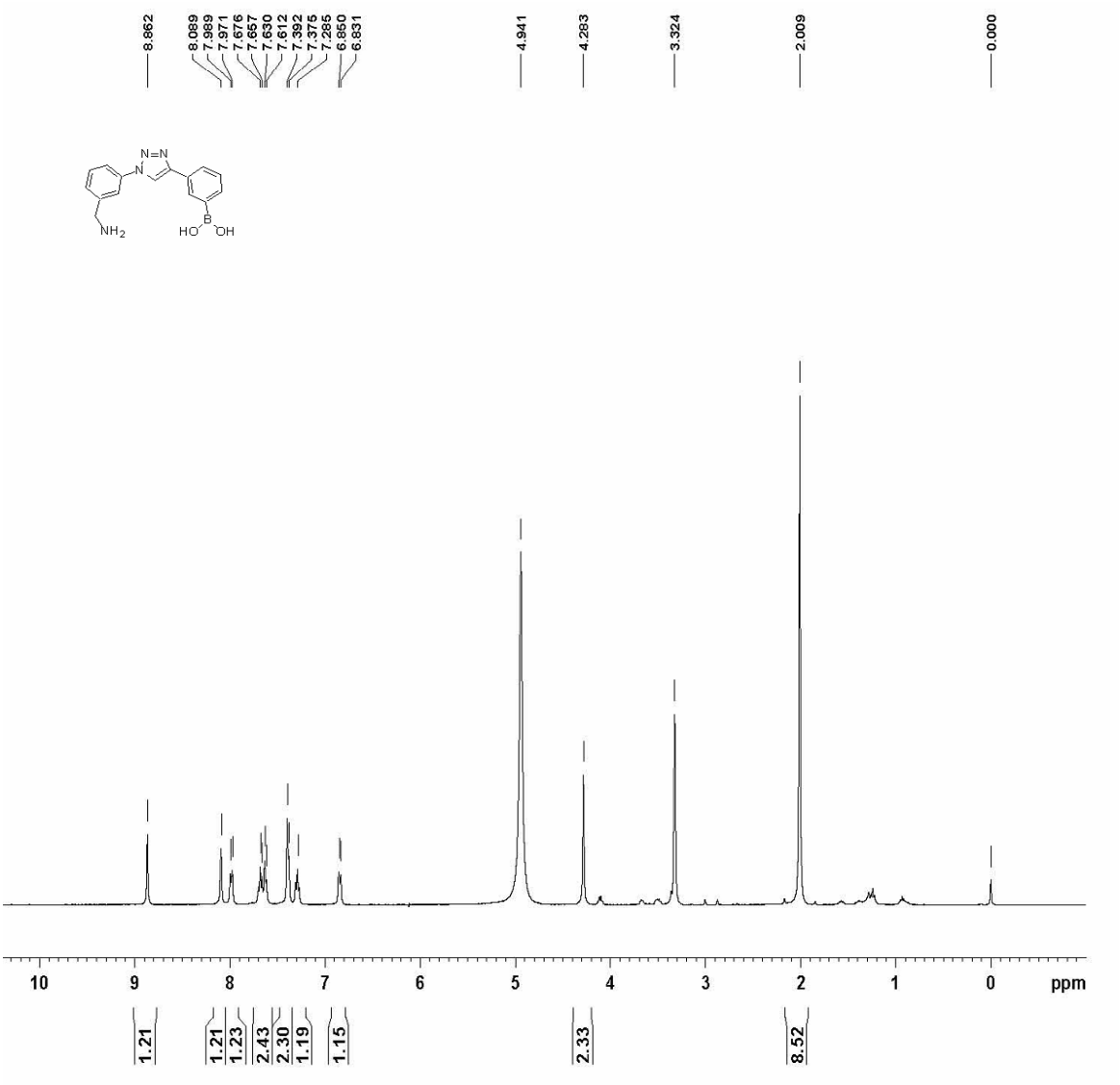
8.862
8.089
7.989
7.971
7.676
7.657
7.630
7.612
7.392
7.375
7.285
6.850
6.831
4.941
4.283
3.324
2.009
0.000
N=N
N
NH2
B
HO
OH
10
9
8
7
6
5
4
3
2
1
0
ppm
1.21
1.21
1.23
2.43
2.30
1.19
1.15
2.33
8.52

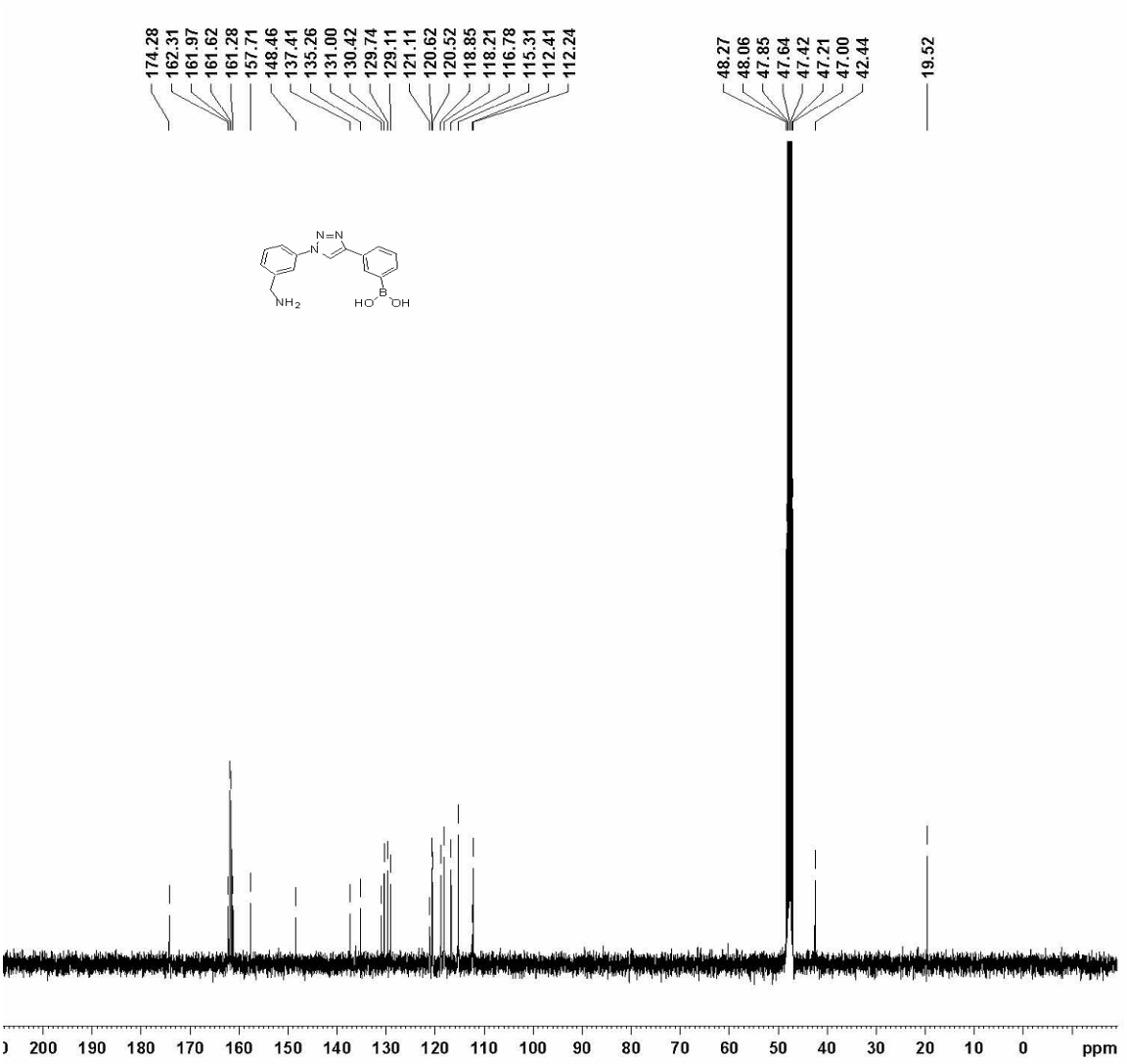
174.28
162.31
161.97
161.62
161.28
157.71
148.46
137.41
135.26
131.00
130.42
129.74
129.11
121.11
120.62
120.52
118.85
118.21
116.78
115.31
112.41
112.24
48.27
48.06
47.85
47.64
47.42
47.21
47.00
42.44
19.52
N=N
NH2
HO
OH
B
200
190
180
170
160
150
140
130
120
110
100
90
80
70
60
50
40
30
20
10
0
ppm

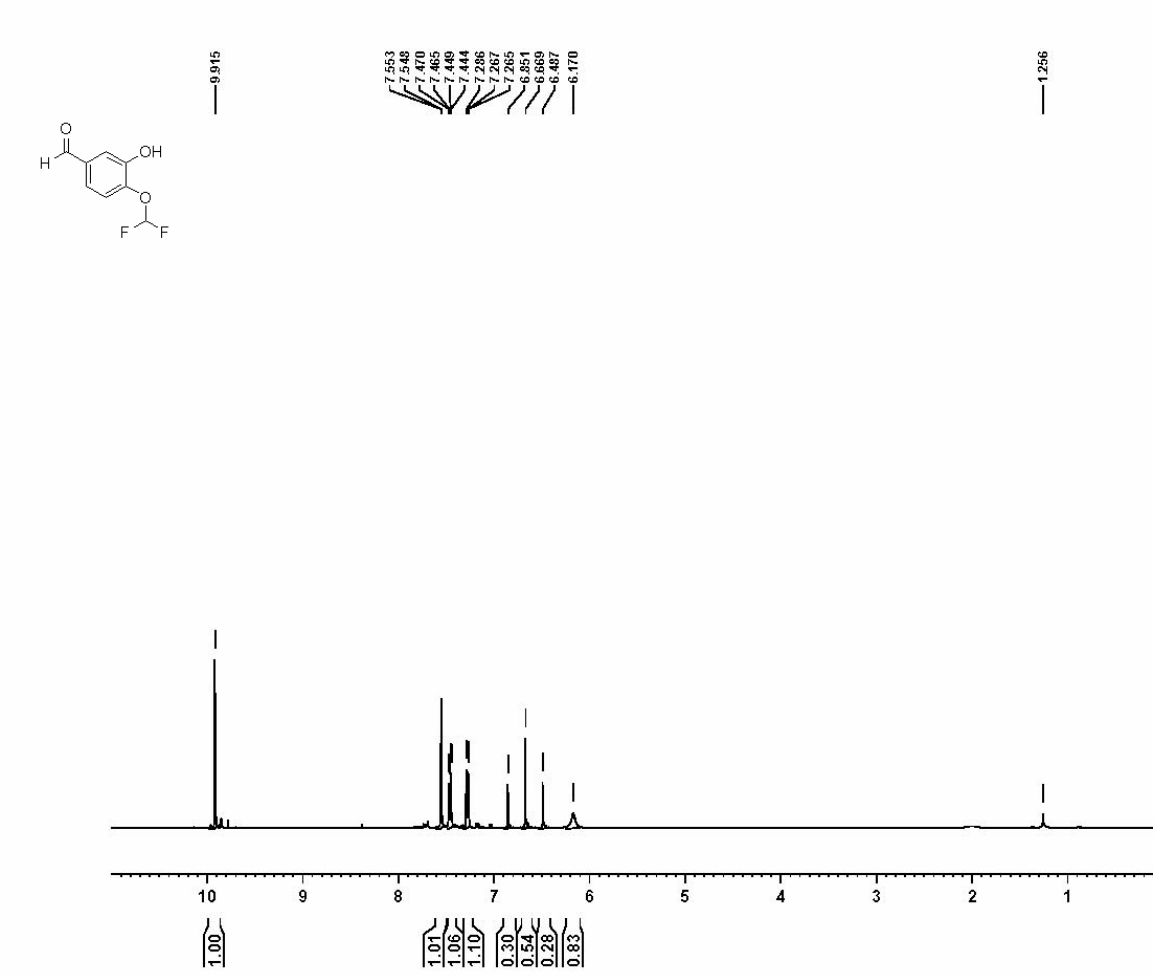
9.915
7.553
7.548
7.470
7.465
7.449
7.444
7.286
7.267
7.265
6.851
6.569
6.487
6.170
1.256
O
H
OH
O
F
F
10
9
8
7
6
5
4
3
2
1
1.00
1.01
1.06
1.10
0.30
0.54
0.28
0.83

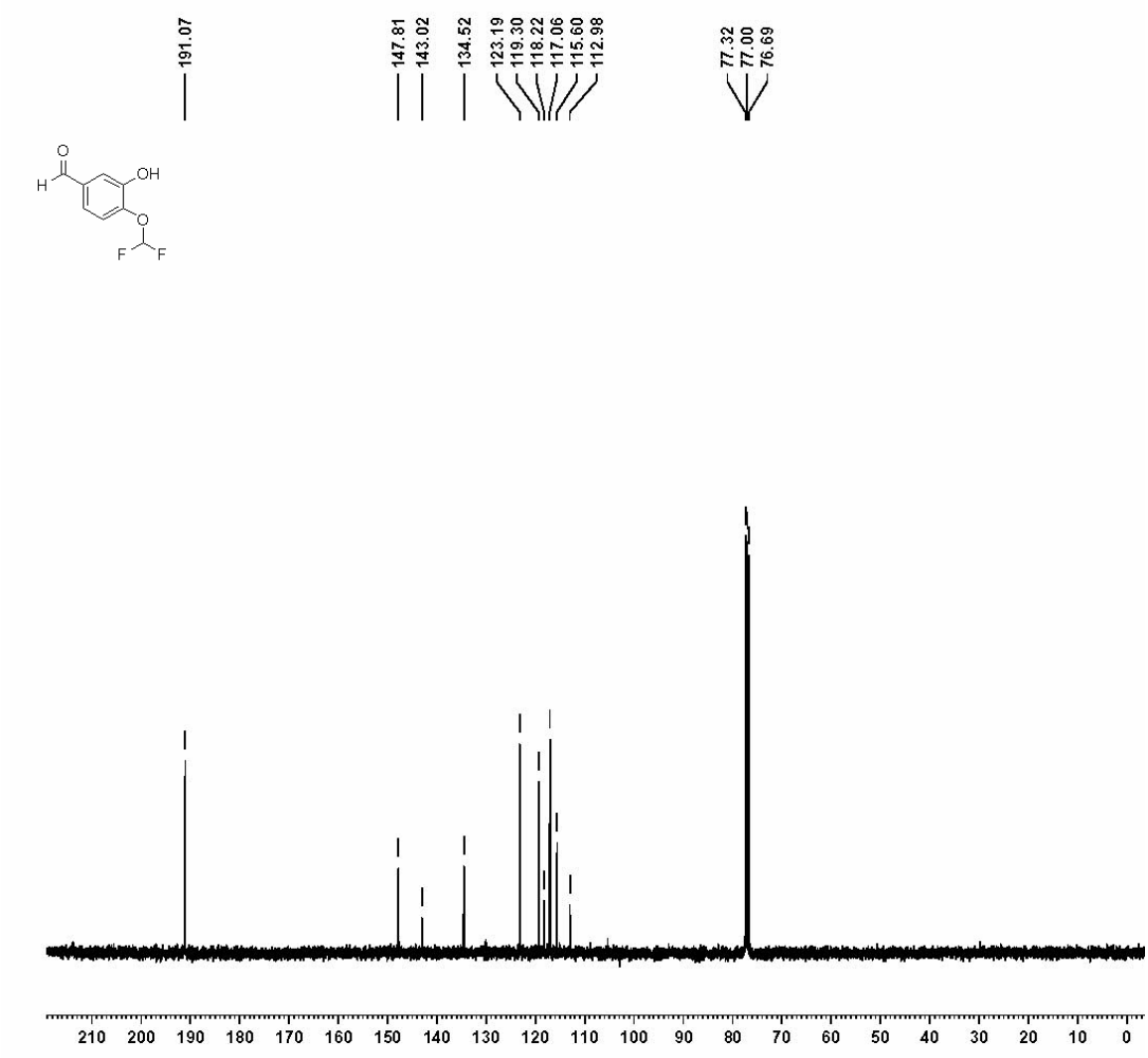
191.07
147.81
143.02
134.52
123.19
119.30
118.22
117.06
115.60
112.98
77.32
77.00
76.69
O
H
OH
O
F
F
210 200 190 180 170 160 150 140 130 120 110 100 90 80 70 60 50 40 30 20 10 0

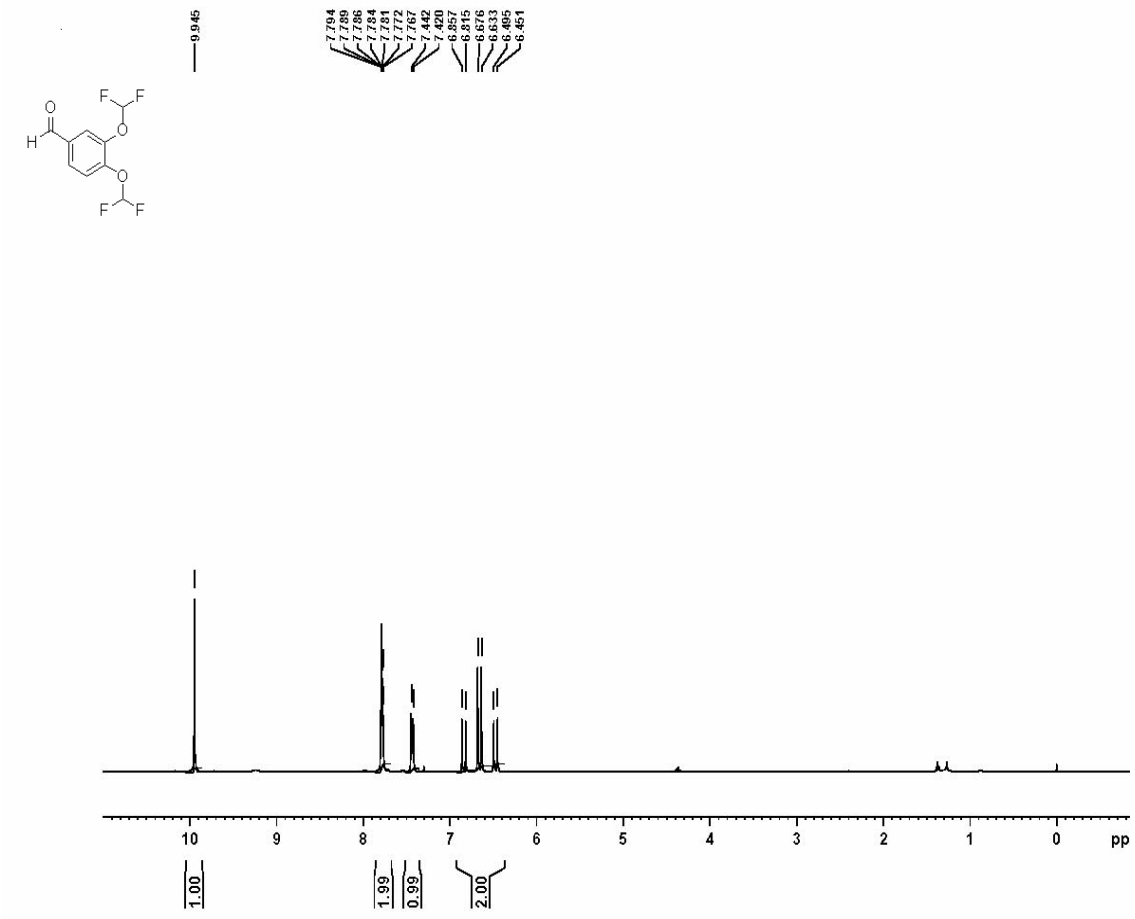
9.945
7.794
7.789
7.786
7.784
7.781
7.772
7.767
7.442
7.420
6.857
6.815
6.676
6.633
6.495
6.451
O
H
F
F
O
O
F
F
10
9
8
7
6
5
4
3
2
1
0
pp
1.00
1.99
0.99
2.00

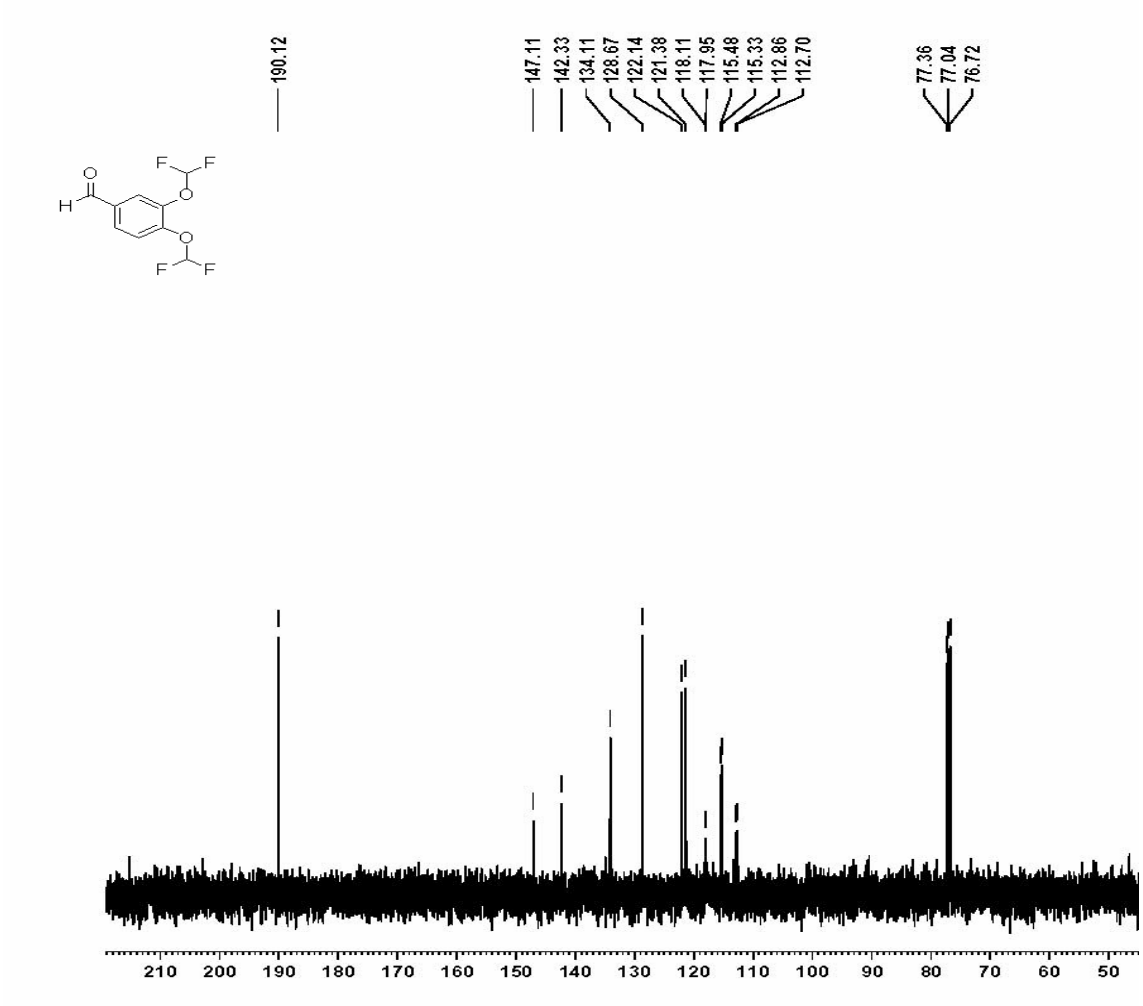
190.12
147.11
142.33
134.11
128.67
122.14
121.38
118.11
117.95
115.48
115.33
112.86
112.70
77.36
77.04
76.72
O
H
F
F
O
O
F
F
210
200
190
180
170
160
150
140
130
120
110
100
90
80
70
60
50

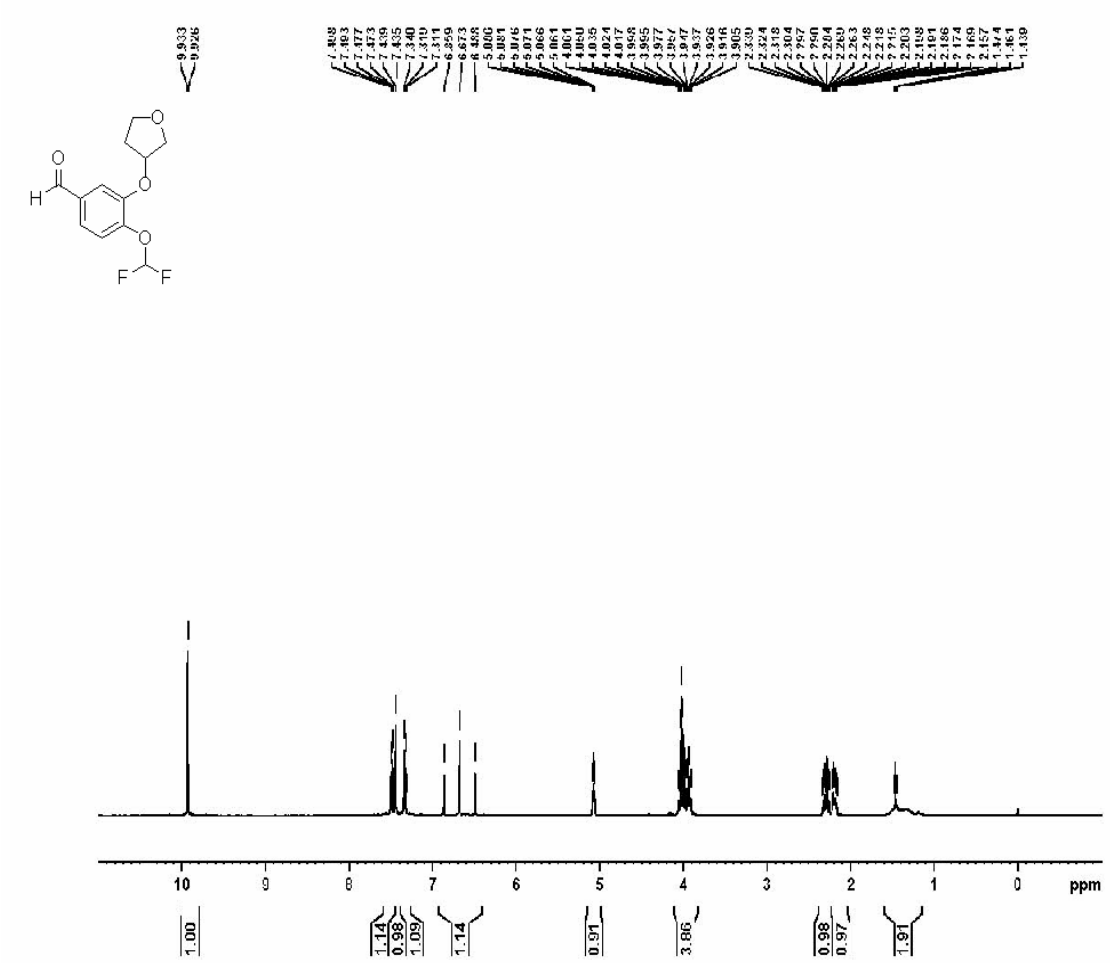
9.933
9.926
O
H
O
O
O
F
F
10
9
8
7
6
5
4
3
2
1
0
ppm
1.00
1.14
0.98
1.09
1.14
0.91
3.86
0.98
0.97
1.91

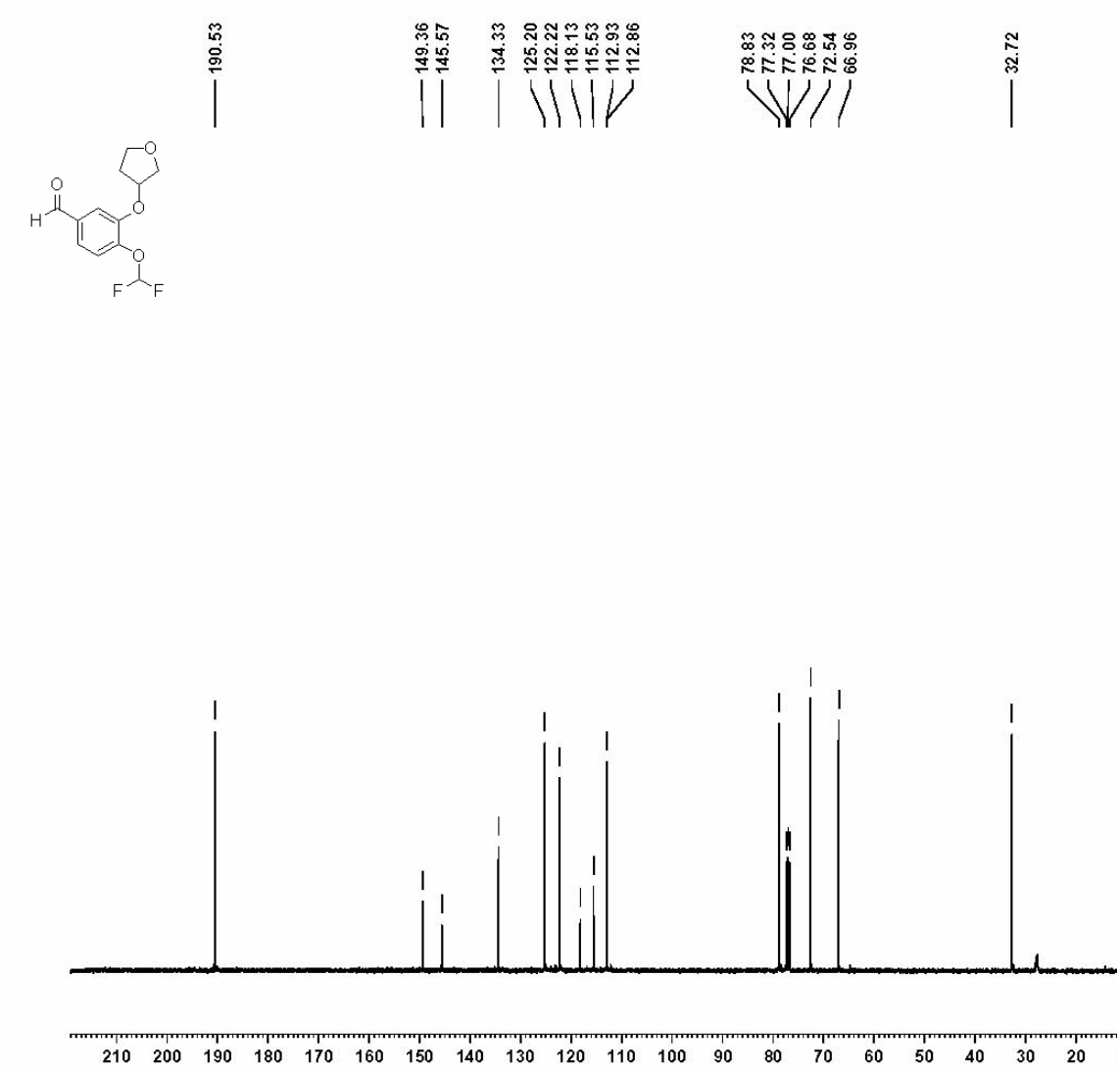
190.53
149.36
145.57
134.33
125.20
122.22
118.13
115.53
112.93
112.86
78.83
77.32
77.00
76.68
72.54
66.96
32.72
O
H
O
O
F
F
210 200 190 180 170 160 150 140 130 120 110 100 90 80 70 60 50 40 30 20

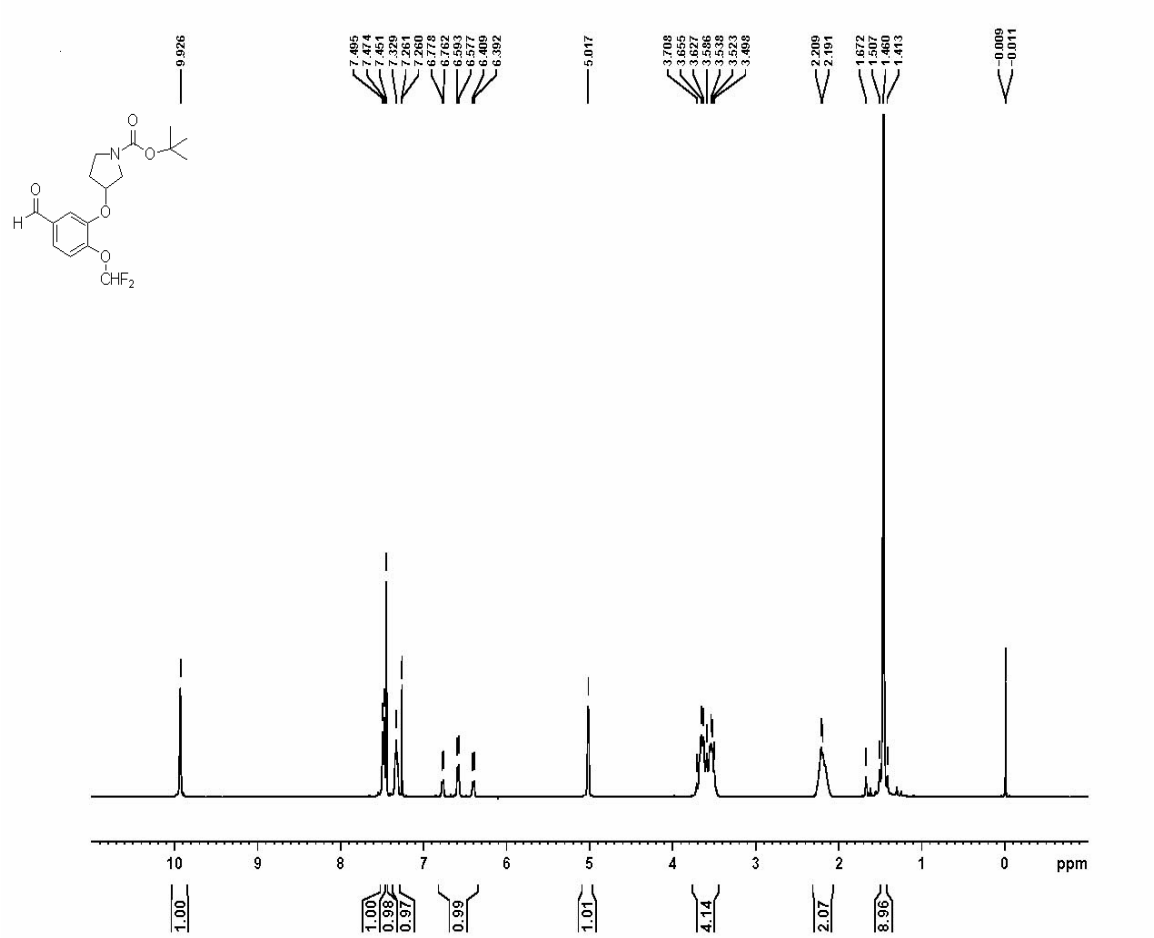
9.926
7.495
7.474
7.451
7.329
7.261
7.260
6.778
6.762
6.593
6.577
6.469
6.392
5.017
3.708
3.655
3.627
3.556
3.538
3.523
3.498
2.209
2.191
1.672
1.507
1.460
1.413
-0.009
-0.011
ppm
1.00
1.00
0.98
0.97
0.99
1.01
4.14
2.07
8.96

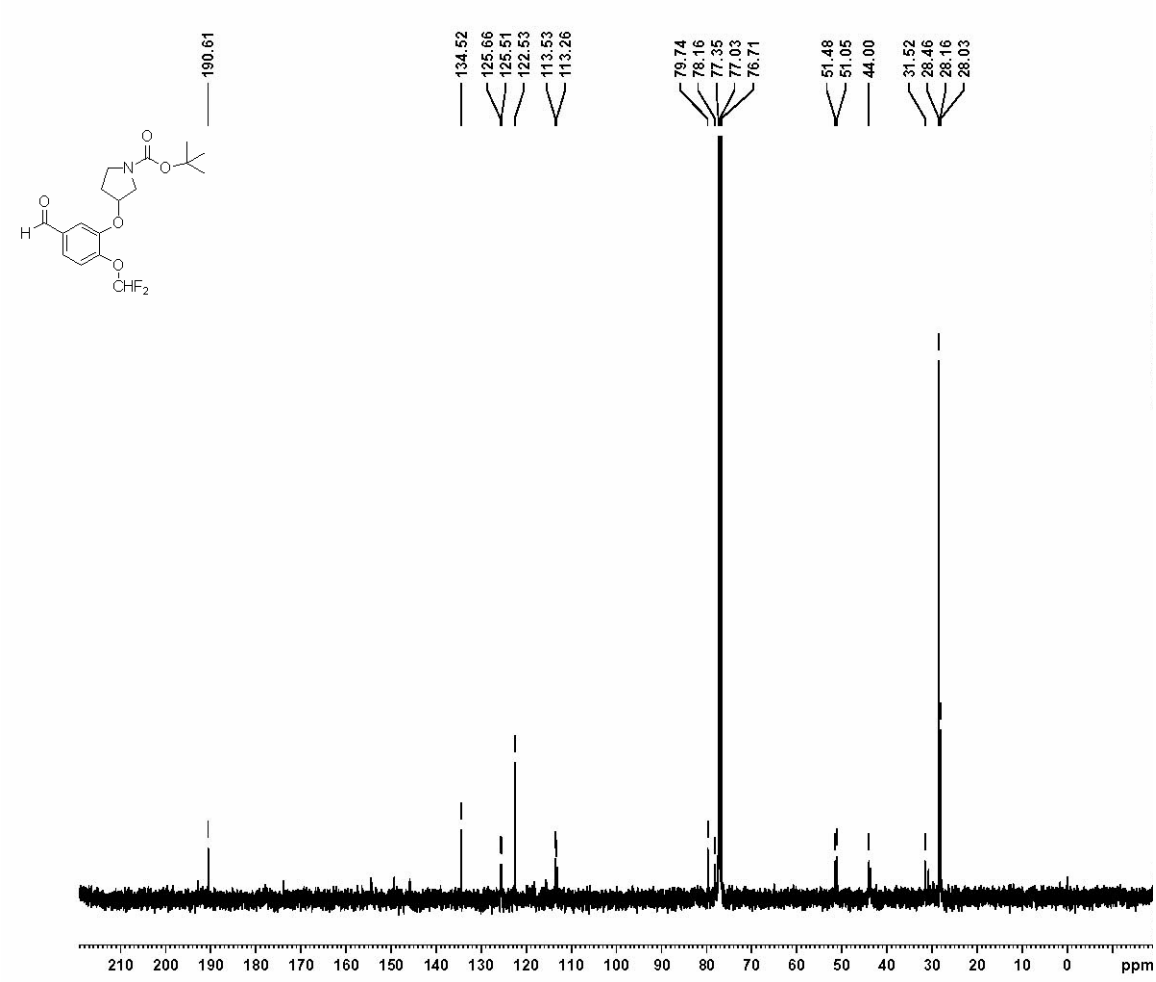
190.61
134.52
125.66
125.51
122.53
113.53
113.26
79.74
78.16
77.35
77.03
76.71
51.48
51.05
44.00
31.52
28.46
28.16
28.03
O
H
N
O
O
O
O
CHF2
210 200 190 180 170 160 150 140 130 120 110 100 90 80 70 60 50 40 30 20 10 0 ppm

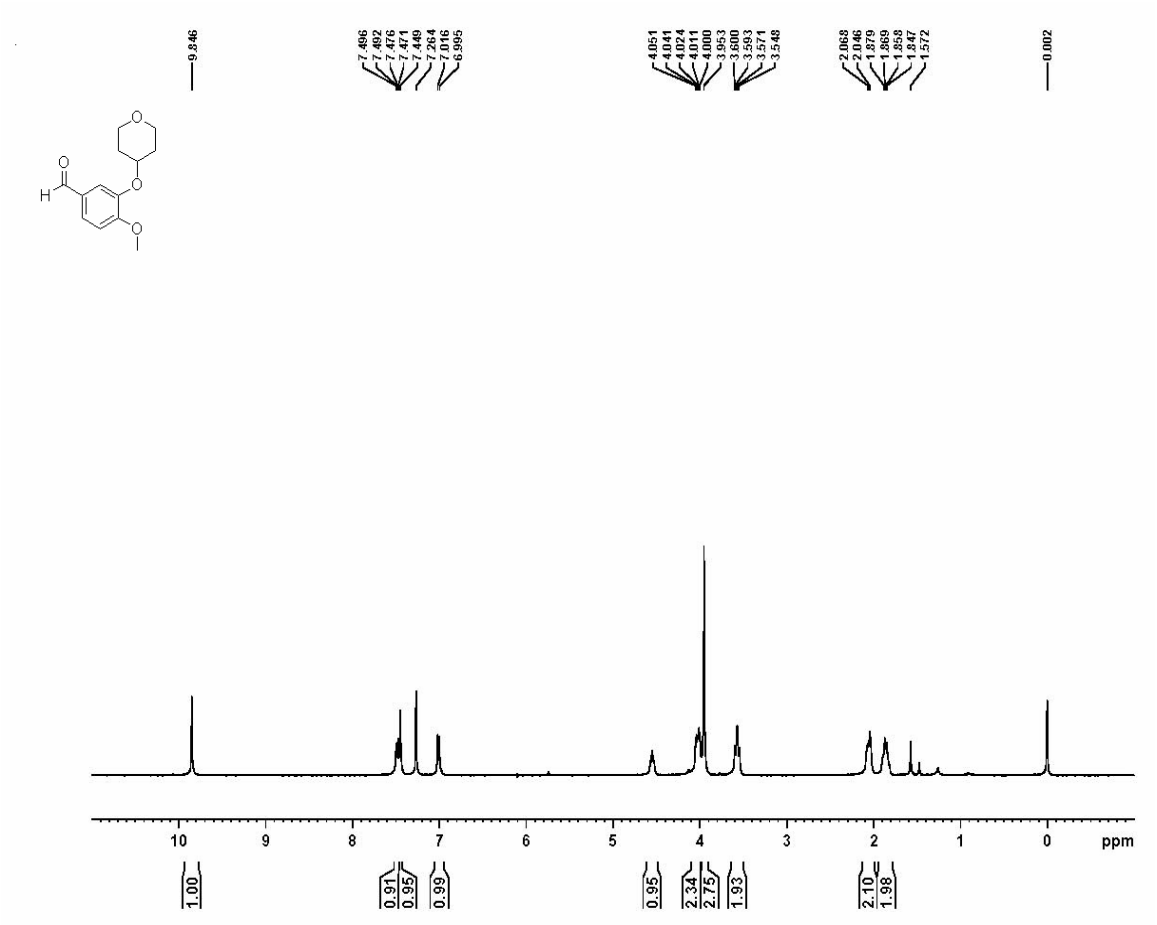
9.846
7.496
7.492
7.476
7.471
7.449
7.264
7.016
6.995
4.051
4.041
4.024
4.011
4.000
3.963
3.600
3.593
3.571
3.548
2.068
2.046
1.879
1.869
1.858
1.847
1.572
0.002
10
9
8
7
6
5
4
3
2
1
0
ppm
1.00
0.91
0.95
0.99
0.95
2.34
2.75
1.93
2.10
1.98

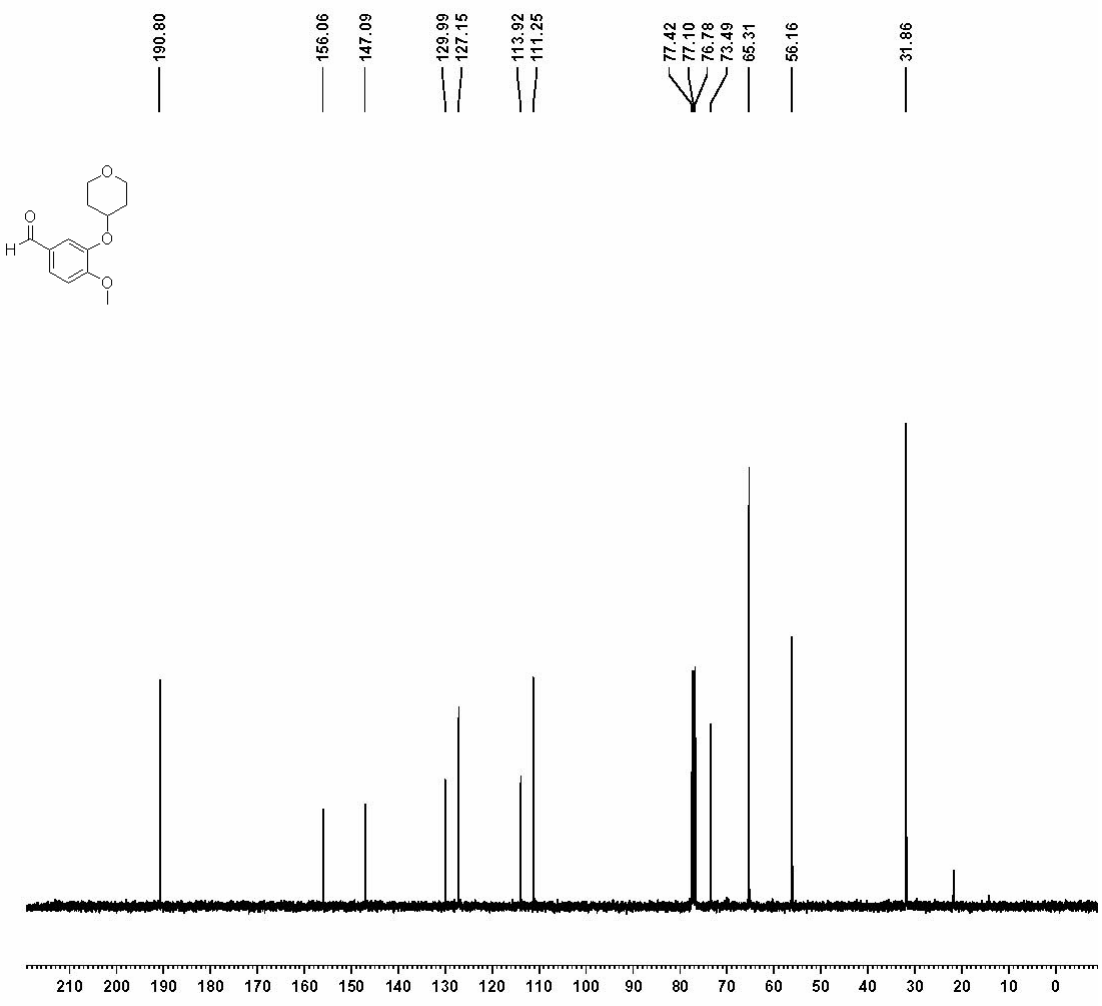
190.80
156.06
147.09
129.99
127.15
113.92
111.25
77.42
77.10
76.78
73.49
65.31
56.16
31.86
O
H
O
O
O
210 200 190 180 170 160 150 140 130 120 110 100 90 80 70 60 50 40 30 20 10 0

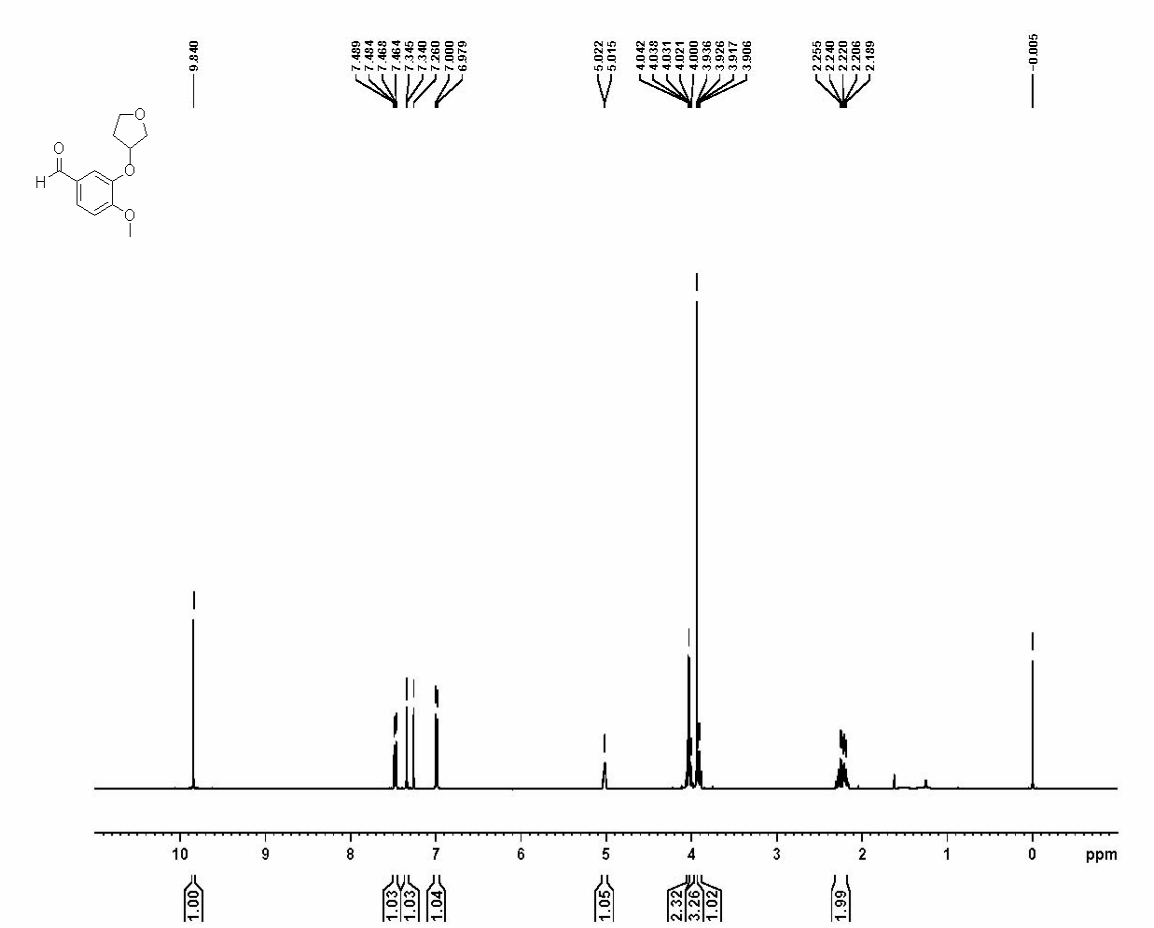
9.840
7.489
7.484
7.468
7.464
7.345
7.340
7.260
7.000
6.979
5.022
5.015
4.042
4.038
4.031
4.021
4.000
3.936
3.926
3.917
3.906
2.255
2.240
2.220
2.206
2.189
0.005
10
9
8
7
6
5
4
3
2
1
0
ppm
1.00
1.03
1.03
1.04
1.05
2.32
3.26
1.02
1.99

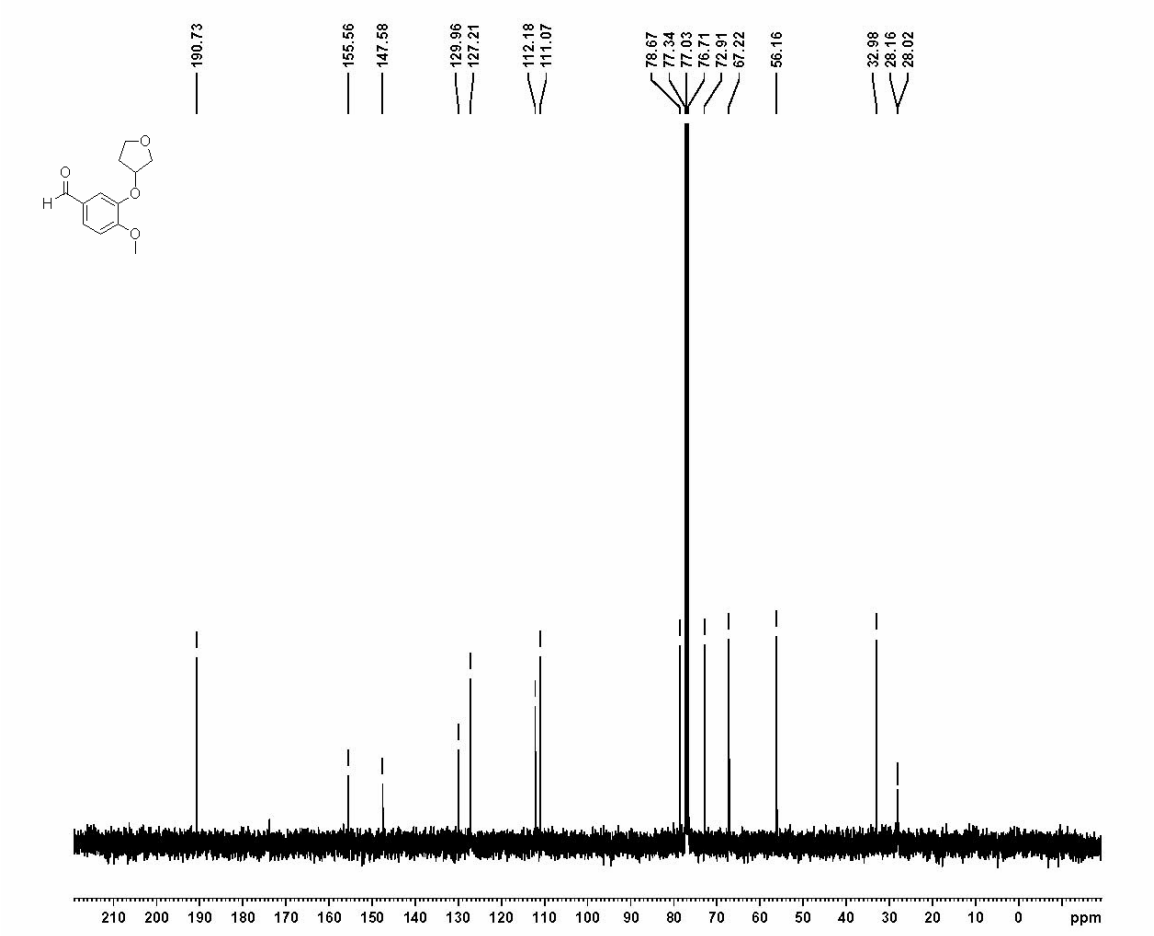
190.73
155.56
147.58
129.96
127.21
112.18
111.07
78.67
77.34
77.03
76.71
72.91
67.22
56.16
32.98
28.16
28.02
210 200 190 180 170 160 150 140 130 120 110 100 90 80 70 60 50 40 30 20 10 0 ppm

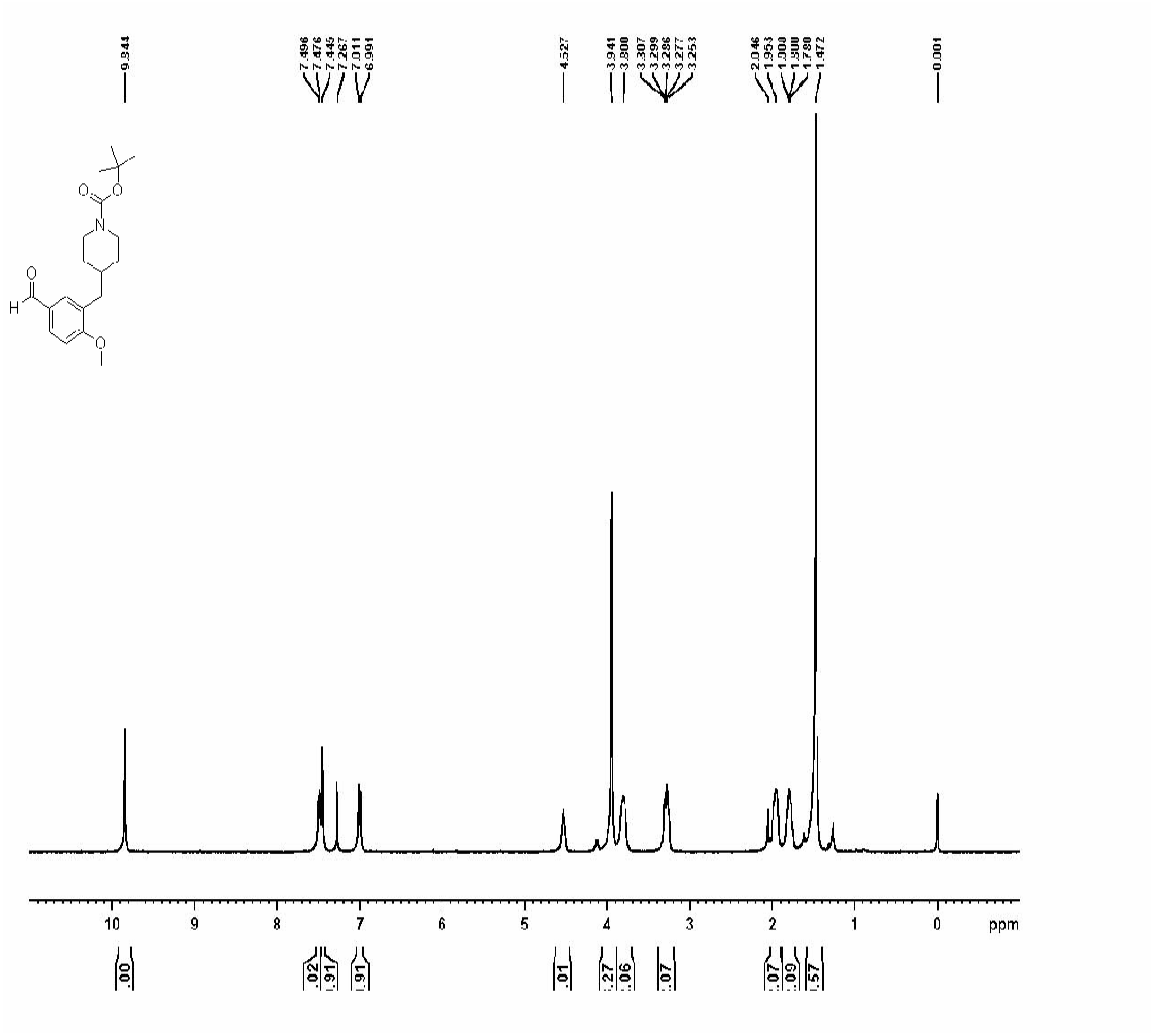
9.944
7.496
7.476
7.445
7.267
7.011
6.991
4.527
3.941
3.808
3.307
3.299
3.286
3.277
3.253
2.046
1.953
1.908
1.808
1.789
1.472
0.001
10
9
8
7
6
5
4
3
2
1
0
ppm
1.00
2.02
1.91
1.91
1.01
2.27
1.06
3.07
2.07
1.09
1.57

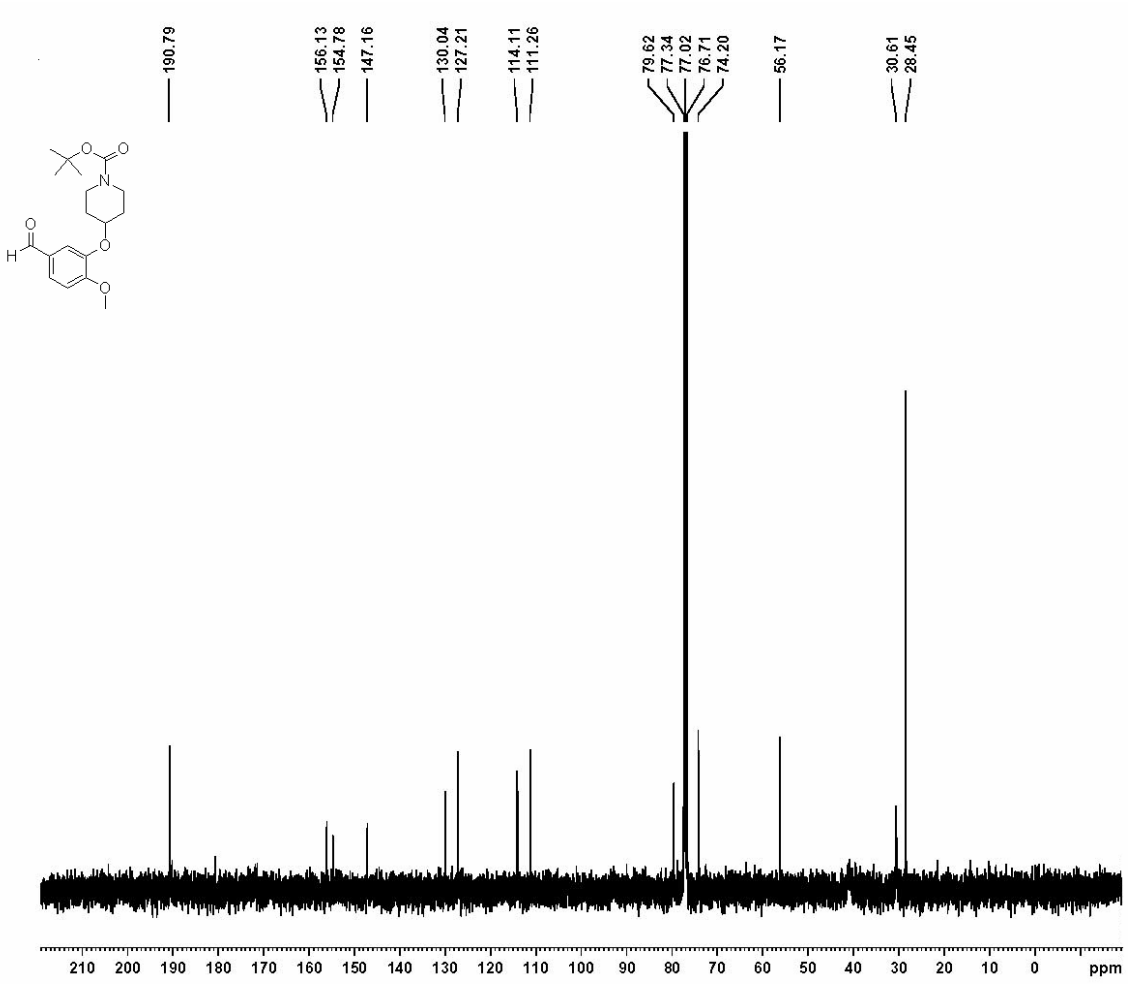
190.79
156.13
154.78
147.16
130.04
127.21
114.11
111.26
79.62
77.34
77.02
76.71
74.20
56.17
30.61
28.45
210 200 190 180 170 160 150 140 130 120 110 100 90 80 70 60 50 40 30 20 10 0 ppm

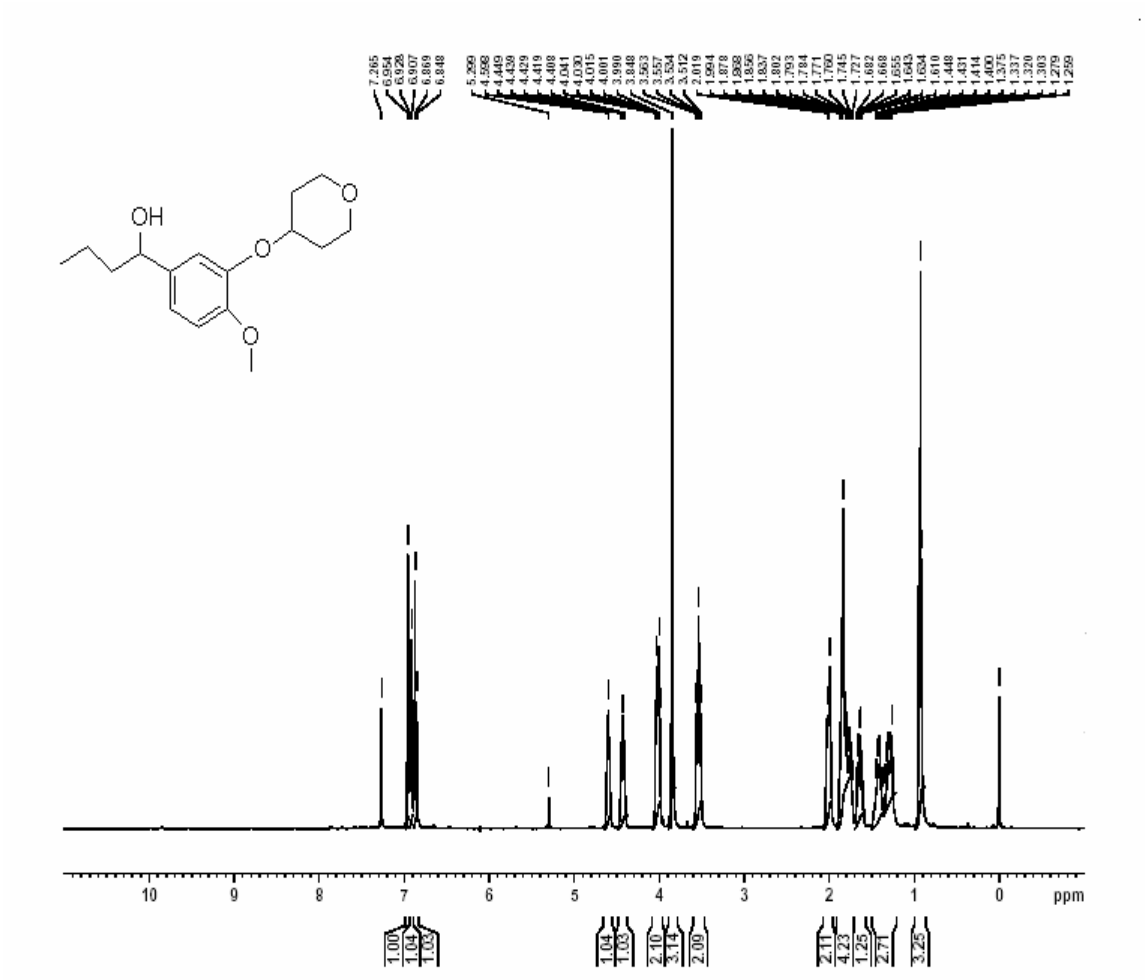
OH
O
O
O
7.265
6.954
6.928
6.907
6.869
6.848
5.299
4.598
4.449
4.439
4.429
4.419
4.408
4.041
4.033
4.015
4.001
3.990
3.848
3.563
3.557
3.534
3.512
2.019
1.994
1.878
1.868
1.856
1.837
1.802
1.793
1.784
1.771
1.759
1.745
1.727
1.682
1.668
1.655
1.643
1.634
1.610
1.448
1.431
1.414
1.400
1.375
1.337
1.320
1.303
1.279
1.259
10
9
8
7
6
5
4
3
2
1
0
ppm
1.00
1.04
1.03
1.04
1.03
2.10
3.14
2.09
2.11
4.23
1.25
2.71
3.25

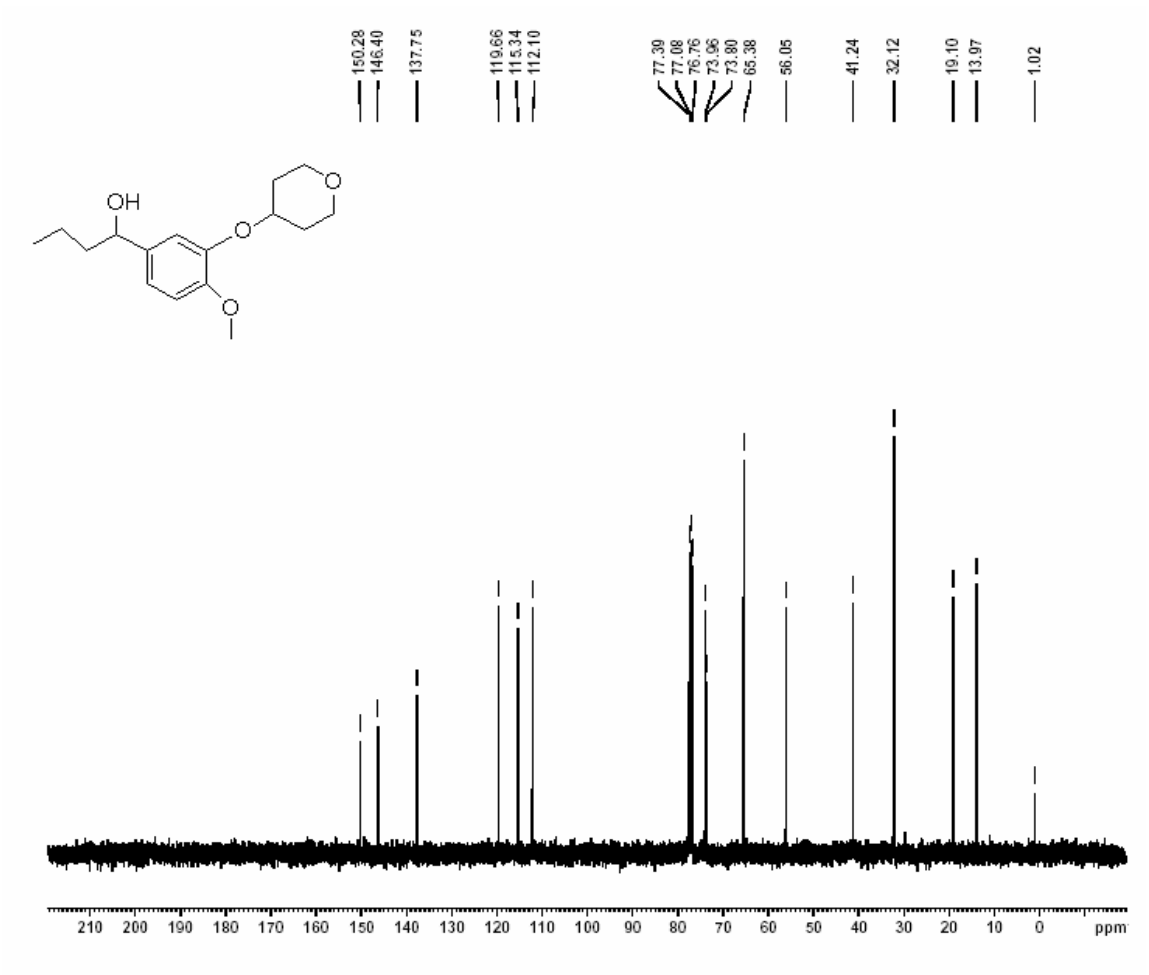
150.28
146.40
137.75
119.66
115.34
112.10
77.39
77.08
76.76
73.96
73.80
65.38
56.05
41.24
32.12
19.10
13.97
1.02
OH
O
O
O
210 200 190 180 170 160 150 140 130 120 110 100 90 80 70 60 50 40 30 20 10 0 ppm

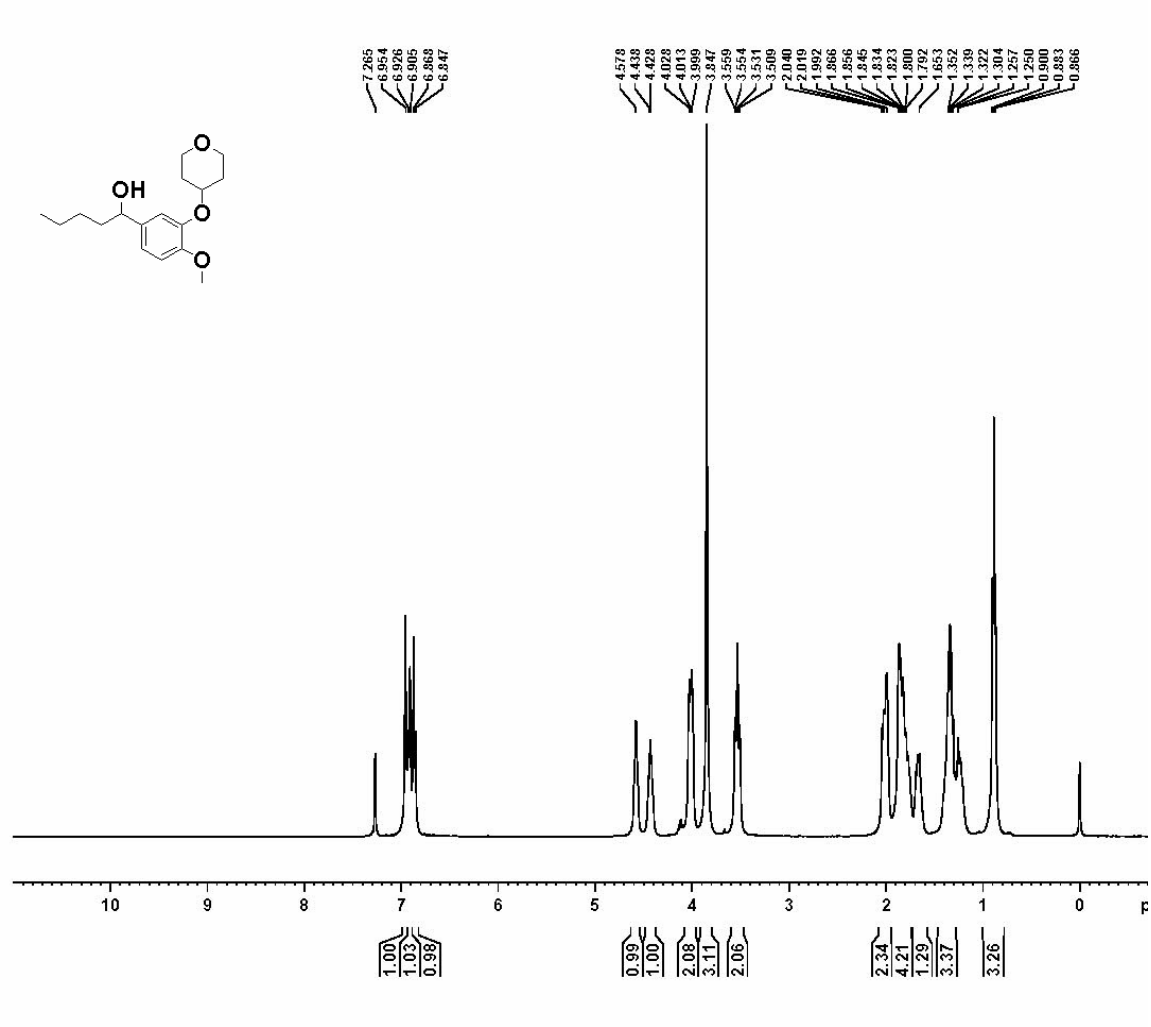
7.265
6.954
6.926
6.905
6.868
6.847
4.578
4.438
4.428
4.028
4.013
3.999
3.847
3.559
3.554
3.531
3.509
2.040
2.019
1.992
1.866
1.856
1.845
1.834
1.823
1.800
1.792
1.653
1.352
1.339
1.322
1.304
1.257
1.250
0.900
0.883
0.866
OH
O
O
O
10
9
8
7
6
5
4
3
2
1
0
1.00
1.03
0.98
0.99
1.00
2.08
3.11
2.06
2.34
4.21
1.29
3.37
3.26

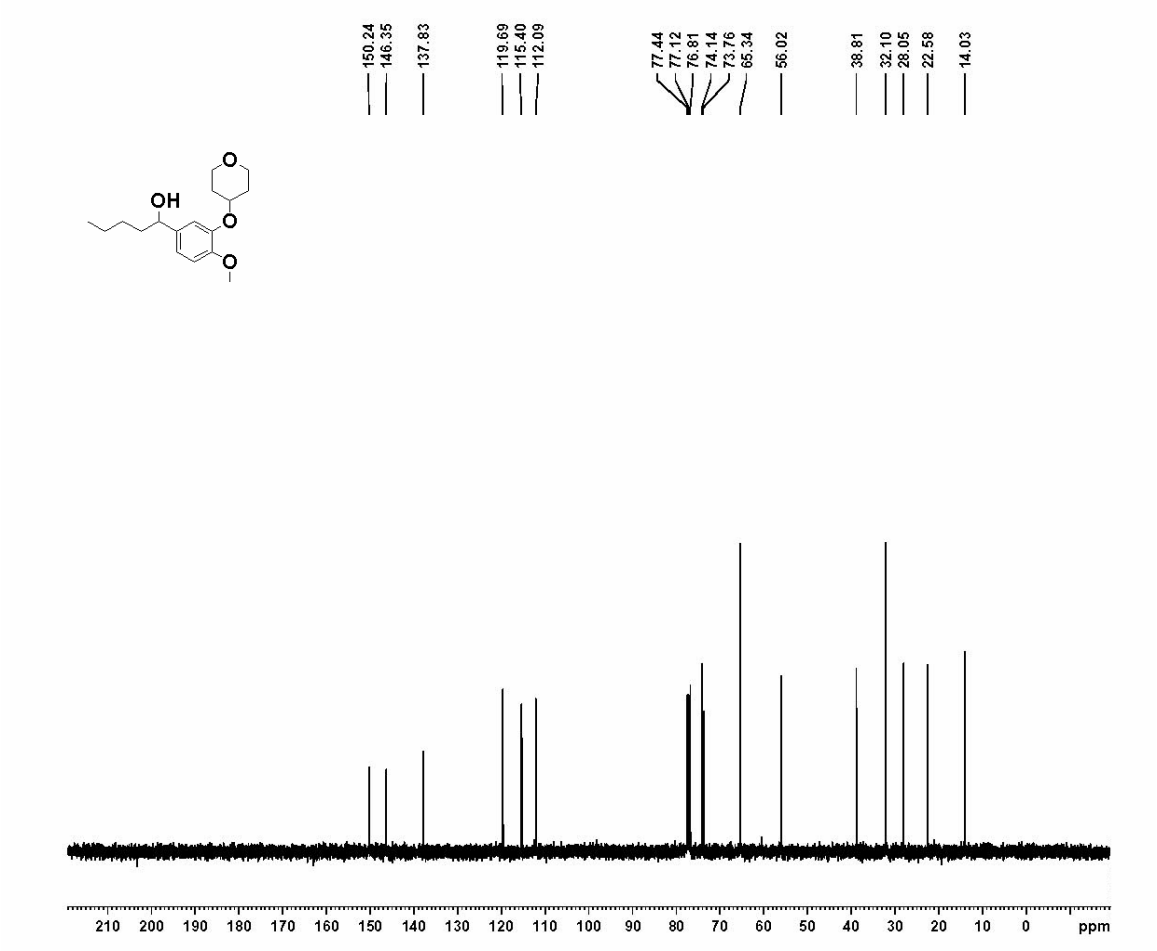
150.24
146.35
137.83
119.69
115.40
112.09
77.44
77.12
76.81
74.14
73.76
65.34
56.02
38.81
32.10
28.05
22.58
14.03
OH
O
O
O
210 200 190 180 170 160 150 140 130 120 110 100 90 80 70 60 50 40 30 20 10 0 ppm

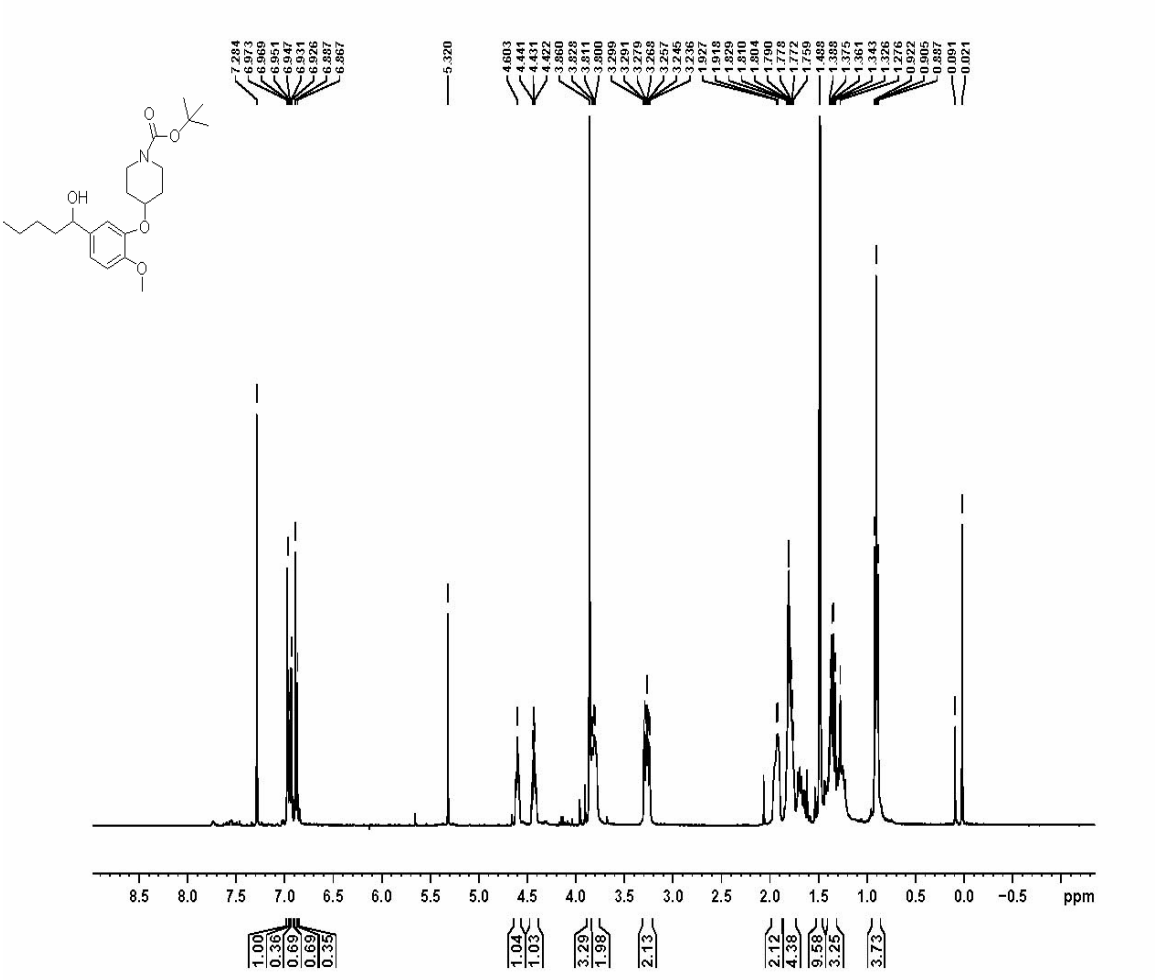
7.284
6.973
6.969
6.947
6.931
6.926
6.887
6.867
5.320
4.603
4.441
4.431
4.422
3.860
3.828
3.811
3.800
3.299
3.291
3.279
3.268
3.257
3.245
3.236
1.927
1.918
1.829
1.810
1.804
1.790
1.778
1.772
1.759
1.498
1.388
1.375
1.361
1.343
1.326
1.276
0.922
0.905
0.887
0.091
0.021
OH
O
N
O
O
O
8.5
8.0
7.5
7.0
6.5
6.0
5.5
5.0
4.5
4.0
3.5
3.0
2.5
2.0
1.5
1.0
0.5
0.0
−0.5
ppm
1.00
0.36
0.69
0.69
0.35
1.04
1.03
3.29
1.98
2.13
2.12
4.38
9.58
3.25
3.73

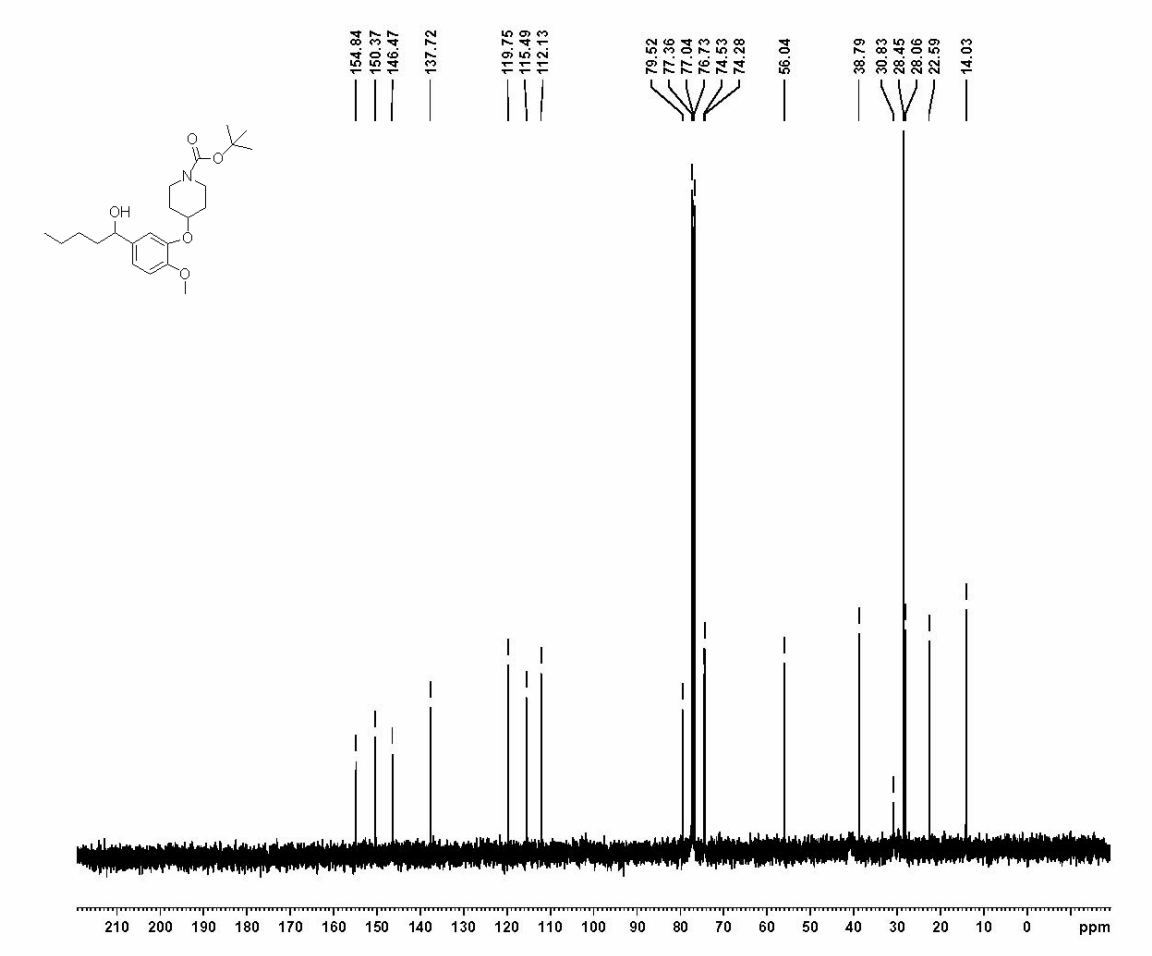
154.84
150.37
146.47
137.72
119.75
115.49
112.13
79.52
77.36
77.04
76.73
74.53
74.28
56.04
38.79
30.83
28.45
28.06
22.59
14.03
OH
O
N
O
O
O
210 200 190 180 170 160 150 140 130 120 110 100 90 80 70 60 50 40 30 20 10 0 ppm

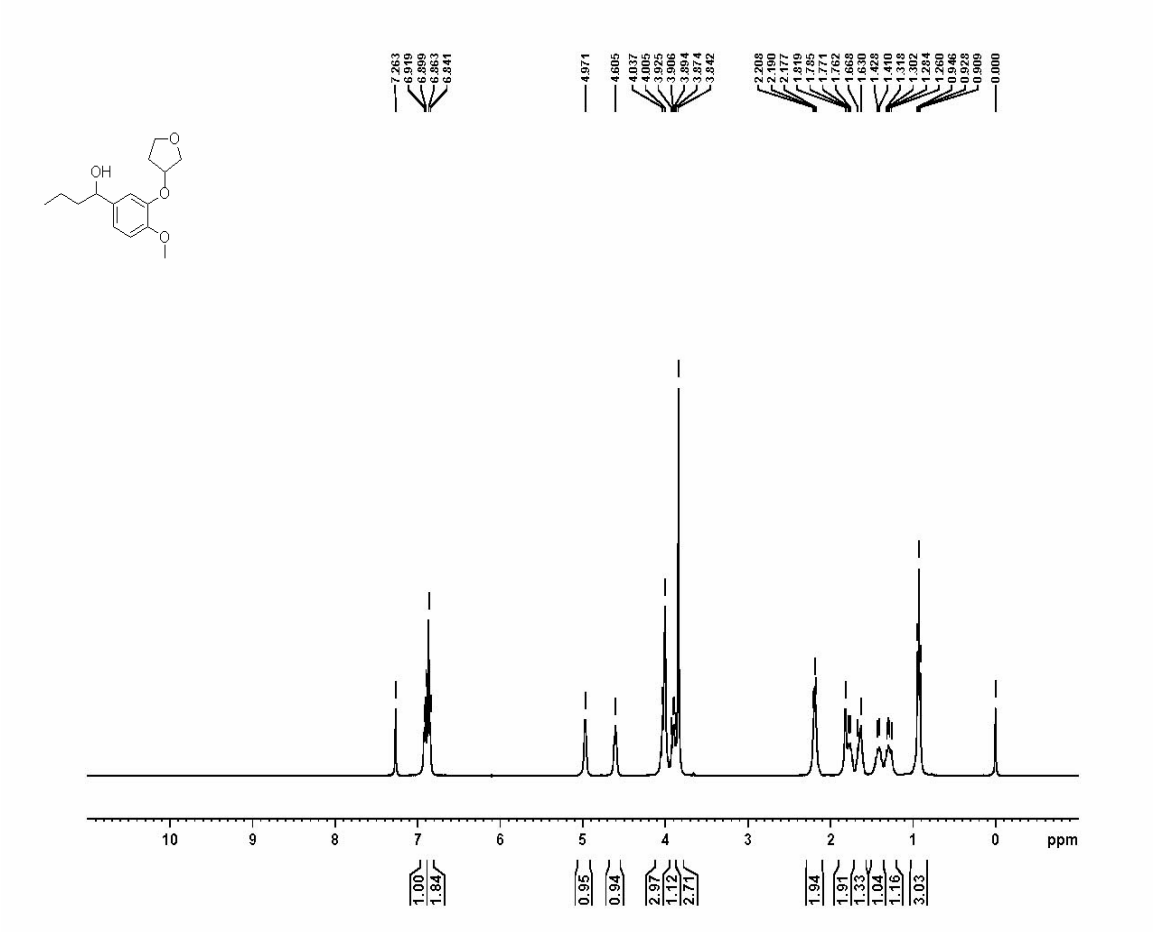
7.263
6.919
6.899
6.863
6.841
4.971
4.605
4.037
4.005
3.925
3.906
3.894
3.874
3.842
2.208
2.190
2.177
1.819
1.785
1.771
1.762
1.668
1.630
1.478
1.410
1.318
1.302
1.284
1.260
0.946
0.928
0.909
0.000
OH
O
O
O
10
9
8
7
6
5
4
3
2
1
0
ppm
1.00
1.84
0.95
0.94
2.97
1.12
2.71
1.94
1.91
1.33
1.04
1.16
3.03

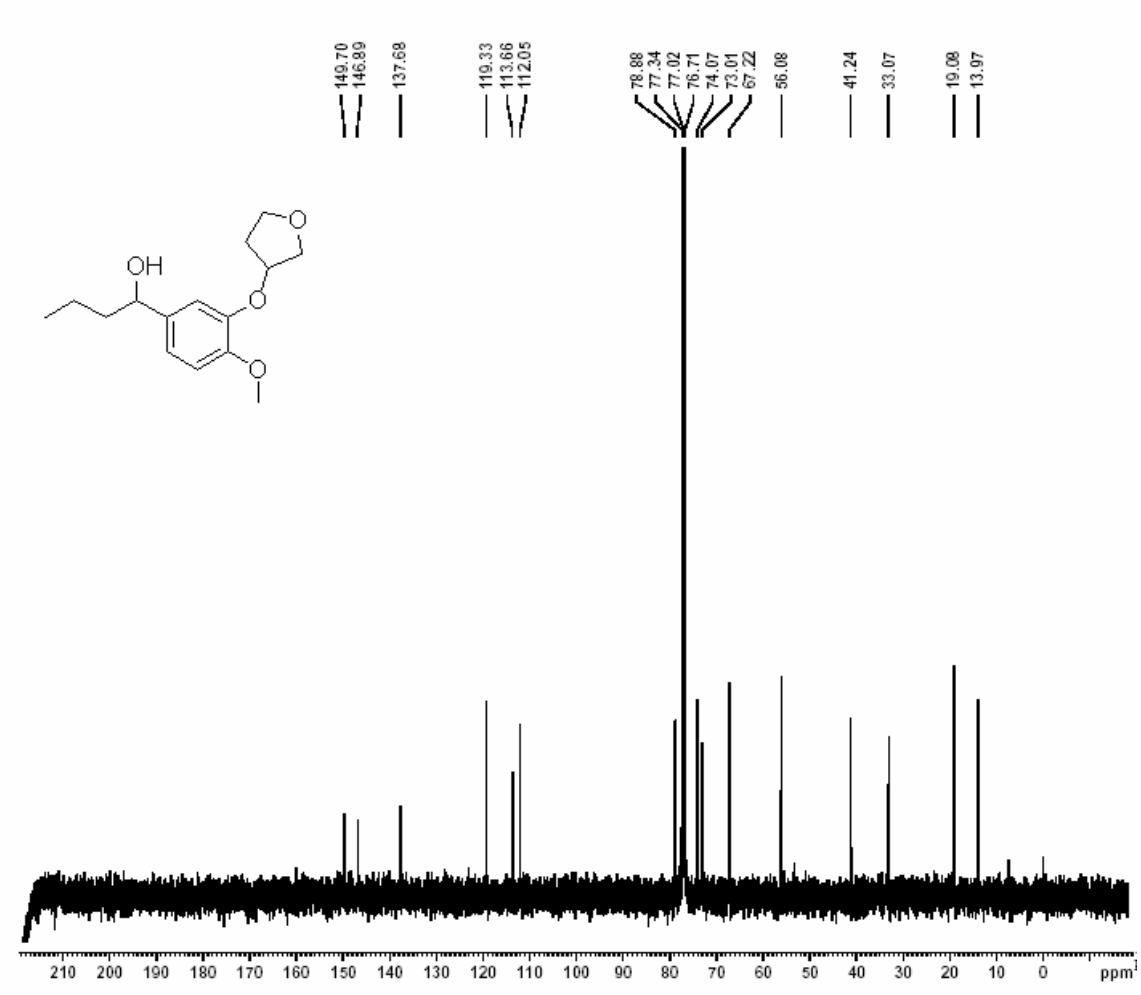
149.70
146.89
137.68
119.33
113.66
112.05
78.88
77.34
77.02
76.71
74.07
73.01
67.22
56.08
41.24
33.07
19.08
13.97
OH
O
O
O
210 200 190 180 170 160 150 140 130 120 110 100 90 80 70 60 50 40 30 20 10 0 ppm

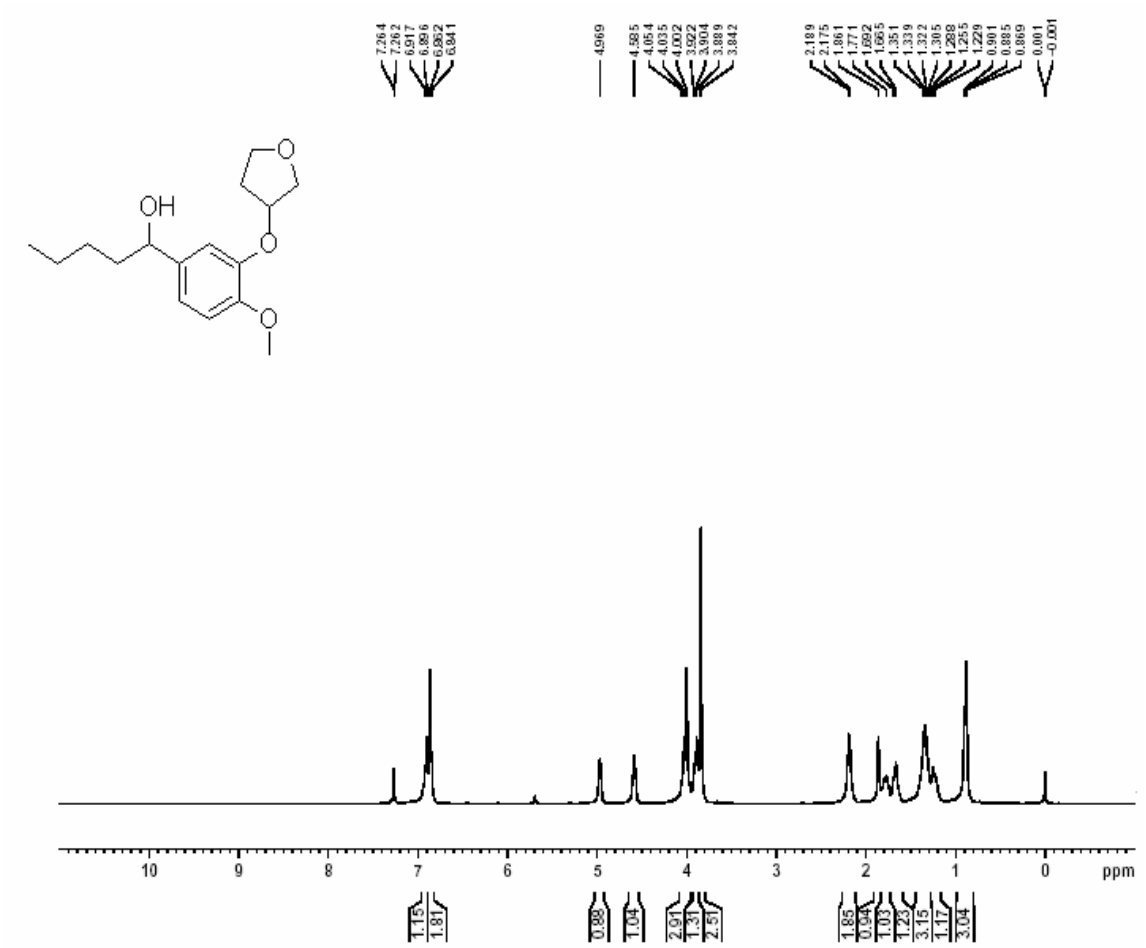
7.264
7.262
6.917
6.876
6.892
6.841
4.969
4.585
4.054
4.035
4.002
3.922
3.904
3.889
3.842
2.189
2.175
1.861
1.771
1.692
1.665
1.351
1.339
1.322
1.305
1.288
1.255
1.229
0.901
0.885
0.869
0.001
-0.001
OH
O
O
O
10
9
8
7
6
5
4
3
2
1
0
ppm
1.15
1.81
0.88
1.04
2.91
1.31
2.51
1.85
0.94
1.03
1.23
3.15
1.17
3.04

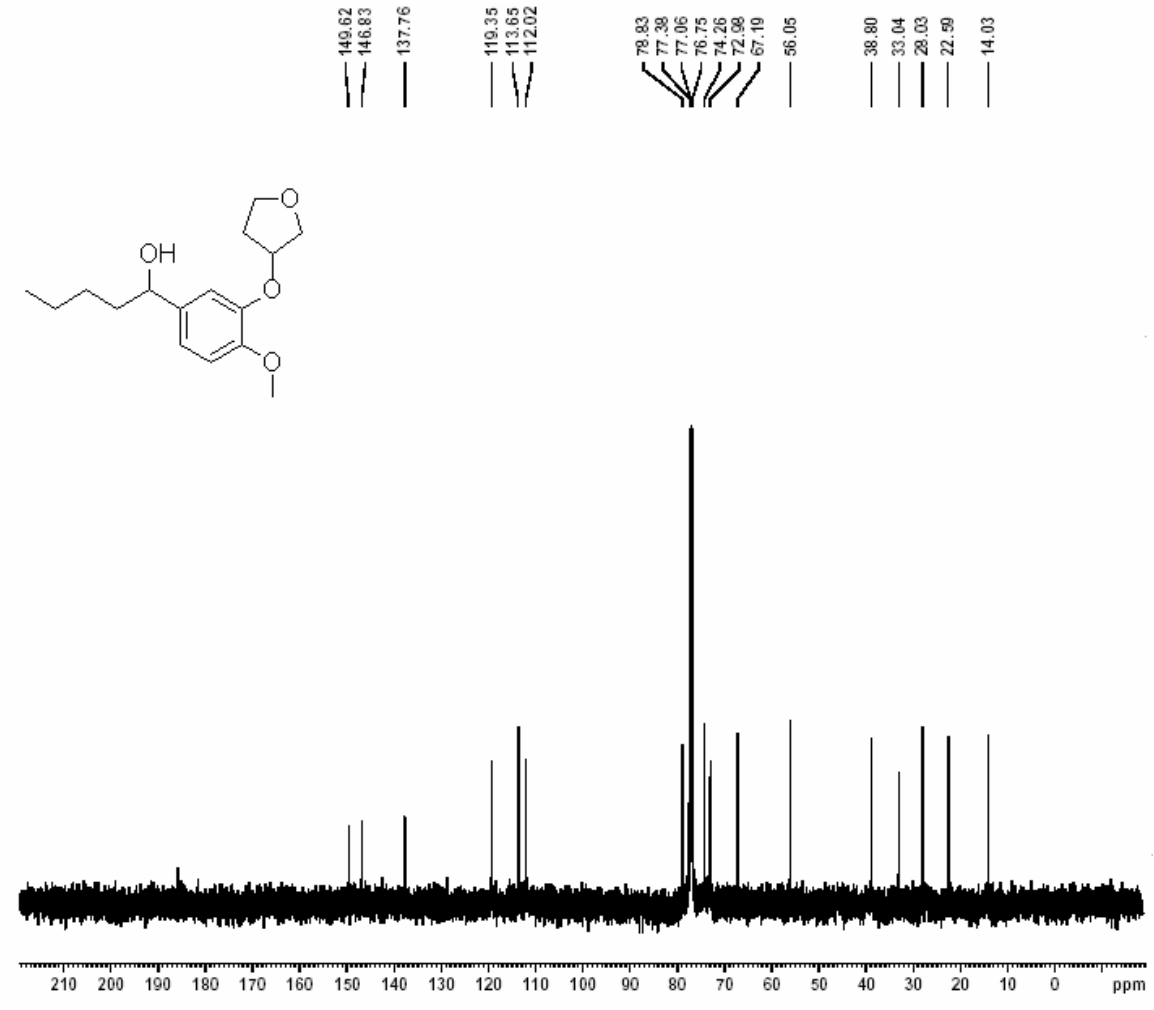
149.62
146.83
137.76
119.35
113.65
112.02
78.83
77.39
77.06
76.75
74.26
72.98
67.19
56.05
38.80
33.04
28.03
22.59
14.03
OH
O
O
O
210 200 190 180 170 160 150 140 130 120 110 100 90 80 70 60 50 40 30 20 10 0 ppm

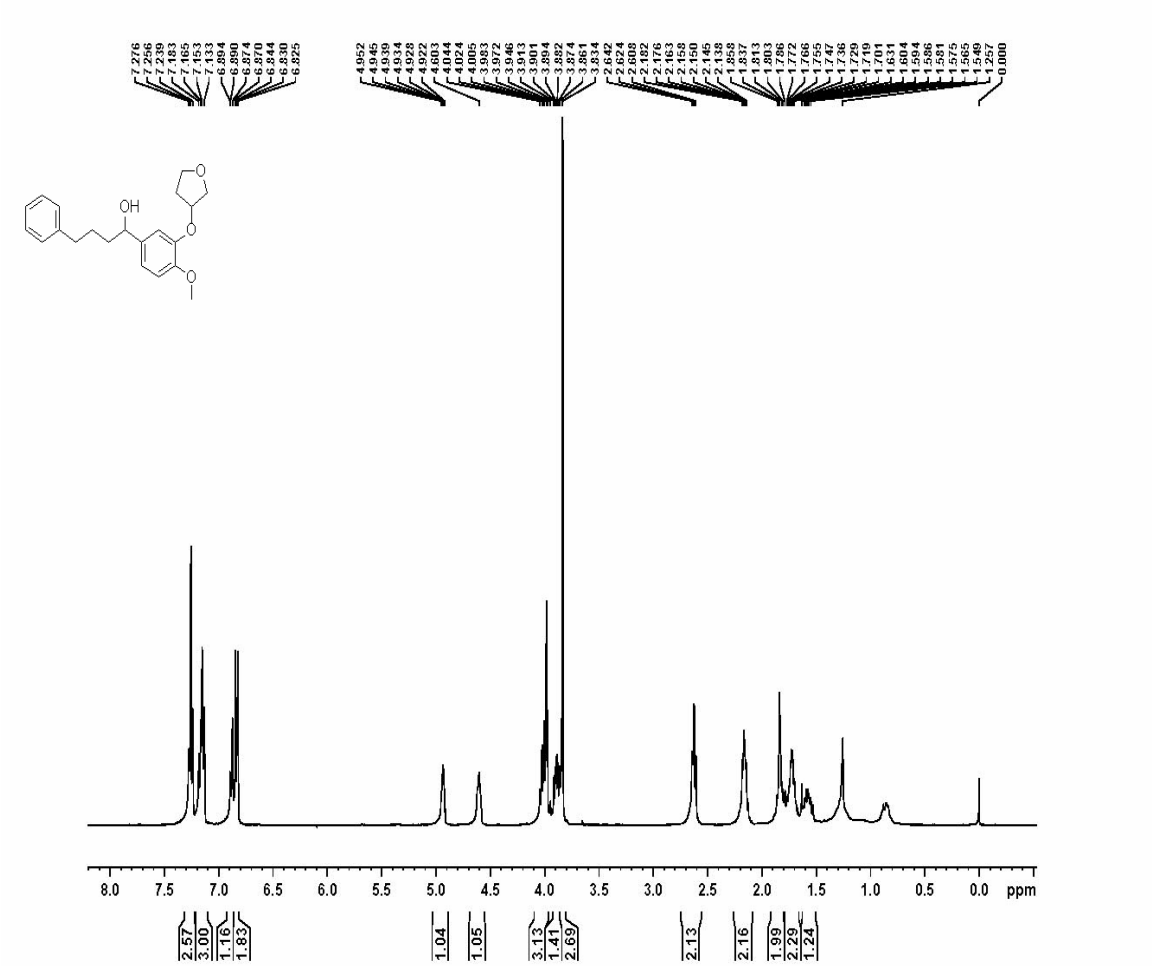
7.276
7.256
7.238
7.183
7.165
7.153
7.133
6.894
6.890
6.874
6.870
6.844
6.830
6.825
4.952
4.945
4.939
4.934
4.928
4.922
4.803
4.044
4.024
4.005
3.983
3.972
3.946
3.913
3.901
3.894
3.882
3.874
3.861
3.854
2.647
2.624
2.608
2.182
2.176
2.163
2.158
2.150
2.145
2.138
1.858
1.837
1.813
1.803
1.786
1.772
1.766
1.755
1.747
1.736
1.729
1.719
1.701
1.631
1.604
1.594
1.586
1.581
1.575
1.565
1.549
1.257
0.000
OH
O
O
O
8.0
7.5
7.0
6.5
6.0
5.5
5.0
4.5
4.0
3.5
3.0
2.5
2.0
1.5
1.0
0.5
0.0
ppm
2.57
3.00
1.16
1.83
1.04
1.05
3.13
1.41
2.69
2.13
2.16
1.99
2.29
1.24

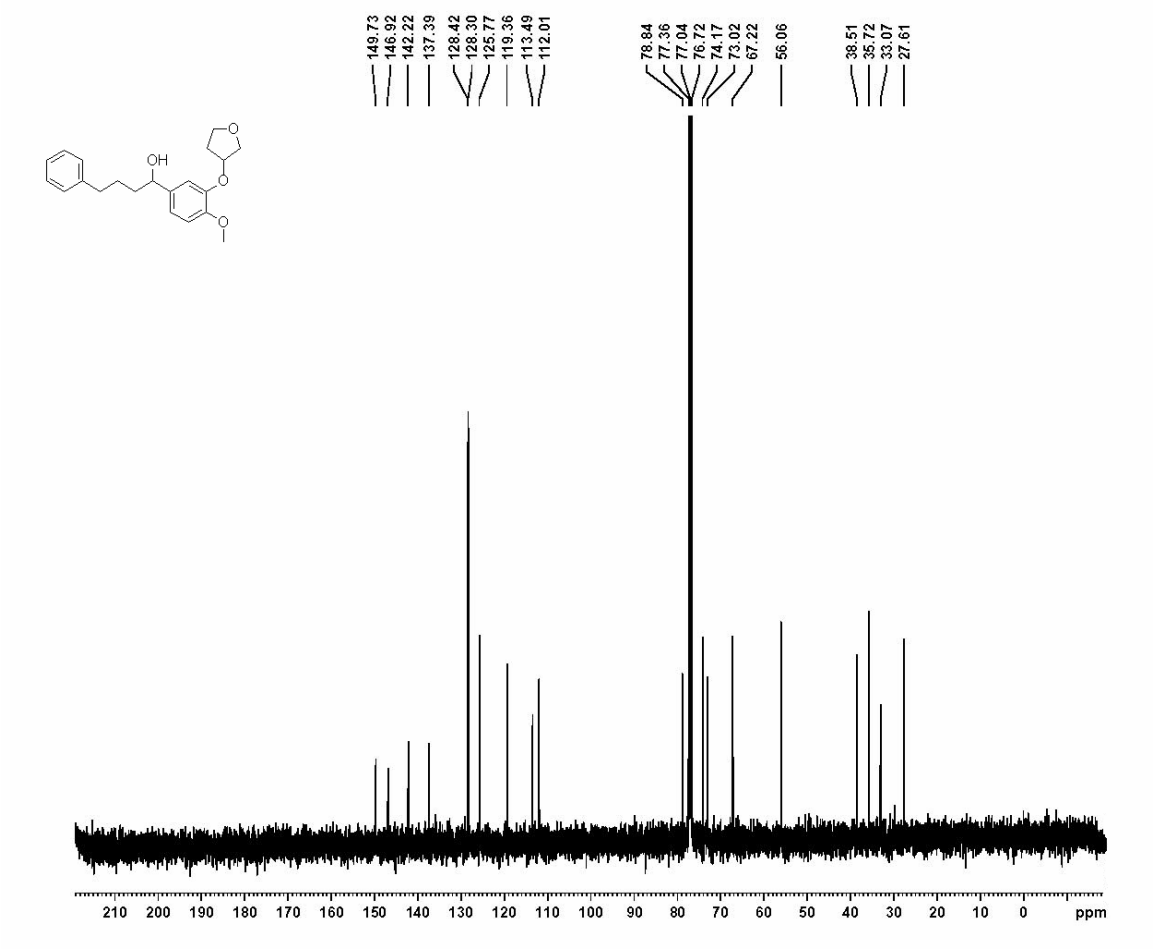
149.73
146.92
142.22
137.39
128.42
128.30
125.77
119.36
113.49
112.01
78.84
77.36
77.04
76.72
74.17
73.02
67.22
56.06
38.51
35.72
33.07
27.61
OH
O
O
O
210 200 190 180 170 160 150 140 130 120 110 100 90 80 70 60 50 40 30 20 10 0 ppm

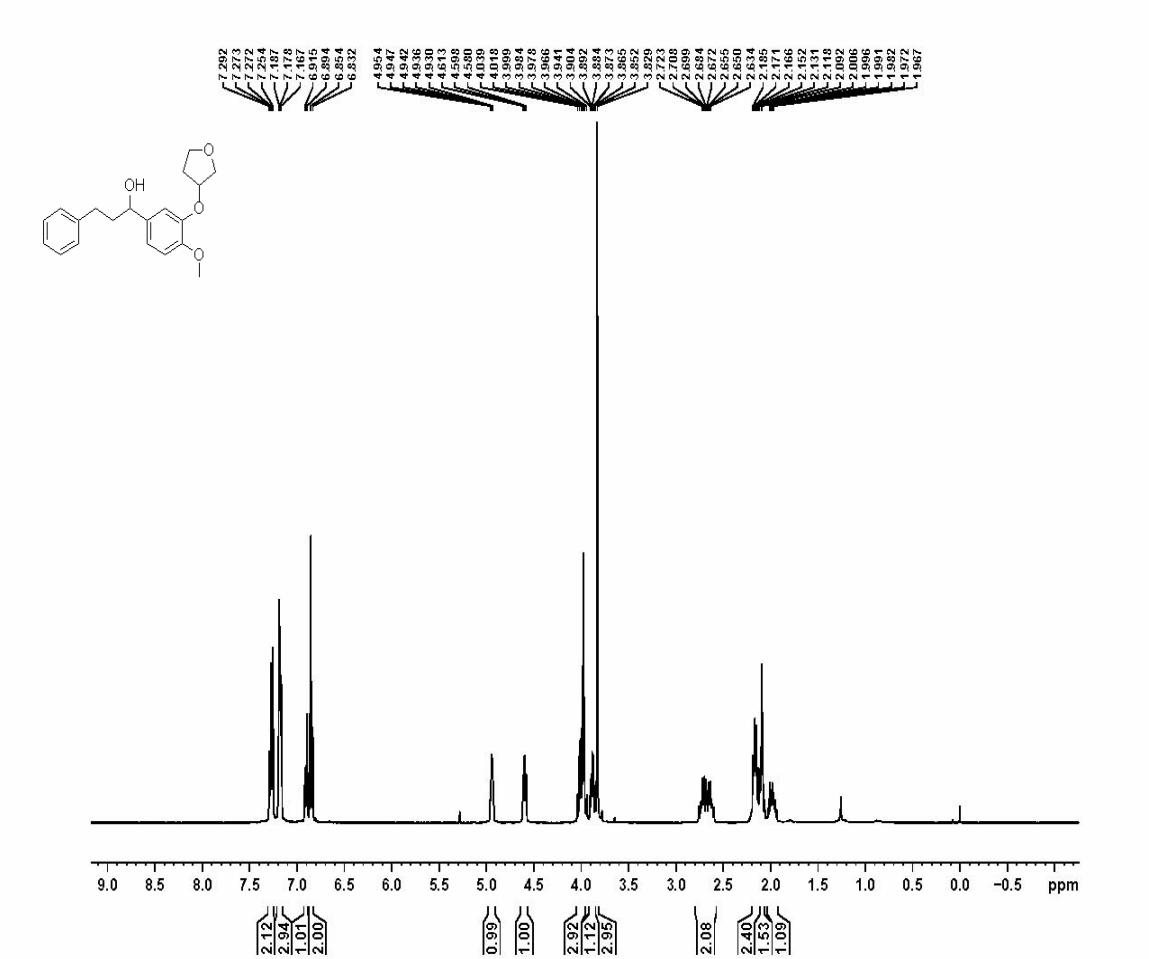
7.292
7.273
7.272
7.254
7.187
7.178
7.167
6.915
6.894
6.854
6.832
4.954
4.947
4.942
4.936
4.930
4.613
4.598
4.580
4.039
4.018
4.000
3.990
3.984
3.978
3.966
3.941
3.904
3.892
3.884
3.873
3.865
3.852
3.829
3.723
2.708
2.699
2.684
2.672
2.655
2.650
2.634
2.195
2.171
2.166
2.152
2.131
2.118
2.092
2.006
1.996
1.991
1.982
1.972
1.967
OH
O
O
O
9.0 8.5 8.0 7.5 7.0 6.5 6.0 5.5 5.0 4.5 4.0 3.5 3.0 2.5 2.0 1.5 1.0 0.5 0.0 −0.5 ppm
2.12
2.94
1.01
2.00
0.99
1.00
2.92
1.12
2.95
2.08
2.40
1.53
1.09

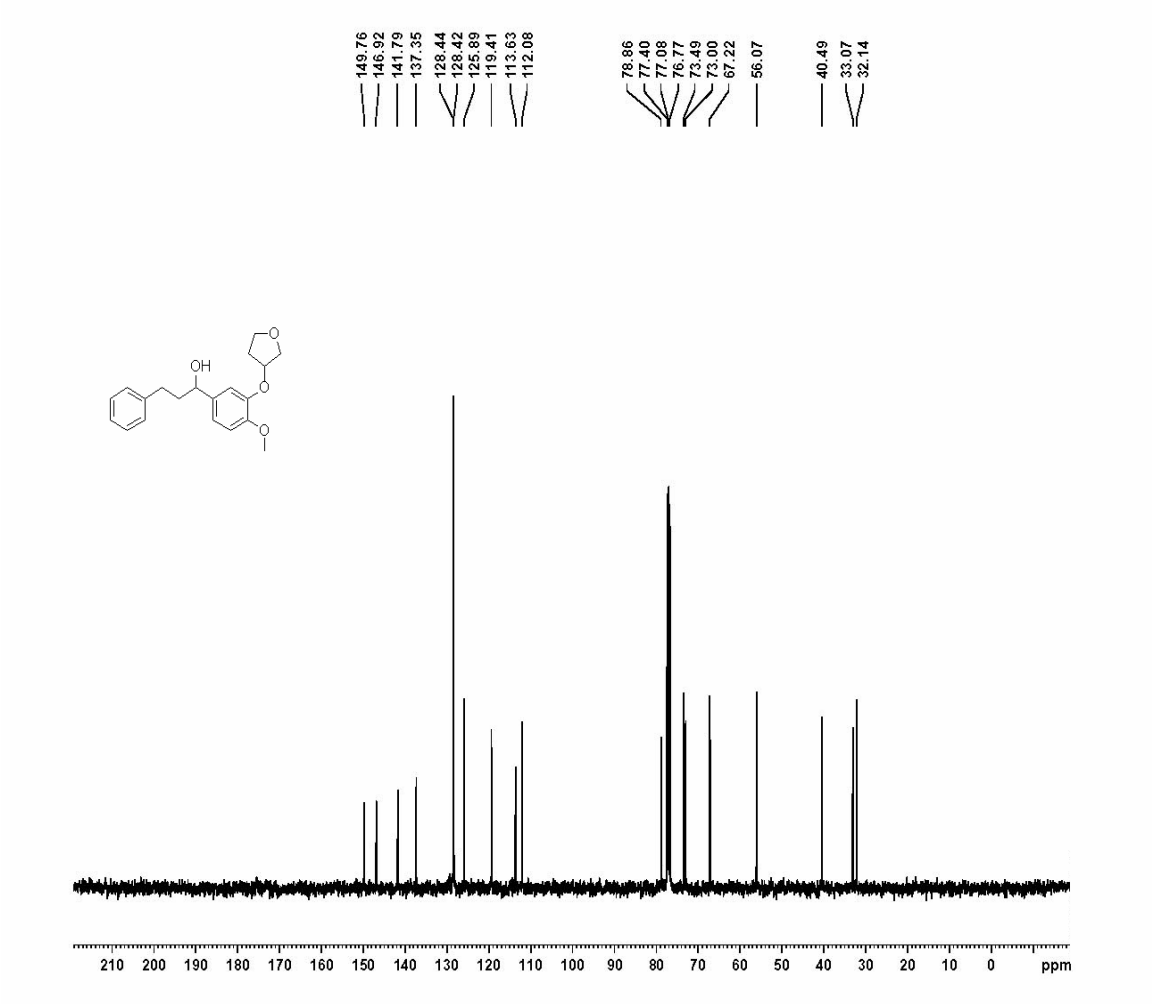
149.76
146.92
141.79
137.35
128.44
128.42
125.89
119.41
113.63
112.08
78.86
77.40
77.08
76.77
73.49
73.00
67.22
56.07
40.49
33.07
32.14
OH
O
O
O
210 200 190 180 170 160 150 140 130 120 110 100 90 80 70 60 50 40 30 20 10 0 ppm

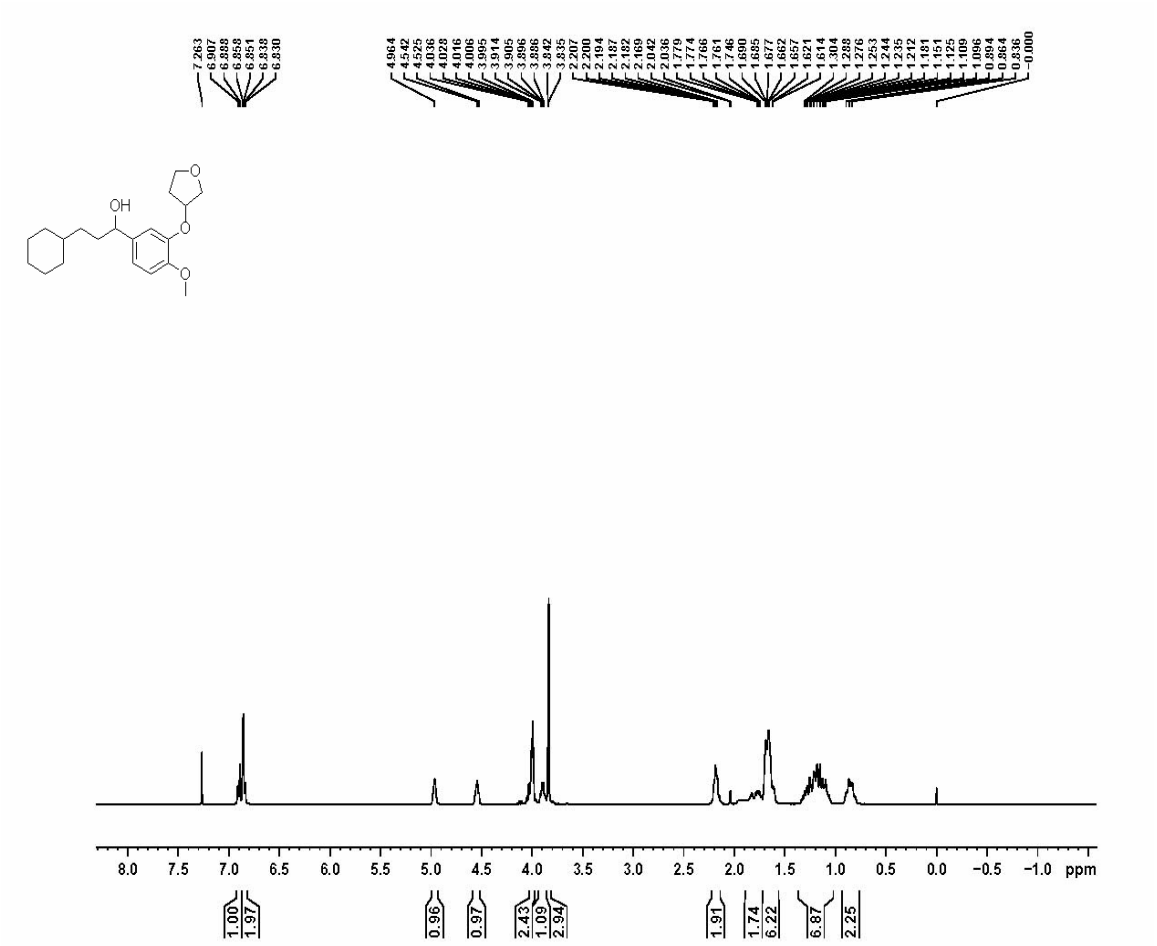
7.263
6.907
6.888
6.858
6.851
6.838
6.830
4.964
4.542
4.525
4.036
4.028
4.016
4.006
3.995
3.914
3.905
3.896
3.886
3.842
3.835
2.207
2.200
2.194
2.187
2.182
2.169
2.042
2.035
1.779
1.774
1.766
1.761
1.746
1.690
1.685
1.677
1.662
1.657
1.621
1.614
1.304
1.298
1.276
1.253
1.244
1.235
1.212
1.181
1.151
1.125
1.109
1.096
0.894
0.864
0.836
0.000
OH
O
O
O
8.0
7.5
7.0
6.5
6.0
5.5
5.0
4.5
4.0
3.5
3.0
2.5
2.0
1.5
1.0
0.5
0.0
−0.5
−1.0
ppm
1.00
1.97
0.96
0.97
2.43
1.09
2.94
1.91
1.74
6.22
6.87
2.25

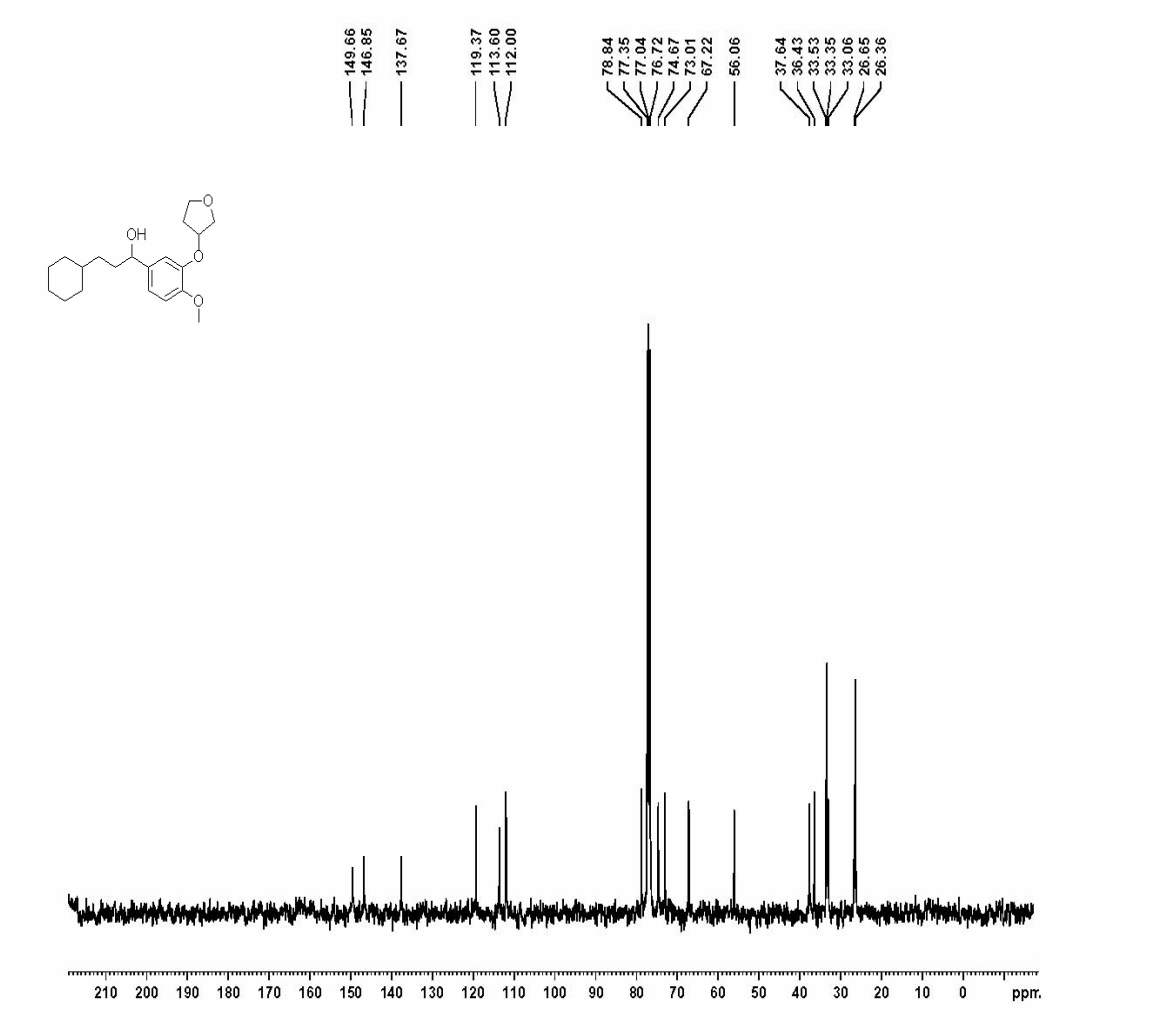
149.66
146.85
137.67
119.37
113.60
112.00
78.84
77.35
77.04
76.72
74.67
73.01
67.22
56.06
37.64
36.43
33.53
33.35
33.06
26.65
26.36
OH
O
O
O
210 200 190 180 170 160 150 140 130 120 110 100 90 80 70 60 50 40 30 20 10 0 ppm

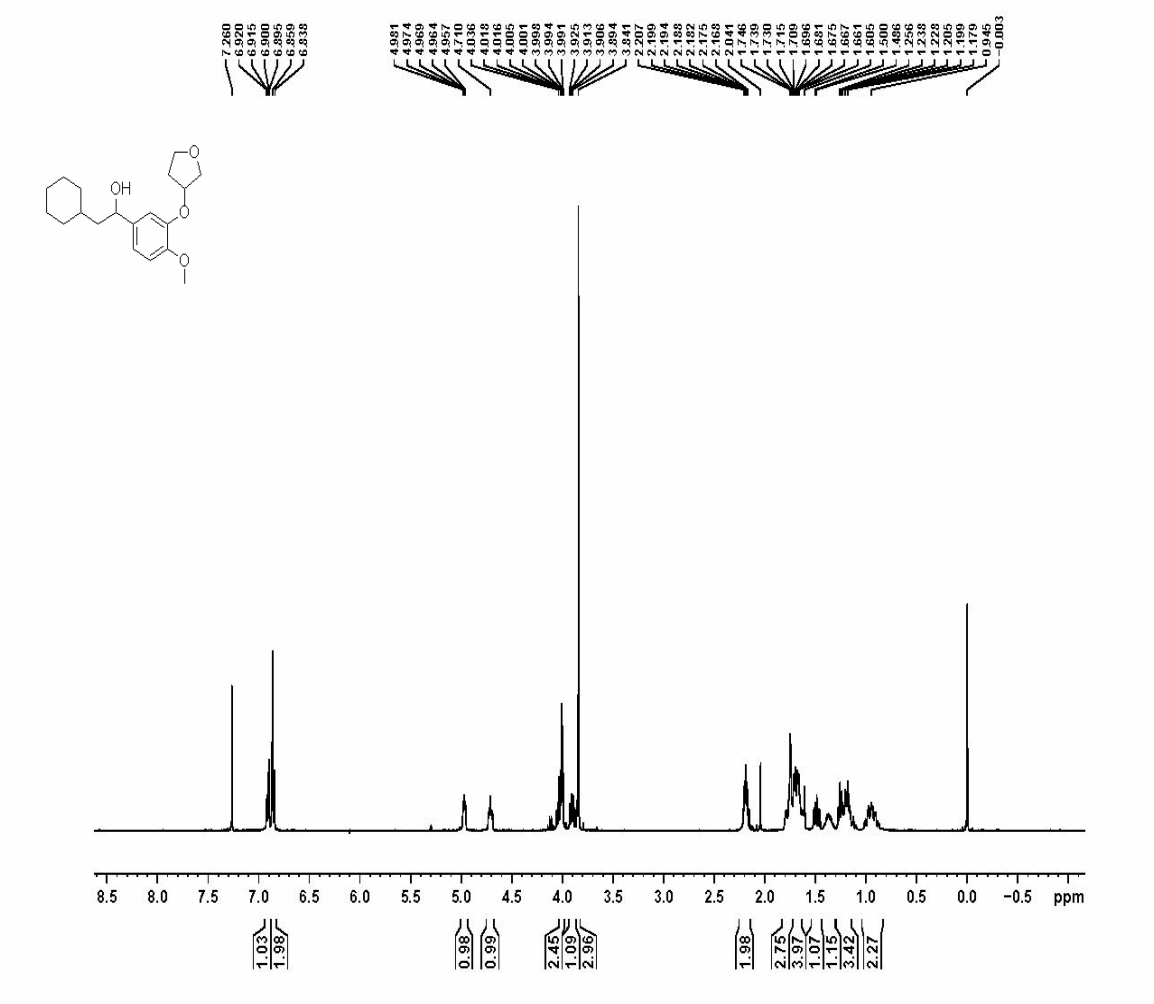
7.260
6.920
6.915
6.900
6.895
6.859
6.838
4.991
4.974
4.969
4.964
4.957
4.710
4.036
4.018
4.016
4.006
4.001
3.998
3.994
3.991
3.925
3.913
3.906
3.894
3.841
2.207
2.199
2.194
2.188
2.182
2.175
2.168
2.041
1.746
1.739
1.730
1.715
1.709
1.696
1.691
1.675
1.667
1.661
1.605
1.500
1.486
1.256
1.238
1.228
1.205
1.199
1.179
0.045
0.003
OH
O
O
O
8.5
8.0
7.5
7.0
6.5
6.0
5.5
5.0
4.5
4.0
3.5
3.0
2.5
2.0
1.5
1.0
0.5
0.0
−0.5
ppm
1.03
1.98
0.98
0.99
2.45
1.09
2.96
1.98
2.75
3.97
1.07
1.15
3.42
2.27

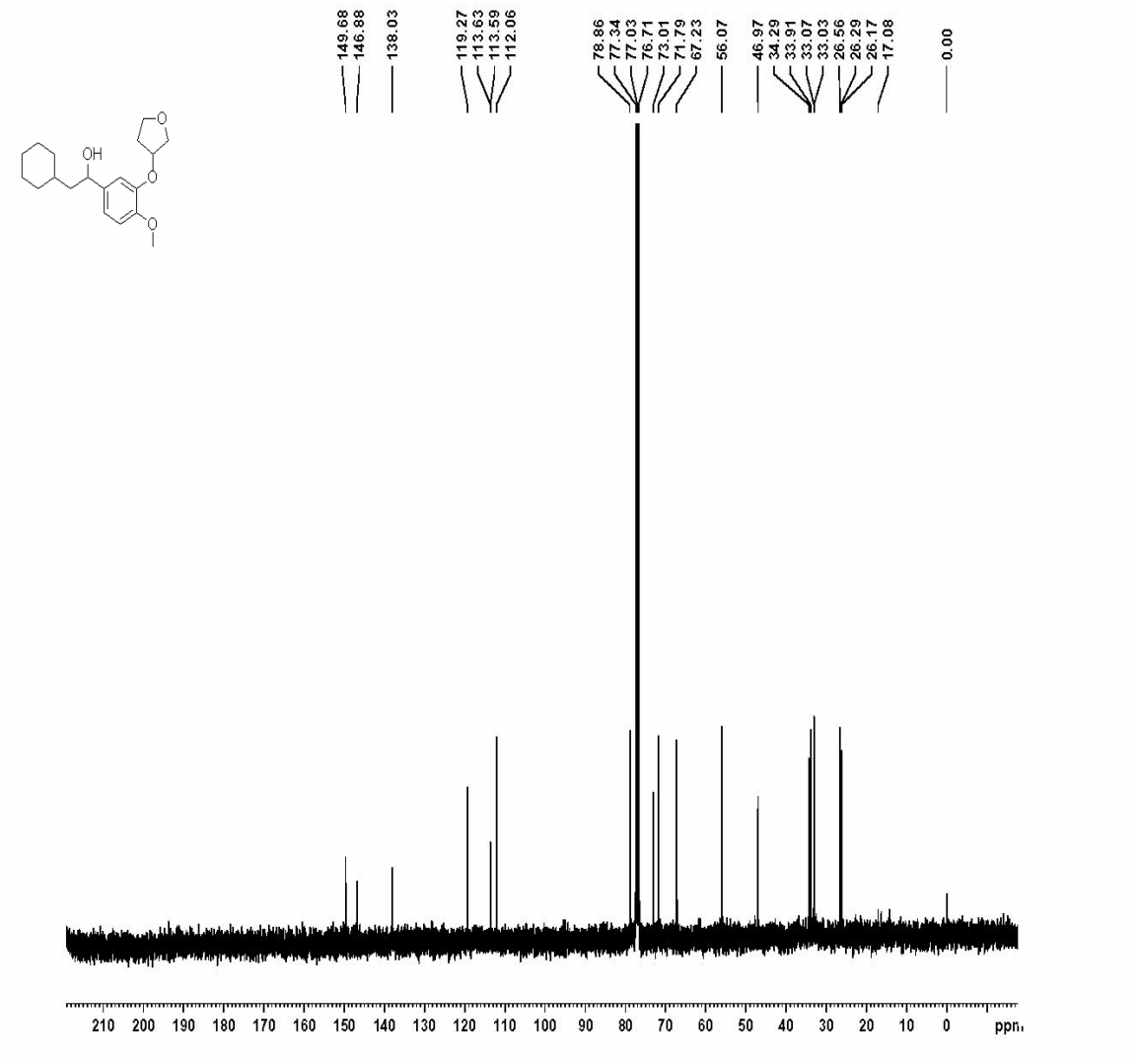
149.68
146.88
138.03
119.27
113.63
113.59
112.06
78.86
77.34
77.03
76.71
73.01
71.79
67.23
56.07
46.97
34.29
33.91
33.07
33.03
26.56
26.29
26.17
17.08
0.00
OH
O
O
O
210 200 190 180 170 160 150 140 130 120 110 100 90 80 70 60 50 40 30 20 10 0 ppm

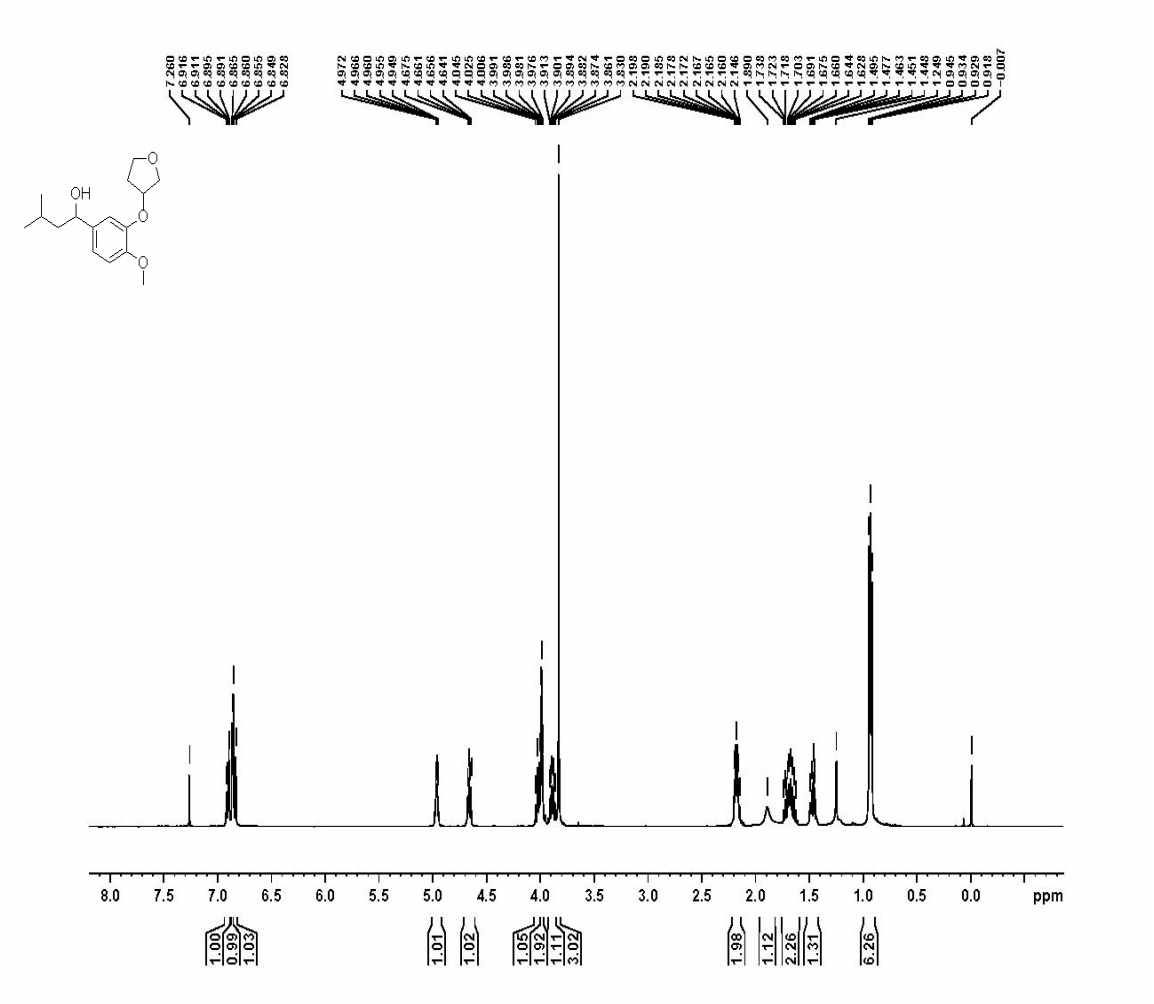
7.260
6.916
6.911
6.895
6.891
6.885
6.880
6.855
6.849
6.828
4.972
4.966
4.960
4.955
4.949
4.675
4.661
4.656
4.641
4.045
4.035
4.006
3.991
3.986
3.981
3.976
3.913
3.901
3.894
3.882
3.874
3.861
3.830
2.198
2.190
2.185
2.178
2.172
2.167
2.165
2.160
2.146
1.890
1.738
1.723
1.718
1.703
1.691
1.675
1.660
1.644
1.628
1.606
1.477
1.463
1.451
1.448
1.249
0.946
0.934
0.929
0.918
0.007
OH
O
O
O
8.0
7.5
7.0
6.5
6.0
5.5
5.0
4.5
4.0
3.5
3.0
2.5
2.0
1.5
1.0
0.5
0.0
ppm
1.00
0.99
1.03
1.01
1.02
1.05
1.92
1.11
3.02
1.98
1.12
2.26
1.31
6.26

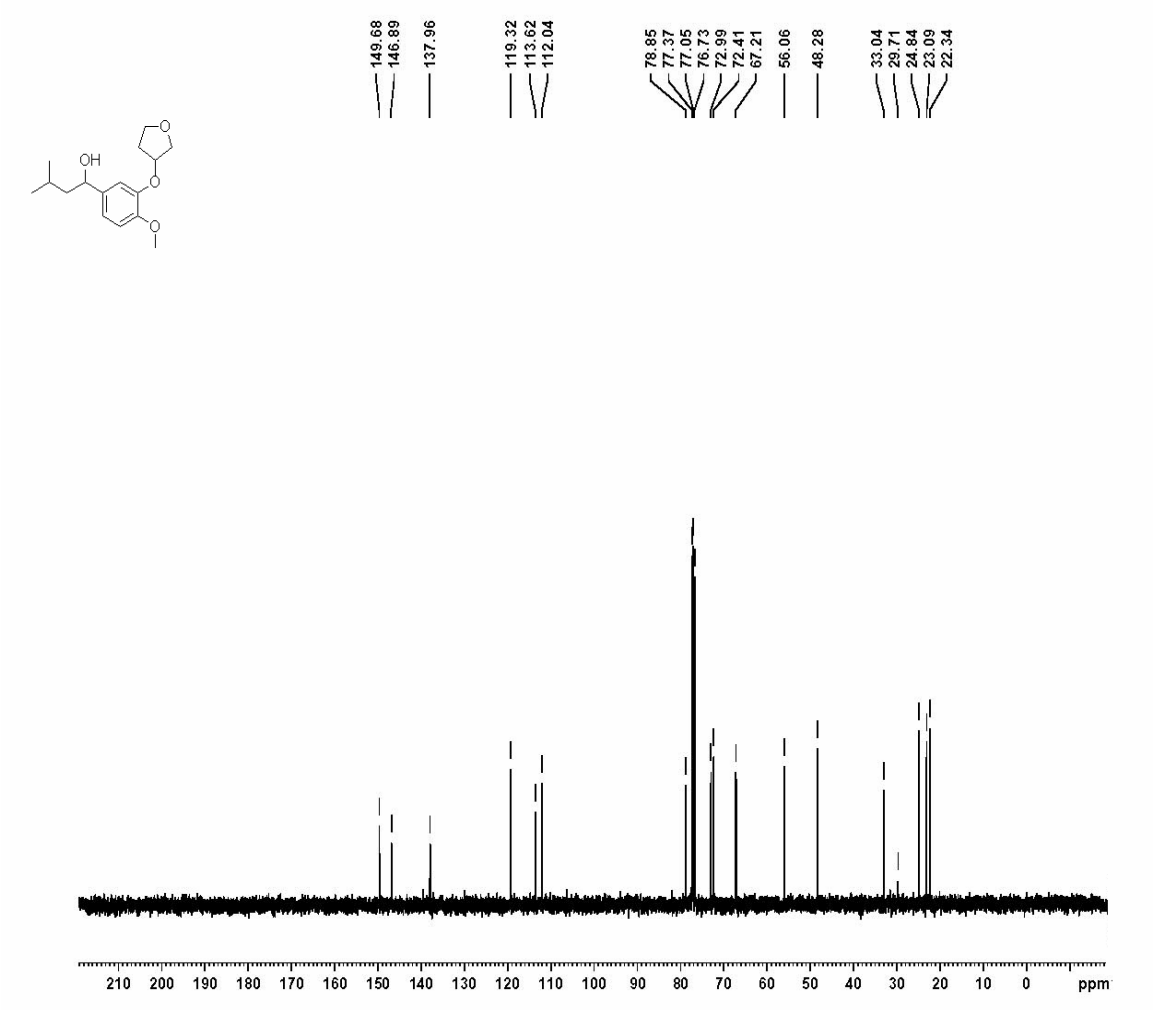
149.68
146.89
137.96
119.32
113.62
112.04
78.85
77.37
77.05
76.73
72.99
72.41
67.21
56.06
48.28
33.04
29.71
24.84
23.09
22.34
OH
O
O
O
210 200 190 180 170 160 150 140 130 120 110 100 90 80 70 60 50 40 30 20 10 0 ppm

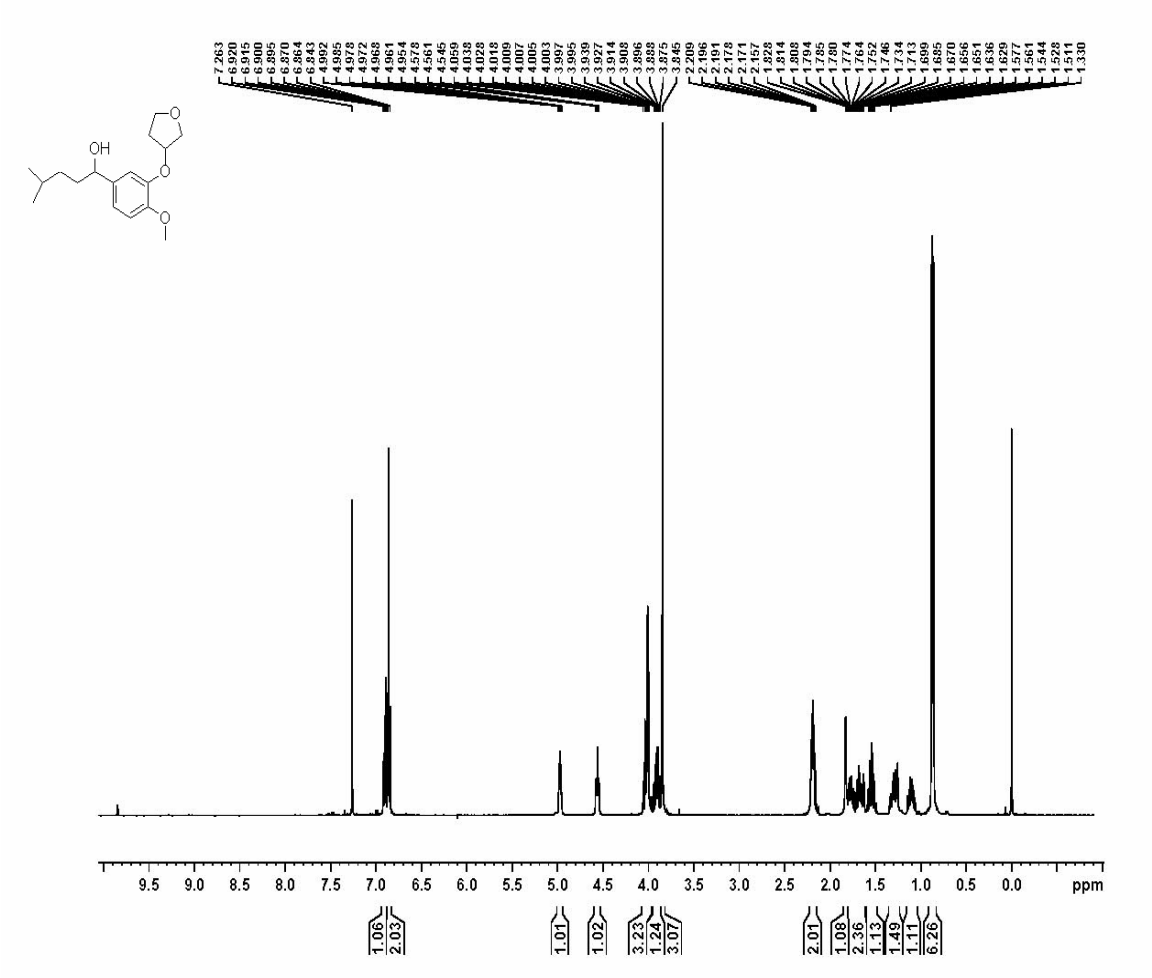
7.263
6.920
6.915
6.905
6.900
6.896
6.870
6.864
6.843
4.992
4.985
4.978
4.972
4.968
4.961
4.954
4.578
4.561
4.545
4.058
4.038
4.028
4.018
4.009
4.007
4.005
4.003
3.997
3.995
3.939
3.927
3.914
3.908
3.896
3.888
3.875
3.845
2.209
2.196
2.191
2.178
2.171
2.157
1.828
1.814
1.808
1.794
1.785
1.780
1.774
1.764
1.752
1.746
1.734
1.713
1.699
1.685
1.670
1.656
1.651
1.636
1.629
1.577
1.561
1.544
1.528
1.511
1.330
OH
O
O
O
9.5 9.0 8.5 8.0 7.5 7.0 6.5 6.0 5.5 5.0 4.5 4.0 3.5 3.0 2.5 2.0 1.5 1.0 0.5 0.0 ppm
1.06
2.03
1.01
1.02
3.23
1.24
3.07
2.01
1.08
2.36
1.13
1.49
1.11
6.26

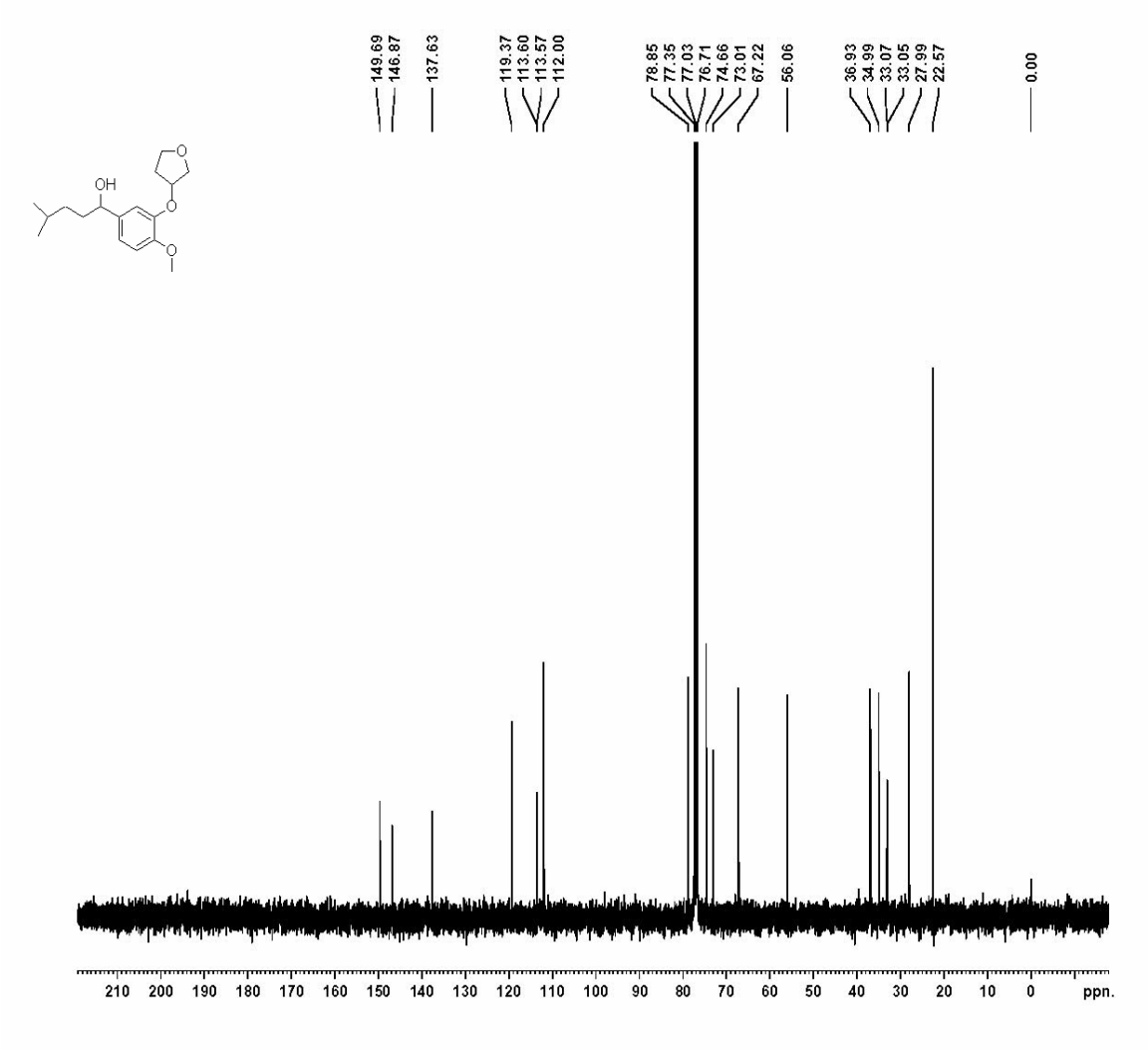
149.69
146.87
137.63
119.37
113.60
113.57
112.00
78.85
77.35
77.03
76.71
74.66
73.01
67.22
56.06
36.93
34.99
33.07
33.05
27.99
22.57
0.00
OH
O
O
O
210 200 190 180 170 160 150 140 130 120 110 100 90 80 70 60 50 40 30 20 10 0 ppn.

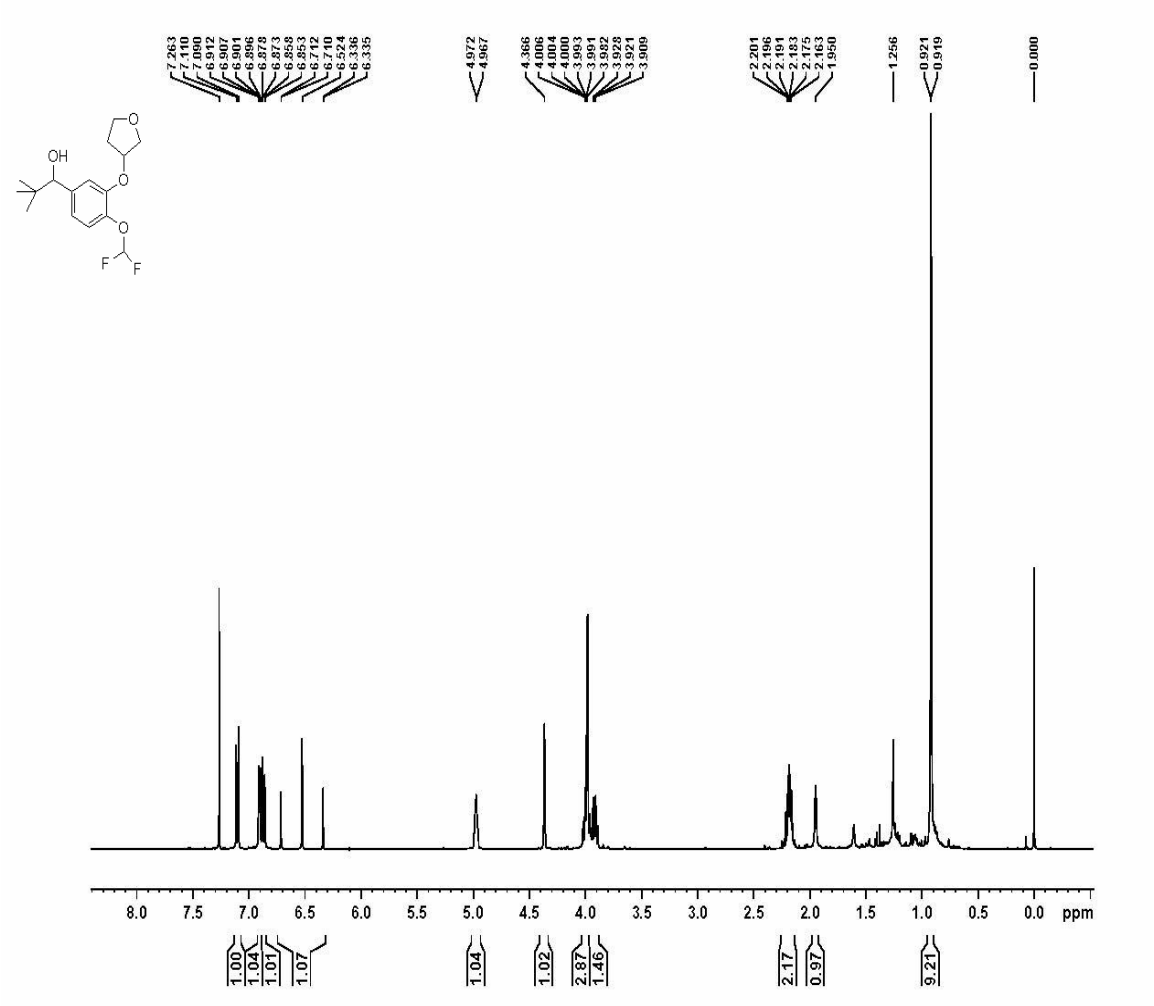
7.263
7.110
7.090
6.912
6.907
6.901
6.896
6.878
6.873
6.858
6.853
6.772
6.710
6.524
6.336
6.335
4.972
4.967
4.366
4.006
4.004
4.000
3.993
3.991
3.982
3.928
3.921
3.909
2.201
2.196
2.191
2.183
2.175
2.163
1.950
1.256
0.921
0.919
0.000
OH
O
O
O
F
F
8.0
7.5
7.0
6.5
6.0
5.5
5.0
4.5
4.0
3.5
3.0
2.5
2.0
1.5
1.0
0.5
0.0
ppm
1.00
1.04
1.01
1.07
1.04
1.02
2.87
1.46
2.17
0.97
9.21

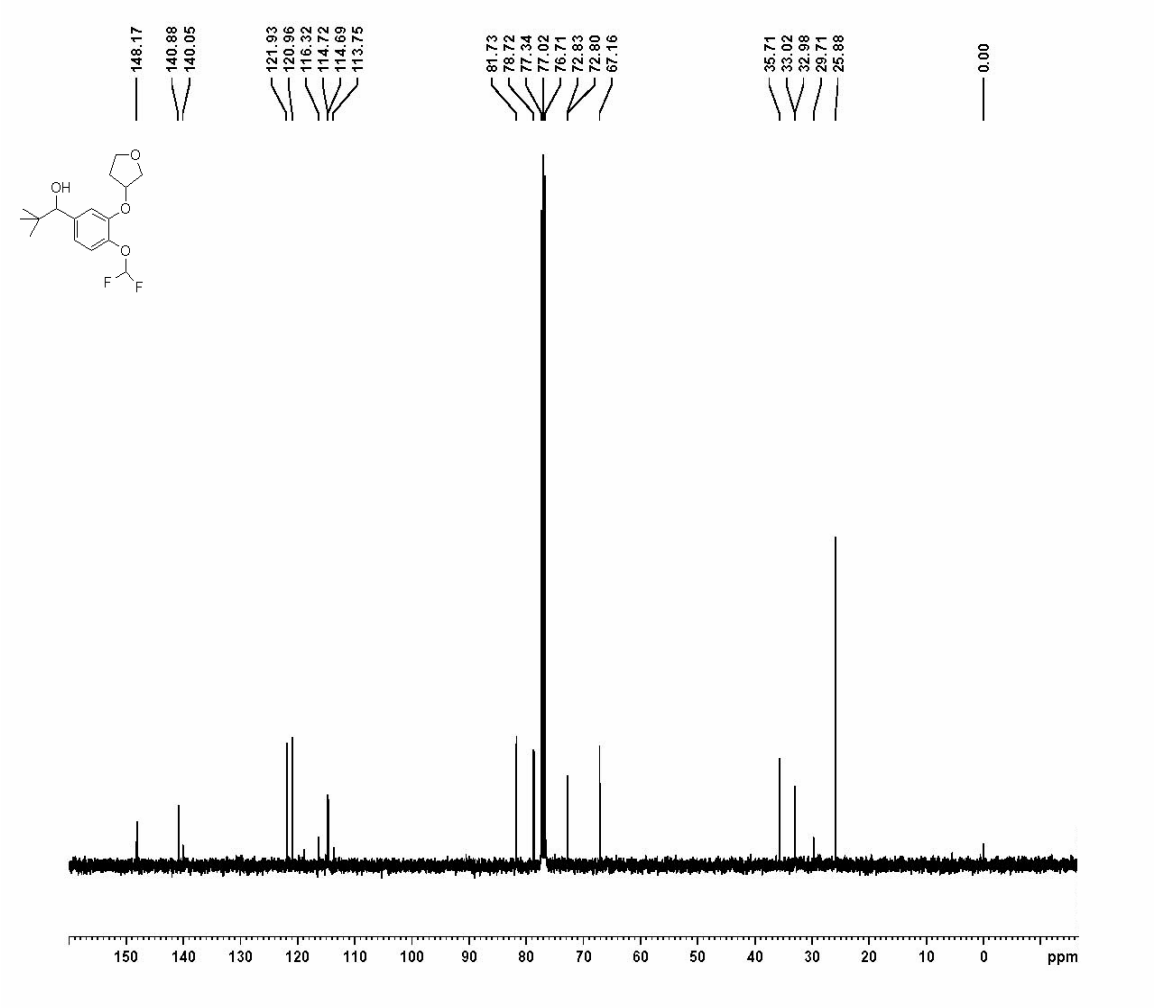
148.17
140.88
140.05
121.93
120.96
116.32
114.72
114.69
113.75
81.73
78.72
77.34
77.02
76.71
72.83
72.80
67.16
35.71
33.02
32.98
29.71
25.88
0.00
OH
O
O
O
F
F
150
140
130
120
110
100
90
80
70
60
50
40
30
20
10
0
ppm

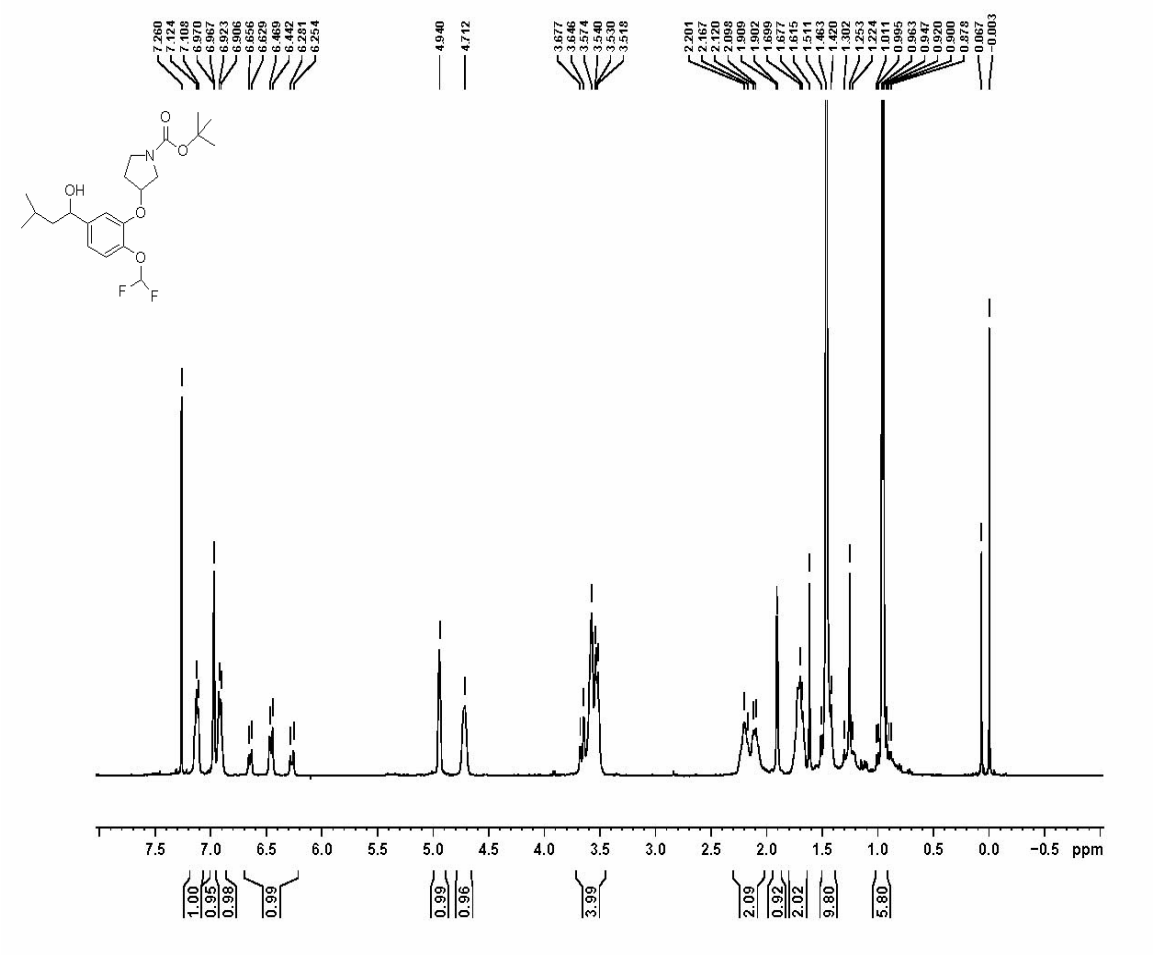
7.260
7.124
7.108
6.970
6.967
6.923
6.906
6.656
6.629
6.469
6.442
6.281
6.254
4.940
4.712
3.677
3.646
3.574
3.540
3.530
3.518
2.201
2.167
2.120
2.099
1.909
1.902
1.699
1.677
1.615
1.511
1.463
1.400
1.302
1.253
1.224
1.011
0.995
0.963
0.947
0.920
0.900
0.878
0.067
-0.003
OH
O
N
O
O
O
F
F
7.5
7.0
6.5
6.0
5.5
5.0
4.5
4.0
3.5
3.0
2.5
2.0
1.5
1.0
0.5
0.0
-0.5
ppm
1.00
0.95
0.98
0.99
0.99
0.96
3.99
2.09
0.92
2.02
9.80
5.80

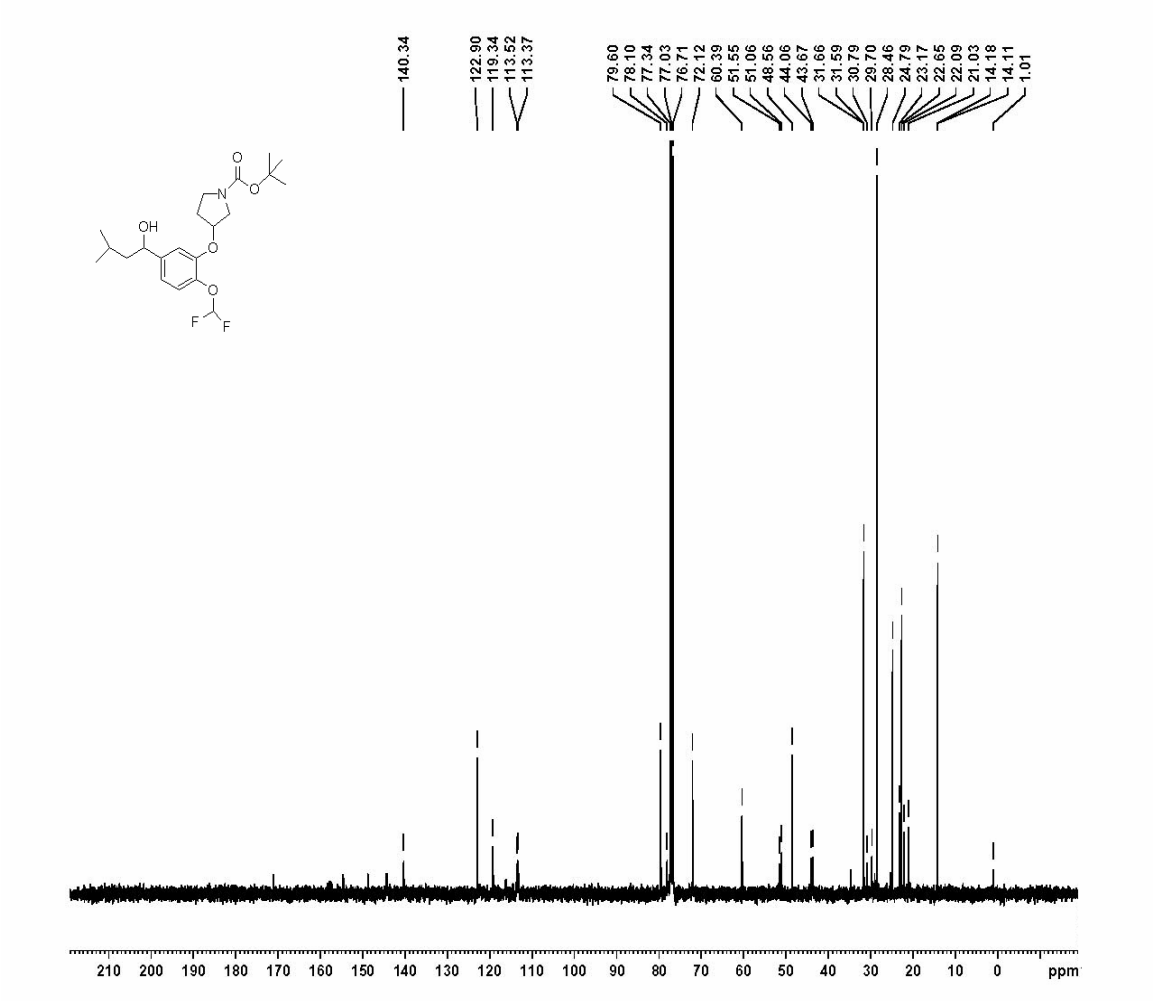
140.34
122.90
119.34
113.52
113.37
79.60
78.10
77.34
77.03
76.71
72.12
60.39
51.55
51.06
48.56
44.06
43.67
31.66
31.59
30.79
29.70
28.46
24.79
23.17
22.65
22.09
21.03
14.18
14.11
1.01
OH
O
N
O
O
O
F
F
210 200 190 180 170 160 150 140 130 120 110 100 90 80 70 60 50 40 30 20 10 0 ppm

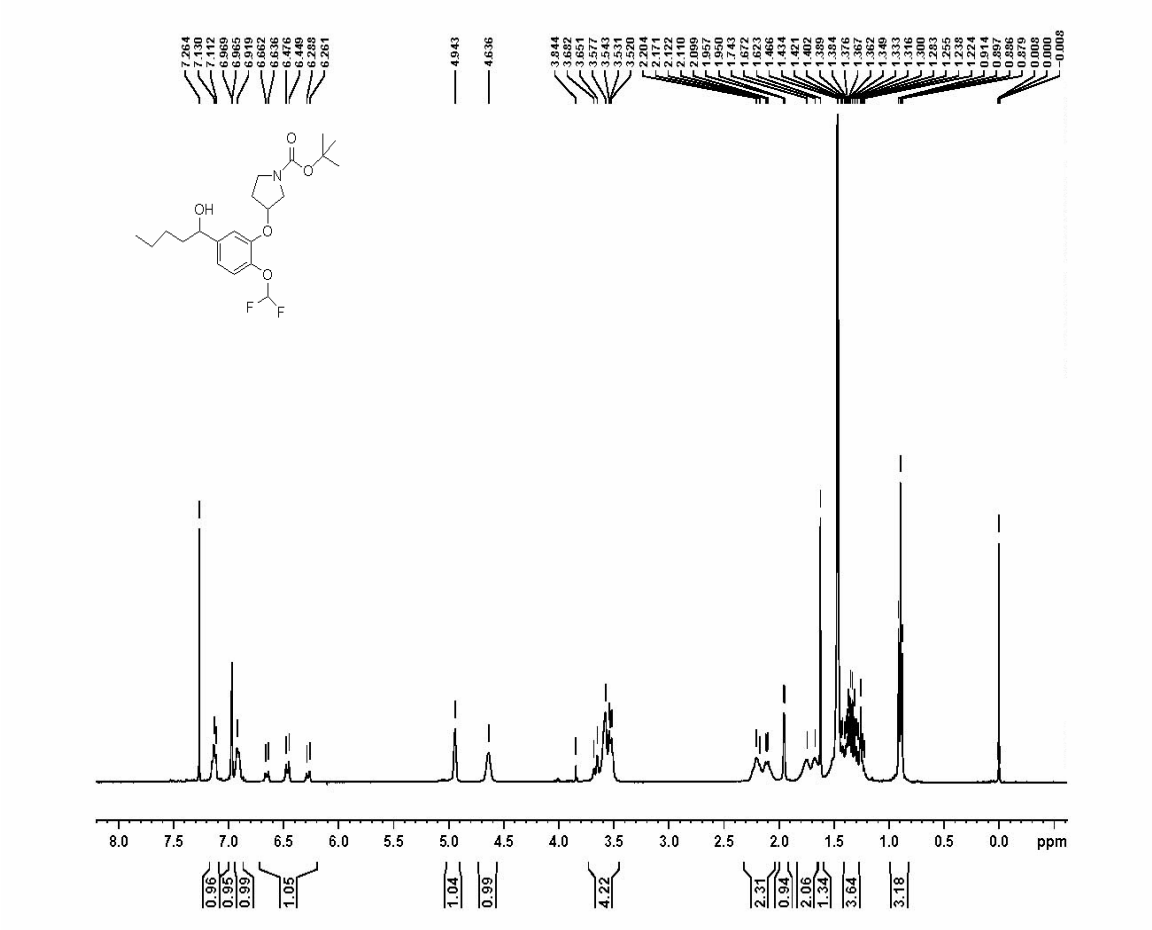
7.264
7.130
7.112
6.969
6.965
6.919
6.682
6.638
6.466
6.446
6.288
6.261
4.943
4.636
3.844
3.692
3.651
3.577
3.543
3.531
3.520
2.204
2.171
2.122
2.110
2.099
1.957
1.950
1.743
1.672
1.623
1.466
1.434
1.421
1.402
1.389
1.384
1.376
1.367
1.362
1.349
1.333
1.316
1.300
1.283
1.255
1.238
1.224
0.914
0.897
0.886
0.879
0.008
0.000
-0.008
OH
O
N
O
O
O
F
F
8.0
7.5
7.0
6.5
6.0
5.5
5.0
4.5
4.0
3.5
3.0
2.5
2.0
1.5
1.0
0.5
0.0
ppm
0.96
0.95
0.99
1.05
1.04
0.99
4.22
2.31
0.94
2.06
1.34
3.64
3.18

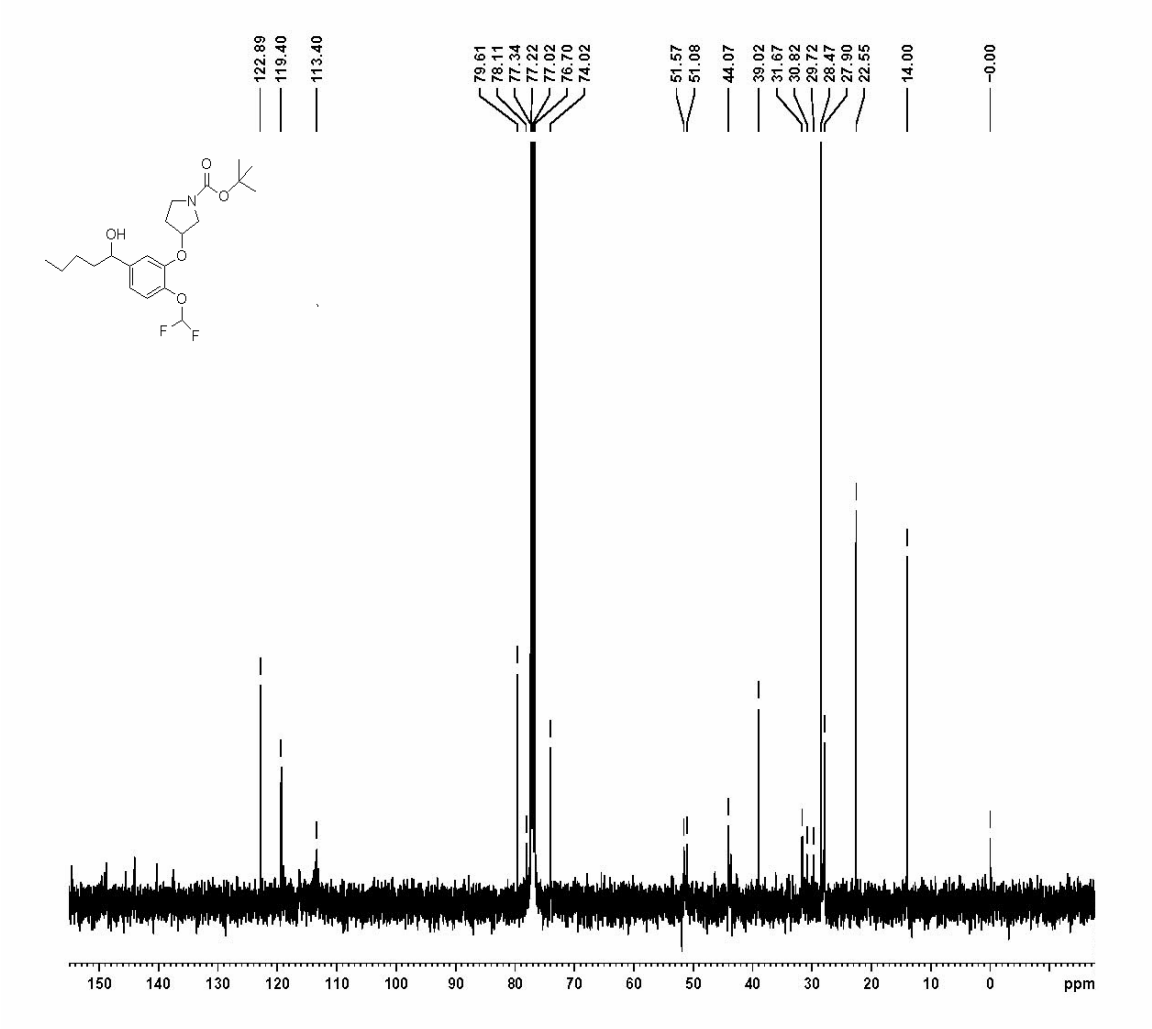
122.89
119.40
113.40
79.61
78.11
77.34
77.22
77.02
76.70
74.02
51.57
51.08
44.07
39.02
31.67
30.82
29.72
28.47
27.90
22.55
14.00
-0.00
OH
O
N
O
O
O
F
F
150
140
130
120
110
100
90
80
70
60
50
40
30
20
10
0
ppm

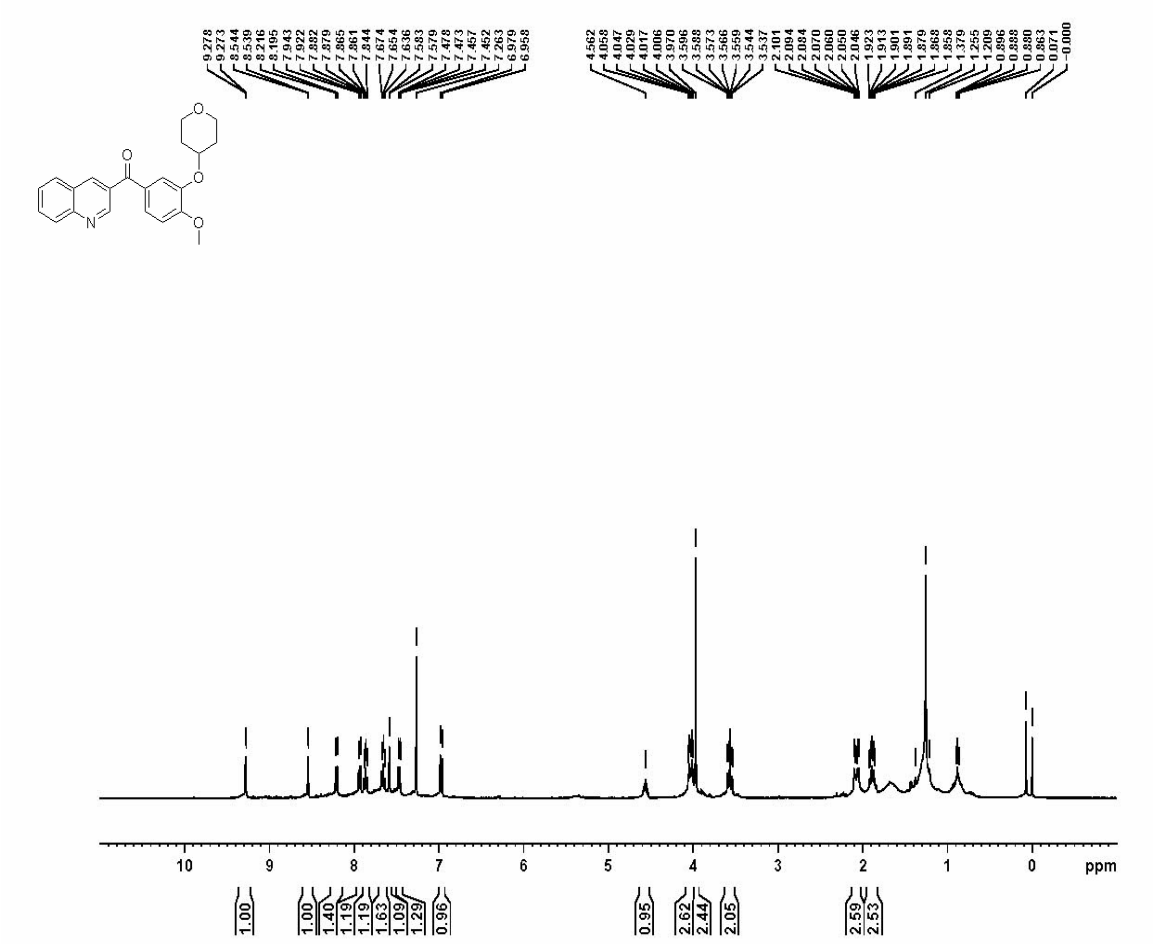
9.278
9.273
8.544
8.539
8.216
8.195
8.044
7.943
7.922
7.882
7.876
7.865
7.861
7.844
7.674
7.654
7.636
7.583
7.579
7.478
7.473
7.457
7.452
7.263
6.979
6.958
4.562
4.058
4.047
4.029
4.017
4.006
3.970
3.596
3.588
3.573
3.566
3.559
3.544
3.537
2.101
2.094
2.084
2.070
2.060
2.050
2.046
1.923
1.913
1.901
1.891
1.879
1.868
1.858
1.379
1.255
1.209
1.206
0.886
0.880
0.863
0.071
0.000
O
O
O
N
O
10
9
8
7
6
5
4
3
2
1
0
ppm
1.00
1.00
1.40
1.19
1.19
1.63
1.09
1.29
0.96
0.95
2.62
2.44
2.05
2.59
2.53

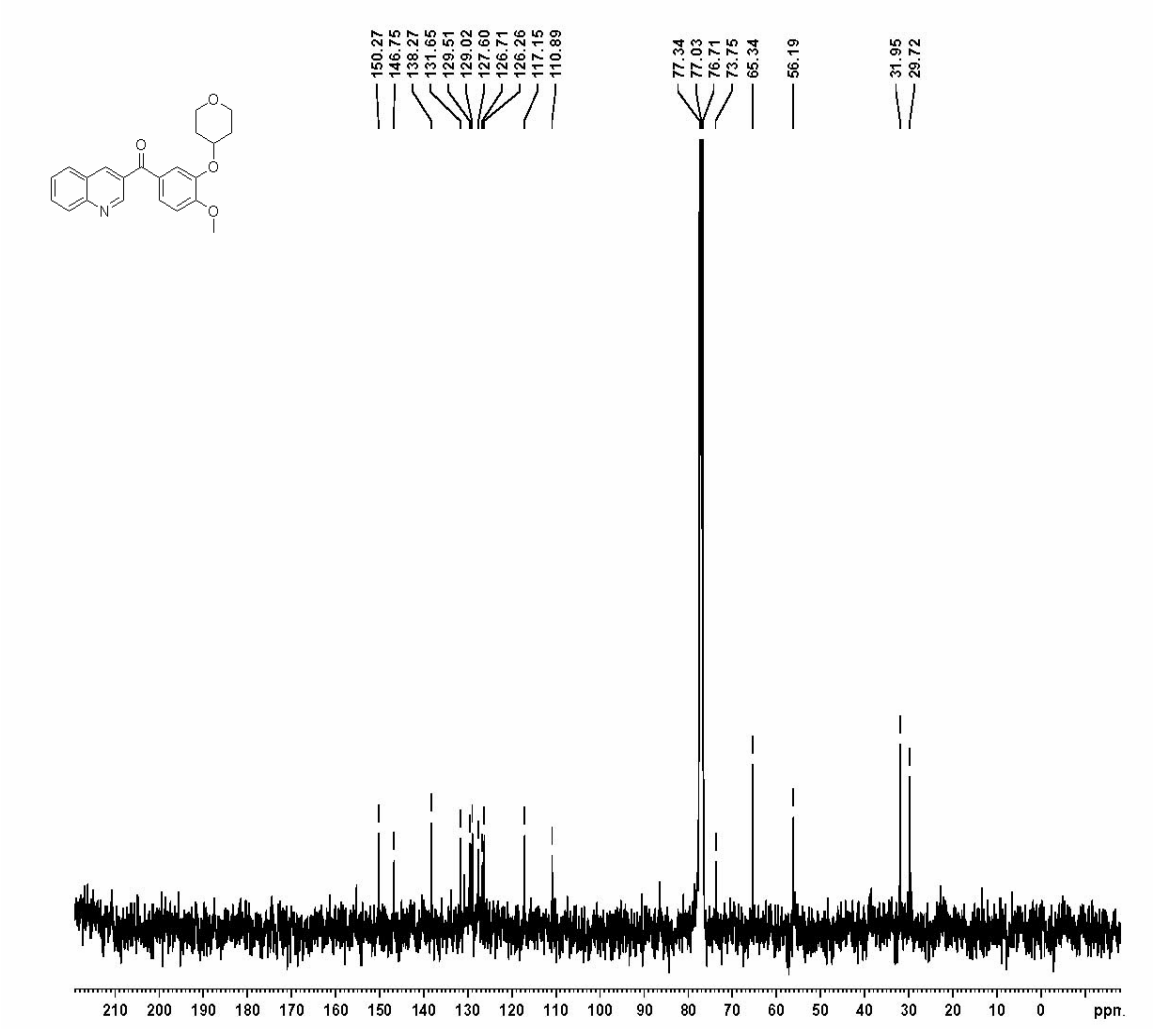
150.27
146.75
138.27
131.65
129.51
129.02
127.60
126.71
126.26
117.15
110.89
77.34
77.03
76.71
73.75
65.34
56.19
31.95
29.72
O
O
O
N
210 200 190 180 170 160 150 140 130 120 110 100 90 80 70 60 50 40 30 20 10 0 ppm

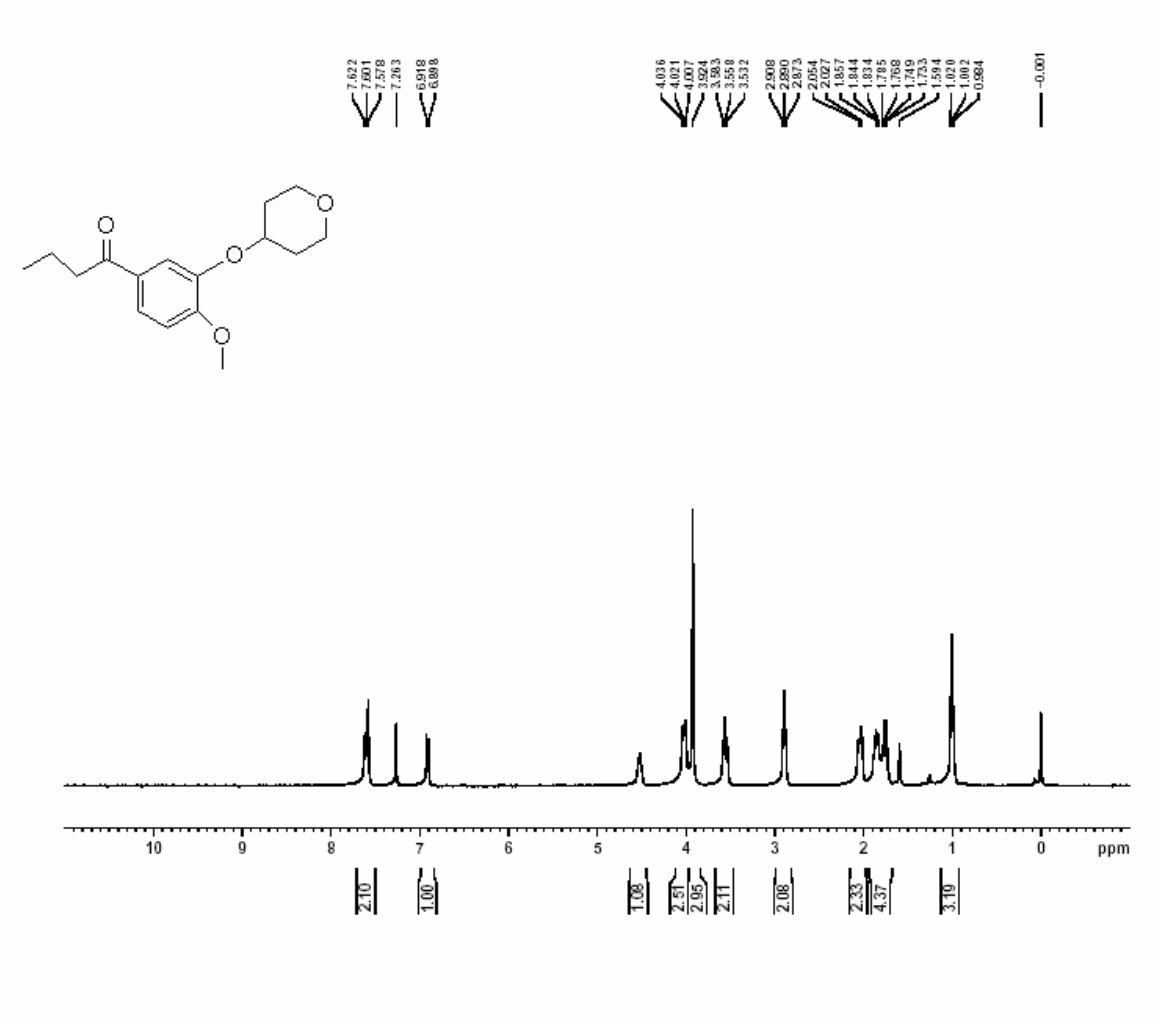
7.622
7.601
7.578
7.263
6.918
6.898
4.036
4.021
4.007
3.924
3.583
3.558
3.532
2.908
2.890
2.873
2.054
2.027
1.857
1.844
1.834
1.785
1.768
1.749
1.733
1.594
1.020
1.002
0.984
-0.001
O
O
O
10
9
8
7
6
5
4
3
2
1
0
ppm
2.10
1.00
1.08
2.51
2.95
2.11
2.08
2.33
4.37
3.19

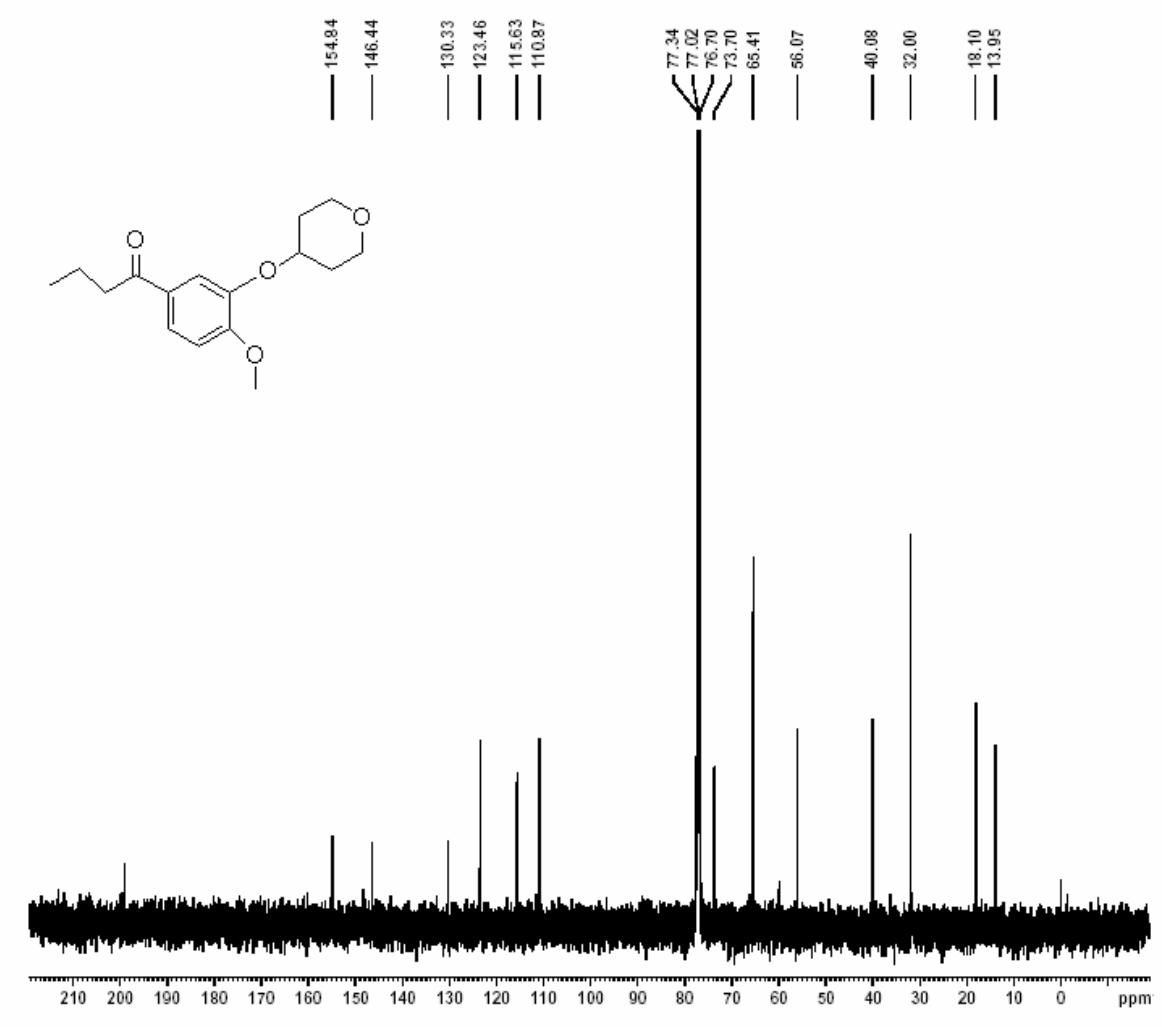
154.84
146.44
130.33
123.46
115.63
110.87
77.34
77.02
76.70
73.70
65.41
56.07
40.08
32.00
18.10
13.95
O
O
O
O
210 200 190 180 170 160 150 140 130 120 110 100 90 80 70 60 50 40 30 20 10 0 ppm

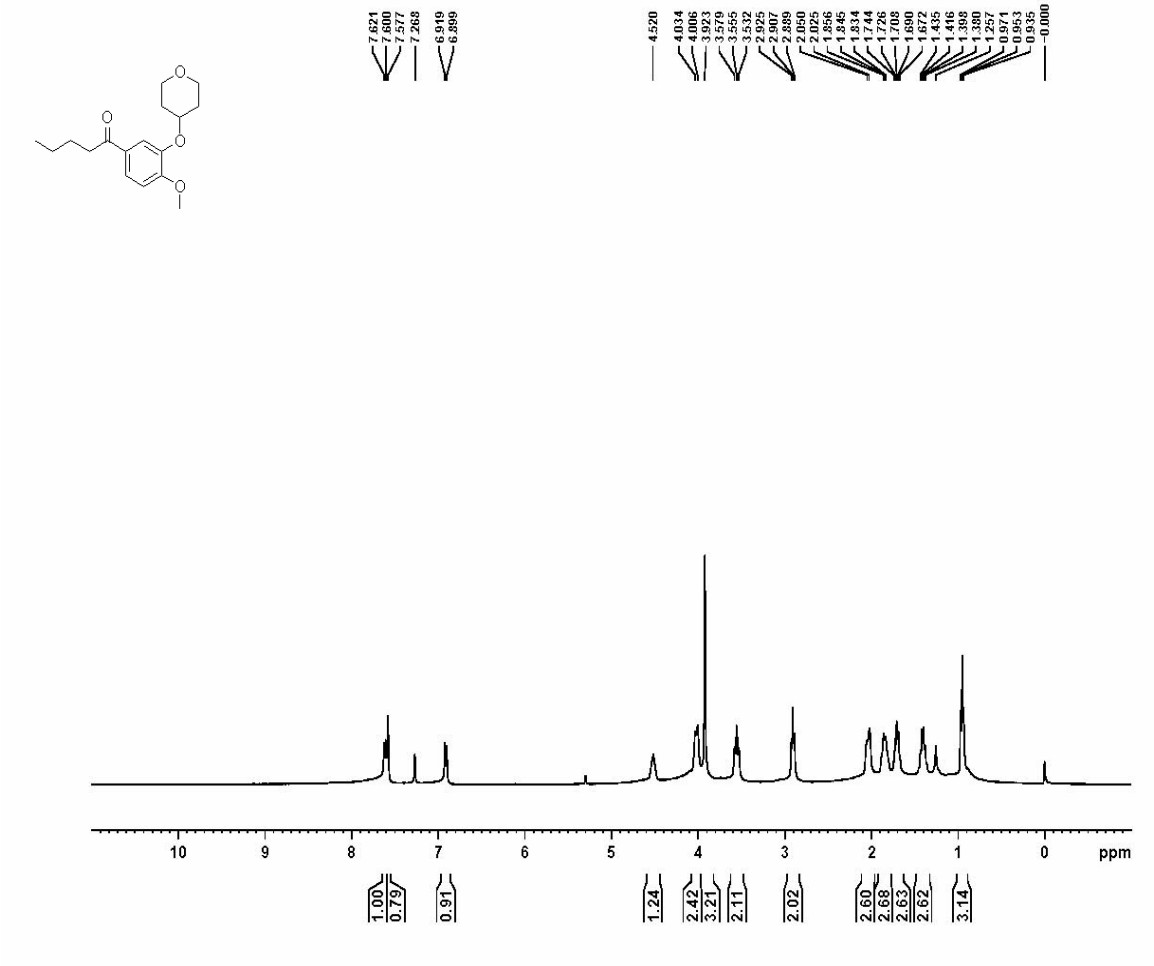
7.621
7.600
7.577
7.268
6.919
6.899
4.520
4.034
4.006
3.993
3.579
3.565
3.532
2.925
2.907
2.889
2.050
2.025
1.856
1.845
1.834
1.744
1.726
1.708
1.690
1.672
1.435
1.416
1.398
1.380
1.257
0.971
0.953
0.935
-0.000
10
9
8
7
6
5
4
3
2
1
0
ppm
1.00
0.79
0.91
1.24
2.42
3.21
2.11
2.02
2.60
2.68
2.63
2.62
3.14

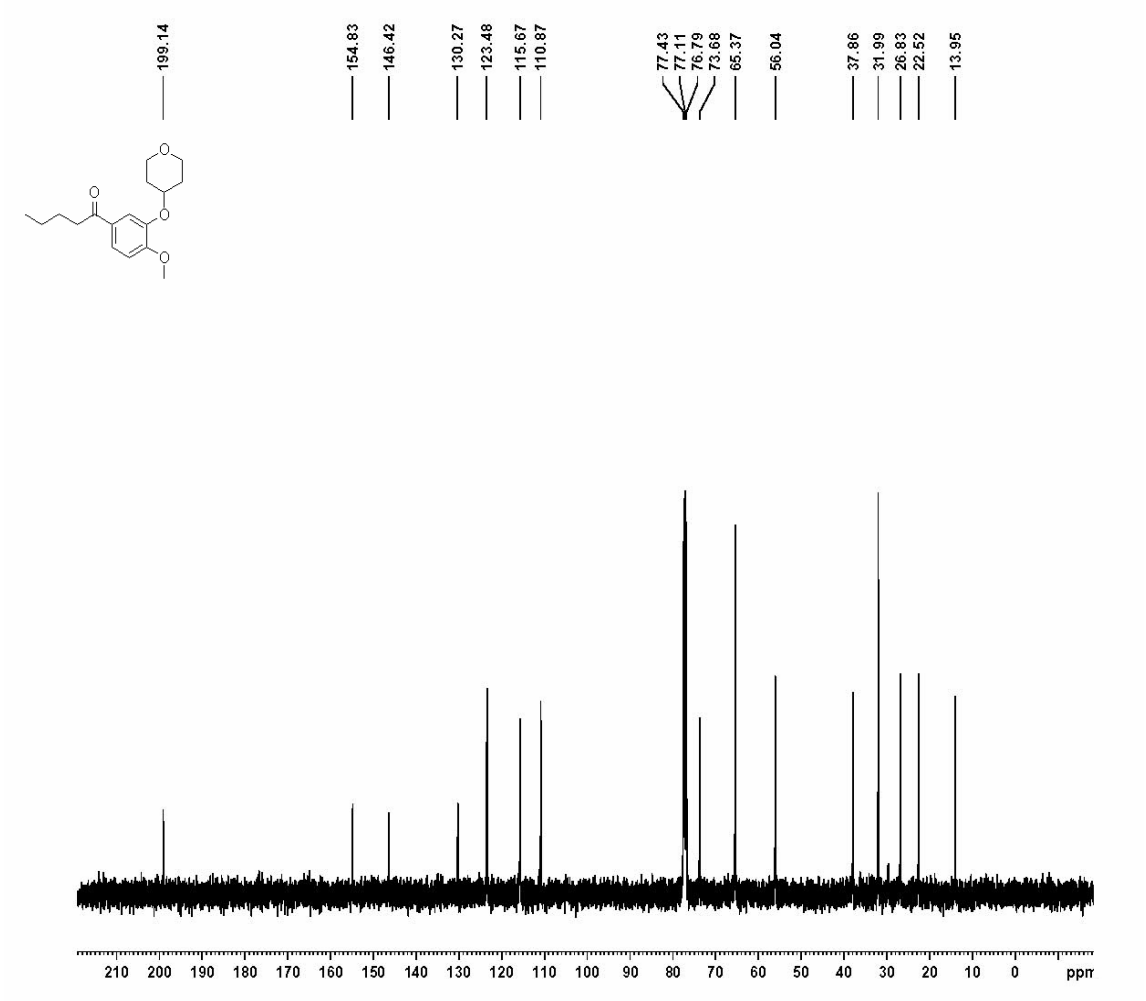
199.14
154.83
146.42
130.27
123.48
115.67
110.87
77.43
77.11
76.79
73.68
65.37
56.04
37.86
31.99
26.83
22.52
13.95
O
O
O
O
210 200 190 180 170 160 150 140 130 120 110 100 90 80 70 60 50 40 30 20 10 0 ppm

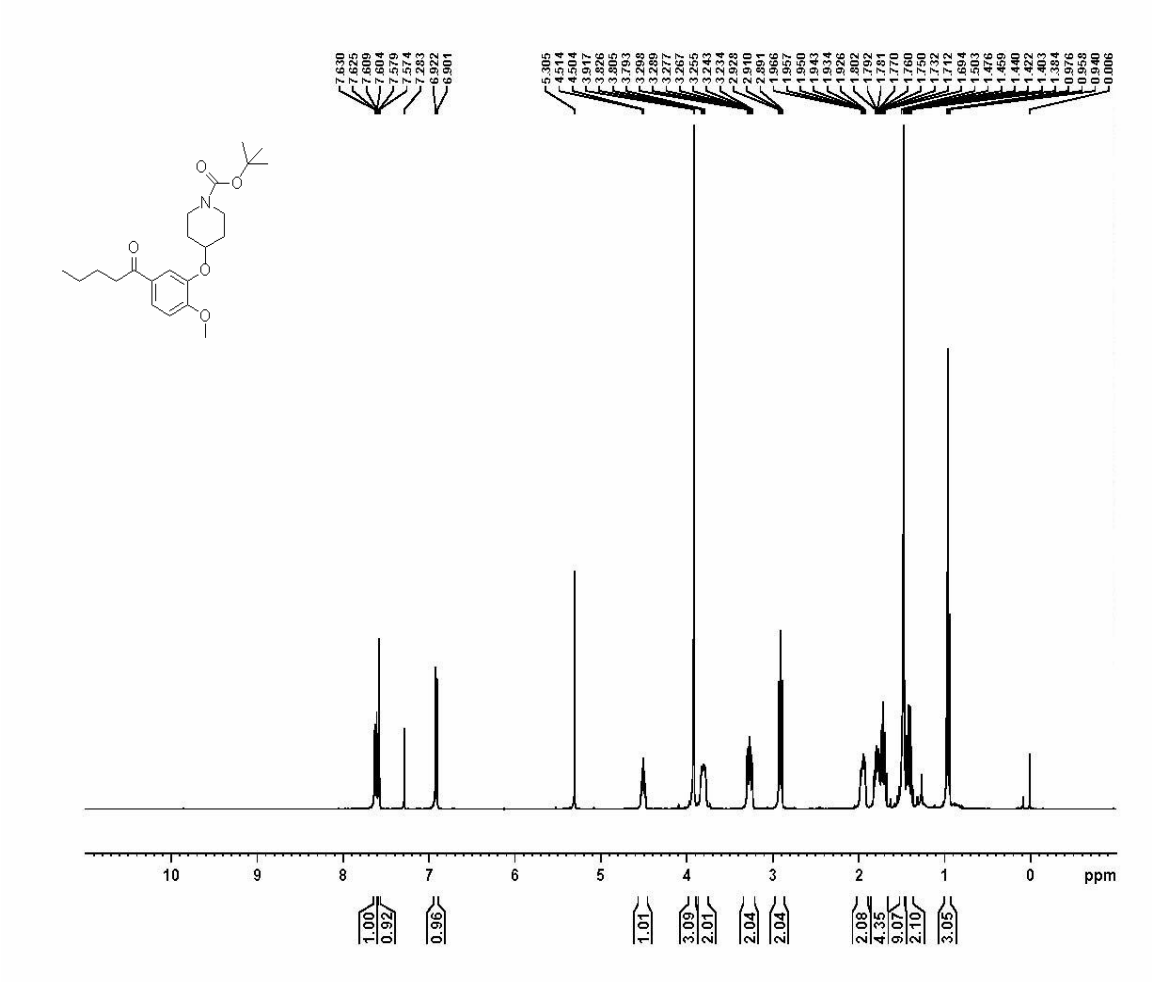
7.630
7.625
7.609
7.604
7.579
7.574
7.283
6.922
6.901
5.305
4.514
4.504
3.917
3.826
3.805
3.793
3.298
3.289
3.277
3.267
3.255
3.243
3.234
2.928
2.910
2.891
1.966
1.957
1.950
1.943
1.934
1.926
1.802
1.792
1.781
1.770
1.760
1.750
1.732
1.712
1.694
1.503
1.476
1.459
1.440
1.422
1.401
1.384
0.976
0.958
0.940
0.006
10
9
8
7
6
5
4
3
2
1
0
ppm
1.00
0.92
0.96
1.01
3.09
2.01
2.04
2.04
2.08
4.35
9.07
2.10
3.05

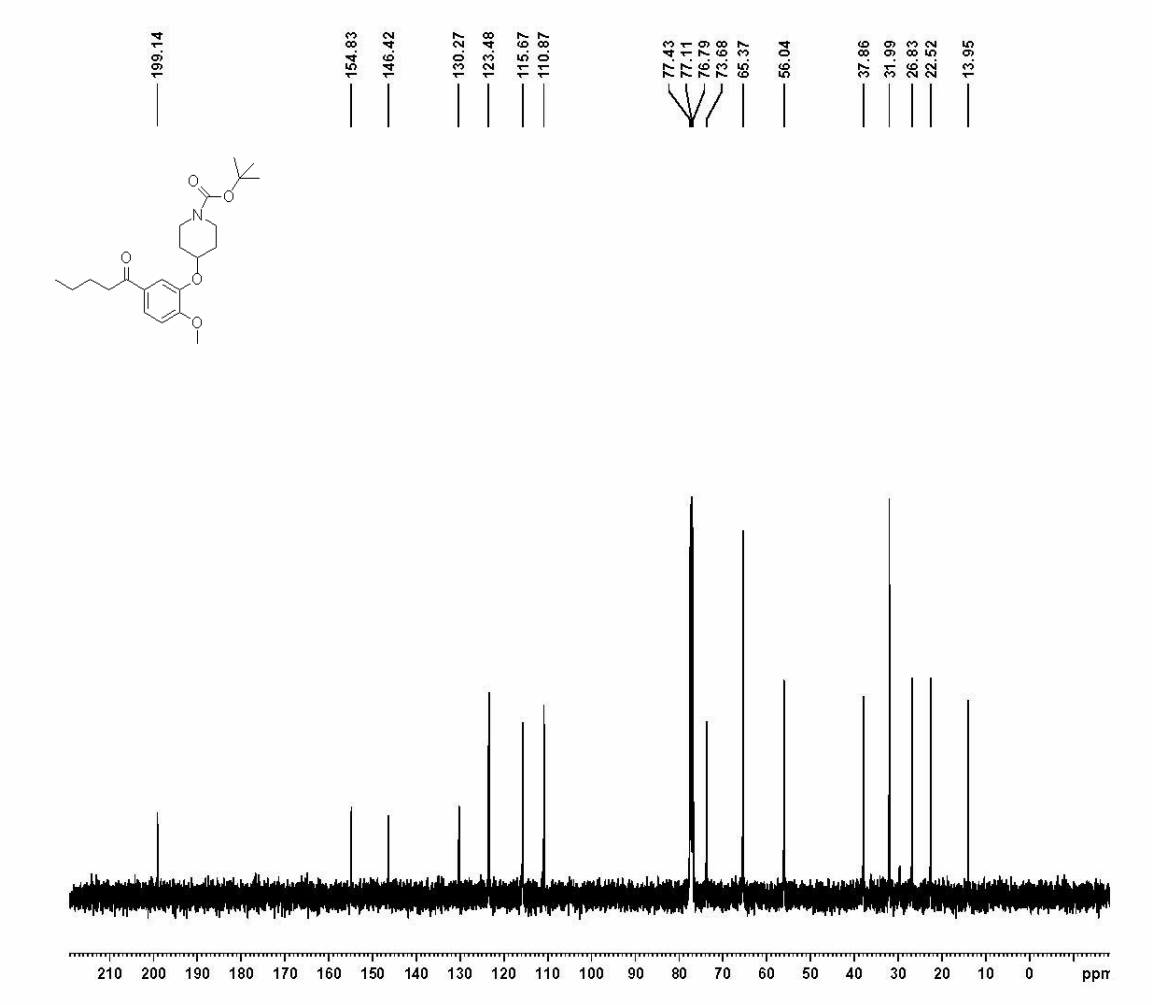
199.14
154.83
146.42
130.27
123.48
115.67
110.87
77.43
77.11
76.79
73.68
65.37
56.04
37.86
31.99
26.83
22.52
13.95
O
N
O
O
O
O
210 200 190 180 170 160 150 140 130 120 110 100 90 80 70 60 50 40 30 20 10 0 ppm

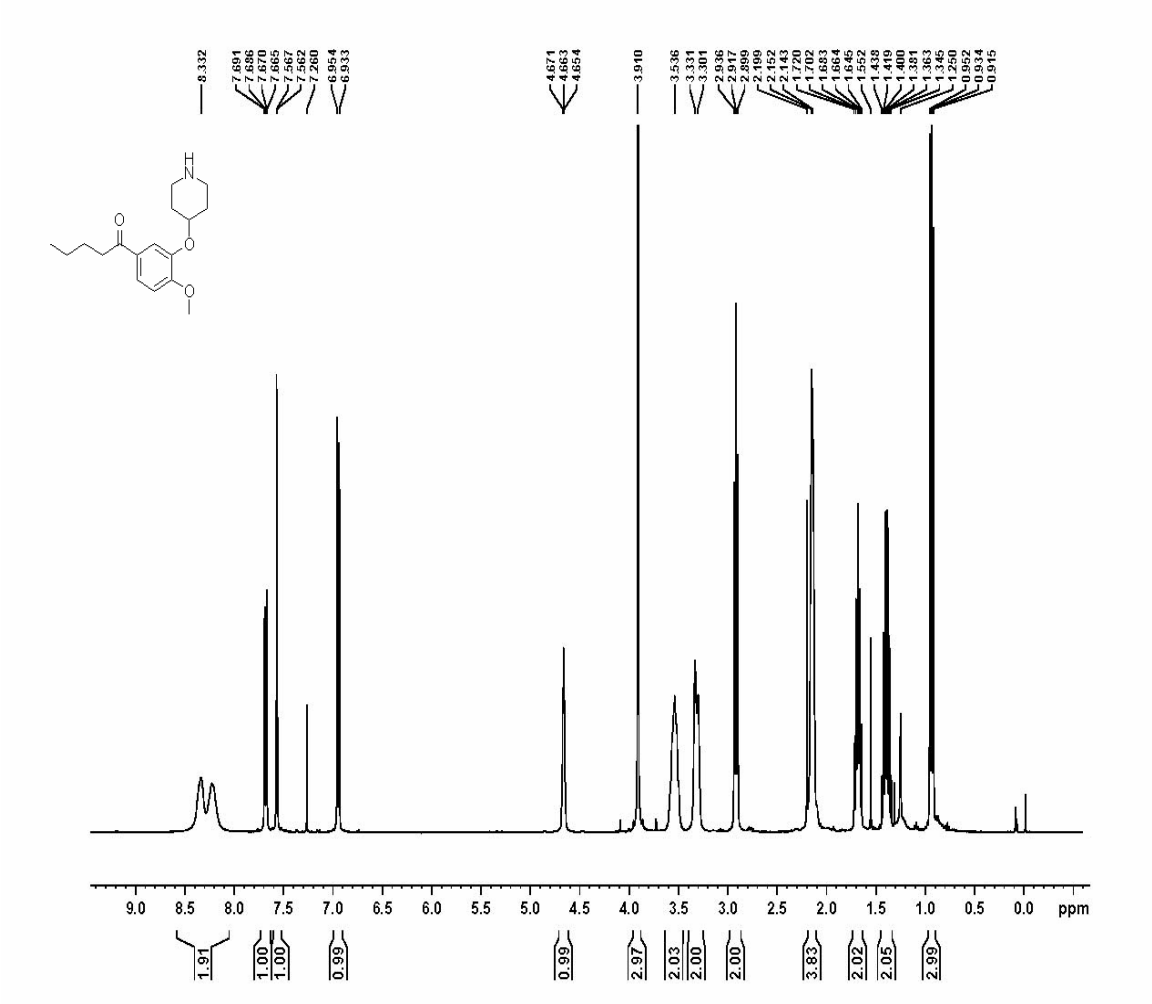
8.332
7.691
7.686
7.670
7.665
7.567
7.562
7.260
6.954
6.933
4.671
4.663
4.654
3.910
3.536
3.331
3.301
2.936
2.917
2.899
2.199
2.152
2.143
1.720
1.702
1.683
1.664
1.645
1.552
1.449
1.400
1.381
1.363
1.345
1.250
0.952
0.934
0.915
9.0 8.5 8.0 7.5 7.0 6.5 6.0 5.5 5.0 4.5 4.0 3.5 3.0 2.5 2.0 1.5 1.0 0.5 0.0 ppm
1.91
1.00
1.00
0.99
0.99
2.97
2.03
2.00
2.00
3.83
2.02
2.05
2.99

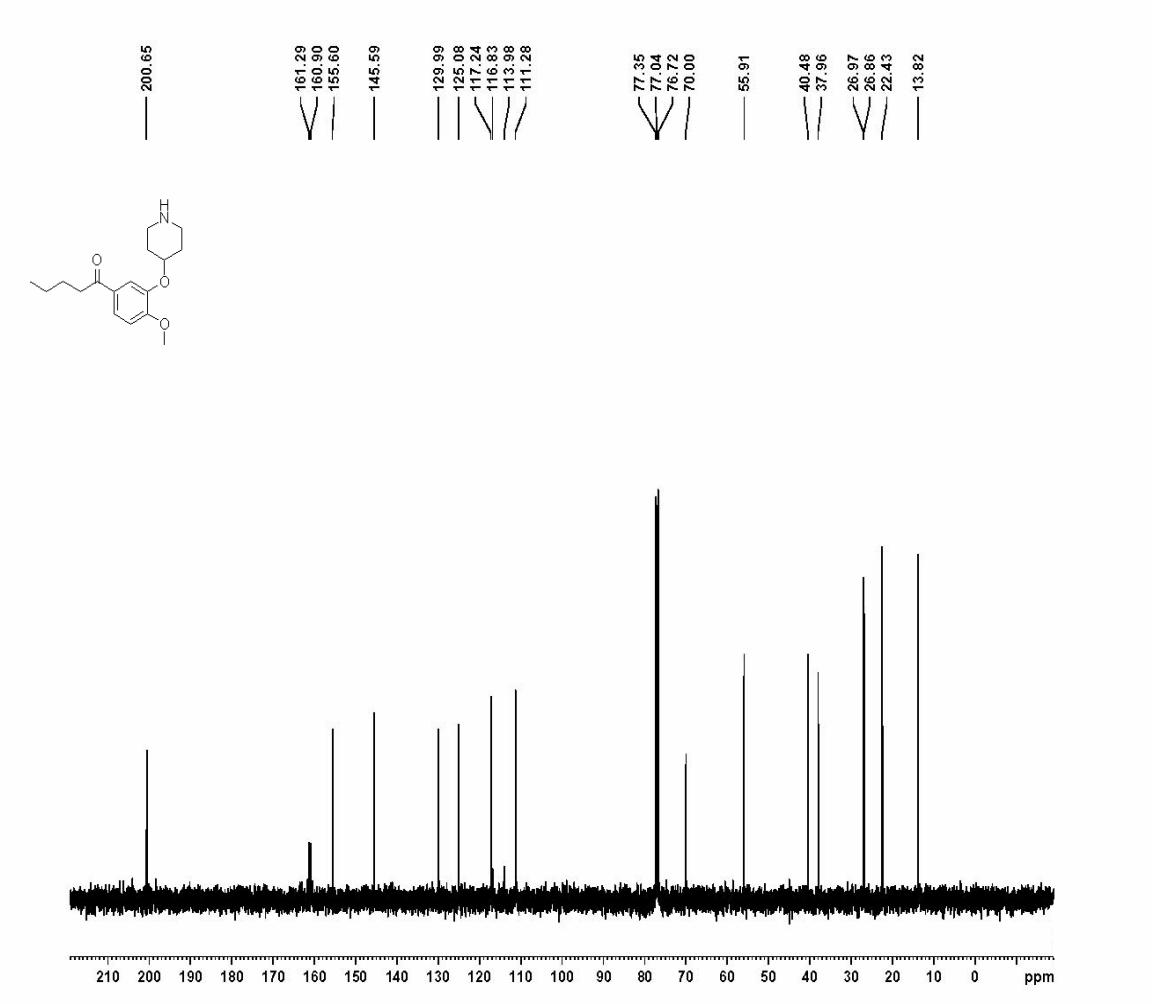
200.65
161.29
160.90
155.60
145.59
129.99
125.08
117.24
116.83
113.98
111.28
77.35
77.04
76.72
70.00
55.91
40.48
37.96
26.97
26.86
22.43
13.82
H
N
O
O
O
210 200 190 180 170 160 150 140 130 120 110 100 90 80 70 60 50 40 30 20 10 0 ppm

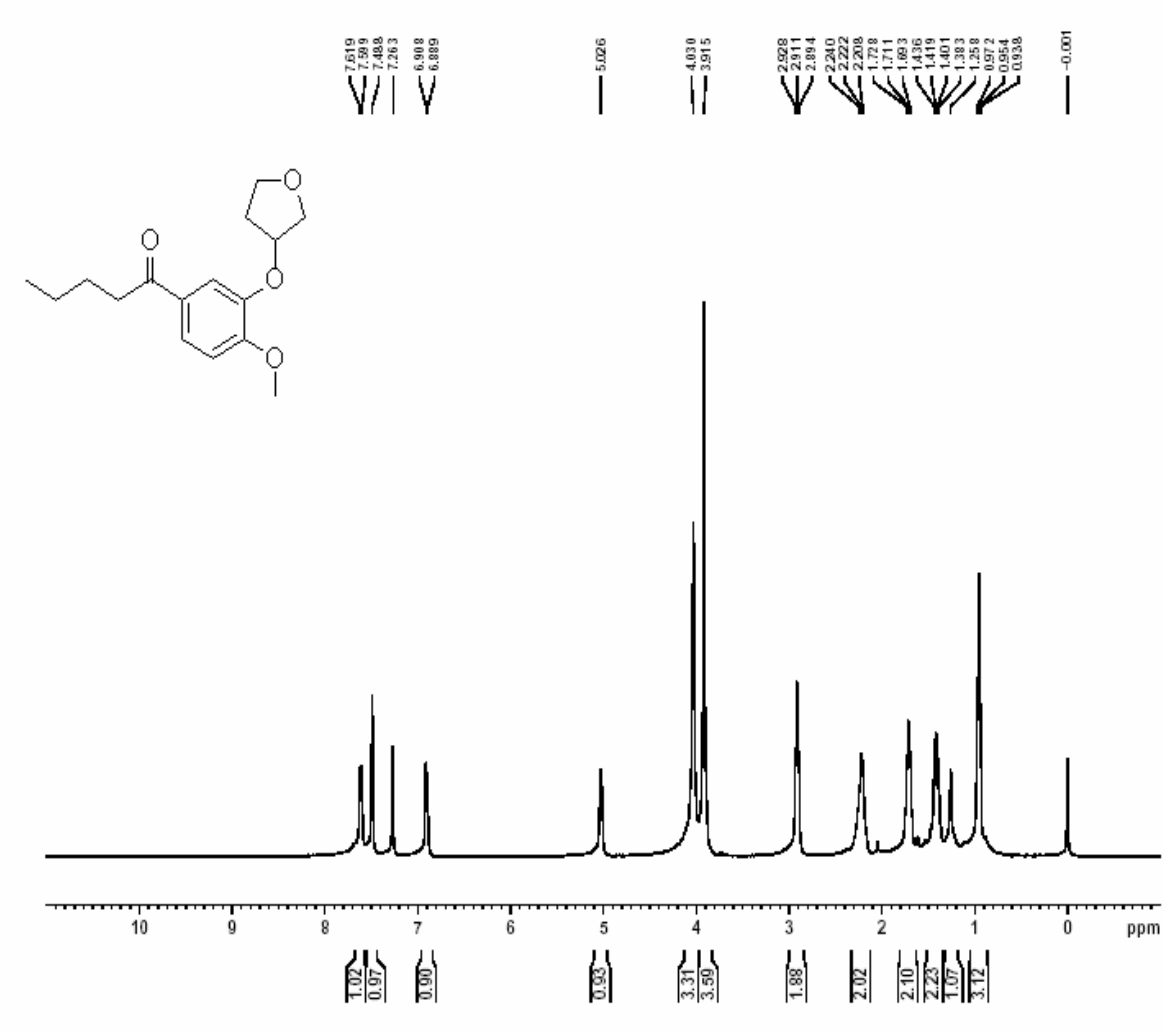
7.619
7.599
7.488
7.263
6.908
6.889
5.026
4.030
3.915
2.928
2.911
2.894
2.240
2.222
2.208
1.728
1.711
1.693
1.416
1.419
1.401
1.383
1.258
0.972
0.954
0.938
-0.001
10
9
8
7
6
5
4
3
2
1
0
ppm
1.02
0.97
0.90
0.93
3.31
3.59
1.88
2.02
2.10
2.23
1.07
3.12

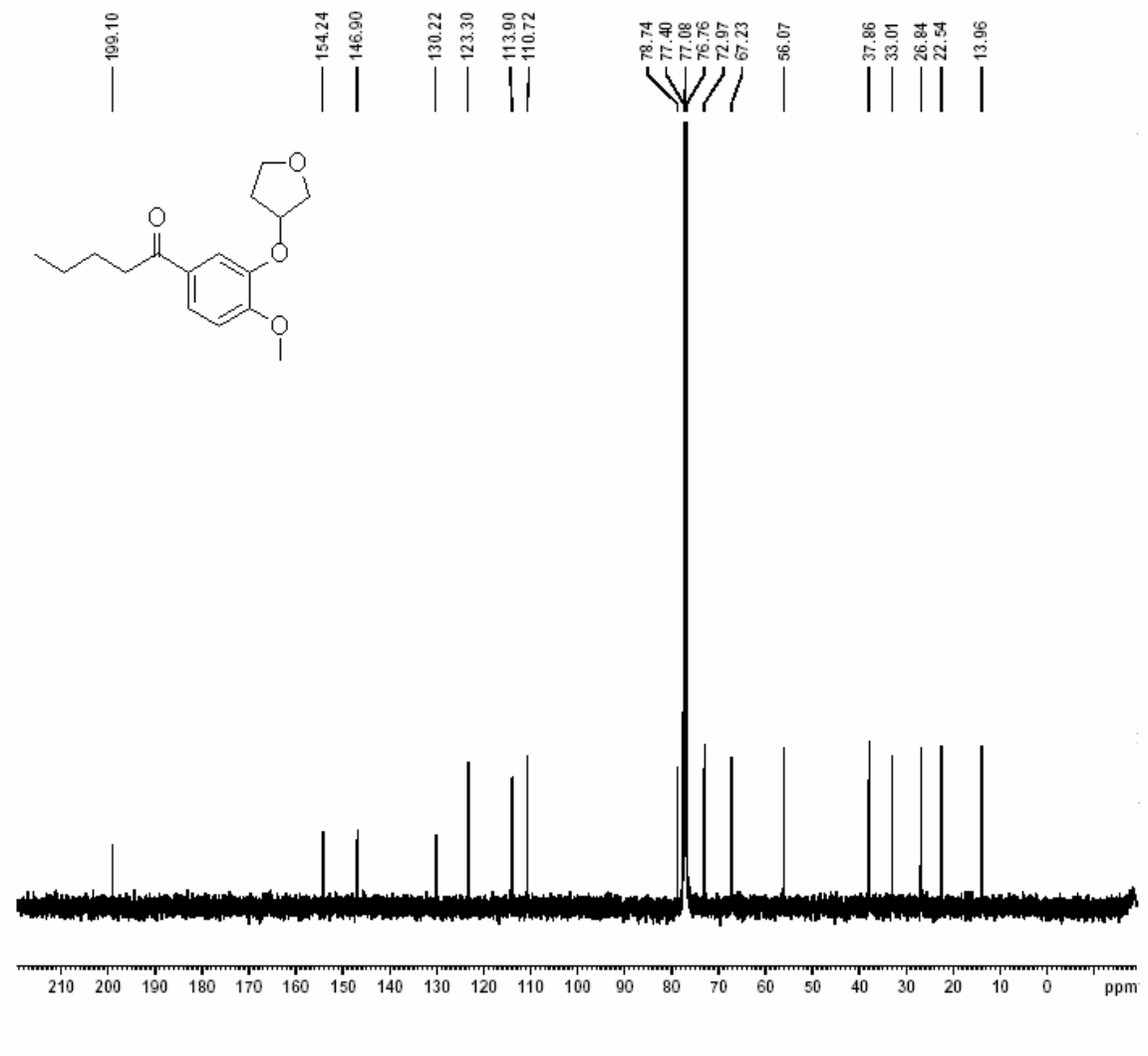
199.10
154.24
146.90
130.22
123.30
113.90
110.72
78.74
77.40
77.08
76.76
72.97
67.23
56.07
37.86
33.01
26.84
22.54
13.96
210 200 190 180 170 160 150 140 130 120 110 100 90 80 70 60 50 40 30 20 10 0 ppm

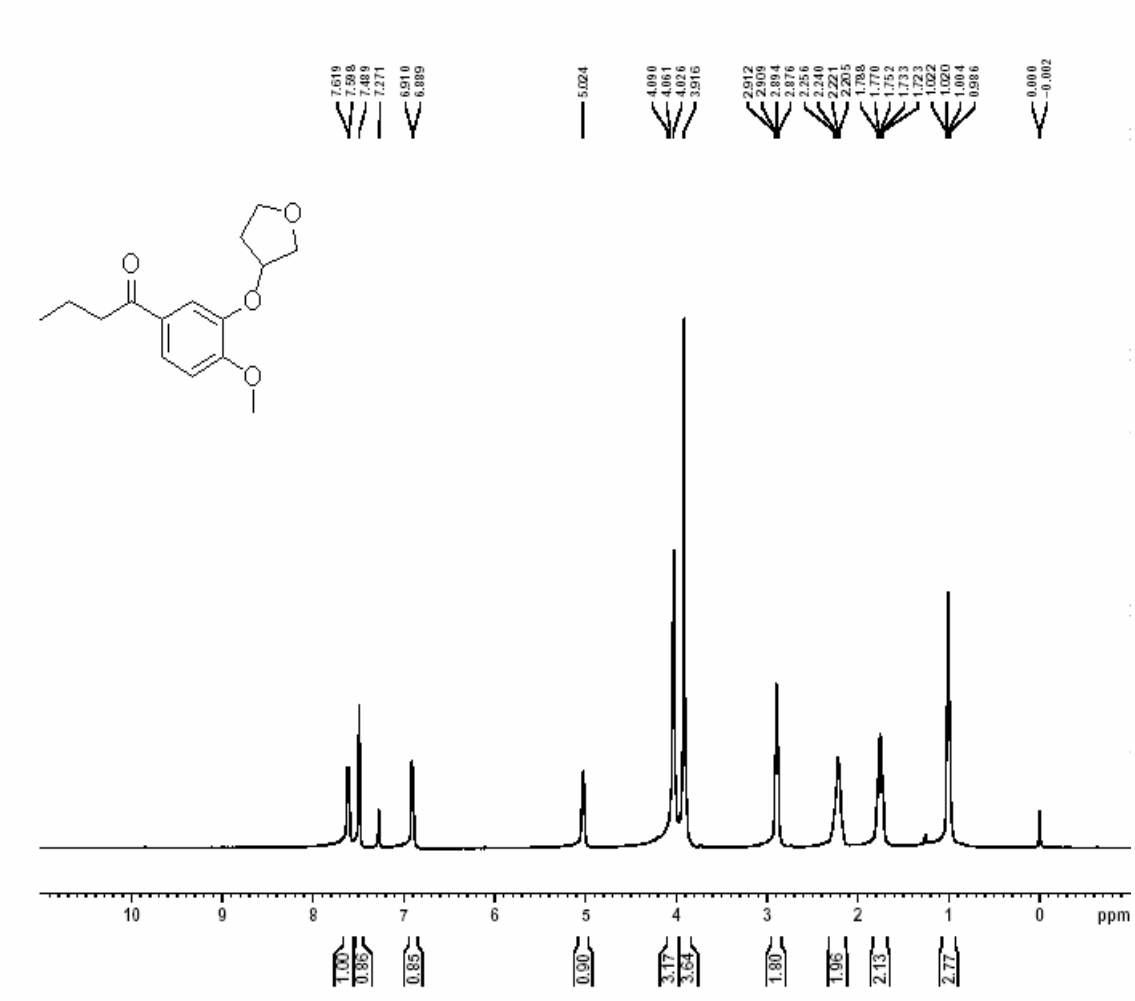
7.619
7.598
7.489
7.271
6.910
6.889
5.024
4.090
4.061
4.026
3.916
2.912
2.909
2.894
2.876
2.256
2.240
2.221
2.205
1.788
1.770
1.752
1.733
1.723
1.022
1.020
1.004
0.986
0.000
-0.002
O
O
O
10
9
8
7
6
5
4
3
2
1
0
ppm
1.00
0.86
0.85
0.90
3.17
3.64
1.80
1.06
2.13
2.77

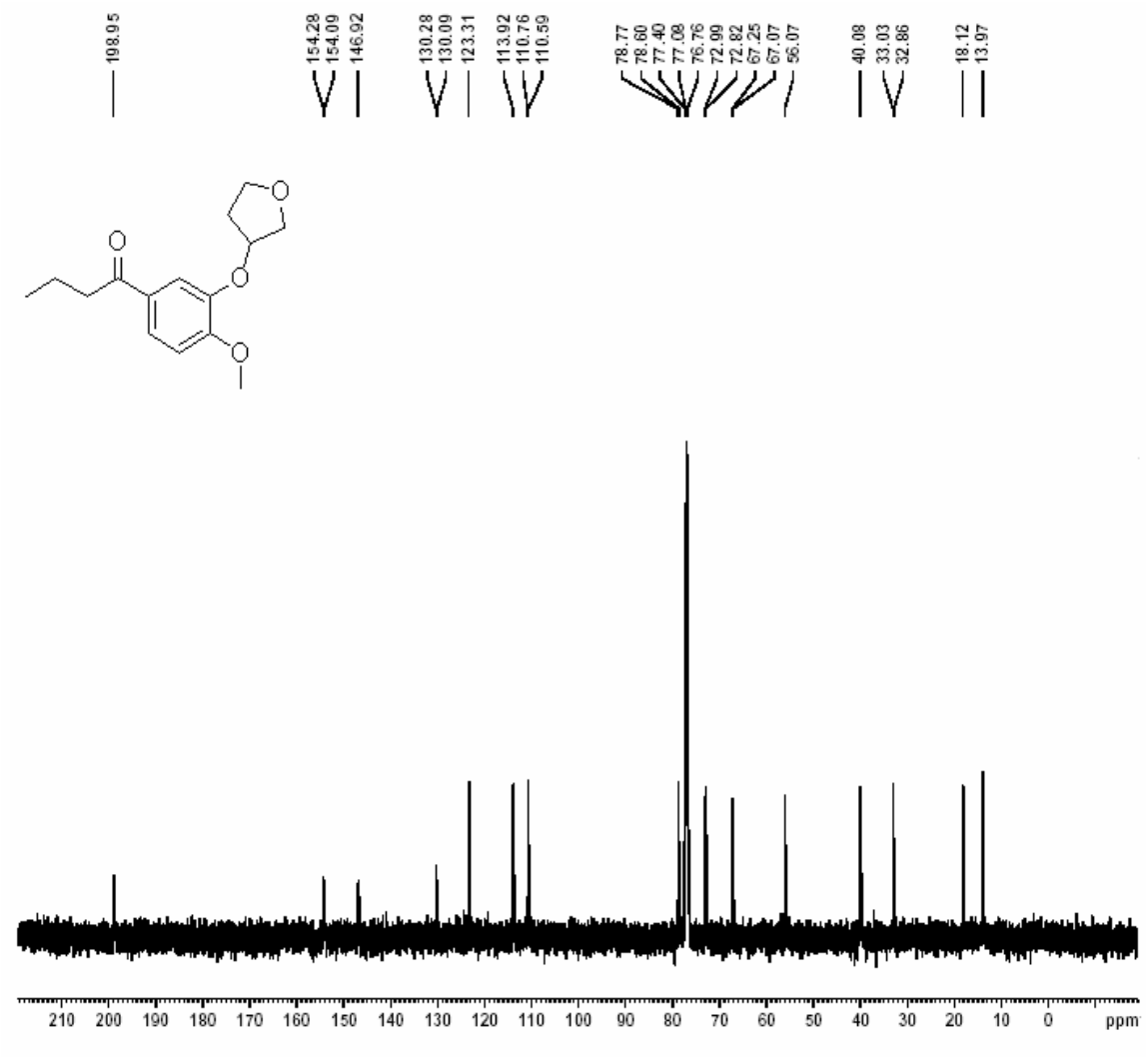
198.95
154.28
154.09
146.92
130.28
130.09
123.31
113.92
110.76
110.59
78.77
78.60
77.40
77.08
76.76
72.99
72.82
67.25
67.07
56.07
40.08
33.03
32.86
18.12
13.97
210 200 190 180 170 160 150 140 130 120 110 100 90 80 70 60 50 40 30 20 10 0 ppm

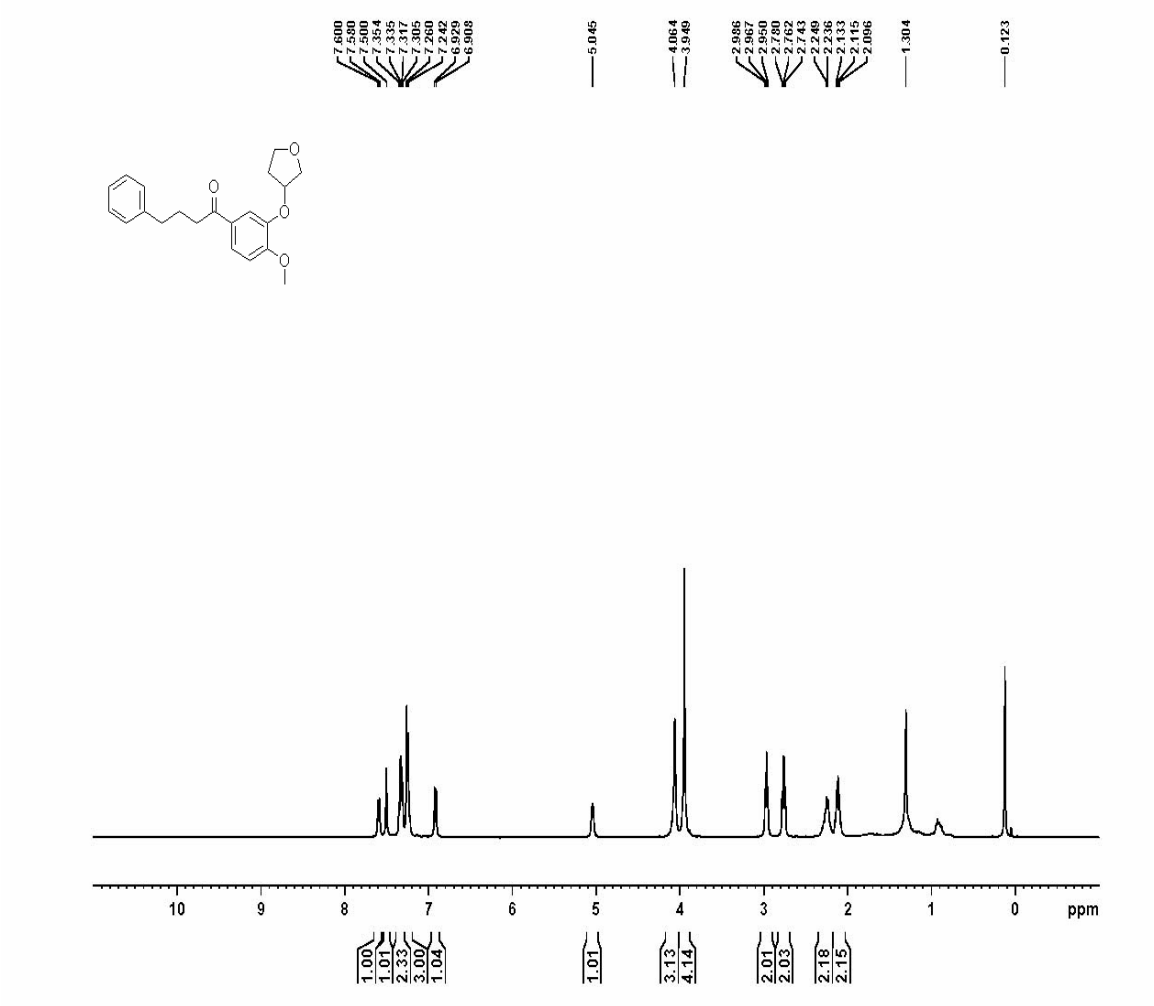
7.600
7.580
7.500
7.354
7.335
7.317
7.305
7.260
7.242
6.929
6.909
5.045
4.064
3.949
2.986
2.967
2.949
2.780
2.762
2.743
2.249
2.236
2.133
2.115
2.096
1.304
0.123
10
9
8
7
6
5
4
3
2
1
0
ppm
1.00
1.01
2.33
3.00
1.04
1.01
3.13
4.14
2.01
2.03
2.18
2.15

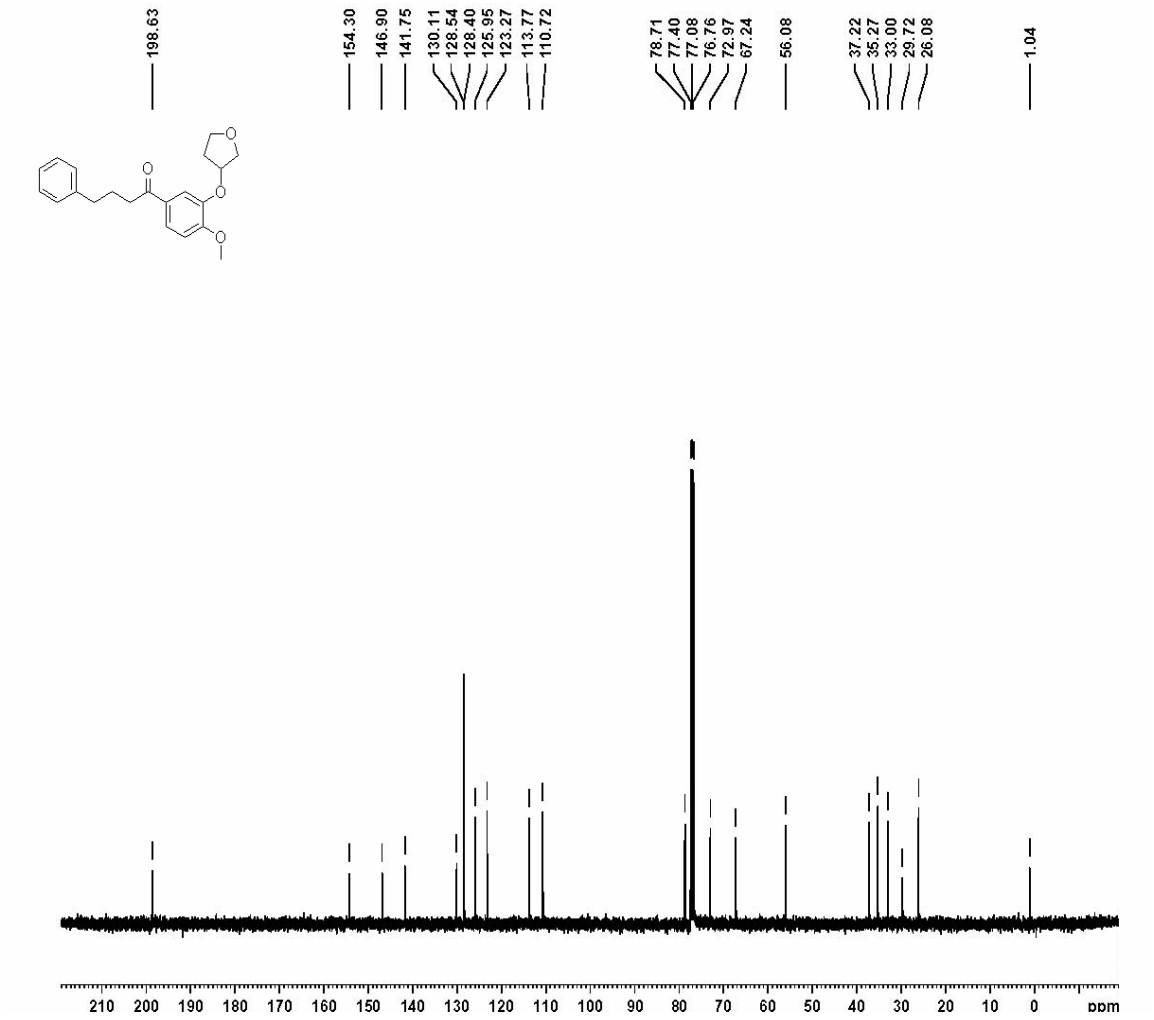
198.63
154.30
146.90
141.75
130.11
128.54
128.40
125.95
123.27
113.77
110.72
78.71
77.40
77.08
76.76
72.97
67.24
56.08
37.22
35.27
33.00
29.72
26.08
1.04
O
O
O
210 200 190 180 170 160 150 140 130 120 110 100 90 80 70 60 50 40 30 20 10 0 ppm

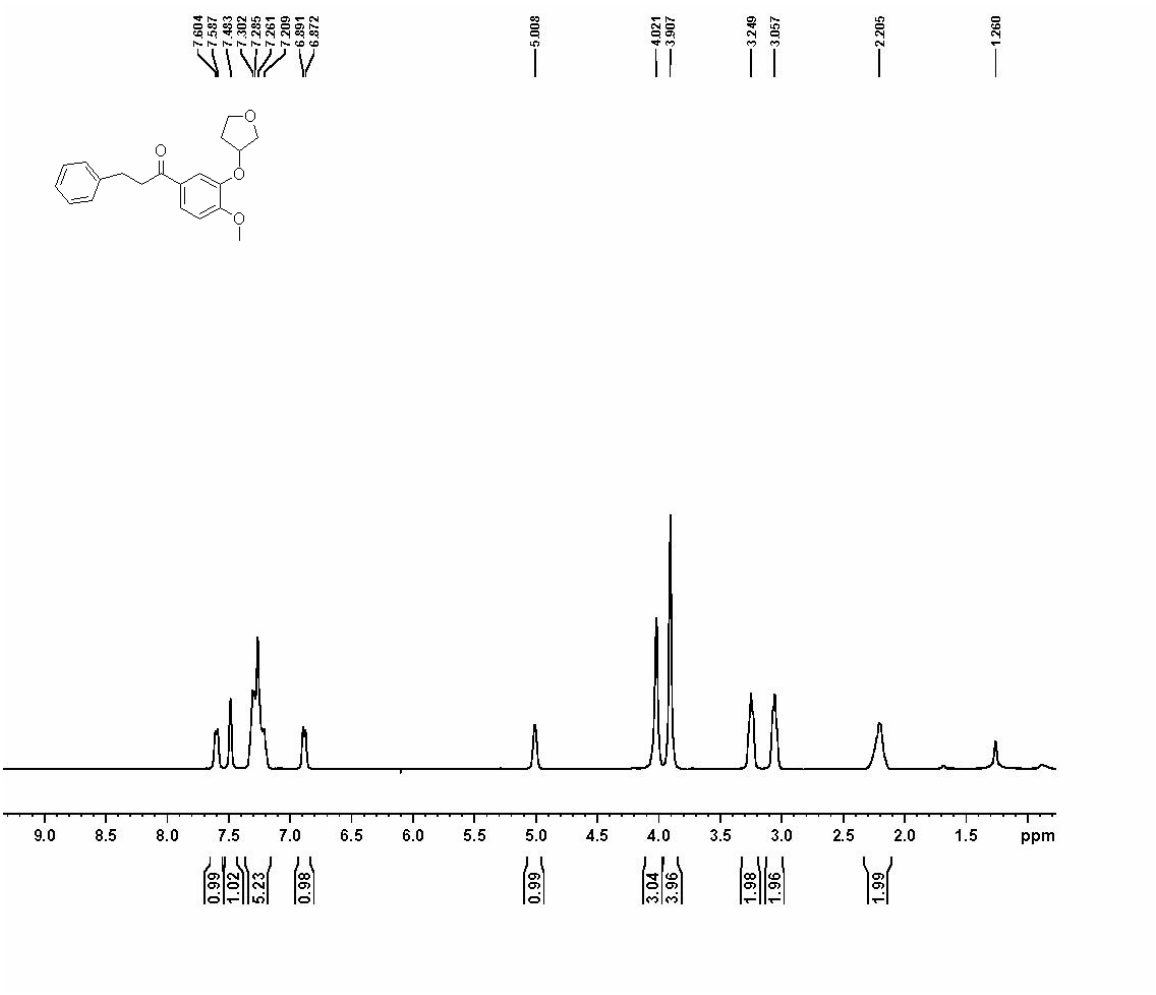
7.604
7.587
7.483
7.302
7.285
7.261
7.209
6.891
6.872
5.008
4.021
3.907
3.249
3.057
2.205
1.260
9.0
8.5
8.0
7.5
7.0
6.5
6.0
5.5
5.0
4.5
4.0
3.5
3.0
2.5
2.0
1.5
ppm
0.99
1.02
5.23
0.98
0.99
3.04
3.96
1.98
1.96
1.99

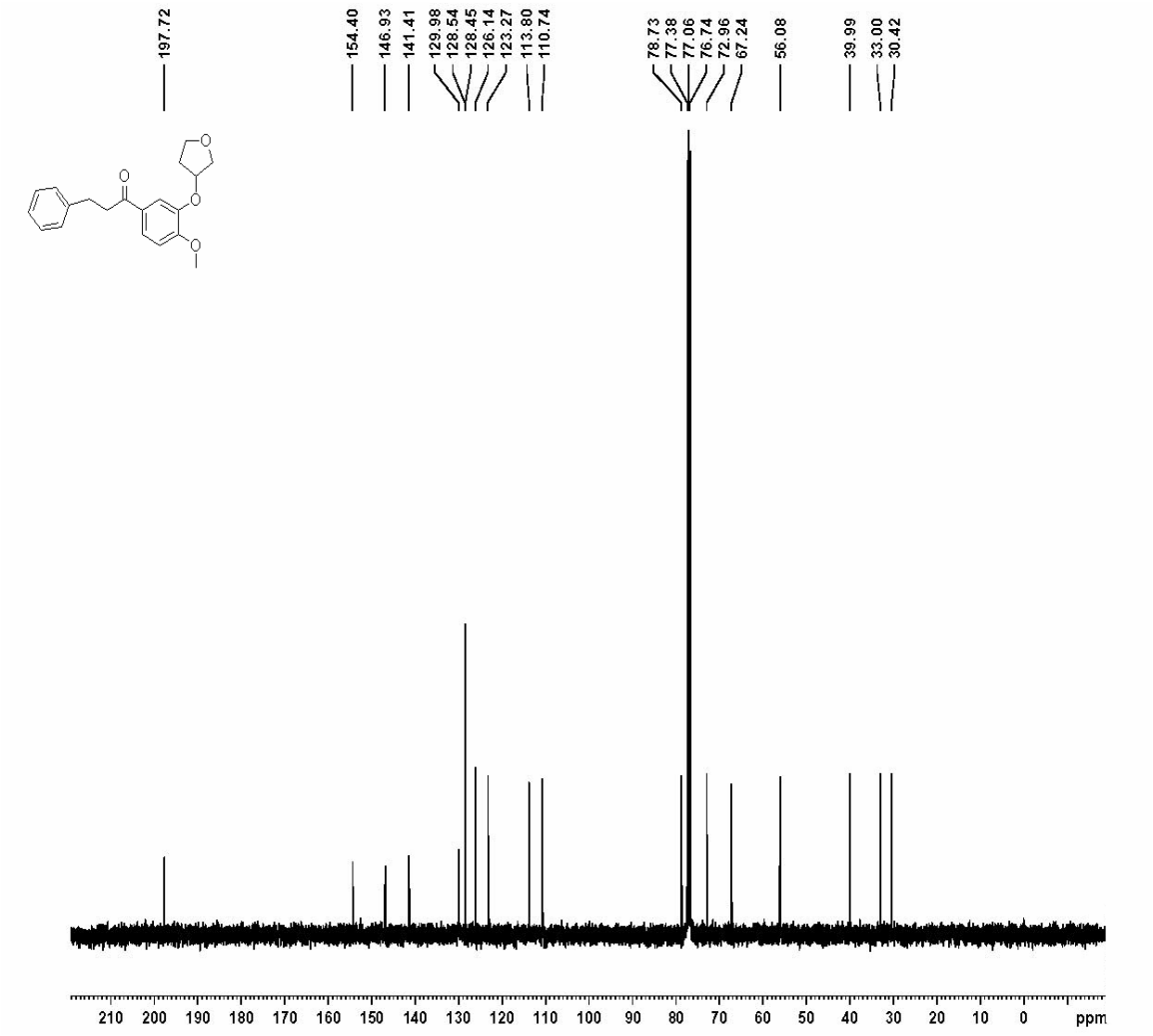
197.72
154.40
146.93
141.41
129.98
128.54
128.45
126.14
123.27
113.80
110.74
78.73
77.38
77.06
76.74
72.96
67.24
56.08
39.99
33.00
30.42
O
O
O
O
210 200 190 180 170 160 150 140 130 120 110 100 90 80 70 60 50 40 30 20 10 0 ppm

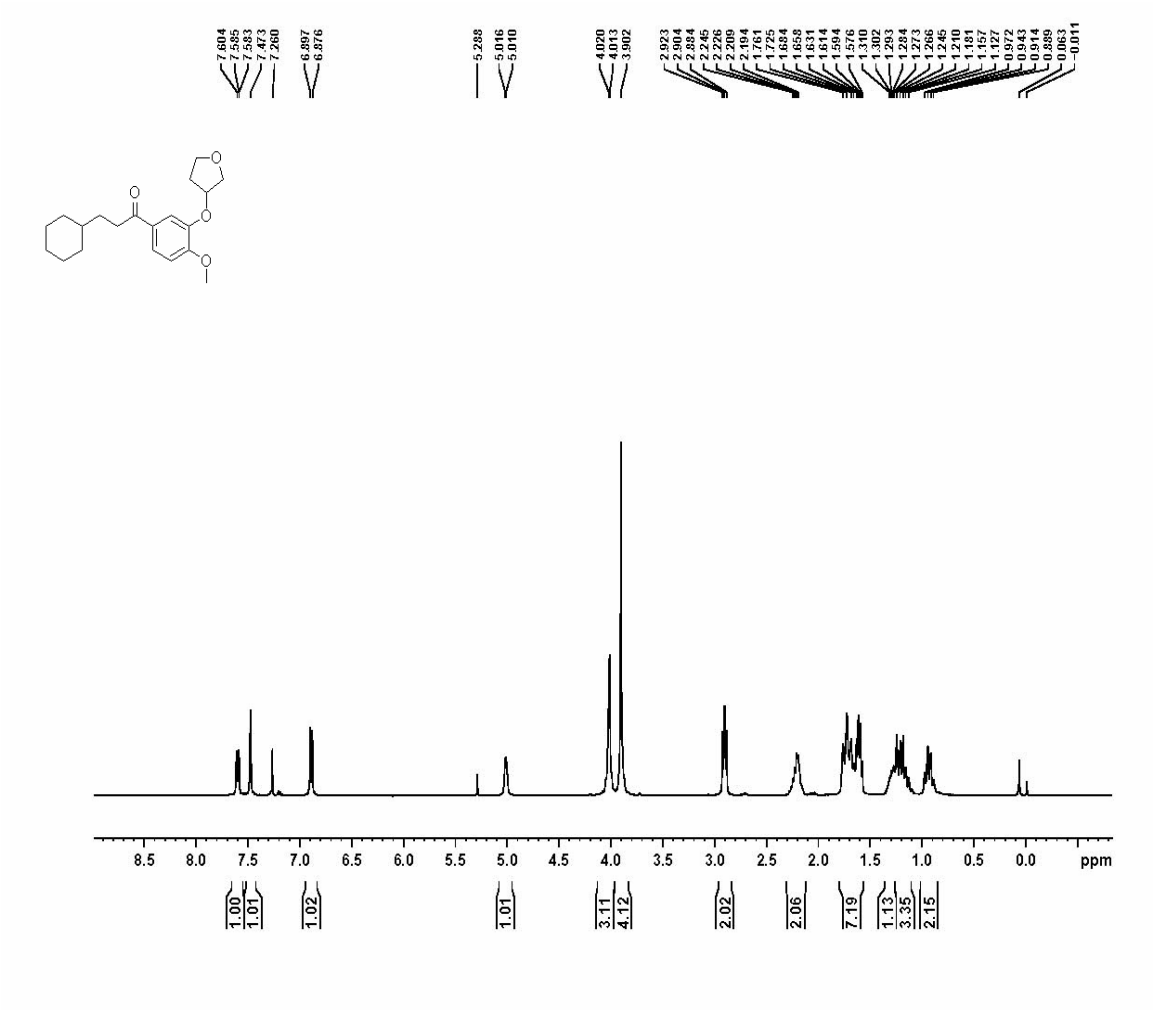
7.604
7.585
7.583
7.473
7.260
6.897
6.876
5.288
5.016
5.010
4.020
4.013
3.902
2.923
2.904
2.884
2.245
2.226
2.209
2.194
1.761
1.725
1.684
1.658
1.631
1.614
1.594
1.576
1.310
1.302
1.293
1.284
1.273
1.266
1.245
1.210
1.181
1.157
1.127
0.972
0.943
0.914
0.889
0.063
-0.011
O
O
O
8.5
8.0
7.5
7.0
6.5
6.0
5.5
5.0
4.5
4.0
3.5
3.0
2.5
2.0
1.5
1.0
0.5
0.0
ppm
1.00
1.01
1.02
1.01
3.11
4.12
2.02
2.06
7.19
1.13
3.35
2.15

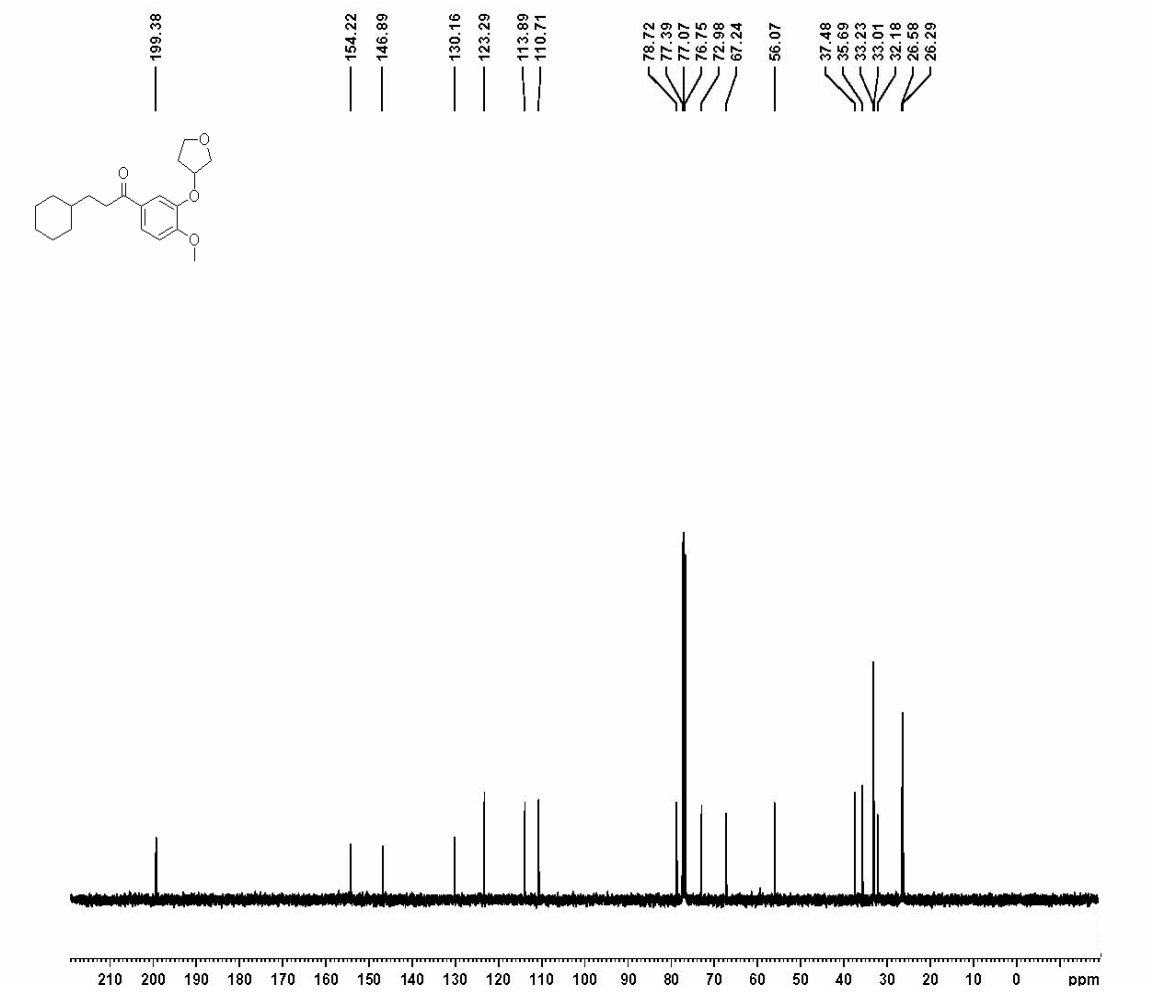
199.38
154.22
146.89
130.16
123.29
113.89
110.71
78.72
77.39
77.07
76.75
72.98
67.24
56.07
37.48
35.69
33.23
33.01
32.18
26.58
26.29
O
O
O
O
210 200 190 180 170 160 150 140 130 120 110 100 90 80 70 60 50 40 30 20 10 0 ppm

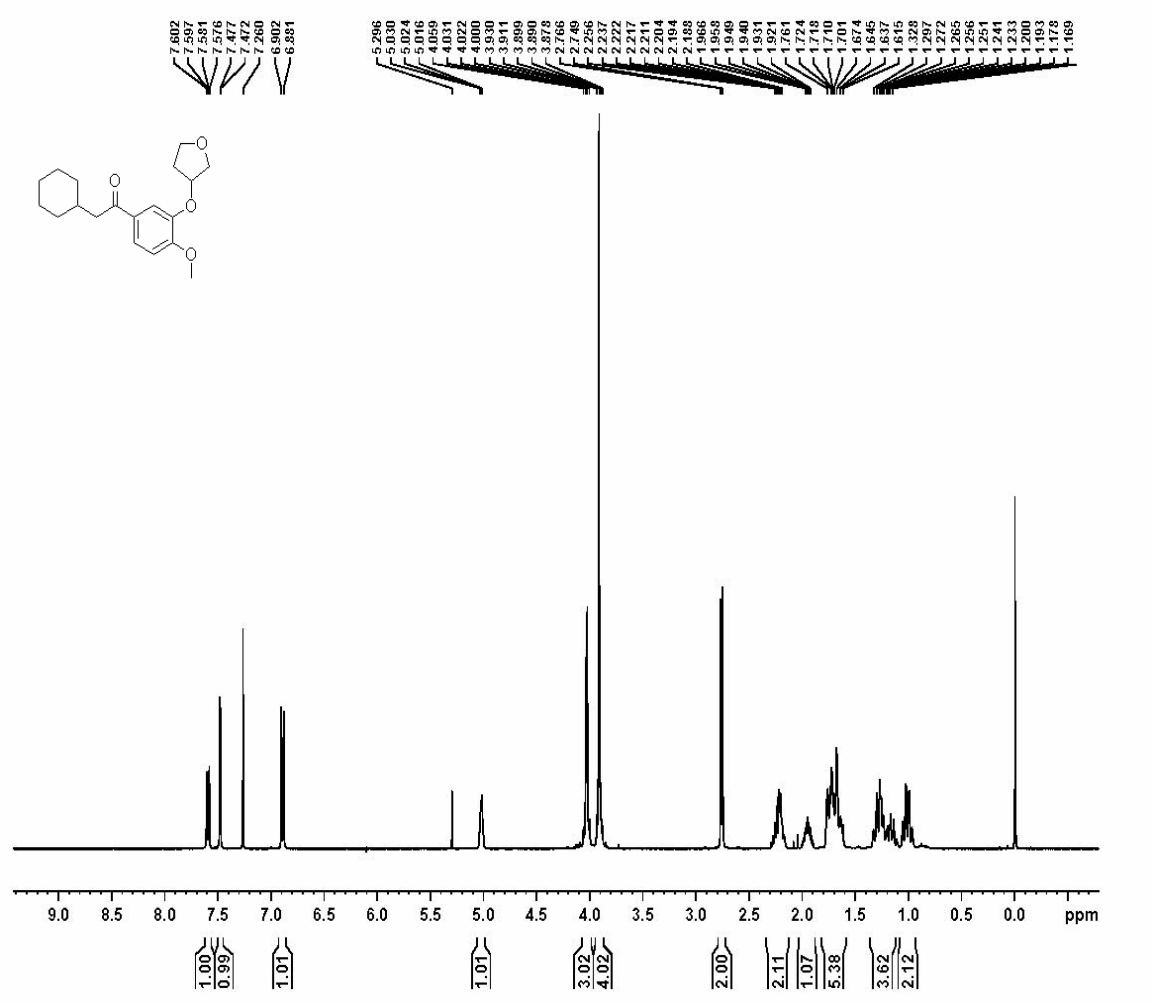
7.602
7.597
7.591
7.576
7.477
7.472
7.260
6.902
6.881
5.296
5.030
5.024
5.016
4.059
4.031
4.022
4.000
3.930
3.911
3.899
3.890
3.873
2.766
2.749
2.256
2.237
2.222
2.217
2.211
2.204
2.194
2.188
1.966
1.958
1.949
1.940
1.931
1.921
1.761
1.724
1.718
1.710
1.701
1.674
1.645
1.637
1.615
1.328
1.297
1.272
1.265
1.256
1.251
1.241
1.233
1.200
1.193
1.178
1.169
O
O
O
9.0
8.5
8.0
7.5
7.0
6.5
6.0
5.5
5.0
4.5
4.0
3.5
3.0
2.5
2.0
1.5
1.0
0.5
0.0
ppm
1.00
0.99
1.01
1.01
3.02
4.02
2.00
2.11
1.07
5.38
3.62
2.12

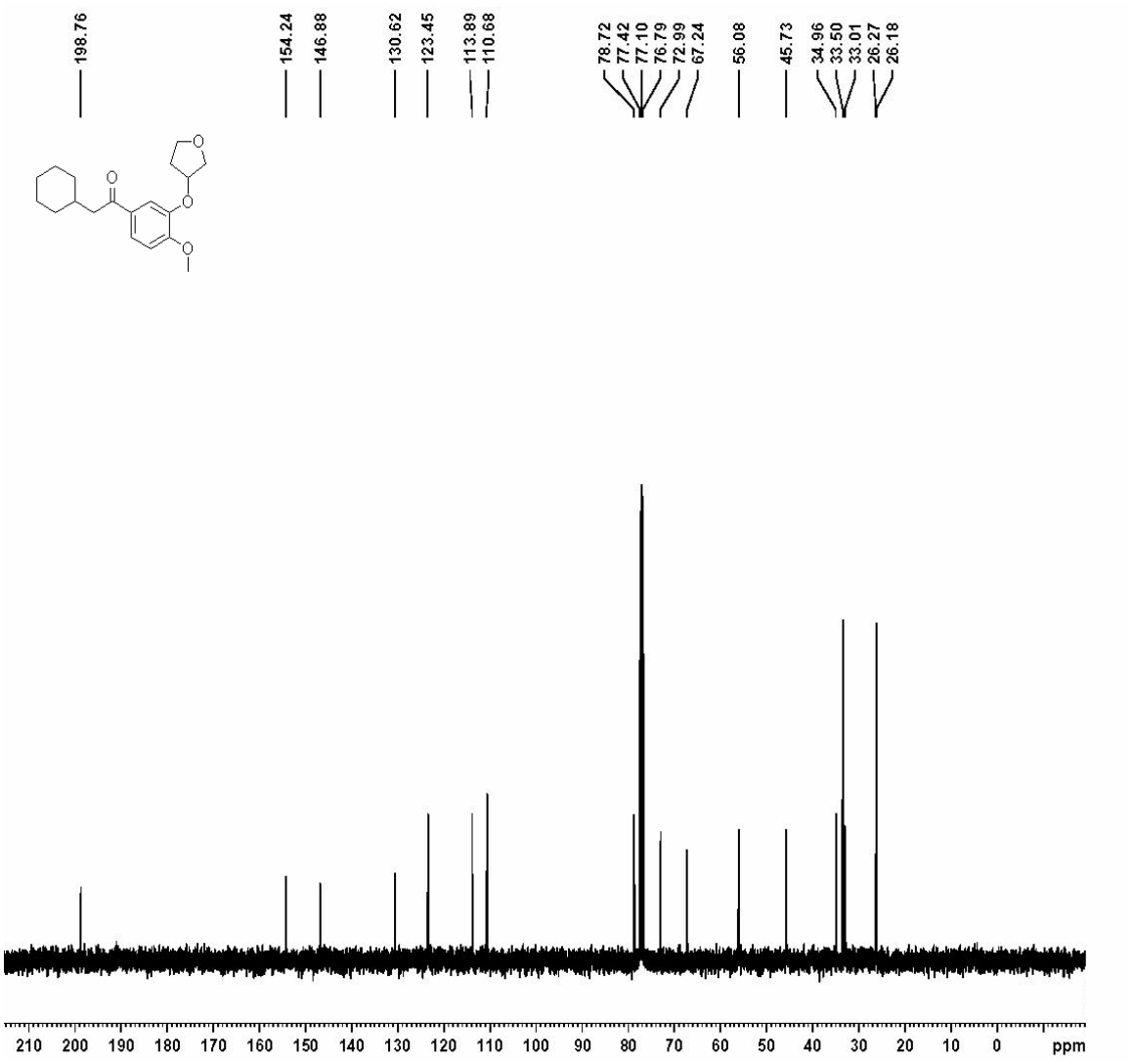
198.76
154.24
146.88
130.62
123.45
113.89
110.68
78.72
77.42
77.10
76.79
72.99
67.24
56.08
45.73
34.96
33.50
33.01
26.27
26.18
O
O
O
210 200 190 180 170 160 150 140 130 120 110 100 90 80 70 60 50 40 30 20 10 0 ppm

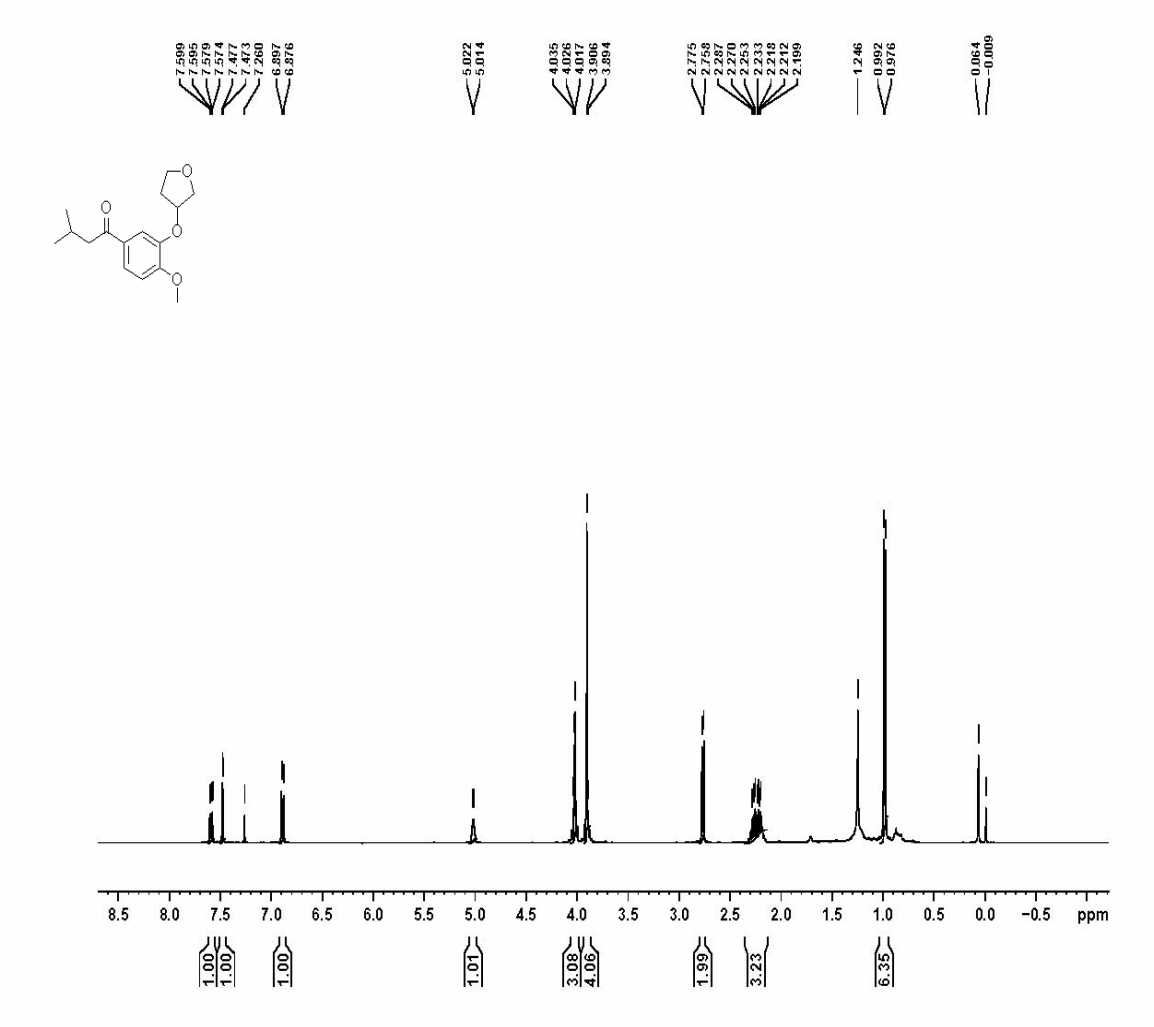
7.599
7.595
7.579
7.574
7.477
7.473
7.260
6.897
6.876
5.022
5.014
4.035
4.026
4.017
3.906
3.894
2.775
2.758
2.287
2.270
2.253
2.233
2.218
2.212
2.199
1.246
0.992
0.976
0.064
-0.009
8.5
8.0
7.5
7.0
6.5
6.0
5.5
5.0
4.5
4.0
3.5
3.0
2.5
2.0
1.5
1.0
0.5
0.0
-0.5
ppm
1.00
1.00
1.00
1.01
3.08
4.06
1.99
3.23
6.35

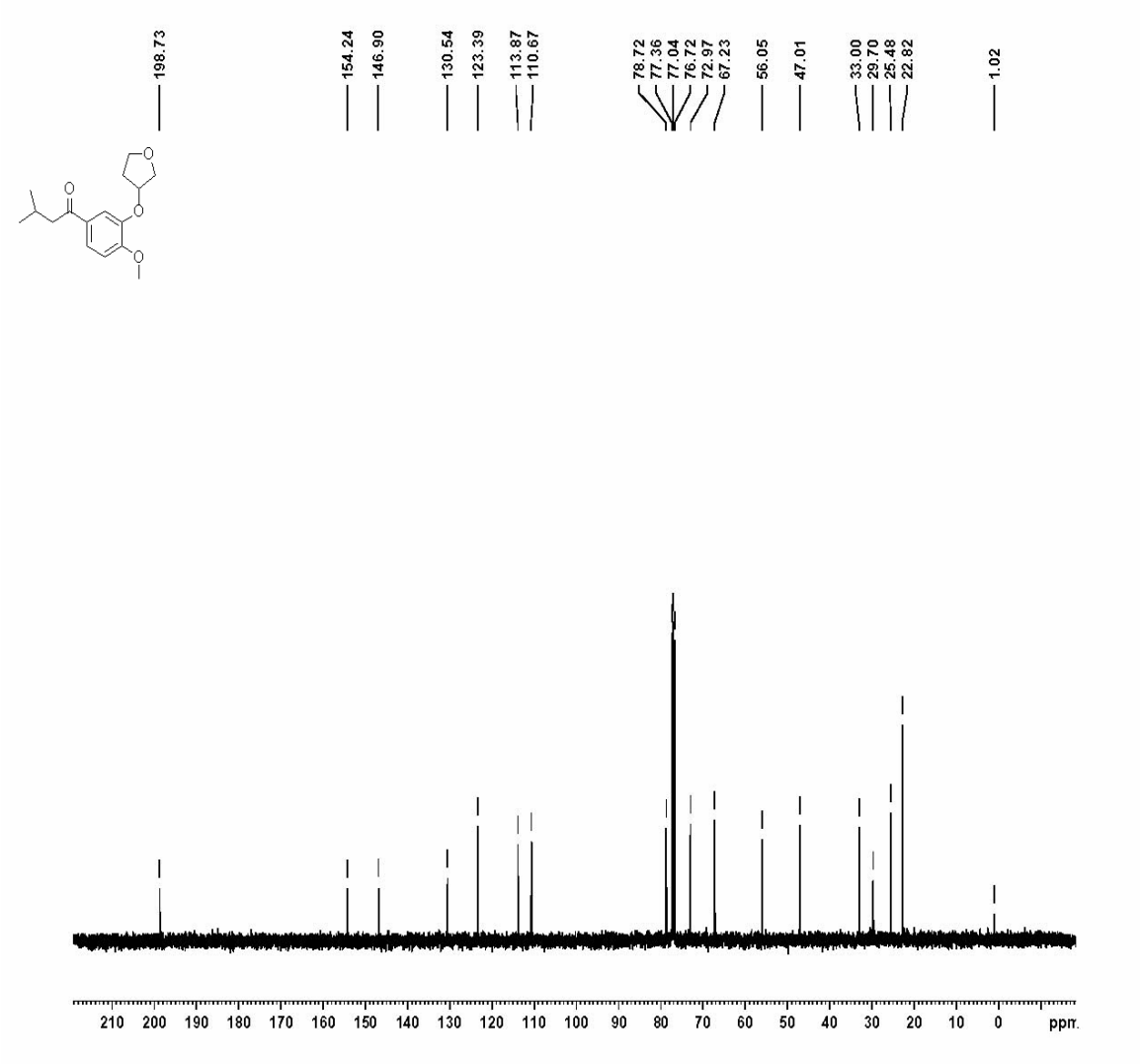
198.73
154.24
146.90
130.54
123.39
113.87
110.67
78.72
77.36
77.04
76.72
72.97
67.23
56.05
47.01
33.00
29.70
25.48
22.82
1.02
O
O
O
210 200 190 180 170 160 150 140 130 120 110 100 90 80 70 60 50 40 30 20 10 0 ppm

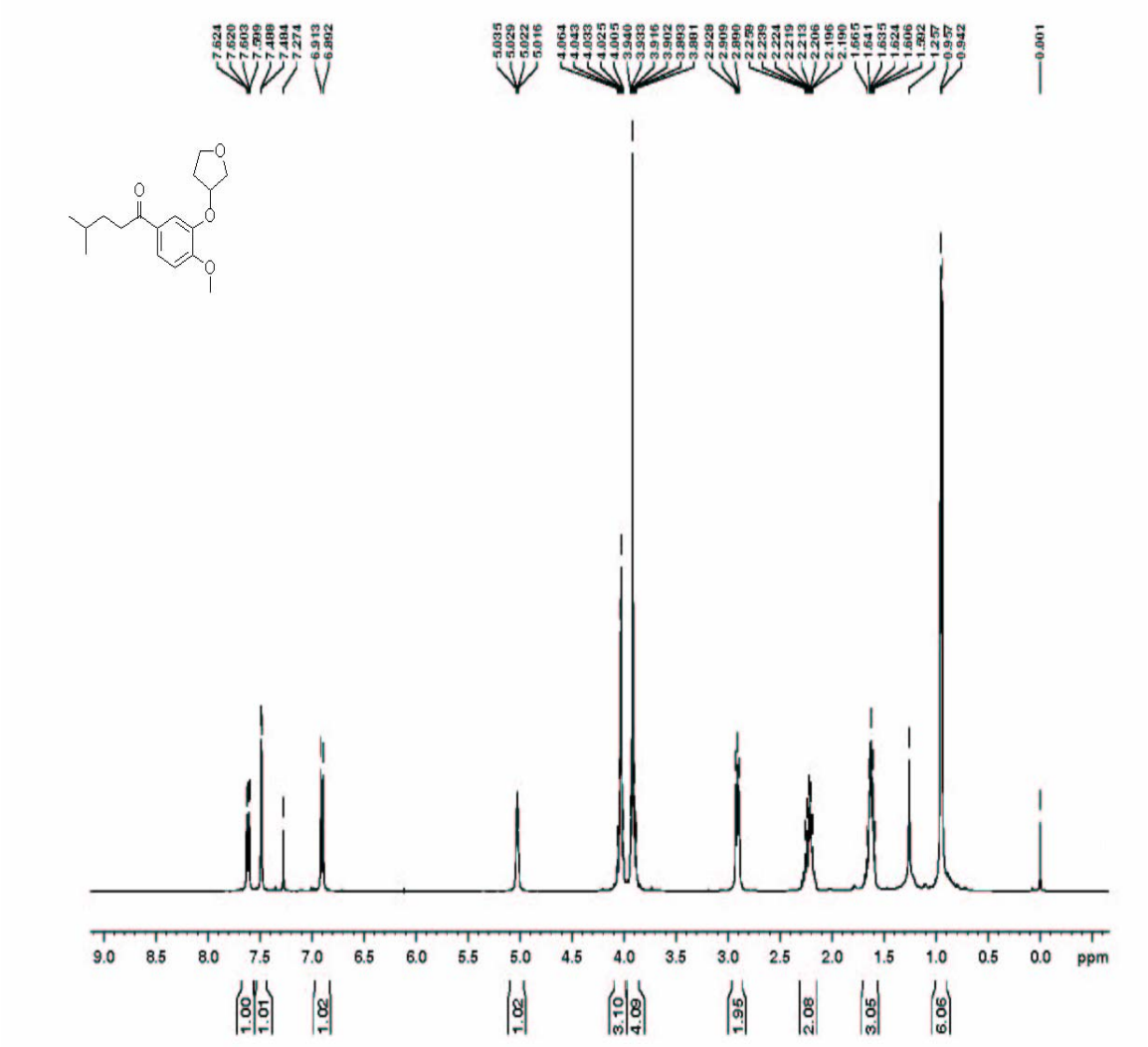
7.624
7.620
7.503
7.499
7.488
7.484
7.274
6.913
6.892
5.035
5.029
5.022
5.016
4.064
4.043
4.033
4.025
4.005
3.940
3.933
3.916
3.902
3.893
3.881
2.928
2.909
2.890
2.239
2.224
2.219
2.213
2.206
2.195
2.189
1.665
1.641
1.635
1.624
1.606
1.592
1.257
0.957
0.942
0.001
9.0 8.5 8.0 7.5 7.0 6.5 6.0 5.5 5.0 4.5 4.0 3.5 3.0 2.5 2.0 1.5 1.0 0.5 0.0 ppm
1.00
1.01
1.02
1.02
3.10
4.09
1.95
2.08
3.05
6.06

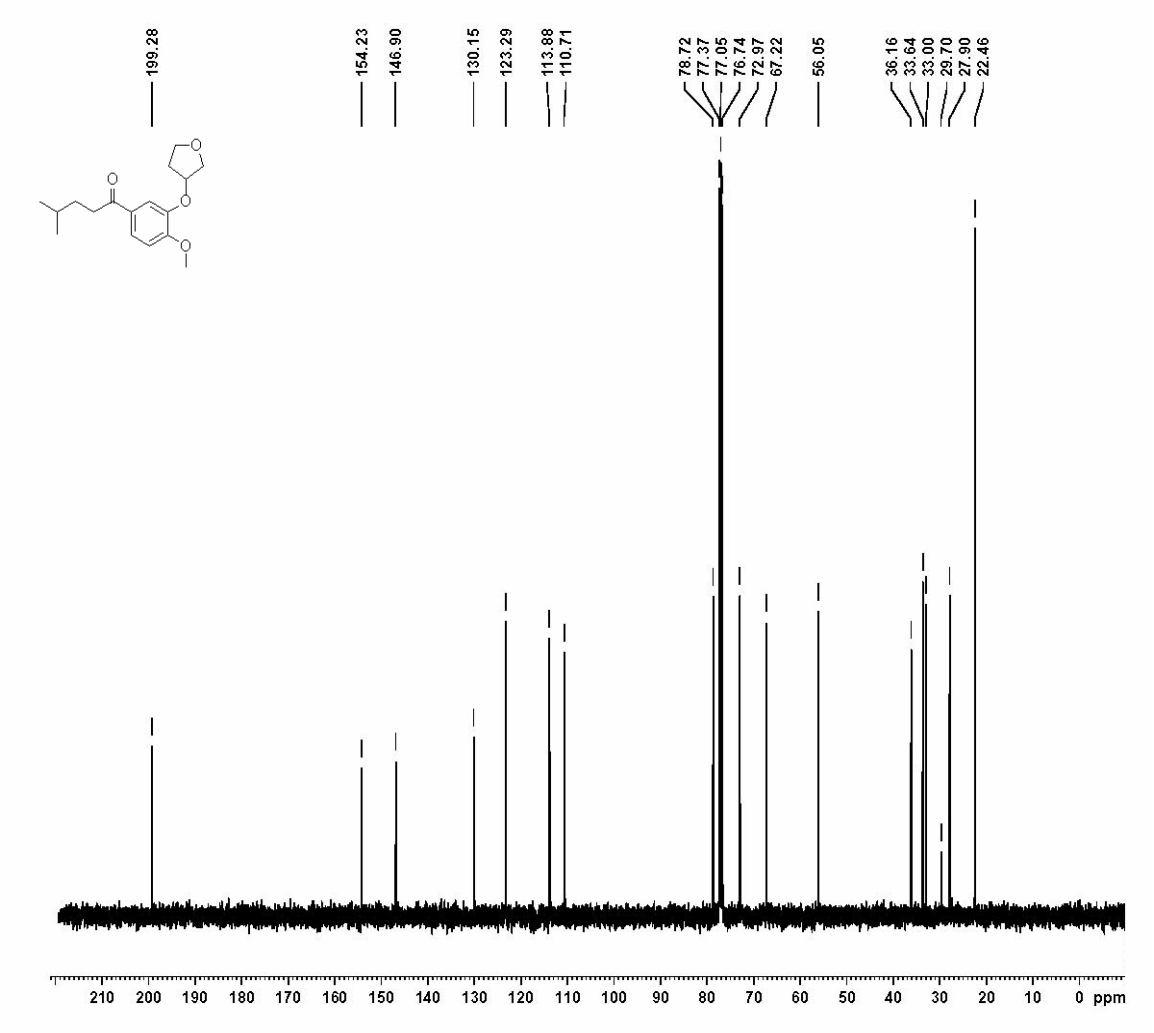
199.28
154.23
146.90
130.15
123.29
113.88
110.71
78.72
77.37
77.05
76.74
72.97
67.22
56.05
36.16
33.64
33.00
29.70
27.90
22.46
210 200 190 180 170 160 150 140 130 120 110 100 90 80 70 60 50 40 30 20 10 0 ppm

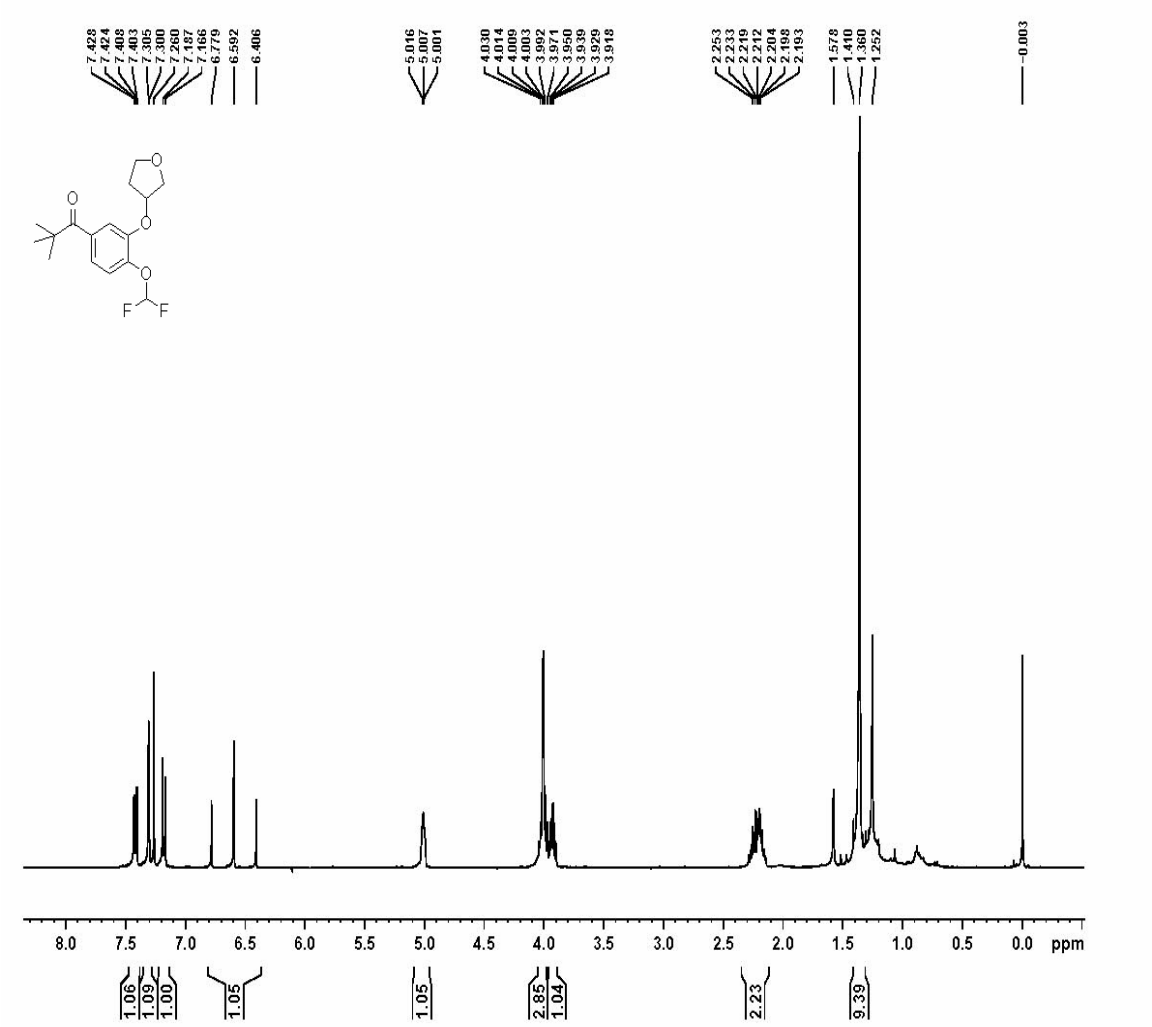
7.428
7.424
7.408
7.403
7.305
7.300
7.260
7.187
7.166
6.779
6.592
6.406
5.016
5.007
5.001
4.030
4.014
4.009
4.003
3.992
3.971
3.950
3.939
3.929
3.918
2.253
2.233
2.219
2.212
2.204
2.198
2.193
1.578
1.410
1.360
1.252
-0.003
O
O
O
F
F
8.0
7.5
7.0
6.5
6.0
5.5
5.0
4.5
4.0
3.5
3.0
2.5
2.0
1.5
1.0
0.5
0.0
ppm
1.06
1.09
1.00
1.05
1.05
2.85
1.04
2.23
9.39

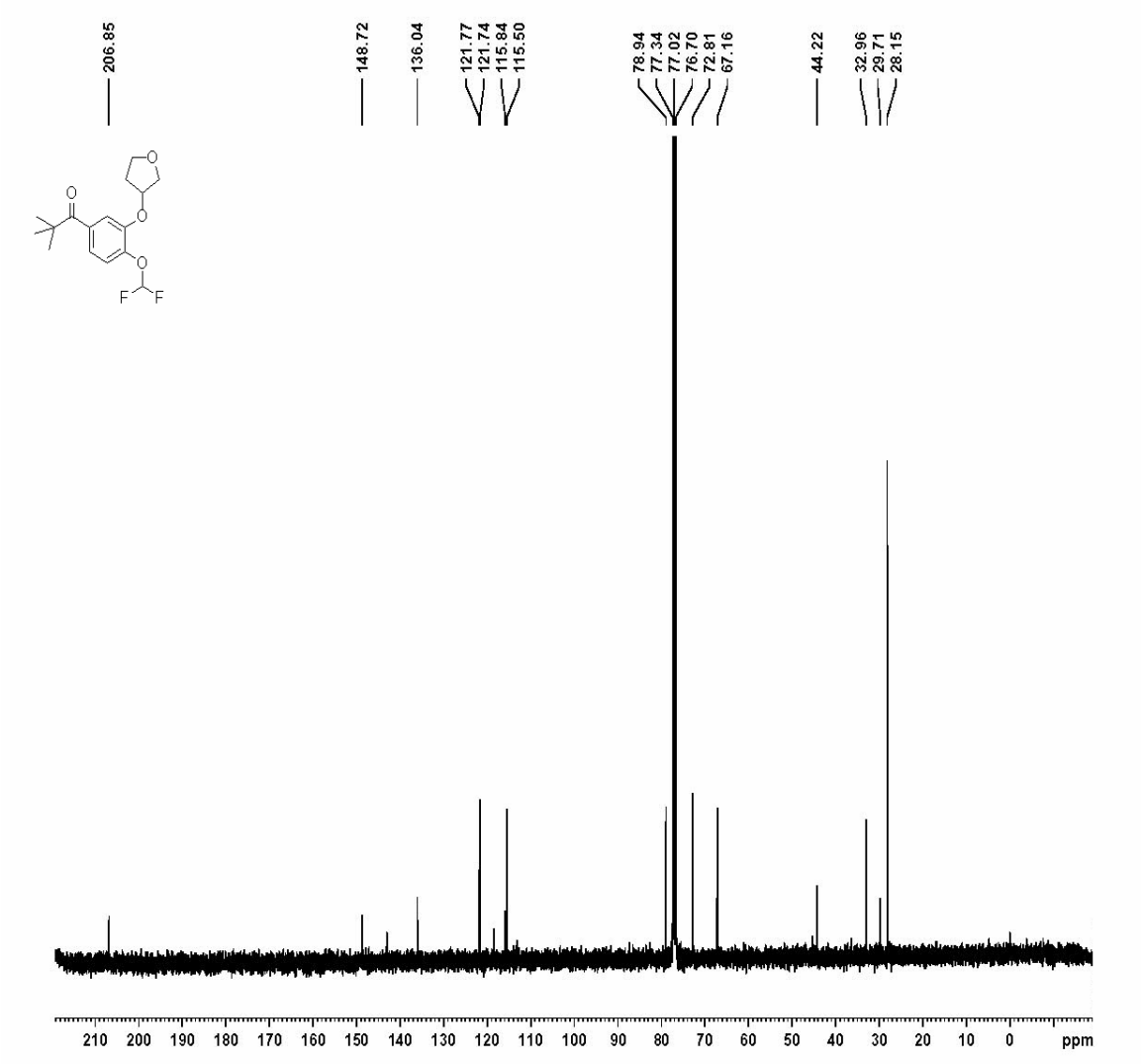
206.85
148.72
136.04
121.77
121.74
115.84
115.50
78.94
77.34
77.02
76.70
72.81
67.16
44.22
32.96
29.71
28.15
O
O
O
F
F
210 200 190 180 170 160 150 140 130 120 110 100 90 80 70 60 50 40 30 20 10 0 ppm

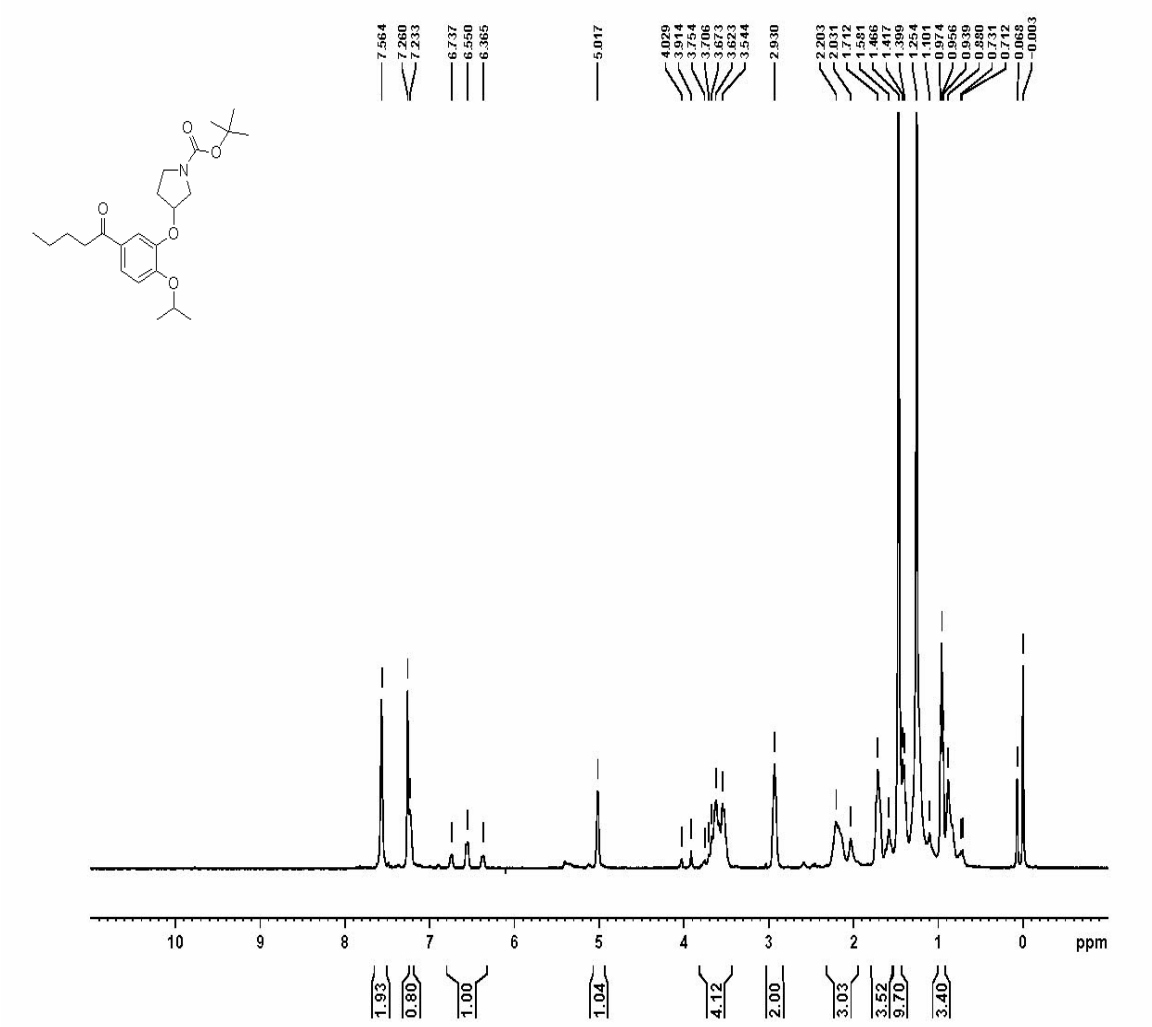
7.564
7.260
7.233
6.737
6.550
6.365
5.017
4.029
3.974
3.754
3.706
3.673
3.623
3.544
2.930
2.203
2.031
1.772
1.581
1.466
1.417
1.399
1.254
1.101
0.974
0.956
0.939
0.880
0.731
0.712
0.068
-0.003
10
9
8
7
6
5
4
3
2
1
0
ppm
1.93
0.80
1.00
1.04
4.12
2.00
3.03
3.52
9.70
3.40

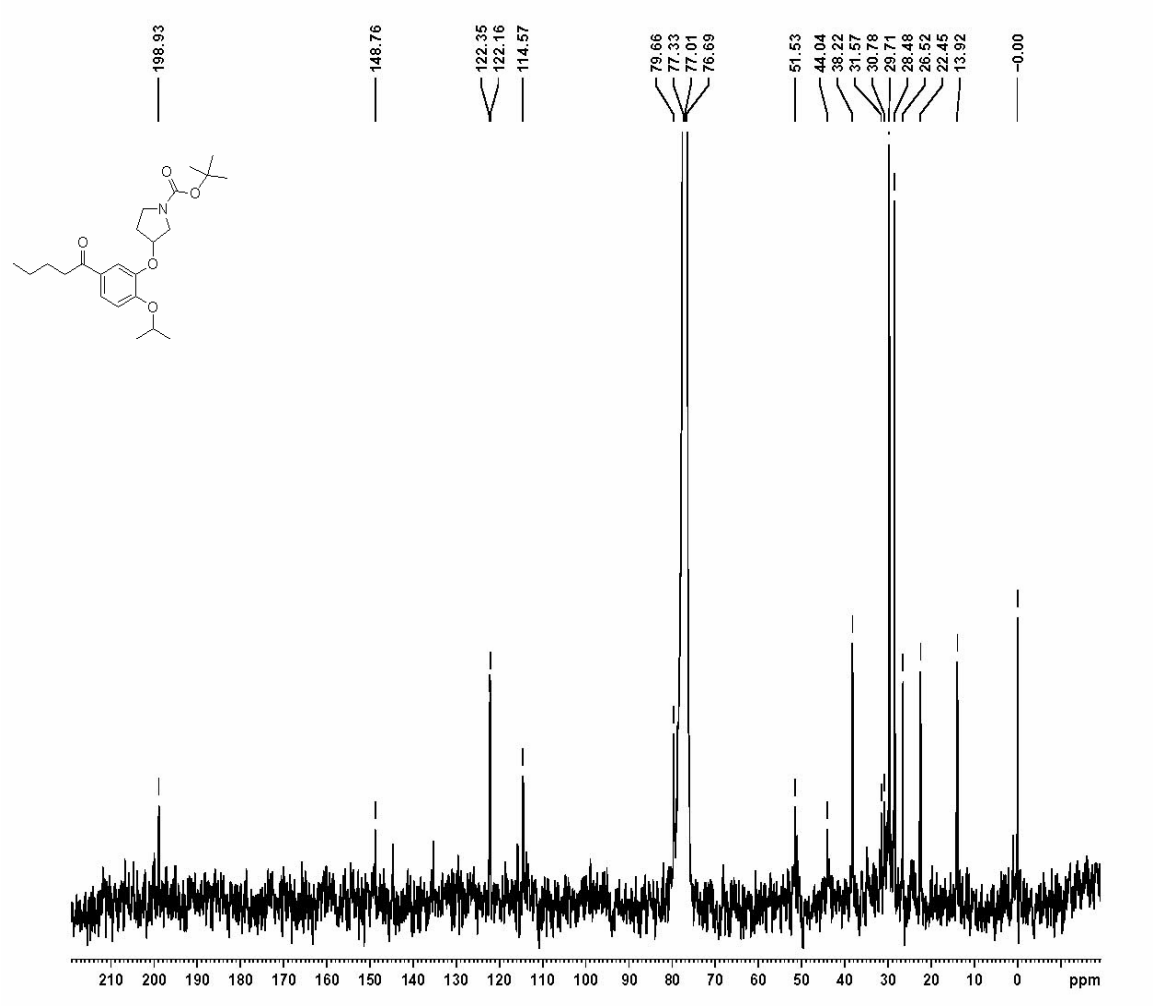
198.93
148.76
122.35
122.16
114.57
79.66
77.33
77.01
76.69
51.53
44.04
38.22
31.57
30.78
29.71
28.48
26.52
22.45
13.92
-0.00
210 200 190 180 170 160 150 140 130 120 110 100 90 80 70 60 50 40 30 20 10 0 ppm

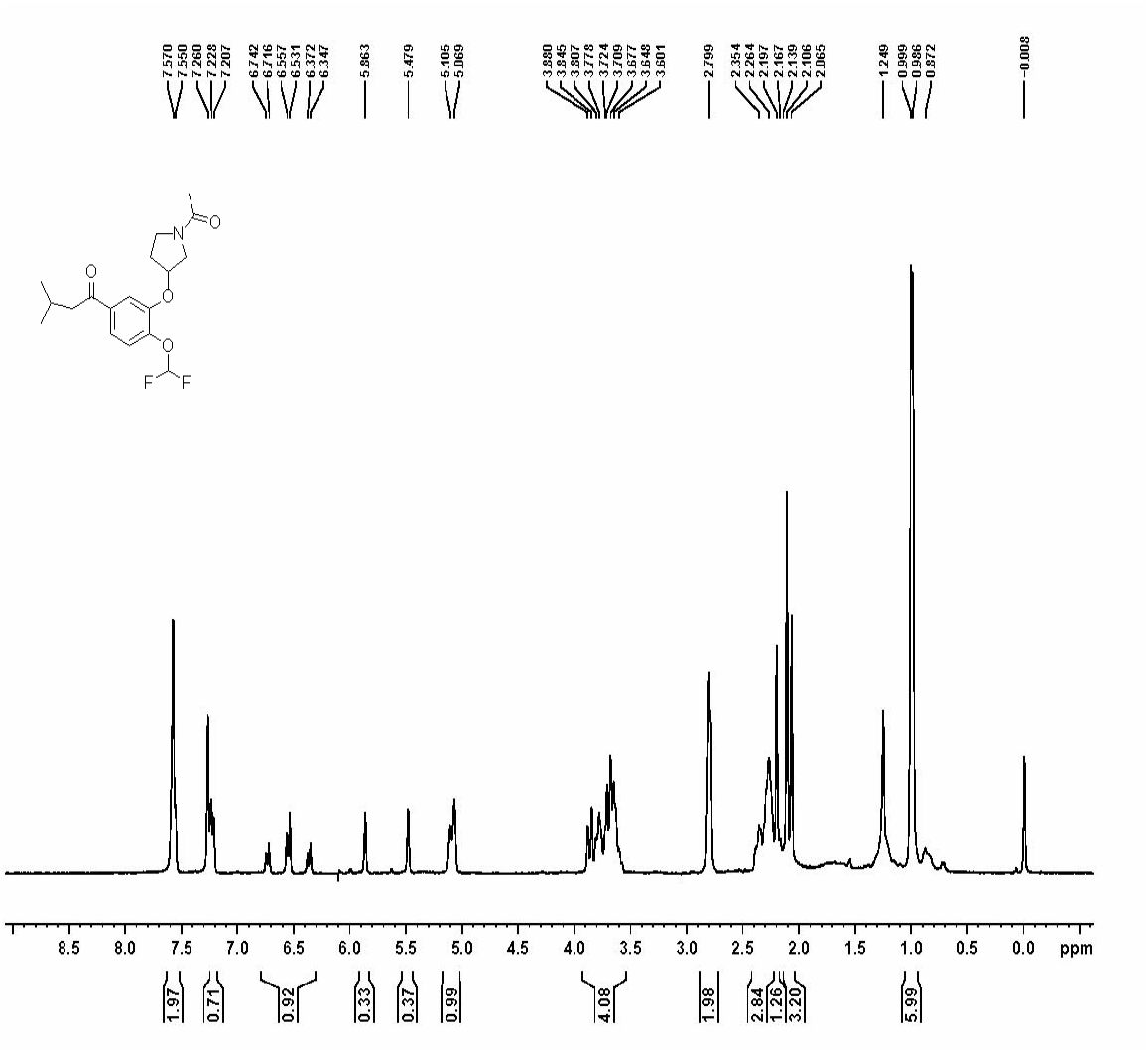
7.570
7.550
7.260
7.228
7.207
6.742
6.716
6.557
6.531
6.372
6.347
5.863
5.479
5.105
5.069
3.880
3.845
3.807
3.778
3.724
3.709
3.677
3.648
3.601
2.799
2.354
2.264
2.197
2.167
2.139
2.106
2.065
1.249
0.999
0.986
0.872
0.008
F
F
8.5
8.0
7.5
7.0
6.5
6.0
5.5
5.0
4.5
4.0
3.5
3.0
2.5
2.0
1.5
1.0
0.5
0.0
ppm
1.97
0.71
0.92
0.33
0.37
0.99
4.08
1.98
2.84
1.26
3.20
5.99

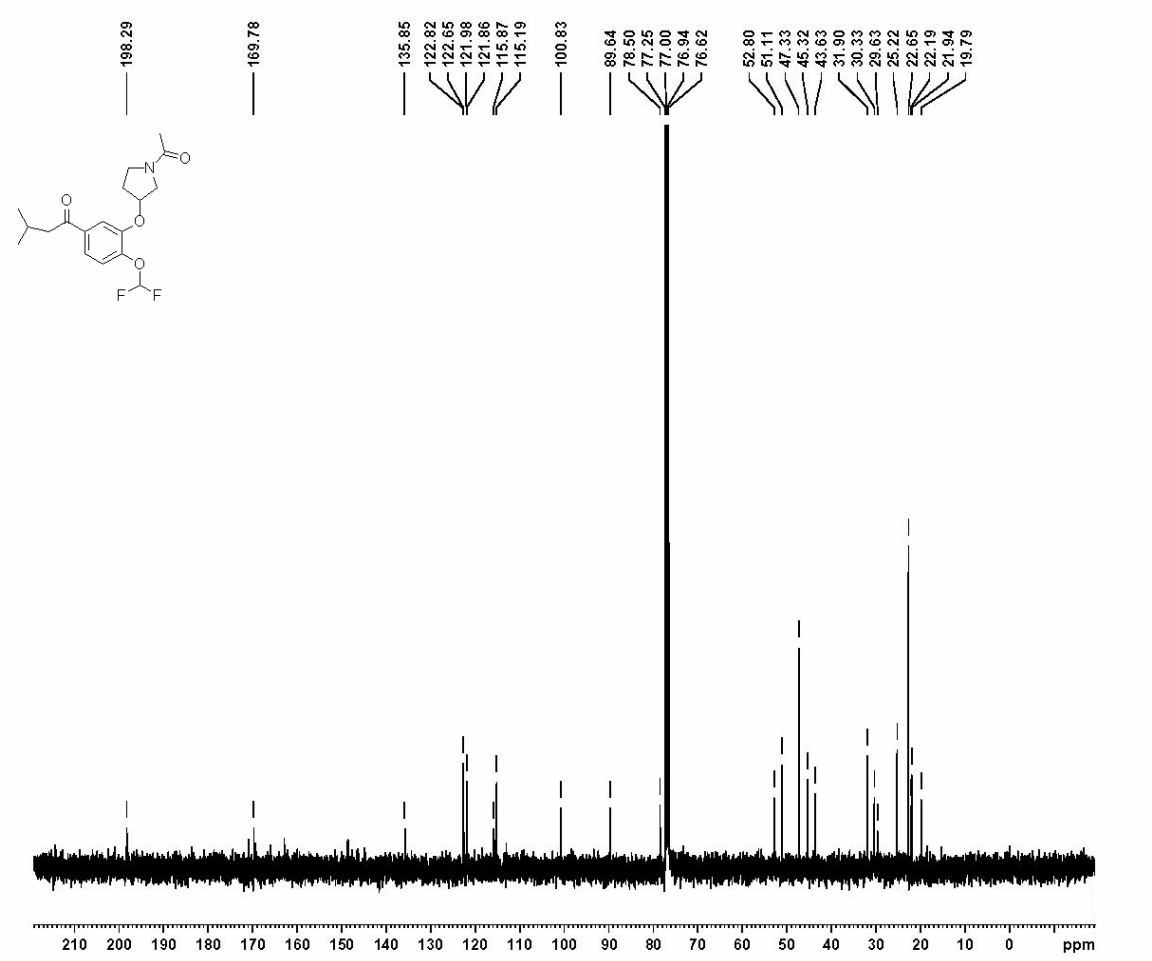
198.29
169.78
135.85
122.82
122.65
121.98
121.86
115.87
115.19
100.83
89.64
78.50
77.25
77.00
76.94
76.62
52.80
51.11
47.33
45.32
43.63
31.90
30.33
29.63
25.22
22.65
22.19
21.94
19.79
O
N
O
O
O
F
F
210 200 190 180 170 160 150 140 130 120 110 100 90 80 70 60 50 40 30 20 10 0 ppm